



POLITECNICO DI TORINO
Repository ISTITUZIONALE

System of Systems conceptual design methodology for space exploration

Original

System of Systems conceptual design methodology for space exploration / Cardile, Diego. - STAMPA. - (2013).

Availability:

This version is available at: 11583/2511716 since:

Publisher:

Politecnico di Torino

Published

DOI:10.6092/polito/porto/2511716

Terms of use:

Altro tipo di accesso

This article is made available under terms and conditions as specified in the corresponding bibliographic description in the repository

Publisher copyright

(Article begins on next page)

POLITECNICO DI TORINO

SCUOLA DI DOTTORATO

Dottorato in Ingegneria Aerospaziale – XXV ciclo

Settore Scientifico Disciplinare: Impianti e sistemi aerospaziali (ING/IND 05)

I Facoltà di Ingegneria

Tesi di Dottorato

**System of Systems conceptual design methodology
for space exploration**



Diego Cardile

Tutori

prof. Sergio Chiesa

ing. Nicole Viola

ing. Giorgio Luigi Ferrari

Coordinatore del corso di dottorato

prof. Fulvia Quagliotti

Aprile 2013

COMMISSIONE GIUDICATRICE
INGEGNERIA AEROSPAZIALE

Il dott. Diego CARDILE ha discusso in data 11 Aprile 2013 presso il Dipartimento di Ingegneria Meccanica e Aerospaziale del Politecnico di Torino la tesi di Dottorato avente il seguente titolo:

System-of-Systems conceptual design methodology for space exploration

Le ricerche oggetto della tesi sono di interesse nel settore

Le metodologie appaiono adeguate

I risultati sono interessanti ed analizzati con adeguato senso critico.

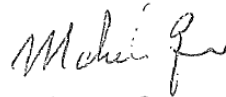
Nel colloquio il candidato dimostra appropriata conoscenza delle problematiche trattate.

La Commissione unanime giudica molto positivamente il lavoro svolto


e propone che al dott. Diego CARDILE venga conferito il titolo di **Dottore di Ricerca**.

Data, 11-04-2013

Prof. Michele GRASSI (Presidente)



Prof. Sergio DE ROSA (Componente)



Prof. Francesco LAROCCA (Segretario)





...just before the Sunrise, June 1889

The Starry Night - Vincent van Gogh

Abstract

The scope of the research is to identify and develop a design methodology for System-of-System (a set of elements and sub-elements able to interact and cooperate in order to complete a mission), based on models, methods and tools, to support the decision makers during the space exploration scenarios design and evaluation activity in line with the concurrent design philosophy.

Considering all combinations of system parameters (such as crew size, orbits, launchers, spacecraft, ground and space infrastructures), a large number of mission concept options are possible, even though not all of them are optimal or even feasible. The design methodology is particularly useful in the first phases of the design process (Phase 0 and A) to choose rationally and objectively the best mission concepts that ensure the higher probability of mission success in compliance with the high level requirements deriving from the “user needs”.

The first phases of the project are particularly critical for the success of the entire mission because the results of this activity are the starting point of the more costly detailed design phases. Thus, any criticality in the baseline design will involve inevitably into undesirable and costly radical system redesigns during the advanced design phases. For this reason, it is important to develop reliable mathematical models that allow prediction of the system performances notwithstanding the poorly defined environment of very high complexity.

In conjunction with the development of the design methodology for system-of-systems and in support of it, a software tool has been developed. The tool has been developed into Matlab environment and provides users with a useful graphical interface. The tool integrates the model of the mission concept, the models of the space elements at system and subsystem level, the cost-effectiveness model or value, the sensitivity and multi-objective optimization analysis. The tool supports users to find a system design solution in compliance with requirements and constraints, such as mass budgets and costs, and provides them with information about cost-effectiveness of the mission.

The developed methodology has been applied for the design of several space elements (Man Tended Free Flyer, Cargo Logistic Vehicle, Rover Locomotion System) and several mission scenarios (Moon surface infrastructure support, Cis-Lunar infrastructure delivering, Cis-Lunar infrastructure logistic support), in order to assess advantages and disadvantages of the proposed method.

The results of the design activity have been discussed and accepted by the European Space Agency (ESA) and have also been compared and presented to the scientific community. Finally, in a particular case, the study of the locomotion system of a lunar rover, the results of the methodology have been verified through the production and testing of the same system.

Table of contents

1	Acronyms	1
1.1	Nomenclatures.....	1
1.2	Notations	4
2	Introduction	11
2.1	Purpose of the research	12
2.2	Research context and state of the art.....	17
3	Methodology	22
4	Models definition	27
4.1	Model Philosophy	27
4.2	Mission concept.....	30
4.3	Habitable Volume	32
4.4	Geometry.....	33
4.5	Structure	38
4.6	Thermal Control System	40
4.7	Power System.....	45
4.8	Propulsion System.....	49
4.9	Life Support System Model & Consumables.....	53
4.10	Communication	60
4.11	Locomotion and mechanisms.....	65
4.12	Launcher.....	70
4.13	Cost.....	74
5	Analysis methods	76
5.1	Value Analysis	76
5.2	Sensitivity and Optimization Analysis	82
5.2.1	Sensitivity analysis: the method of Morris.....	83
5.2.2	Multi-objective Optimization.....	84
6	Scenario Evaluator Tool.....	87
6.1	Tool scope	87
6.2	Tool description.....	87
6.2.1	Tool general description.....	87
6.2.2	Scenario tab	90
6.2.3	Building Block tab	94
6.2.4	Results tab	96
6.2.5	Analysis tab	97
7	System design.....	100
7.1	Free-Flyer	100
7.1.1	Mission objectives.....	100
7.1.2	System requirements	100
7.1.3	Mission Reference Scenario.....	101
7.1.4	Operation Concept.....	102
7.1.5	System Configuration Definition	110
7.1.6	System description	117
7.1.7	System budgets.....	126
7.2	Cargo Logistic Vehicle.....	128
7.2.1	Mission objectives.....	128
7.2.2	System requirements	128
7.2.3	Mission Reference Scenario.....	128
7.2.4	System description	130
7.2.5	System budgets.....	149

7.3	Rover Locomotion System.....	153
7.3.1	Applied design methodology	153
7.3.2	Mission objective	155
7.3.3	System requirements	155
7.3.4	Preliminary performance.....	156
7.3.5	Wheel design assessment	157
7.3.6	Wheel sizing.....	160
7.3.7	Resized wheel.....	164
7.3.8	Scaled wheel.....	166
7.3.9	Resized wheel design revision	168
8	Mission design.....	171
8.1	Moon surface infrastructure support	171
8.1.1	Study 1: Number of crew members and mission duration	174
8.1.2	Study 2: Anytime return	175
8.1.3	Study 3: Lunar Base	176
8.2	Cis-Lunar infrastructure delivering	179
8.3	Cis-Lunar infrastructure Logistic	195
9	Conclusions	203

1 Acronyms

1.1 Nomenclatures

A5	Ariane 5
A5ME	Ariane 5 Mid Life Evolution
ACS	Attitude Control System
AMCM	Advanced Missions Cost Model
AO	Atomic Oxygen
AO	Asteroid Orbit
AOCS	Attitude and Orbit Control System
ARS	Air Revitalization System
AS	Asteroid Surface
ATCS	Active Thermal Control System
ATO	Asteroid Transfer Orbit
ATV	Automated Transfer Vehicle
BER	Bit Error Rate
BOL	Begin Of Life
bps	bit per second
CAP	Capsule
CC	Cargo Carrier
CDF	Concurrent Design Facility
CE	Concurrent Engineering
CLV	Cargo Logistic Vehicle
CMU	Decentralized command and Monitoring Units
COAS	Crew Optical Alignment Sight
cVV	crew Visiting Vehicle
DO	Deimos Orbit
dod	depth-of-discharge
DS	Deimos Surface
DTO	Deimos Transfer Orbit
E/E	End to End
EADS	European Aeronautic Defense and Space Company
ECLS	Environmental Control and Life Support
ECLSS	Environmental Control and Life Support System
ECSS	European Cooperation for Space Standardization
EIRP	Effective Isotropic Radiated Power
EML	Earth-Moon Lagrangian point
EMLP1O	Earth-Moon Lagrangian Point 1 Orbit
EMLP1TO	Earth-Moon Lagrangian Point 1 Transfer Orbit
EMLP2O	Earth-Moon Lagrangian Point 2 Orbit
EMLP2TO	Earth-Moon Lagrangian Point 2 Transfer Orbit
EOL	End Of Life
EPS	Electric Power System
ES	Earth Surface
ESA	European Space Agency
ESAS	Exploration System Architecture Study
EVA	Extra-Vehicular Activity
FDS	Fire Detection and Suppression
FEM	Finite Element Method
FES	Fluid Evaporator System

GEO	GEostationary Orbit
GNC	Guidance, Navigation And Control
GOX	Gas OXYgen
GPS	Global Positioning System
GTO	Geosynchronous Transfer Orbit
GUI	Graphical User Interface
HEO	High Elliptic Orbit
HR	High Rate
IBDM	International Berthing and Docking Mechanism
IM	Inflatable Module
IMU	Inertial Measurement Unit
IOC	Initial Operating Capability
ISS	International Space Station
JPL	Jet Propulsion Laboratory
LAM	Lunar Ascent Module
LDM	Lunar Descent Module
LEO	Low Earth Orbit
LH	Liquid Hydrogen
LH2	Liquid Hydrogen
LIDAR	LIght Detection And Ranging
LLO	Low Lunar Orbit
LM	Laboratory Module
LMET	Liquid METHane
LOI	Lunar Orbit Injection
LOX	Liquid OXYgen
LRV	Lunar Roving Vehicle
LS	Lunar Surface
LS	Launch System
LSAM	Lunar Surface Access Module
LTO	Lunar Transfer Orbit
LV	Logistic Vehicle
MCC	Master Control Computer
MDPS	Micrometeoroids and Debris Protection System
MET	Mobile Equipment Transporter
MIT	Massachusetts Institute of Technology
MLI	Multi-Layer Insulation
MMH	Mono-Methyl-Hydrazine
MMM	Mass Memory Module
MO	Mars Orbit
MOEA/D	Multi-Objective Evolutionary Algorithm Based on Decomposition
MON	Mixed Oxides of Nitrogen
MOPSO	Multi-Objective Particle Swarm Optimization
MPCV	Multi-Purpose Crew Vehicle
MS	Mars Surface
MTO	Mars Transfer Orbit
N/A	Not Available
NAFCOM	NASA-Air Force Cost Model
NASA	National Aeronautics and Space Administration
NEO	Near-Earth Objects
NSGA	Non-dominated Sorting Genetic Algorithm
NTO	Nitrogen Tetra-Oxide

OBDH	On Board Data Handling
OCS	Orbit Control System
OGA	Oxygen Generation Assembly
OML	Outer Mold Line
OP	Outpost
ORS	Oxygen Regeneration System
PCDU	Power Control and Distribution Unit
PICA	Phenolic Impregnated Carbonaceous Ablator
PMD	Propellant Management Devices
PO	Phobos Orbit
PSO	Particle Swarm Optimization
PTCS	Passive Thermal Control System
PTO	Phobos Transfer Orbit
RM	Resource Module
RT	Resonance Transfer
RvD	Rendezvous and Docking
SCWO	Super Critical Waste Oxidation
SET	Scenario Evaluator Tool
SoS	System of Systems
SSIM	Space Station Integrated Module
SSN	Space Station Node
SSSM	Space Station Service Module
STD	STanDard
STEPS	Systems and Technologies for the ExPLoration of Space
STS	Space Transportation System
TAS	Thales Alenia Space
TCS	Thermal Control System
TDRSS	Tracking and Data Relay Satellite System
TEI	Trans-Earth Injection
THC	Temperature and Humidity Control
TLI	Trans-Lunar Injected
TOF	Time Of Flight
TPS	Thermal Protection System
TPS-a	ablative Thermal Protection System
TPS-r	reusable Thermal Protection System
TS	Transfer Stage
TWTA	Traveling Wave Tube Amplifier
UHF	Ultra-High Frequency
UOP	Utility Outlet Panel
US	United States
USSR	Union of Soviet Socialist Republics
VHF	Very-High Frequency
WCS	Waste Collection System
WRS	Water Recovery System
wrt	with respect to
WSB	Weak Stability Boundary

1.2 Notations

A	Ground contact area
A_n	Cross-section area
A_{rad}	Radiators area
A_{sa}	Solar array area
b	Tank wall thickness
B_n	System's block number
b_w	Wheel width
c	Speed of light
C	Cost
c_c	Coulombian coefficient of cohesion of the soil
C_d	Drag coefficient
C_{launch}	Launch cost
D	Drag
$D_{antenna}$	Diameter of the antenna
D_c	Programmatic and technical development and production complexity
D_{CP}	External diameter of the platform (cylinder coupled to platform geometry)
d_e	Diameter of the upper base of the truncated cone
D_e	Diameter of the lower base of the truncated cone
D_{et}	Tank external diameter
df	Duty factor
d_i	Diameter of the upper base of the internal free volume of the truncated cone
D_i	Diameter of the lower base of the internal free volume of the truncated cone
D_{it}	Tank internal diameter
D_{MH-e}	External diameter of the cylinder for Manned Habitat
D_{MH-i}	Diameter of the internal pressurized compartment of the Manned Habitat
DP	Drawbar pull
dpy	Solar cells degradation per year
D_{RM}	External diameter of the cylinder for Resource Module
D_{tank}	Diameter of the propellant tanks
D_w	Wheel diameter
E	Elastic modulus
E_{bat}	Energy of the batteries
E_{fc}	Fuel cells energy
eff_{sc}	Energy conversion efficiency of the solar cells
F	Maximum thrust that can be generated by the motor-wheel
f	System global functionality
f_c	Carrier frequency
f_r	Coefficient of rolling resistance
G	Gain
g	Acceleration of gravity
g_0	Standard gravity
G_r	Receiver antenna gain
G_t	Transmitter antenna gain
H	Maximum horizontal propelling force that can be generated
h_e	Height of the truncated cone
h_i	Height of the internal free volume of the truncated cone
I	Inertial force generated by the acceleration
I_{ass}	Solar cells degradation due to design and assembly inefficiencies
I_d	Inherent degradation

Inst	Mass margin for battery installation
I_s	Solar cells shadowing inefficiency
I_{sp}	Specific impulse
I_t	Solar cells temperature inefficiencies
k	Boltzmann constant
k_{ACC}	Mass proportional coefficient for ACC system
k_{ATCS}	Mass proportional coefficient for thermal control system components
k_{bat}	Battery specific energy density
k_{bo}	Boil-off proportional coefficient
k_c	Modulus of the soil deformation due to the soil cohesive ingredients
K_c	Modulus of cohesion of soil deformation
$k_{c/e\ sup}$	Mass proportional coefficient for cooking/eating supplies
k_{closet}	Mass proportional coefficient for closet
$k_{dispensewipes}$	Mass proportional coefficient for dispense wipes
k_f	Number of factors
k_{fcs}	Fuel cell energy density
k_{food}	Mass proportional coefficient for food
$k_{heatH2O}$	Heat of vaporization of the water
$k_{heatR134A}$	Heat of vaporization of the Freon
k_{hr}	Heat-rejection coefficient
$k_{hygiene\ kit}$	Mass proportional coefficient for hygiene kit
k_{ii}	Mass proportional coefficient for internal TPS
$k_{k/o\ clean\ supp}$	Mass proportional coefficient for kitchen/oven cleaning supplies
k_{MDPS}	Mass proportional coefficient for MDPS
k_{MDPS}	Mass proportional coefficient of MDPS
k_{MLI}	Mass proportional coefficient for MLI
k_{OML}	Mass proportional coefficient for OML structure
k_{ot}	Mass proportional coefficient for oxygen tank
k_{PVS}	Mass proportional coefficient for pressurized vessel structure
k_{Qcrew}	Heat generated by a person
k_{rad}	Mass proportional coefficient for radiators
$k_{recreational\ item}$	Mass proportional coefficient for recreational items
k_{rp}	Residual propellant proportional coefficient
k_{sa}	Mass proportional coefficient for solar array
k_{SA}	Mass proportional coefficient for sleep provisions
$k_{sleep\ accommodation}$	Mass proportional coefficient for sleep accommodation
k_{suit}	Mass proportional coefficient for suit
$k_{susp/steering}$	Mass proportional coefficient for the suspension and steering system
k_{tank}	Ratio between the diameter of the cylindrical tank and its length
k_{THC}	Mass proportional coefficient for venting and thermal conditioning system
k_{ti}	Mass proportional coefficient for tank insulation layers
k_{TPS-a}	Mass proportional coefficient for ablative thermal protection system
k_{TPS-r}	Mass proportional coefficient for reusable thermal protection system
$k_{trashbag}$	Mass proportional coefficient for trash bags
k_w	Mass proportional coefficient for wheel system
k_{wm}	Mass proportional coefficient for wheel motor
k_{wt}	Mass proportional coefficient for water tank
K_γ	Modulus of density of soil deformation
k_ϕ	Modulus of the soil deformation due to the soil frictional ingredients
L	Lift
$L_{antenna}$	Length of the antenna

l_{con}	Length of the cylindrical section of the launcher fairing
l_{CP}	Length of the module (cylinder coupled to platform geometry)
L_d	Solar cells lifetime degradation
l_{fix}	Length of the cylinder for internal equipment
L_{fs}	Propagation loss
l_{MH-e}	Length of the cylinder for Manned Habitat
l_{MH-i}	Length of the internal pressurized compartment of the Manned Habitat
L_{other}	Other link loss
LOX	Liquid oxygen
l_{RM}	Length of the cylinder for Resource Module
l_{tank}	Length of the propellant tank
l_{tank}	Length of the cylindrical tank
l_{tap}	Length of the tapered section of the launcher fairing
M	Link margin
m	mass
m_0	Initial total mass of the spacecraft
m_{ACC}	Mass of the atmosphere contaminant control system
$m_{accessories}$	Mass of the accessories for the crew
$m_{antenna}$	Mass of the antenna
m_{ATCS}	Mass of the active thermal control system components
$m_{atm\ control}$	Mass of the atmosphere supply and control system
$m_{basic\ supply}$	Mass of the basic supplies
m_{bo}	Mass of propellant lost due to the boil off
$m_{c/e\ supp}$	Mass of the cooking/eating supplies
m_{COAS}	Mass of the Crew Optical Alignment Sight
$m_{conventional\ ovens}$	Mass of the conventional ovens
M_d	Dry mass of the system in Pounds
$m_{dispensewipes}$	Mass of the dispense wipes
$m_{emergency\ kit}$	Mass of the emergency kit
$m_{equivalent\ rack}$	Mass of the equivalent racks for system, payloads accommodation
m_{fcs}	Mass of the fuel cell system
m_{food}	Mass of the food
m_{fuel}	Mass of fuel
$m_{generic\ tools}$	Mass of the generic tools for the crew
$m_{hatches}$	Mass of the hatches
$m_{hygiene\ kit}$	Mass of the hygiene kit
m_i	Inert mass of the spacecraft
m_{ji}	Mass of internal TPS
$m_{k/o\ clean\ supp}$	Mass of the kitchen/oven cleaning supplies
m_{lander}	Mass of the lander
$m_{landingsys}$	Mass of the landing system
$m_{lighting}$	Mass of the lighting equipment
$m_{main-engine}$	Main engine mass
m_{MDPS}	Mass of the micrometeoroids and debris protection system
$m_{microwave\ ovens}$	Mass of the microwave ovens
m_{MLI}	Mass of MLI
m_{OML}	Mass of the OML structure
m_{other}	Mass of other equipment
$m_{ox\ tank}$	Mass of the oxygen tank
m_{oxygen}	Mass of oxygen
m_p	Mass of the propellant

m_{payload}	Payload mass
$m_{\text{primary structure}}$	Mass of the primary structure
m_{PVS}	Mass of the pressurized vessel structure
$m_{\text{pyrotechnic}}$	Mass of the pyrotechnic mechanisms
m_{R134A}	Mass of the Freon for FES
m_{rack}	Mass of racks
m_{rad}	Mass of the radiators
$m_{\text{recreational item}}$	Mass of the recreational items
$m_{\text{restrains}}$	Mass of the restrains
m_{rp}	Mass of the residual propellant
m_{sa}	Mass of all the solar array
m_{SA}	Mass of the sleep provisions
$m_{\text{secondary structure}}$	Mass of the secondary structure
$m_{\text{secondary-engine}}$	Secondary engine mass
m_{sink}	Mass of the sink & spigot for hydration of food and drinking water
$m_{\text{sleep accommodation}}$	Mass of the sleep accommodation
$m_{\text{smoke detector}}$	Mass of the smoke detector system
$m_{\text{SS transmitter}}$	Mass of the Solid State transmitter
m_{suit}	Mass of the space suit
$m_{\text{survival kit}}$	Mass of the survival kit
$m_{\text{susp/steering}}$	Mass of the suspension and steering system
$m_{\text{suspended}}$	Suspended mass
m_{tank}	Tank mass
$m_{\text{tank support}}$	Mass of the tank support structure
$m_{\text{test equipment}}$	Mass of the test equipment
m_{THC}	Mass of the venting and thermal conditioning system
m_{ti}	Mass of the tank insulation
m_{tot}	Total mass
$m_{\text{TPS-a}}$	Mass of ablative thermal protection system
$m_{\text{TPS-r}}$	Mass of reusable thermal protection system
m_{trashbag}	Mass of the trash bags
$m_{\text{TWTA transmitter}}$	Mass of the TWTA transmitter
$m_{\text{umbilicals}}$	Mass of the EVA umbilical and support system
$m_{\text{vacum trash bag}}$	Mass of the vacuum trash bags
m_{w}	Mass of water
$m_{\text{water-vap}}$	Mass of the water for FES
$m_{\text{wet tank}}$	Mass of the empty tanks and propellant
m_{wheels}	Mass of the wheels
m_{windows}	Mass of the windows
m_{wm}	Mass of the wheel motor
m_{wt}	Mass of the water tank
n	Exponent of soil deformation
N_{c}	Terzaghi's bearing capacity factors in general shear failure
n_{crew}	Number of crew members
$n_{\text{day mission}}$	Duration of the manned mission in days
n_{hatches}	Number of hatches
n_{rack}	Number of equivalent racks
n_{rack}	Number of racks
n_{RvD}	number of RvD
n_{ti}	Numbers of tank insulation layers
N_{γ}	Terzaghi's bearing capacity factors in general shear failure

O/F	Oxidizer-to-fuel mass ratio
p	Mission success ratio
P	Number of dimension levels
P_0	Ideal power per unit area
P_{BOL}	Power per unit area produced at the begin of life
P_d	Average power required during daylight
P_e	Average power required during eclipse
P_{EOL}	Power per unit area produced at the end of life
p_l	Launch probability-of-success
P_{launch}	Launch probability of success
P_{min}	Minimum pressure to guarantee inside the tank
P_n	System performance
P_{RvD}	RvD probability of success
P_{sa}	Power that the solar array shall provide during daylight
p_t	Internal pressure of the tank
P_t	Transmitted power
p_w	Ground contact pressure
P_w	Power to be generated by the locomotion system wheel
Q	Total thermal load
Q_{ATCS}	Total thermal load
Q_{crew}	Thermal load due to the presence of the crew
Q_e	Development and production quantities
Q_{fesH2O}	Heat to be dissipated by the FES water
$Q_{fesR134A}$	Heat to be dissipated by the FES Freon
r	Tank mean radius
R	Universal gas constant
r_1	Radius of the initial orbit when performing change of orbit inclination
r_2	Radius of the orbit where performs the change of orbit inclination
R_b	Bulldozing resistance
R_c	Compaction resistance
R_{cf}	Compaction resistance for deformable wheel
R_{cr}	Compaction resistance for rigid wheel
R_d	Data-rate
r_e	Radius of the upper base of the truncated cone
R_e	Radius of the lower base of the truncated cone
R_e	Number of elementary effects
R_g	Gravitational resistance
r_i	Radius of the lower base of the internal free volume of the truncated cone
R_i	Radius of the lower base of the internal free volume of the truncated cone
R_r	Rolling resistance
R_{tot}	Sum of the motion resistances for locomotion system
s	Slant range
S_{CP}	Total surface (cylinder coupled to platform geometry)
S_{CP-cil}	Surface of the internal cylinder (cylinder coupled to platform geometry)
$S_{CP-plat}$	Surface of the platform (cylinder coupled to platform geometry)
S_e	Total surface of the truncated cone
$S_{e\ lateral}$	Lateral surface of the truncated cone
$S_{e\ lower}$	Surface of the lower base of the truncated cone
$S_{e\ upper}$	Surface of the upper base of the truncated cone
S_{exp}	Exposed surface of the spacecraft
S_h	Surface of hatch

S_i	Total surface of the internal free volume of the truncated cone
$S_{i \text{ lateral}}$	Lateral surface of the internal free volume of the truncated cone
$S_{i \text{ lower}}$	Surface of the lower base of the internal free volume of the truncated cone
$S_{i \text{ upper}}$	Surface of the upper base of the internal free volume of the truncated cone
SM	Service module
S_{MH-e}	Total surface of the cylinder for Manned Habitat
S_{MH-i}	Total surface of the internal pressurized compartment of the manned habitat
S_{MLI}	Surfaces covered by MLI material
SNR	Signal to noise ratio
SNR_{avail}	Signal to noise ratio received
SNR_{required}	Signal to noise ratio required
S_p	Specification
S_{RM}	External surface of the cylinder for Resource Module
$S_{RM \text{ base}}$	Surface of the base of the cylinder for Resource Module
$S_{RM \text{ lat}}$	Lateral surface of the cylinder for Resource Module
S_t	Tank external surface
S_{w-h}	Surface of windows and hatches
T	Engine vacuum thrust
t	Distance of rupture
T	Torque
T0	Inlet temperature of the fluid in the radiator system
T4	Outlet temperature of the fluid from the radiator system
t_{bat}	Batteries utilization time
t_d	Duration of daylight period per orbit
t_{delay}	End to end delay time
t_e	Duration of eclipse period per orbit
T_E	Radiator temperature at the equilibrium
T_{gas}	Temperature of the gas
t_{mission}	Duration of the manned mission in days
T_n	System noise temperature
$t_{\text{propagation}}$	Delay time due to propagation
T_r	Receiver system temperature
T_{sink}	Temperature of the heat sink
$t_{\text{transmission}}$	Delay time due to transmission
V	Value
v	Velocity
v_e	Effective exhaust velocity of the rocket
V_F	View factor
$V_{\text{habitable}}$	Habitable volume
$V_{\text{habitable/crew}}$	Habitable volume per crew member
V_i	Velocity before and after the burn to change plane
V_p	Pressurized volume
$V_{\text{pressurized}}$	Pressurized volume
$V_{\text{pressurizedequipment}}$	Volume of the equipment inside the pressurized section
V_{prop}	Volume of propellant
V_{tank}	Volume of the tank
VV	Visiting vehicle
W	Vertical load acting on the wheel
W_{bat}	Power required by the batteries
w_t	Distance between the internal and external surface of the truncated cone
x	Messages per second

X_d	Efficiency of the paths from the solar arrays directly to the loads
X_e	Efficiency of the paths from the solar arrays thru the batteries to the loads
y	Number of bytes per message
z	Size of the block of data
z_w	Maximum wheel sinkage
α	Sidewall angle of the truncated cone
α_a	Angle of approach
γ	Specific weight of soil
Δ	Width of the step
δ	Ratio between the inert and total mass of a spacecraft
ΔV	Delta velocity
δ_w	Wheel deflection
ε	Surface emissivity
η	Antenna efficiency
η_{fcs}	Fuel cells efficiency
θ	Angle of orbit change
θ_s	Slope angle
μ	Mean
μ_{gas}	Molar mass of gas
ρ	Specific weight
ρ_{fuel}	Specific weight of fuel
$\rho_{oxidizer}$	Specific weight of oxidizer
σ	Standard deviation
σ_c	Yield strength
Φ	Diameter of the cylindrical section of the launcher fairing
ϕ	Coulombian angle of internal friction of the soil
ω	Velocity of the wheel

2 Introduction

Exploration is the action of exploring an unfamiliar area, ref. [1]. Thus, exploration implies to do something aimed at discovering resources and/or information inherent to an area of which we do not have any knowledge or experience of. In the particular case of space exploration, the area is intended as the physical universe beyond the earth's atmosphere.

Only in the recent history, with the development of space access vehicles, the exploration of the space, i.e. the closed observation of the object in the space, has become possible. First than the 20th century, only space observation was possible. Astronomy is the science that deals with the observation of objects places at high distance from the Earth.

Since the ancient time, humans observe the objects in space. The Ancient Egyptians, like many other early civilizations, performed observation of the sky. The discoveries that they achieved were useful to have an accurate calendar so that they would know when to plant and harvest crops to provide food. They understand that there were a correlation between the flooding of the River Nile and the position of the stars in the sky. In fact, the Nile floods every year at the summer solstice that occurs exactly when the axial tilt of the Earth's semi-axis is most inclined towards the Sun during summer. Although they never understand the real reasons and motivation of this, they exploited the flooding of the Nile to grow their crops.

It is only in the modern era, with the invention of the telescope, that astronomy evolved in a modern science and more important discoveries have been possible. The invention of the telescope pushed the developing and built of new and modern astronomy observatories. The Greenwich observatory was founded with the intention of develop new and more exact star catalogues and maps that sailors could utilize to orientate during the sea travel. The cost of the structure was repaid by the sale of the star maps to the navigators.

The recent technological evolution allowed the developing of new space observation devices. A space observatory, for example, is an artificial satellite equipped with instruments designed for the observation and study of objects and phenomena in outer space or to study the Earth's atmosphere. The observation of the Earth has become an indispensable tool for studying a wide range of phenomena from forest fires to meteorological events. The importance of the meteorology, i.e. the study of the atmosphere, is linked to the fact that all the human activities directly or indirectly are affected by weather and climate. The capability to perform weather forecast allows safe transports, more efficient food production, optimization of logistics for industries and so on.

Space exploration is certainly more costly than space observation because the needing to travel up to the site of interest in the space. The costs of a manned or robotic exploration mission are in the order of the billions of dollars and find a justification to a so expensive activity is certainly difficult and in any case questionable. The typical question is “Could the same amount of money be devoted to help people, here on Earth, to solve problems instead of to send a spacecraft on a planet?”.

Instead of looking for a justification for such a huge expenditure, it is more interesting and useful to show the economical, technical and social benefits deriving from space exploration activities. The choice to accept or not investments in space activities is then subjective and based on the self-concept of cost and benefits.

The social poverty is not due to the lack of money but to the lack of wealth, which is the value of goods and services. The wealth is produced (and the income is generated) in the form of added value. Thus, the social poverty cannot be solved by giving money but producing wealth. In fact, the pumping of money in a poor nation would contribute to reduce

the value of the money and to increase the inflation. In economy, instead, the method to increase the wealth is through investment of money to generate additional wealth.

Space exploration is a means to generate new wealth. Thus, a space exploration mission will be never a direct source of food but it will be a means to generate new wealth and technologies useful to get food. The money spend in space activities is not an end in itself but it always impacts on economy and industry. The space business allows the development of technological economy that stimulates the birth of new technological districts, the attraction of new investors and the creation of new employments. This is a process that generates income aimed to increase the wealth of a large part of the population because through the redistribution of the money allows increasing of the wealth not only in the space sector.

NASA definition for spin-off technology is “*a technology, originally developed to meet NASA mission needs, that has been transferred to the public and now provides benefits for the Nation and world as a commercial product or service*”, ref. [2]. Thus, a spin-off is a product that incorporates technology and "know-how" deriving from the space activities and provides practical benefits to the general public. This implies that the research activity, performed in the framework of aerospace, has a practical benefit for the people. The examples of technology spin-off are numerous and only NASA has documented nearly 1800 spin-off technologies in the annual NASA Spin-off publication, ref. [3]. The technologies deriving from space exploration enhance many aspects of daily life, including health and medicine (light-emitting diodes also called LED, infrared ear thermometers, ventricular assist device, artificial limbs, invisible braces, scratch-resistant lenses), transportation (aircraft anti-icing systems, highway safety, improved radial tires, chemical detection), public safety (video enhancing and analysis systems, fire-resistant reinforcement, firefighting equipment), consumer goods (temper foam, enriched baby food, portable cordless vacuums, freeze drying), energy and environment (water purification, solar energy, pollution remediation), information technology (structural analysis software, remotely controlled ovens, NASA Visualization explorer, space race blastoff), and industrial productivity (powdered lubricants, improved mine safety, food safety).

It is important to understand that, any significant scientific or technological progress is never for its own sake but it is the results of the effort performed by the technicians to reach a more important objective. Often, the solution to a technical problem is not obtained by a direct approach, but through the approach to a more important and ambitious objective that justify the technological effort. Thus, the needing to solve the technological problems associated to the exploration missions stimulates the imagination of the engineers.

The first space activities were pushed by the competition between the Soviet Union (USSR) and the United States (US) for supremacy in space exploration which were seen as necessary for national security and symbolic of technological and ideological superiority. The space competition ended with the landing of the Apollo spacecraft on the Moon. Then, the increasing costs associated to space exploration pushed the two nations (and the other that contemporary started their own space programs) to collaborate in order to share resources. Today, space exploration represents an opportunity of collaboration between the nations, enables people to see beyond their narrow confines, to overcome diversities, struggles and wars, suggesting a common goal.

2.1 Purpose of the research

Especially in the last years, space missions have become more complex than before because the attention of the space agencies has shifted toward new ambitious programs.

Complicated space missions implies very complex systems and very complex systems implies more expensive systems. Cost is a fundamental limitation to nearly all space missions and is becoming more so. Thus, every day, it becomes more evident that it is necessary to manage the increased complexity in order to decrease the SoS cost.

Engineering design is a challenging activity for any product. In particular, the design of space systems represents a challenge of the highest order since the significant uncertainties in environmental and system parameters. The design challenge comes from the combination of performance, cost, reliability, safety, operability, and schedule requirements and demands the best of engineering skill, organization, communication, integration, and judgment.

The design of space-exploration missions begins with a mission statement that defines what the mission needs to achieve, what the qualitative goals are, and why one shall perform the mission itself. The mission architecture defines how the mission will work in practice and all elements that will take part in it. It includes such issues as the synergies of manned and robotic resources, mission control, and the mission timeline. The mission architecture design activity is an iterative process aimed at maximizing the cost effectiveness (or value) of the mission. The target is reached searching the solution that maximizes benefits and minimizes costs and other negative effects. This is performed by successive meaningful comparisons and evaluation of the generated alternatives. Considering all the system combination of space elements and functionalities allocation, a large number of possible solutions are possible and the process results a very demanding activity.

Figure 1 attempts to schematize the mission architecture design process. The analysis of the mission statements allows the definition of the main mission objectives that must be compatible with the technical capabilities, physical realities and available budgets so that the activity can proceed. At this level, also potential partners can be identified, in order to recognize possible external contributions involving secondary mission objectives and first high level requirements, such as actions to be performed at the desired target site, number of crewmembers, system needed, etc. Once the mission objectives and constraints are known, the space elements, consistent with orbits, trajectories and cost constraints, can be selected to develop all the potential mission concepts. The set of candidate architectures must be large enough to scan all possible combinations, resulting from major and minor variations, but also small enough to make the detailed definition and evaluation manageable. The list of options can be illustrated by a tree of alternatives where major variations are located at the root of the tree and minor variations are located at the extremities. There are several structured methods useful to develop all possible system combinations. The process to construct and prune a trade tree of available options is one of these. After the main systems drivers have been identified, this method consists in mechanically creating the list of all possible combinations of mission options reducing then the number of options to those that are actually feasible or even also reasonable. The concept-tree is the output of this crucial activity that must be performed with particular attention in order not to exclude solutions that at a first sight may seem non-optimal but that are actually optimal.

At this point, each mission concept must be subjected to qualitative and/or quantitative evaluations, taking into account issues such as mass, risk, cost and exploration performances. In order to perform these analyses, first of all the major system drivers that affect the main features of the space elements have to be identified, then trade off analyses aimed at selecting the best solution have to be carried out. Generally, trade off analyses are performed for all those systems and subsystems where multiple options exist, as life support system, power generation, thermal control, propulsion, entry and landing systems, structures, environmental control EVA approaches, GN&C, layout, surface mobility approaches, science support, etc.. Moreover, also mission operations such as crew timelines, mission event sequencing and

control, back up and emergency procedures, maintenance and repair, science activities, contingency approaches, communication methods must be considered to complete the analyses. The design process ends with an assessment of the cost effectiveness of each concept solutions, in order to identify the most promising option.

It is evident that the design process of a space exploration mission is a very demanding activity both in terms of time and computational effort. The process seems to be quite sequential and orderly but iterations are frequent as well as the simultaneous working on several steps of the process and at multiple levels of details.

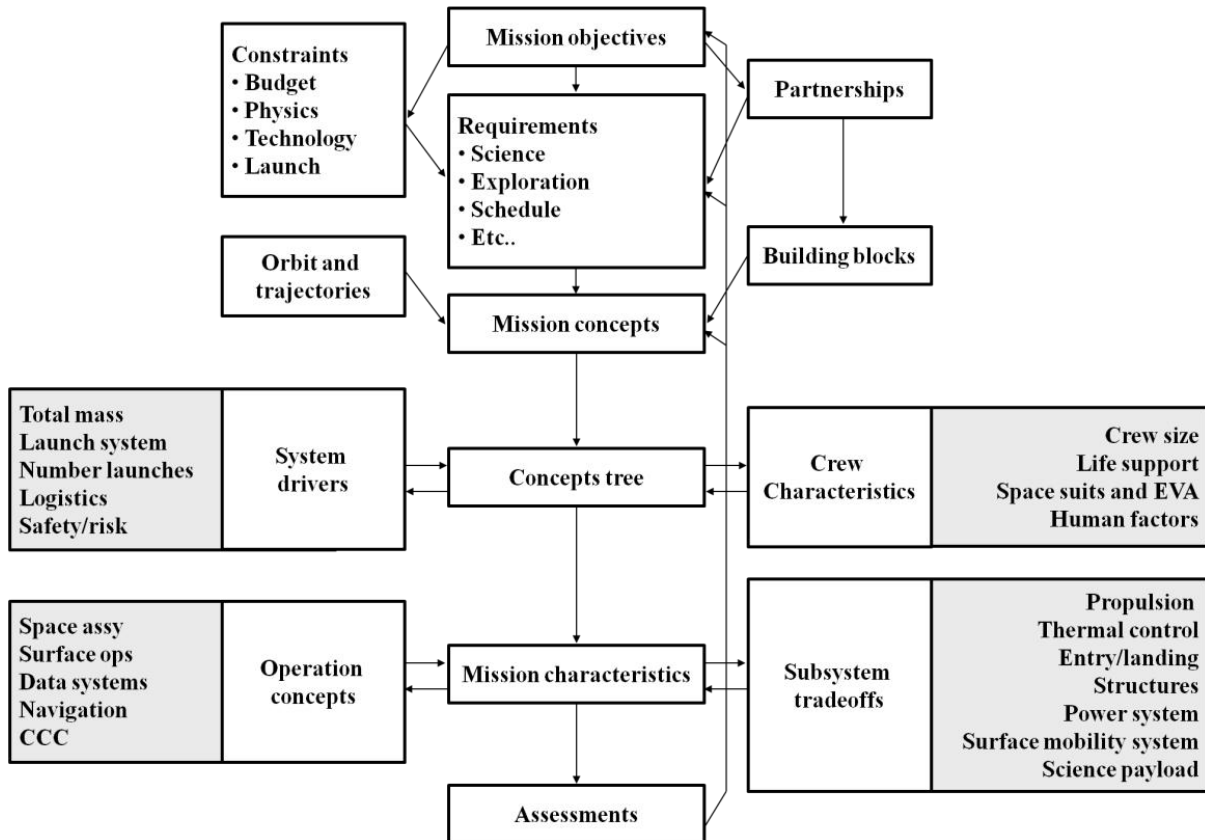


Figure 1 Mission design process (ref. [4])

The main purpose of this research is to identify and develop a methodology, based on models, methods and tools, to support the decision makers during the space exploration scenarios design and evaluation activity, which requires innovative solutions and technologies.

The thesis is aimed at merging a flexible modeling framework for complex systems design with analysis techniques such as value analysis, sensitivity analysis and multi-objective optimization techniques, by keeping the concurrency of the design process and providing information on the behavior of the system and its components to the decision maker and supporting the major trade-off.

The objectives are then:

- to analyze the space exploration scenarios by identifying and developing the methodology, based on models, methods and tools to support the decision makers during the space exploration scenarios design and evaluation activity, which requires innovative solutions and technologies
- to identify and analyze the engineering tools and techniques in support of system design. Understand systems engineering process for development of

system baselines (requirements, design details, verification plans, cost and performance estimates)

- to develop the modeling framework and the mathematical models for mission architecture, system engineering and assessment, coupling with concurrent design methodologies to assess system behavior also in terms of interactions and sensitivity
- to develop a software tool to support the space mission design process (mission architect and building block engineering) aimed at reduce time and computational effort, merging system design techniques, developed models analysis and concurrent methodologies

The fulfillment of the above mentioned objectives has been achieved following a step-by-step philosophy identifying specific activities/tasks to be developed in a progressive timeline along the project life.

The identified tasks are here below listed:

- Literature survey on design methodologies for complex engineering systems
- Overview of the existing studies on exploration scenarios
- Development and implementation of the design methodology
- Demonstration of the methodology: simple SoS example
 - Development / implementation of suitable space exploration scenarios
 - Detailed mathematical models for the identified space exploration scenario
 - Analyses of the first space exploration scenario
- Improvement of the design methodology
- Extension of the literature survey and system metallization
- Methodology applied to a new space exploration scenarios, with new mathematical models
- Development of the tool in support of the design of mission concepts and Space exploration systems
- Software integration with concurrent design methodologies
- Tool application at several space-exploration scenarios for Gap-analysis studies

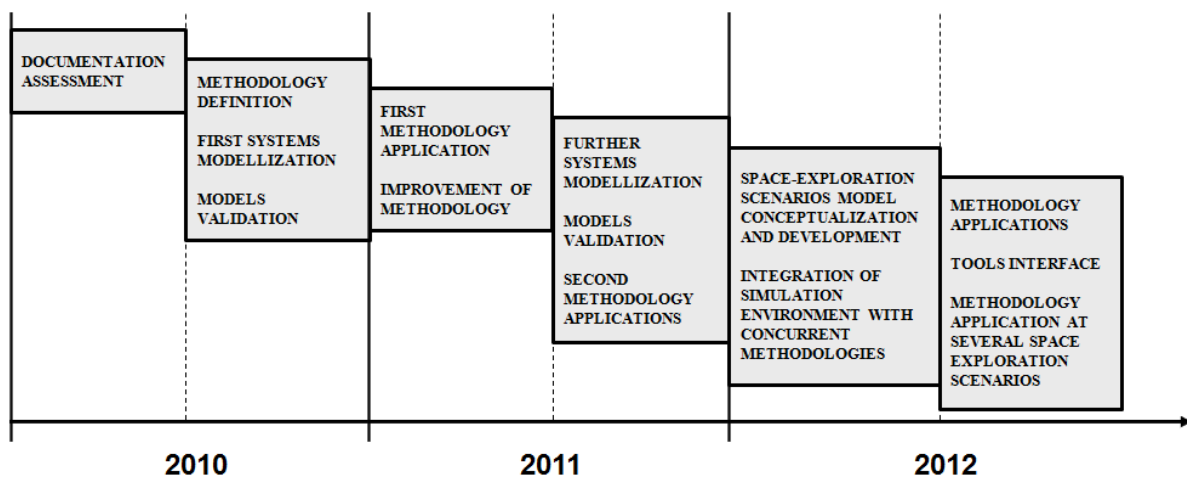


Figure 2 Work schedule

The methodology that has been implemented for the mission and spacecraft conceptual design is explained in section 3 together with the logical flow for mission concept and spacecraft design and analysis.

The modelling framework philosophy together with the description of the analytical models implemented in support of the system requirements, design, analysis, verification and validation activities is provided in section 4. First, the mission concept definition is provided and then the detailed descriptions of the analytical models of the main components possibly integrated in a space exploration system are presented. Finally, the analytical model of the launcher system based on a database of existing launcher is provided.

The value analysis is a technique aimed to identify the solutions with the highest cost-effectiveness. In section 5, the concept of value, articulated in mission-functionality and cost, is introduced to evaluate the system and mission architectures. The sensitivity and the optimization analyses have been then introduced. The sensitivity analysis allows identification of the most relevant design variables on the considered performances. The multi-objective optimization algorithm, performed only with the important factors, provided the set of optimal design-factor levels.

The “ESA Scenario Studies” is a research program aimed to the assessment of the optional European scenarios for future human spaceflight and exploration in the next 20 years. In this framework, several exploration system concept studies have been performed with the intention to identify the necessary technologies and system performances. This research activity allowed application of the developed and implemented system models and analysis techniques, thus to provide validation of the result through discussion of the results with ESA experts. The studies concern the analysis of mission objectives and main high level requirements, the identification and development of high level system trade off, the mission profile definition and finally the system concept definition as result of the analyses and trade-offs performed. The main results of the design concept activities are presented section 7.

Coupling the modeling framework and the analysis methodologies implemented, a simulation tool has been developed and presented in section 6. Scenario Evaluator Tool (SET) supports the design team in the framework of the space mission design process allowing mission architecture and building block engineering with a significantly reduction of time and computational effort. The software allows the characterization, comparison and optimization of exploration scenarios and exploration systems. The characterization of particular mission architecture is provided by information about mass budget of the space elements, cost index and exploration capabilities. The comparison and optimization are provided by information about equivalent possible solutions.

The simulation tool has been utilized in order to provide example of utilization and potentialities. The tool has been applied to hypothetical exploration scenarios of the Cis-lunar space and in three simple design sessions aimed to test and provide comparison of the results with similar studies that can be found in literature.

Finally, the main conclusion and recommendations are given in section 9. The tool developed support designers and decision makers during the preliminary design phases of a complex system (as a mission scenario) by keeping the concurrency of the design process and providing information on the behavior of the system and its components also in terms of interactions and sensitivity. Such activity is performed currying out the design of space building block evaluating them in the context of a particular mission architecture. The tool is

then useful for Gap-analysis studies allowing identification of the gaps between existing technologies and technologies needed to complete a future space exploration mission.

2.2 Research context and state of the art

The traditional approach for systems development is sequential and it is called “waterfall model”. The waterfall model is a structured system development method that, starting from the requirements and through successive design steps, reaches the full development of the system. Figure 3 shows a schematization of the waterfall model.

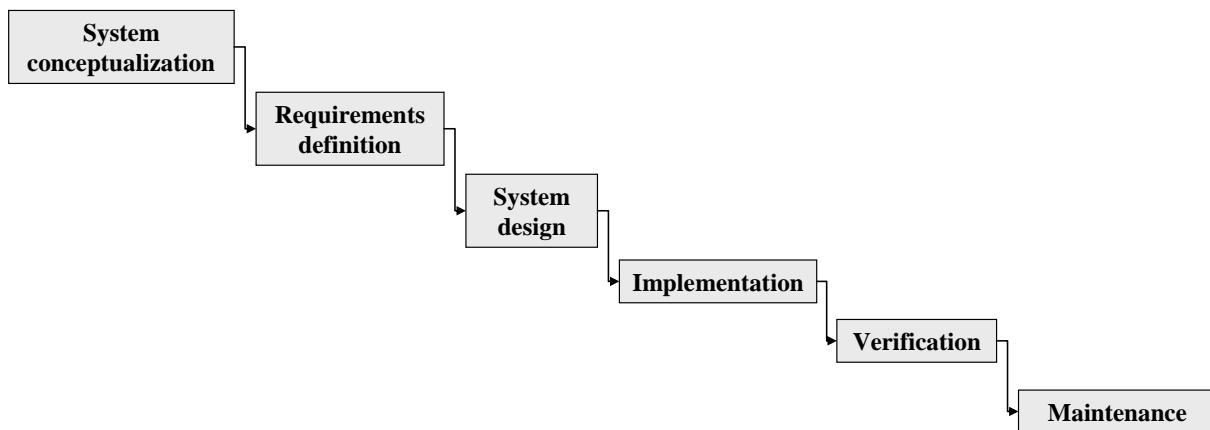


Figure 3 Waterfall model

The standard waterfall model for systems development is an approach that goes through the following steps:

- System conceptualization
- Identification and analysis of the system requirements
- Design of the system, thus
 - Braking of the system into subsystems or components thus identifying the architectural design
 - Detailed design of each subsystems or components
- Implementation of the system
 - Construction, implementation or coding of each subsystem or component and individual test
 - Integration of the system elements
- Testing and debugging of the entire system to eventually have validation of the performances
- Deploying of the system and maintenance during system operations

Thus, the classical design approach starts from the system conceptualization that refers to the establishment of the mission goals and formulation of the top-level system requirements (needs, wants, desires, capabilities, constraints and external interfaces) and concept of operations that describes how the system will be operated during the life-cycle phases to meet stakeholder expectations. Then, the process continues with the system analysis to assess the system requirements and how they are allocated to subsystems, people, or processes. The system requirements definition process foresees the overall understanding of the constraints, of how the system will be operated, of the possible use-case scenarios and the assessment of the physical and functional interfaces with which the system must interact other than the definition of the performances. Once the requirements have been defined the design activity starts. Essentially, the design activity translates the requirements set into a design

solution. In the most general case, the design activity foresees the analysis of alternative solutions that through detailed trade studies are successively selected. The preferred configuration will be then fully defined into a final design solution that will satisfy the technical requirements. The currently accepted design approach to space systems is to compartmentalize by subsystems and to decompose the subsystem design tasks into discipline tasks. The inherent problem with compartmentalization and decomposition is that they necessarily create artificial boundaries in the process and organization. These boundaries create the tendency towards sandboxing or territorial syndromes. Both create communication problems in properly exchanging interacting parameters and data. In this method the system design is accomplished by assembling these separately designed subsystems, etc., iterating, or balancing between conflicting outputs.

The final design solution allows the generation of the end product specifications, necessary to produce the final product and to conduct the verification activities. During the production activity, the elementary system/subsystem components are produced, acquired, or coded and then integrated into higher level assemblies. These assemblies are then verified and again integrated with other assemblies up to the system level. Once the entire system is created, testing and debugging activities start. The scope of these activities is to be ensured that the final product works correctly and efficiently. The final step foresees the operation of the system and the maintenance activities.

The waterfall model is widely used although it is rigid and inflexible. The main criticisms of the waterfall model include:

- the requirements shall be fixed before the system is designed because otherwise the development method would be unstable
- the design team does not look backwards or forewords and thus it is unable to discover and fix problems until system testing
- the system performance cannot be tested until the system is almost/fully implemented
- in the case that something does go wrong, the design usually must be scrapped or heavily altered

Since the waterfall model can be very expensive and it is associated to the failure of a large number of programs, ref. [5], alternative approaches have been developed.

Concurrent engineering is an alternative to the traditional waterfall method. The definition that ESA have adopted for the concurrent engineering is, ref. [6]:

"Concurrent Engineering (CE) is a systematic approach to integrated product development that emphasizes the response to customer expectations. It embodies team values of co-operation, trust and sharing in such a manner that decision-making is by consensus, involving all perspectives in parallel, from the beginning of the product life-cycle."

Behind the concurrent engineering there are methodologies, techniques and instruments that allow an integrated approach to the product design and to the associated production process. The concurrent engineering approach allows reduction of the development time and costs and allows both higher flexibility of the development activity and quality of the final product.

The difference between the waterfall model and the concurrent engineering is that while the first method moves linearly as described before, the concurrent engineering is iterative so that all the issues concerning the lifecycle of the system are taken into account since the first development phases. This allows a more evolutionary approach to design. The basic concept is that, especially in complex systems, each component has an impact on other

components and that any design change will be propagated through the system. Thus, the early assessment of the impact of changes is essential to ensure that the design process converges on an optimized solution. Figure 4 shows a schematization of the concurrent engineering approach.

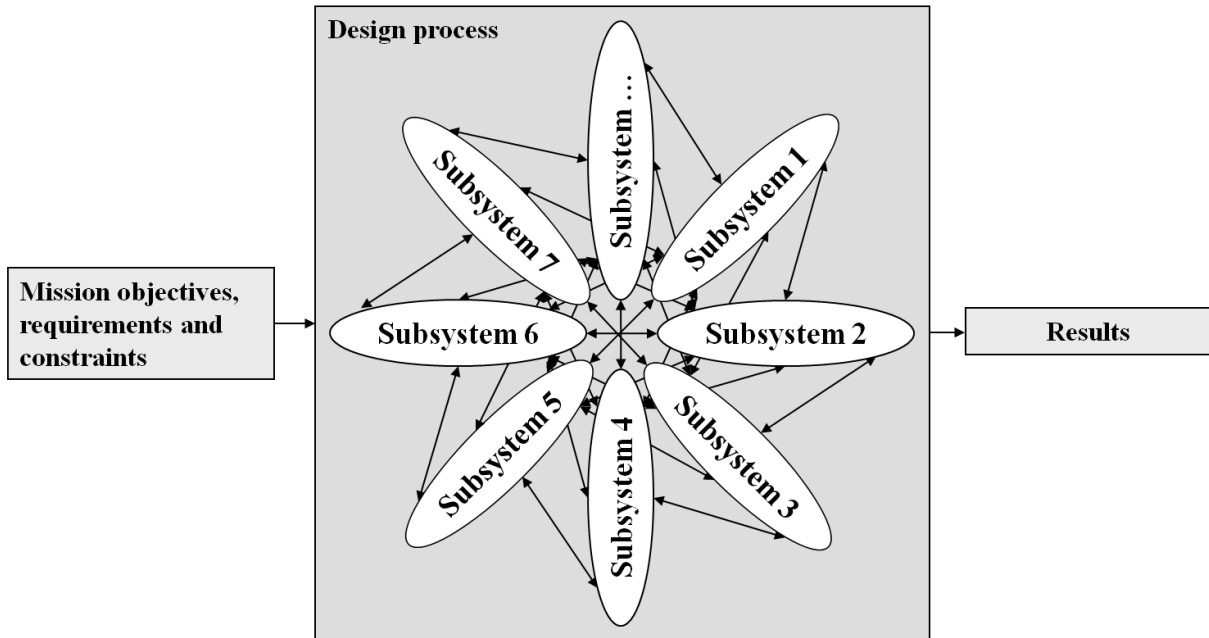


Figure 4 Concurrent engineering

The process starts with the analysis of the mission objectives so that the mission requirements and constraints can be formalized. The set of requirements such as the constraints (coming from budgets, physical issues, technological issues, political issues and heritage) are then used as inputs for the design process. A complex system is formed of several interconnected components that can be grouped into subsystems. The complexity derives from the many interactions between the components that generate a behavior of the final product that cannot be derived from the properties of the individual parts that form it in an obvious way. This is because any change of a component has an effect on the overall system. Thus, in order to ensure that the system design reaches the optimized configuration, it is necessary to assess the impact of a design change as soon as possible. For its nature the design process in concurrent engineering is iterative and evolutionary. For these reasons, tools are necessary to evaluate and in case relax dependencies. The overall lifecycle of the product is taken into account since the first development phases so that at the end of the development a huge amount of development time and money can be saved. If the concurrent engineering process is well structured and supported, any change in the set of requirements (that, for example could derive from new needs) does not generate instability in the design process that leads to an increasing of the development time and costs such as for the traditional design approach.

The main critical issue concerning the concurrent engineering is that being the cooperation of a multi-disciplinary team a key factor, communication is fundamental. Thus, the final result depends on an efficient communication between engineers and teams and software (compatibility). All these three kinds of communication can be very difficult in practice leading to a process that may not work effectively.

With the objective to create a practical application of the concurrent engineering process to find a way to perform mission and system design in a more efficient way, ESA has

created the Concurrent Design Facility (CDF). CDF is based on five key elements: a process, a multidisciplinary team, an integrated design model, a facility, and an infrastructure. The process is derived from the concurrent engineering approach, thus communication is the core element. For this reason, periodical meetings and working sessions are foreseen to pursue collaboration, efficient communication and the iteratively nature of the process. The team that works in each session is composed of specialists equipped with the necessary tools for design modeling, calculations and data exchange. It is fundamental that the multidisciplinary team is highly motivated to adopt a new method of working, to co-operate, to perform design work and provide answers in real-time and to contribute to the team spirit. Since, in concurrent engineering, the assessment of how design changes impact on the entire system is fundamental, the process is model-driven. The utilized models are parametric and expandable. The parametric models can be utilized for various mission/technological scenarios in real time and further levels of detail can be introduced to refine the design of a system. The utilization of mathematical models allows to quickly exchange the design parameters throughout the other disciplines so that any impact can immediately be identified and collectively assessed. The CDF activities are performed in a room that supports and promotes interaction, cooperation and involvement of the specialists. Finally, the software infrastructure includes tool for generation and integration of the models, documentation production and storage.

Concurrent engineering process is not a new and exclusive approach in industry. In fact, many industrial sectors were used to adopt it, even before it was introduced in aerospace industry. In the word, other examples of concurrent engineering approach application in the space field are performed by other agencies and research institutes such as NASA/JPL (with the Project Design Center-PDC), ASI, CNES, JAXA and DLR, by industries such as Thales Alenia Space (TAS), EADS Astrium, J-CDS and by universities such as TU Munich, MIT, Stanford, Cranfield, and La Sapienza.

The concurrent design facilities are not the only application for mission and system design. SpaceNet (ref. [7]) is a NASA-funded and integrated modelling and simulation software environment for analysis of space exploration missions and campaigns from a logistics point of view. It was developed for NASA by the Massachusetts Institute of Technology, Jet Propulsion Laboratory and California Institute of Technology with support from Payload Systems Inc. and United Space Alliance LLC.

SpaceNet assists the work of the decision makers to assess what is needed to support (manned) space exploration missions in the Earth, Moon and Mars system. The software does not allow the design of space elements but, considering their features, assess a particular mission architecture and/or supply chain strategy. The software simulates the mission taking into account its feasibility (mainly ΔV and associated fuel consumptions, utilization of consumables and supply) and provides an evaluation on the base of logistics measures of effectiveness. Since the software does not only aim at the analysis of a mission concept but in a more general way at the analysis of a mission scenario, it allows the detailed simulation and analysis of multi-year campaigns.

The basic constituents of SpaceNet are the elements, the supplies/demands and the network. The space elements are physical objects that move through the space and can hold or transport supplies (crew, cargo, and propellant) and may or may not have propulsive capability. Supplies/demands are any items that move through the network and include consumables, science equipment, surface vehicles, and spares. Finally, the network consists of nodes, that represent the spatial location in the solar system, and arcs. The nodes include surface nodes, orbital nodes, and Lagrangian nodes. The arcs are trajectories between these locations.

SpaceNet allows the opportunity to optimize a specific mission scenario from the logistic point of view. The software finds the optimal logistics architecture to supply a specific mission (or series of missions).

3 Methodology

Figure 5 illustrates the methodology that has been considered for the mission and spacecraft conceptual design. First, the mission statement defines why a mission shall be performed, which the mission needs are and what kind of qualitative goals shall be reached. After application of the methodology for the mission and spacecraft conceptual design, the information obtained is utilized as inputs for the more detailed design phases. The ECSS standards (European Cooperation for Space Standardization) divide the life cycle of space projects into 7 phases as follows, ref. [8]:

- Phase 0: Mission analysis/needs identification
- Phase A: Feasibility
- Phase B: Preliminary Definition
- Phase C: Detailed Definition
- Phase D: Qualification and Production
- Phase E: Utilization
- Phase F: Disposal

The phases 0, A and B are mainly aimed to the analysis of the mission statement with the intention of identify the system functional and technical requirements and the deriving system concept(s) compliant with the technical and programmatic constraints. The initial phases of the project provide the identification of all the necessary activities and resources necessary to develop the system and allow the initial assessment of technical and programmatic risk. After the activities of phase C and D, the system is completely developed and qualified. Phase E is about the operations of the system. It includes all the activities concerning the launch, commissioning, utilization and maintaining of the system. At the end of the phase E, all the activities concerning the safely disposal of the system start. The identified methodology is applicable to the initial phases of the project (0, A) so that the information obtained are utilized to the detailed design of the space elements.

The methodology for mission and spacecraft conceptual design can be divided into two main steps. The first one allows the definition of the mission concept baseline including the identification of the spacecraft and the mission operation concepts. The second step allows the preliminary definition of each spacecraft which is part of the mission scenario. The spacecraft definition includes information about the preliminary design of the spacecraft, the list of the necessary technologies and the spacecraft operation concept.

Once the mission objectives have been identifies, the requirements definition activity starts. The requirements engineering process includes the interpretation and analysis of the customer needs and the identification of the constraints deriving from budgets, political, physical and technical issues. The requirements definition process shall take into account of the heritage, i.e. the know-how of the design team deriving from previously performed activities. The outcome of the requirements definition activity is the set of requirements that the system shall meet. The set of requirements, in the most general case, includes the functional requirements (what the system shall perform to satisfy the objective), the missions requirements (what the system shall do to perform the functional requirement), the interfaces requirements (which interfaces the system shall have towards external World and between internal modules), the environmental requirements (the conditions under which the system shall perform the work), the physical requirements (the boundary conditions for which the system shall ensure physical compatibility), the operational requirements (how the operability of the system shall be), the human factor requirements (which human capabilities the system shall comply with), the logistic support requirements (the logistic constraints the system shall comply with), the product assurance requirements (the product assurance constraints the

system shall comply with), the configuration requirements (the configuration constraints the system shall comply with), the design requirements (the design constraints the system shall comply with), the verification requirements (the verification constraints the system shall comply).

Once the set of requirements has been established, the functional analysis shall be performed. The functional analysis is an iterative activity that allows the definitions of the high and low level functions to be performed to meet the requirements. The functional analysis supports the identification and definition of the performance and functional requirements and supports the selection of the products and processes that satisfy the performance and functional requirements, taking into account the project constraints. One of the outputs of the functional analysis is the functional architecture which *describes the functional arrangements and sequencing of sub-functions resulting from the breaking down of the set of system functions to their sub-functions, and is documented in the function tree*, ref. [8]. At the end of the functional analysis, the configurations that lead with the functional architecture is identifiable.

The requirements set and the functional architecture allows the generations of several possible mission concepts. Each option shall be then analysed, evaluated and in case discarded until one (or few) option is chosen. The concepts assessment shall take into account mass and cost budgets, potential performances and robustness. A solution is considered robust, if it is stable to perturbations such as a small variation of the requirements.

Once the mission concept baseline is defined, the spacecraft definition activity starts. The activity is performed iteratively and for each spacecraft included in the mission scenario. The design methodology for the spacecraft is very similar to that for the mission concept. The information concerning the mission concept is utilized to assess the mission objectives of each spacecraft. With this information is possible to define the set of requirements. Also in this case, the design activity takes into account of the heritage and of the constraints deriving from budget and physical, political, technological issues. Once the set of requirements is established, the functional analysis allows the definition of the functional architecture. The spacecraft definition document includes information about the spacecraft conceptual design, the main technologies to be considered and the operation concept. The spacecraft definition is the results of several trade-off activities aimed to identify the most effective solution which is compliant with the set of requirements and constraints. Once all the alternatives to solve a problem are identified, to select the most effective, a trade-off methodology shall be chosen. In general, the trade-off analysis can be performed in a qualitative (on the base of heritage, engineering judgment, observations, etc.) and/or quantitative (i.e. on the base of numerical analyses performed through the use of models) way. In both cases, it is necessary to setup a choosing criteria including weighting factors where appropriate. Finally, the analysis of the results allows to choose the most appropriate configuration.

All the described activities are iterative. This means that the design activity is performed more times until convergence of the results. The first results will be obtained on the base of preliminary assumptions and very high level analytical models. The higher will be the number of iterations, the higher will be the accuracy of the obtained results (obtained also through implementation of detailed mathematical models). Thus, the information out-coming from the mission and spacecraft conceptual design will be considered acceptable when it will be considered sufficiently detailed and robust.

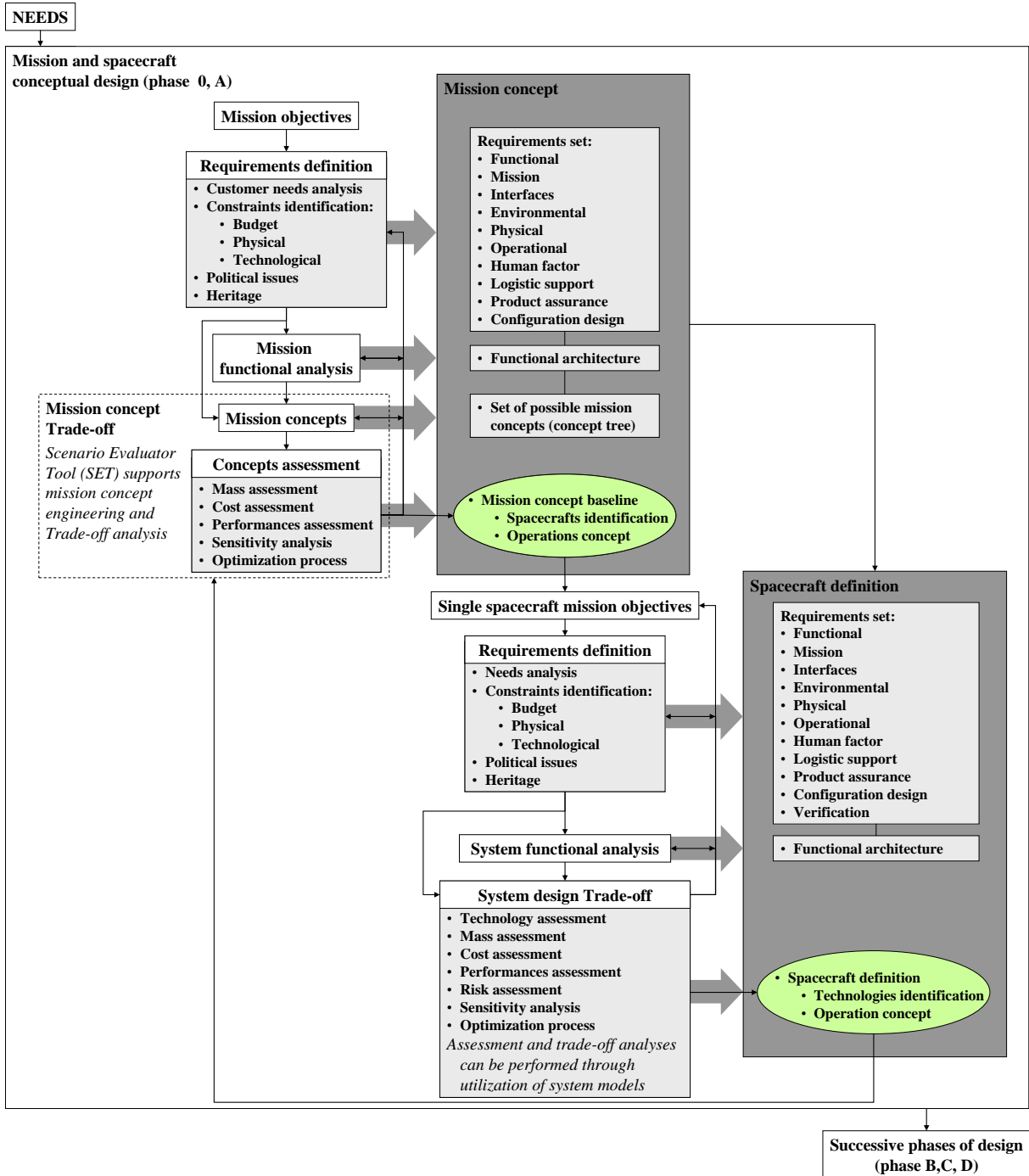


Figure 5 Mission and spacecraft conceptual design methodology flow-chart

One of the results of the research activity presented in this document is a simulation tool in support of the decision makers during the trade-off analyses for the mission concept and spacecraft design. The tool is called SET (Scenario Evaluator Tool) and allows the possibility to evaluate a particular mission scenario in terms of mass, cost and exploration capabilities. It includes the model of several space elements allowing the possibility to evaluate their main features in the framework of a particular mission concept. The detailed description of the tool is provided in the section 6.

Figure 6 shows the logical flow for mission concept and spacecraft design and analysis. This is also the high-level logic that has been then partially translated in the SET software tool. Figure 6 shows what are the logical steps to be performed in order to analyse a mission scenario and allows to understand how SET is integrated in the previously presented design methodology. The logical flow shall be intended as an alternative way (with higher detail level) to read the design methodology presented in Figure 5.

The logical flow consists of two main parts. The first one describes the logical flow for the developing and implementation of the spacecraft and mission concept model. The second one describes the logical flow for the analysis of the mission concept and spacecraft performances. The first activity to be performed is the identification of the space elements that will be present in the mission scenario. At this point, it is necessary to choose the level of detail of the models of each space element. For the first preliminary analyses, high level models will be sufficient but the confidence level of the results will be very low. To increase the confidence level of the results, it will be necessary the utilization of more detailed models obtained through a conceptual design activity of the spacecraft.

Once the models of all the spacecraft are available, the mission concept shall be defined. Thus, the starting and target location of the spacecraft and the nodes shall be identified. The starting and target positions can be orbit or points on the surface of planets. The nodes are that points in the space where docking or undocking manoeuvres are performed. Since the spacecraft moves through these locations, transfer strategies shall be chosen. The transfer strategies will imply an associated ΔV budget. Once, all the transfer strategies have been conceived, the associated ΔV shall be considered. The ΔV will be obtained through manoeuvres performed by the spacecraft. It is necessary to identify the active and passive space elements of each mission phase. The active space elements are intended as those spacecraft that perform the manoeuvres in a particular mission phase. The passive space elements are intended as those spacecraft that act as payload in a particular mission phase.

Once all the mission concepts to be analysed have been conceived and implemented, the analyses of the mission can be performed. Two different kinds of analyses can be performed. The first one consists in the simple evaluation of the mission concepts performances. The second one consists in the possibility to perform sensitivity analyses, to assess the relative influence of the design parameters on the considered performances, and/or optimization analyses to find the set of equivalent optimal solutions (i.e. the solutions for which is not possible to increase a performance level without decrease another performance level).

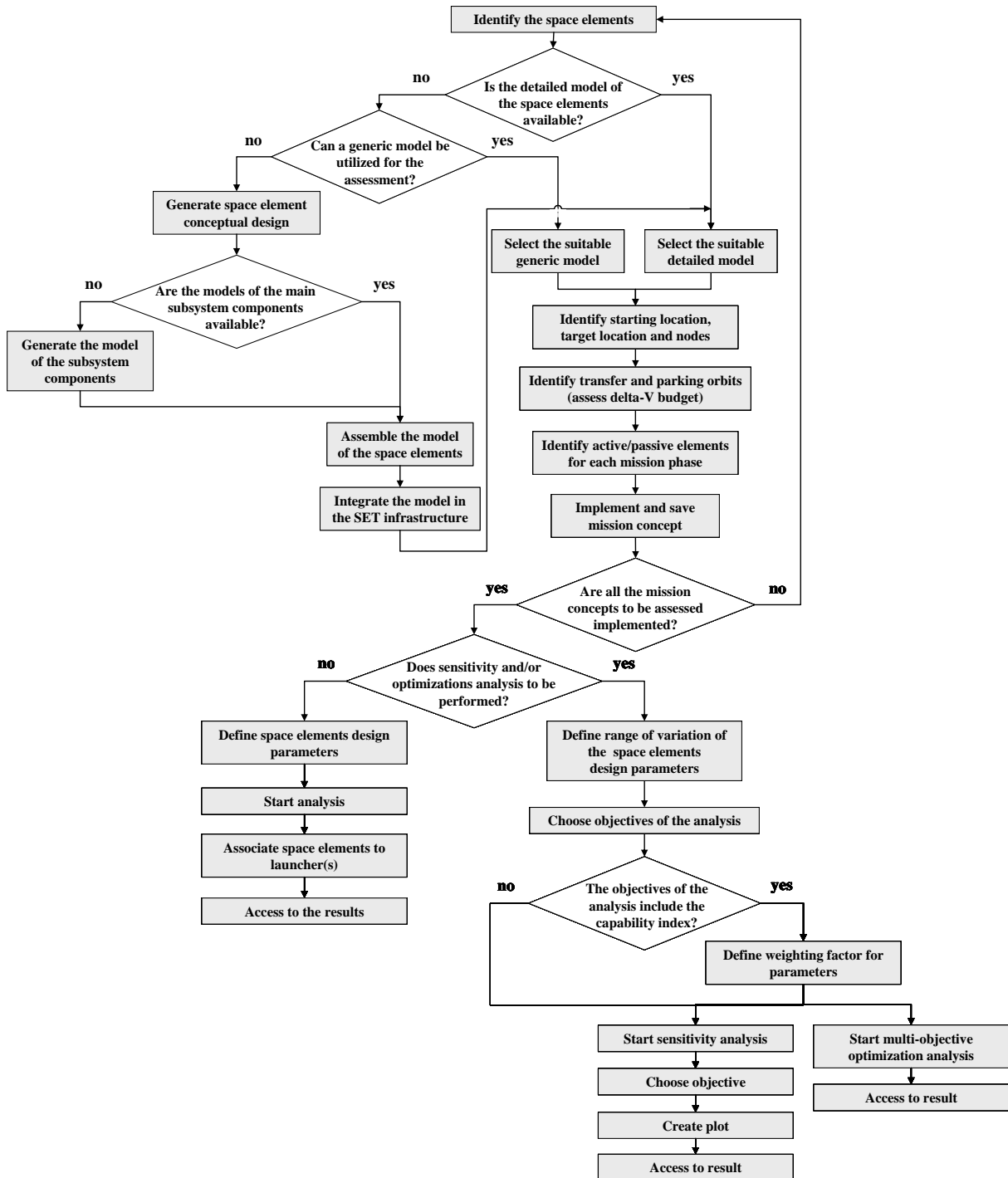


Figure 6 Logical flow for mission concept and spacecraft design and analysis

4 Models definition

4.1 Model Philosophy

The currently accepted design approach to space System-of-Systems is to create a fragmentation by subsystems and to decompose the subsystem design tasks into discipline tasks. Doing so, artificial boundaries are introduced in the process and in the organization thus creating communication problems in properly exchanging data. The system design is accomplished by assembling these separately designed subsystems, iterating or balancing between conflicting outputs. In this process, the scope of systems engineering is to make sure that the development process happens in a way that leads to the most cost-effective final system. The basic idea is that before those decisions that are hard to undo are made, the alternatives should be carefully assessed. This can be achieved only if there is an efficient communication between the various disciplines that concur to the system definition. Tools can help designers towards this purpose.

With the objective of supporting the design team and the decision-makers during the design of complex systems, a modeling framework for SoS design has been developed.

The SoS, as we intend it, is formed of several interacting elements and sub-elements whose overall behavior is usually different than the sum of the effects of the single elements. The mathematical models, which are linked together in the modeling framework, provide the design team with qualitative and quantitative information, both at SoS and system level, enabling an efficient understanding of the differences and common aspects of dissimilar architectures, the effect of the design parameters on the design and the emergent behaviors coming from the interactions between different SoS elements.

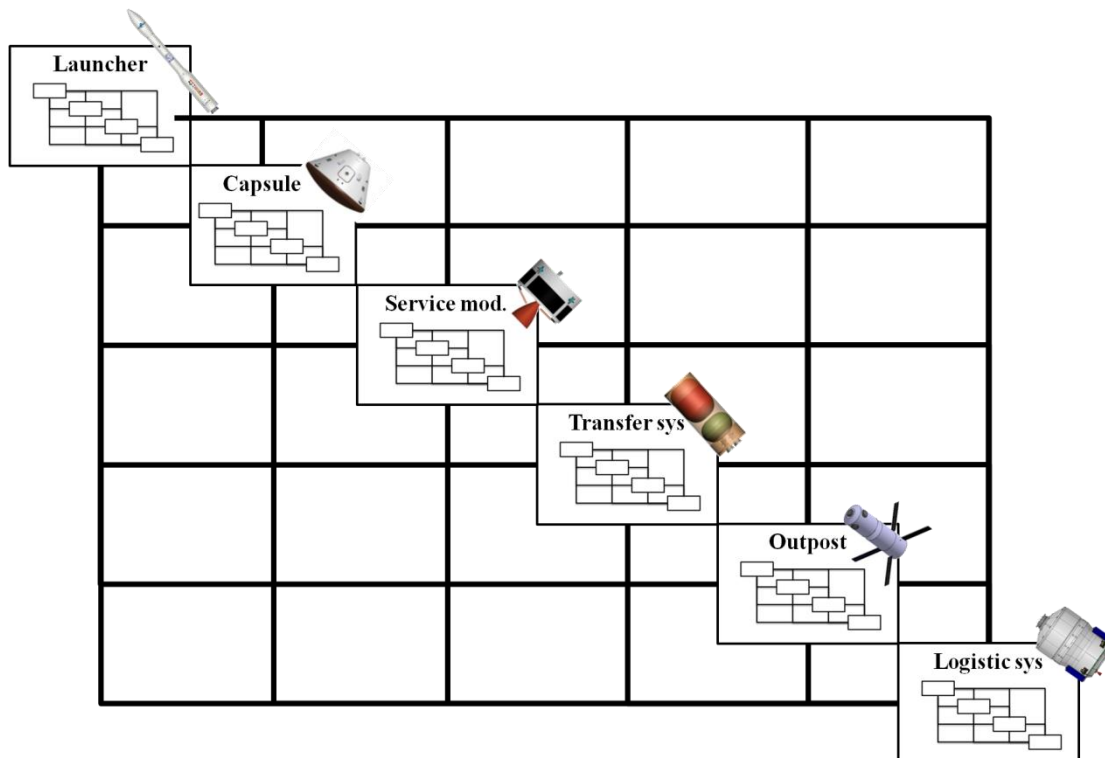


Figure 7 Modellization approach for system and subsystem design

A schematization of all the relationships and interactions amongst the elements of a generic SoS for space exploration is shown in Figure 7. The blocks represent the

mathematical models of the space elements, while feed-forward and feed-back lines indicate a flow of data among the elements that are coupled together. The presence of feed-backs in the modeling framework forces the process to iterate before reaching convergence. The same modeling philosophy has been maintained both at high and low SoS level, thus within every block of Figure 7. Figure 8 shows an example of systems engineering representation of a generic space element. The model of the spacecraft is obtained by merging the “elementary” models of the subsystems which are part of it. The models of the spacecraft subsystems are represented by the blocks and the exchange of information at system level is represented by the lines. The model of the system is provided with an input and output interface in order to exchange information at higher SoS level. Thus, the spacecraft model receives in input requirements and design parameters, elaborates them and provides in output to the other SoS elements information about performances and features of itself. The same SoS decomposition can be repeated at lower level for each spacecraft subsystem.

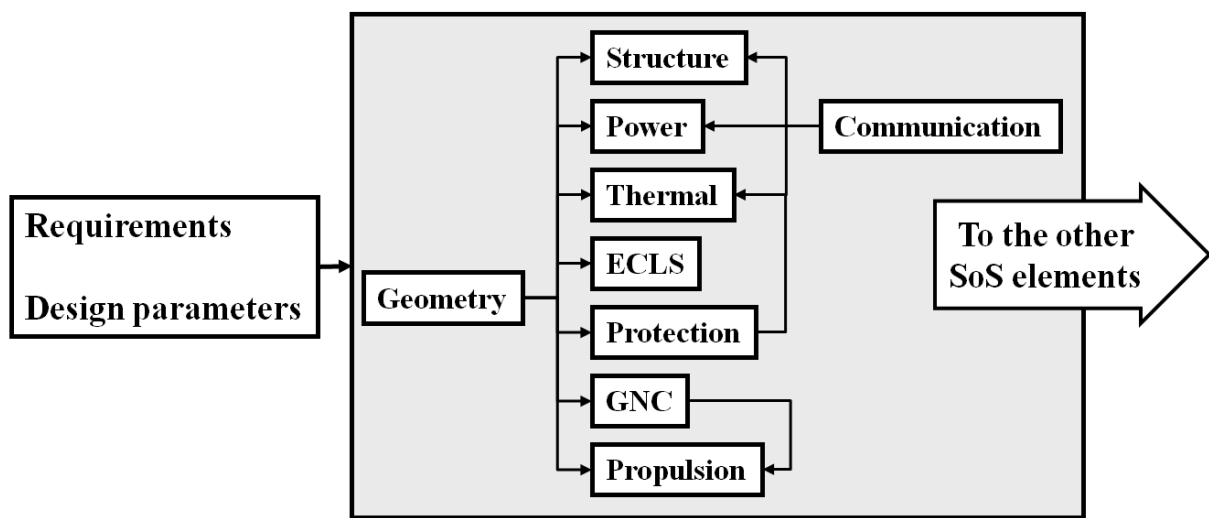


Figure 8 Systems engineering representation of a system analytical model

The combination of the models is possible only if information can be exchanged at different levels of the SoS, thus internally at spacecraft system/subsystem level and externally at SoS level. In the modeling framework the exchange of information is possible thanks to a “data-bus” on which information can be exchanged opportunely. The interface of each model is organized so that the indexed parameters can be read or written without allocation errors. This has been possible because each parameter has been provided with a structured nomenclature that allows identification of the associated space element and design feature.

The non-hierarchical decomposition of the mathematical models, provided by the modeling framework, implies a sort of modularity that allows for a certain degree of flexibility and expandability. The blocks can easily be substituted with more or less accurate models providing only the necessary interfaces with the other blocks of the system. This allows the user to increase or decrease the accuracy of the modellization at his discretion and on the base of the necessary information to be obtained by the study. The model of new systems can be easily obtained through reassembling of the “elementary” models and, in case, introduction of the missing with a general reduction of the modellization effort. Figure 9 graphically explains the modularity concept. The suitable interfaces of the models allow integration of the analytical models at any SoS level. Thus, the model of each spacecraft subsystem is obtained by assembling the model of each component that is part of it, the model of the spacecraft is obtained by assembling the model of each subsystem and the model of the SoS at its higher level is obtained by coupling together the model of each spacecraft.



Figure 9 Modularity of the modellization

In order to evaluate different configurations of a SoS for space exploration, the traditional approach for the design activity of a spacecraft cannot be applied and it is necessary to move up to an higher design level. In fact, in a traditional design approach, the space exploration scenario is well defined as well as the requirements of each system part of it. The spacecraft design activity is limited to the allocation of the functions to its subsystems and to the sizing of them. But when the space exploration scenario shall be conceived and only the main goals and constraints are known, the number, typology and performance of the space elements that will part of it are not known and different solutions are possible. The functions to be implemented shall be defined as well as the functional allocation to the different exploration systems of the mission scenario. The concept of each spacecraft is so obtained by the identification and grouping of the functions to be performed. It is evident that several architectural solutions are possible and that each of them shall be evaluated to identify the best one. The detailed design of each spacecraft will be then performed, during a second design loop, doing reference to the traditional design approach.

Figure 10 shows the design approach for space exploration SoS. The mission needs allow identification of the mission requirements thus providing information about the input and the output to be obtained by the SoS. Although these information are available, the SoS shall be designed defining the space elements and the relationships between them. This process is performed identifying and grouping together the functions that each space element will perform. Thus, the detailed design of each spacecraft can be then carried out doing reference to the traditional design approach for complex systems. The functions to be performed by the space element are known and the design can be performed allocating the functions to the several subsystems thus allowing trade-offs and sizing.

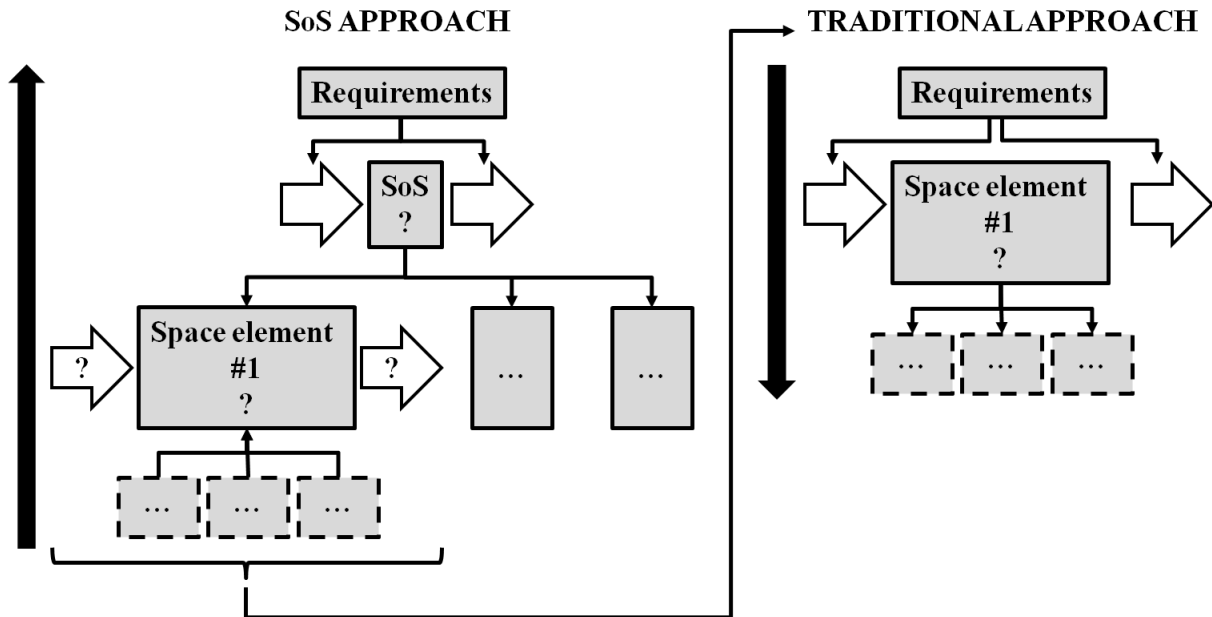


Figure 10 Space exploration SoS design approach

Although, a large number of design solutions are possible, literature research shows that generally, the typology of systems for space exploration can be summarized in a limited number of space elements although, not always, a clear distinction exists:

- The launcher is a system able to transport a payload from the surface of a planet to an orbit, giving to the payload the necessary velocity to stay into orbit for the necessary time.
- The capsule is a system able to house a crew and eventually provide entry, descent and landing on the surface of a planet with atmosphere.
- The capsule service module is an unpressurized system containing a variety of support systems used for spacecraft operations. Generally, but not always, it provides propulsion, power and other supporting capabilities such as thermal dissipation and consumable storing.
- The transfer stage is a system able to transport a payload from one orbit to another.
- The lander is a system able to descent and land a payload on the surface of a planet. If the planet has an atmosphere, the landing occurs after an initial re-entry phase.
- The ascent vehicle is a system able to get orbit from the surface of a planet. Generally, it is docked to a lander that, after completion of the mission, remains on the surface of the planet and performs launch pad functionalities.
- The space station is a system placed in an orbit around a celestial body generally able to support the presence of a crew for e determinate period of time and on-orbit operations.
- The rover is a system able to move a payload on the surface of a planet.
- The Satellite is an unmanned on-orbit system that can have several purposes such as telecommunication, observation and so on.

4.2 Mission concept

The mission statement defines what the mission needs to achieve, what the qualitative goals are, and why one shall perform the mission itself. The mission architecture includes all the physical and functional elements of a mission and defines how the mission will work in

practice and all elements that will take part in it. It includes such issues as the synergies of manned and robotic resources, mission control, and the mission timeline. Considering all the possible combinations of people, orbits, launch systems, space vehicles, surface facilities and supporting infrastructures we end up with a large number of possible mission architectures also if obviously, not all of them are optimal, or even feasible. The mission concept is the part of the architectural plan that defines how people and systems will work to meet the mission objectives and to satisfy the needs. The main constituents of the mission concept are the exploration elements (or space elements), the orbits utilized and the mission operations. The exploration elements include space access elements, space elements and surface elements. The space access elements include the launch facilities, launch systems and propulsion systems that place a payload in orbit. The space elements include the orbiting space vehicles (e.g. space station), the transportation vehicles (e.g. transfer stage) and vehicle for re-entry, descent, landing and ascent. The surface elements include the habitats, structures and vehicles on the surface of a planet. The orbit is the trajectory of a spacecraft. The set of orbits considered in the mission concept implies the mission duration and the reference space environment. The mission operation concerns the operations to be performed on orbit and on the ground, the operation functions, the space logistics, the command, control and communication.

Figure 11 shows an example of mission concept for an hypothetical logistic mission to a space station orbiting around the Moon. The logistic vehicle is launched in a high elliptic orbit (HEO) by the Ariane 5. After separation from the launcher, the logistic vehicle performs on board systems initialization, deploying of the solar arrays and the necessary orbit stabilization maneuvers. Then, the transfer phase starts and the logistic vehicle moves towards the Moon by Resonance Transfer. Resonance transfer implies from 3 months to 1 year to reach the Moon in outer space. In proximity of the space station, the logistic vehicle performs final approach and docking maneuvers automatically. During the docking phase, the logistic vehicle has the automatic or manual (from ground) capability to trigger a collision avoidance maneuver should in case of problem. After attachment accomplishment, the logistic vehicle gets dormant operational mode until crew arriving if it is not yet on the space station. The space station supplies the logistic vehicle with power. Before crew arriving, the logistic vehicle performs systems initialization thus to be ready for the unloading and loading operations. After the logistic vehicle is loaded with waste, it undocks and performs the disposal maneuvers that put logistic vehicle in an orbit without long-term effects.

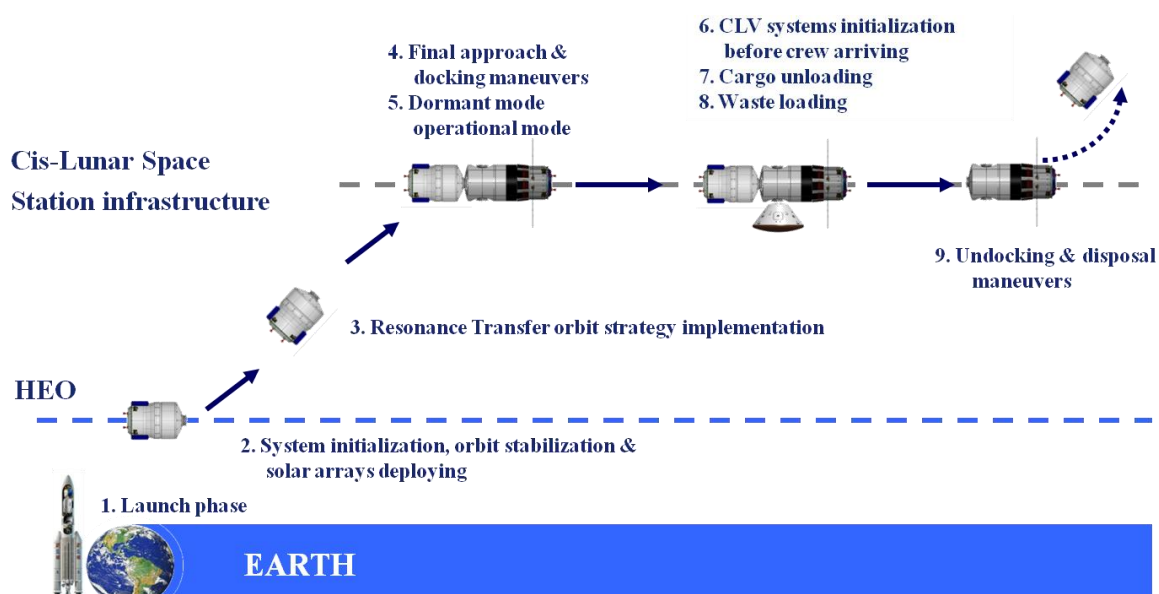


Figure 11 Example of mission concept for logistic mission

4.3 Habitable Volume

The habitable volume per crew member depends on the mission duration and on the crew comfort level for which a system must be operated during the mission. In general, the total habitable volume that must be ensured to the crewmembers increases as the mission get longer. The total habitable volume can be estimated according to the NASA-STD-3000 (ref. [9]), see Figure 12. It shows how the mission duration and the comfort level (tolerable limit, performance limit and optimal) affect the total habitable volume per crewmembers.

Once the mission duration, the comfort level, and the number of crew members are determined, the amount of net habitable volume for the crew is computed considering equation [1]:

$$V_{habitable} = V_{habitable/crew} \cdot n_{crew} \quad [1]$$

The total pressurized volume ($V_{pressurized}$) will be so computed summing the net habitable volume ($V_{habitable}$) and the volume needed for the pressurized equipment ($V_{pressurized_equipment}$). The volume for pressurized equipment can be estimated on the basis of existing hardware datasheets or according to literature data (ISS, Space Shuttle or Spacelab available data) by performing similar assumptions or considering a mean density (for example the mean density for payload can be assumed equal to 245 kg/m^3 according to ATV performances, ref. [10]).

$$V_{pressurized} = V_{habitable} + V_{pressurized\ equipment} \quad [2]$$

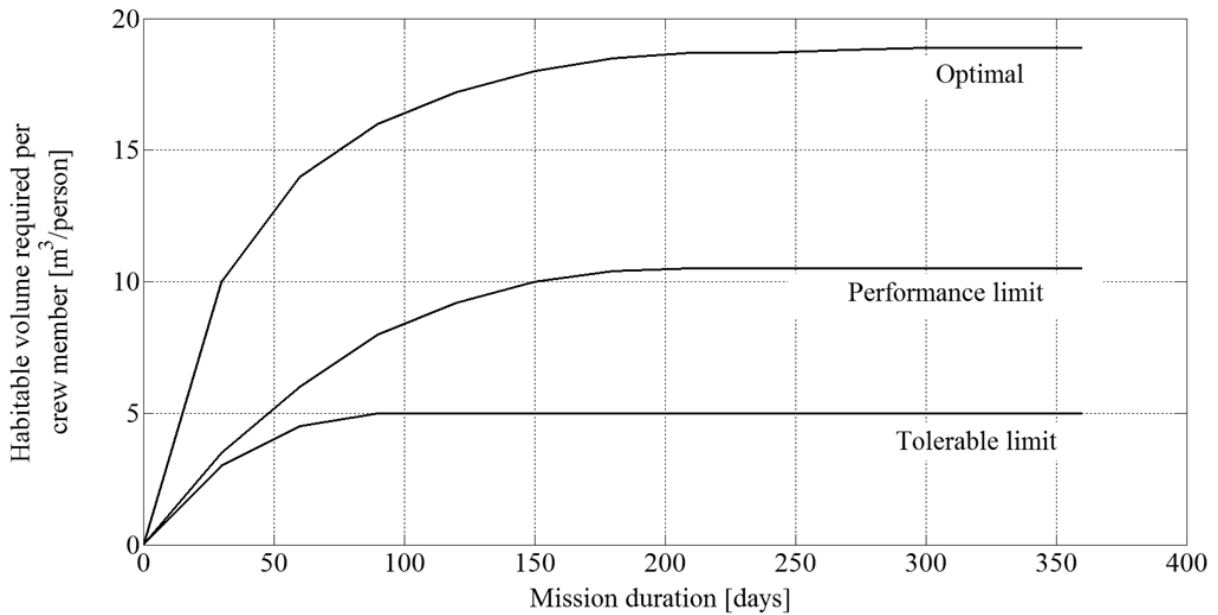


Figure 12 Habitable volume vs. Mission duration

4.4 Geometry

The external layout of the space exploration systems can be schematized into few simple three-dimensional geometric figures. Generally, the shape can be assimilated to cylinder, hollow cylinder, cone, truncated cone, sphere and so on.

For example, the external shape of a capsule is very important for the determination of the aero-thermal loads during the re-entry phases and for the optimization of the internal-external volume ratio. The shape is chosen in front of the desired lift-to-drag (L/D) ratio. Generally, capsules with low L/D have cone or truncated cone shape, capsules with mid L/D have more complex shape and generally similar to a combination of cylinders, cones and spheres. Finally, re-entry vehicles with high L/D are lifting body thus vehicle with complex shape generally consisting of a fuselage with wings (e.g. the Space Shuttle is an example of lifting body.).

Figure 13 shows the shape of a truncated cone and defines the design parameters useful to the development of the geometry model. The considered truncated cone is cave so that internally free volume is available. The variables D_e and d_e are the lower base diameter and the upper base diameter of the truncated cone respectively. The variables D_i and d_i are the lower base diameter and the upper base diameter of the internal free volume respectively. The variable α is the sidewall angle, h_e and h_i are the height of the truncated cone and the height of the internal free volume respectively.

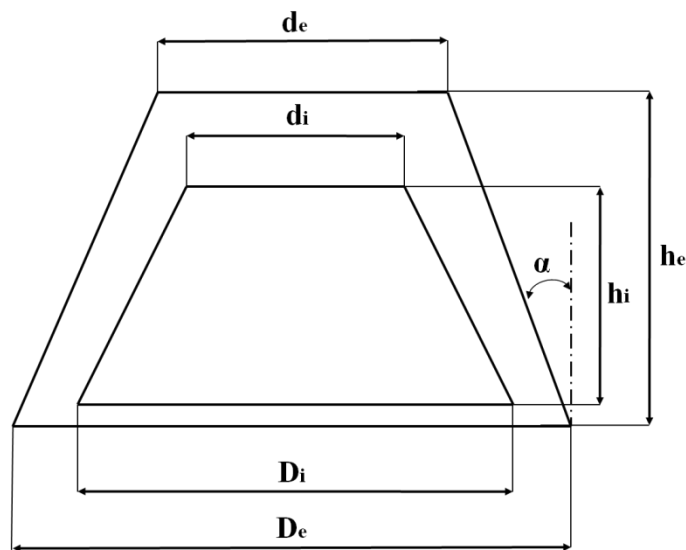


Figure 13 Truncated cone geometry parameters

Classical geometry equations have been utilized to evaluate external and internal surfaces of the truncated cone. The model assumes as input the ratios h_i/R_i and h_e/R_e where R_i is the radius of the lower base of the internal free volume of the truncated cone and R_e is the radius of the lower base of the truncated cone.

The ratio between the radius of the lower base (r_i) and upper base (R_i) of the internal free volume of the truncated cone and can be evaluated as:

$$\frac{r_i}{R_i} = 1 - \frac{h_i}{R_i} \cdot \tan(\alpha) \quad [3]$$

So R_i , r_i and h_i can be calculated as:

$$R_i = \frac{D_i}{2} = \left(\frac{3 \cdot V_{\text{pressurized}}}{\pi \cdot \frac{h_i}{R_i} \cdot \left(1 + \frac{r_i}{R_i} + \left(\frac{r_i}{R_i} \right)^2 \right)} \right)^{\frac{1}{3}} \quad [4]$$

$$r_i = \frac{d_i}{2} = R_i \cdot \frac{r_i}{R_i} \quad [5]$$

$$h_i = R_i \cdot \frac{h_i}{R_i} \quad [6]$$

In the same way, the dimensions of the external geometry of the truncated cone can be evaluated as:

$$D_e = 2 \cdot R_e = 2 \cdot (R_i + w_t) \quad [7]$$

$$d_e = 2 \cdot r_e = 2 \cdot R_e \cdot \left(1 - \frac{h_e}{R_e} \cdot \tan(\alpha) \right) \quad [8]$$

$$h_e = R_e \cdot \frac{h_e}{R_e} \quad [9]$$

Where R_e is radius of the lower base of the truncated cone, w_t is the distance between the internal and external surface of the truncated cone, r_e is the radius of the upper base of the truncated cone.

Finally, the internal and external surfaces of the truncated cone can be evaluated as:

$$S_{i \text{ lateral}} = \pi \cdot (r_i + R_i) \cdot \sqrt{h_i^2 + (R_i - r_i)^2} \quad [10]$$

$$S_{i \text{ lower}} = R_i^2 \cdot \pi \quad [11]$$

$$S_{i \text{ upper}} = r_i^2 \cdot \pi \quad [12]$$

$$S_i = S_{i \text{ lateral}} + S_{i \text{ lower}} + S_{i \text{ upper}} \quad [13]$$

$$S_{e \text{ lateral}} = \pi \cdot (r_e + R_e) \cdot \sqrt{h_e^2 + (R_e - r_e)^2} \quad [14]$$

$$S_{e\text{ lower}} = R_e^2 \cdot \pi \quad [15]$$

$$S_{e\text{ upper}} = r_e^2 \cdot \pi \quad [16]$$

$$S_e = S_{e\text{ lateral}} + S_{e\text{ lower}} + S_{e\text{ upper}} \quad [17]$$

Where $S_{i\text{ lateral}}$ is the lateral surface of the internal free volume of the truncated cone, $S_{i\text{ lower}}$ is the surface of the lower base of the internal free volume of the truncated cone, $S_{i\text{ upper}}$ is the surface of the upper base of the internal free volume of the truncated cone, S_i is the total surface of the internal free volume of the truncated cone, $S_{e\text{ lateral}}$ is the lateral surface of the truncated cone, $S_{e\text{ lower}}$ is the surface of the lower base of the truncated cone, $S_{e\text{ upper}}$ is the surface of the upper base of the truncated cone and S_e is the total surface of the truncated cone.

In the particular for the re-entry capsule, the lower surface of the truncated cone can be increased of a 15 % due to the curvature of the thermal shield and the surface of windows and hatches (S_{w-h}) can be considered constant and equal to 3.2 m².

The external shape of a resource module (of a capsule or of a free-flyers and so on) can be assumed similar to a cylinder. The Figure 14 shows the shape of a cylinder and defines the design parameters useful to the development of the geometry model. The variables D_{RM} and l_{RM} are respectively the external diameter and the length of the cylinder.

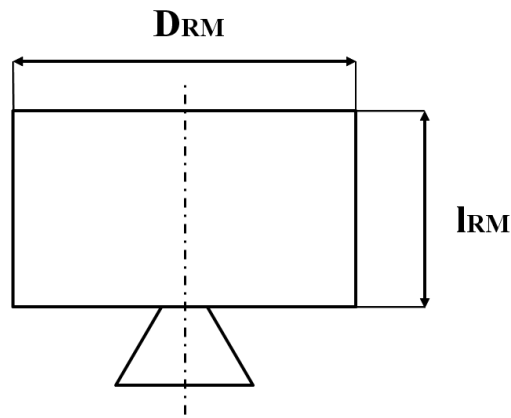


Figure 14 Resource modules

The model developed assumes the outer diameter of the resource module as an input. This shall be chosen, mainly, taking into account envelopes of internal equipment, other module interface and launcher payload fairing constraints.

The length of the module is assumed proportional to the length of the propellant tanks (l_{tank}) plus a fixed value (l_{fix}) to take into account the installation of other internal equipment such as avionics components, tanks for consumables storage, Thermal Control System (TCS) elements, Electric Power System (EPS) elements and so on. Thus, the value of l_{fix} shall be assumed considering functional allocation to the resource module and mission objectives of the system.

$$l_{RM} = l_{\text{fix}} + l_{\text{tank}} \quad [18]$$

As for the truncated cone, also the geometrical features of the cylinder can be evaluated through pure geometrical equations. The external surface (S_{RM}) of the cylinder can be calculated as the sum of the lateral surface of the cylinder ($S_{RM\ lat}$) and the surface of the bases ($S_{RM\ base}$):

$$S_{RM\ lat} = D_{RM} \cdot \pi \cdot l_{RM} \quad [19]$$

$$S_{RM\ base} = \frac{D_{RM}^2}{4} \cdot \pi \quad [20]$$

$$S_{RM} = S_{RM\ lat} + 2 S_{RM\ base} = D_{RM} \cdot \pi \cdot l_{RM} + 2 \frac{D_{RM}^2}{4} \cdot \pi \quad [21]$$

Also, the external shape of a manned habitat can be assumed similar to a cylinder, see Figure 15. Nevertheless, the geometry model of the cylinder for manned habitat changes with respect to the cylinder for a resource module because of the different input parameters.

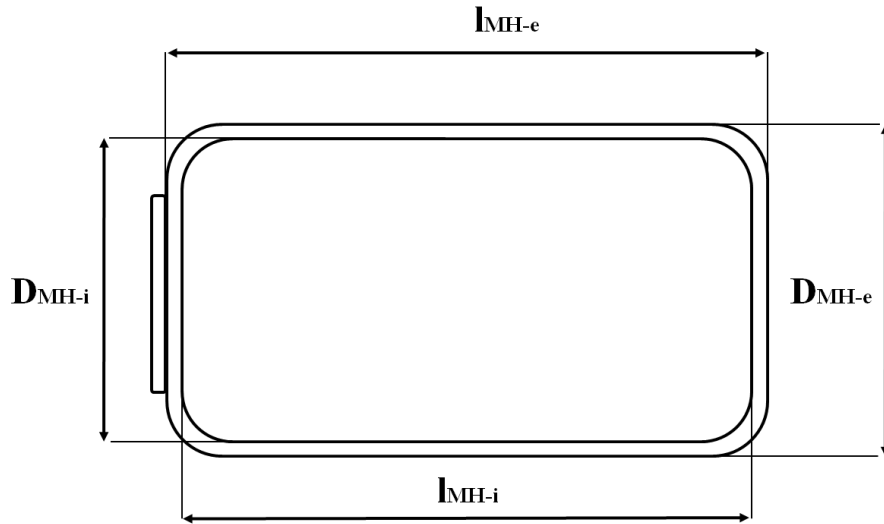


Figure 15 Manned Habitat

In general the available pressurized volume is very important for manned habitat as well as the external diameter (D_{MH-e}). The pressurized volume is necessary to ensure sufficient habitable volume to the crew members and to the internal payload and equipment. The external diameter is important because together with the external length of the module (l_{MH-e}) defines the maximum envelopes.

Considering pure geometrical equations, the length of the internal pressurized compartment of a manned habitat (l_{MH-i}) can be calculated as:

$$l_{MH-i} = \frac{4 \cdot V_{pressurized}}{\pi \cdot D_{MH-i}^2} \quad [22]$$

Where l_{MH-i} is the length of the internal pressurized compartment of the manned habitat and D_{MH-i} is the diameter of the internal pressurized compartment of the manned habitat. The external envelopes of the module can be calculated assuming the wall thickness

of the pressurized compartment (w_t). A typical value of this variable for manned habitat is 0.1 m. Finally, the external diameter of the manned habitat (D_{MH-e}) and the external length (l_{MH-e}) can be calculated considering equation [23] and [24]:

$$D_{MH-e} = D_{MH-i} + 2 \cdot w_t \quad [23]$$

$$l_{MH-e} = l_{MH-i} + 2 \cdot w_t \quad [24]$$

The external and internal surface of the cylinder can be calculated according to equation [25] and [26] respectively:

$$S_{MH-i} = 2 \cdot \frac{D_{MH-i}^2}{4} \cdot \pi + D_{MH-i} \cdot \pi \cdot (l_{MH-i}) \quad [25]$$

$$S_{MH-e} = 2 \cdot \frac{D_{MH-e}^2}{4} \cdot \pi + D_{MH-e} \cdot \pi \cdot l_{MH-e} \quad [26]$$

Where S_{MH-i} is the total surface of the internal pressurized compartment of the manned habitat and S_{MH-e} is the total surface of the external cylinder of the manned habitat.

In general, pressurized modules have one or more hatches. A typical value for the surface of each hatch (S_h) is 4 m², value that is obtained from ref. [11].

Finally, there are modules with a shape similar to that of Figure 16. Essentially, a cylinder is coupled together with two circular platforms at the bases. The geometry of the module foresees that the two platforms have a diameter bigger than the diameter of the central cylinder. In general, propulsive stages or Moon lander adopt this particular shape to optimize their mass.

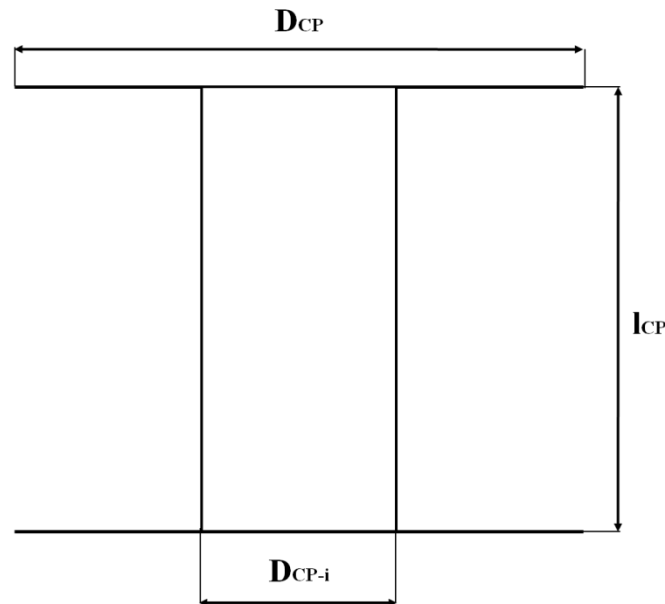


Figure 16 Cylinder coupled to platforms

The input parameter is the external diameter of the platforms (D_{CP}), assumed equal in geometry. The diameter of the internal cylinder (D_{CP-i}) can be calculated as difference between the diameter of the platforms and the diameter of the propellant tanks (D_{tank}). The equation [27] can be considered:

$$D_{CP-i} = D_{CP} - 2 \cdot D_{tank} \quad [27]$$

The length of the module (l_{CP}) can be assumed equal to the length of the tanks. The internal equipment will be accommodated in the internal cylinder or in the stand-off volumes between the propellant tanks.

$$l_{CP} = l_{tank} \quad [28]$$

The surface of the internal cylinder (S_{CP-cil}) can be calculated doing reference to equation [29]:

$$S_{CP-cil} = D_{CP-i} \pi l_{CP} \quad [29]$$

The surface of each platform $S_{CP-plat}$ can be calculated as:

$$S_{CP-plat} = \frac{D_{CP-e}^2}{4} \pi - 2 \frac{D_{CP-i}^2}{4} \pi \quad [30]$$

Finally, the total surface (S_{CP}) of the module can be calculated:

$$S_{CP} = S_{CP-cil} + 2 \cdot S_{CP-plat} \quad [31]$$

4.5 Structure

The structure is the subsystem of a spacecraft that ensures the structural integrity of the spacecraft for the entire mission life cycle. The main functionalities of the structure are to carry ground handling loads, flight accelerations and operational loads, to support equipment in stable position and to protect sensitive components from the environments such as shock and vibration by dissipating energy or transforming the vibration to make it less damaging.

The structure can be divided into three main categories:

- Primary structure
- Secondary structure
- Tertiary structure

The primary structure carries the main loads acting on the spacecraft. The secondary structure carries and support equipment such as booms, solar panels, racks. The secondary structure attaches directly to the primary structure. Finally, the tertiary structure includes all the small structures such as brackets, boxes and printed circuit boards.

The mass of the structure can be assumed proportional to the surface area of the module. In particular for the capsule, to estimate the mass of the pressurized vessel structure (including secondary structure), a uniform mass distribution per unit area can be assumed. Thus, the resulting mass is scaled with respect to the surface area of the pressurized vessel. With reference to the geometry model presented in the section 4.4, the mass of the pressurized vessel can be calculated as:

$$m_{PVS} = k_{PVS} \cdot (S_i - S_{w-h}) \quad [32]$$

Where m_{PVS} is the mass of the pressurized vessel structure in Kg, k_{PVS} is the scalar factor (assumed scaling factor for aluminum honeycomb is 20.3 Kg/m^2 , ref. [11]) and S_{w-h} is the surface of windows and hatches that can be considered constant and equal to 3.2 m^2 .

The same design method is adopted for the mass of the OML structure of a capsule:

$$m_{OML} = k_{OML} \cdot (S_e - S_{w-h}) \quad [33]$$

Where m_{OML} is the mass of the OML structure in Kg and k_{OML} is the scalar factor (assumed scaling factor for composite skin panels, including attachment structure, is 11.6 Kg/m^2 , ref. [11]).

The structure of a resource module includes the unpressurized structure and the dedicated tank support structure. The unpressurized structure provides structural attachment for the other subsystem components as radiators, solar arrays, avionics systems or propulsion devices and ensures the proper interface with the launcher. It can be assumed that the resource module structure design and construction is very similar to the Apollo service module structure. Thus, we can utilize database data to estimate the primary structure mass ($m_{\text{primary structure}}$) with good approximation. The equation considered is a power law relationship based on the lateral external surface area ($S_{\text{RM lat}}$ expressed in m^2) of the Resource Module:

$$m_{\text{primary structure}} = 6.6515 \cdot S_{\text{RM lat}}^{1.1506} \quad [34]$$

The mass dedicated to the tank support structure ($m_{\text{tank support}}$) is not negligible. Its mass can be estimated as proportional to the wet tank mass ($m_{\text{wet tank}}$) which is the mass of the empty tank and propellant (see equation [69], [70] and [74]):

$$m_{\text{tank support}} = 0.008 m_{\text{wet tank}} \quad [35]$$

The mass of the pressurized vessel and of the OML structure of a manned habitat can be calculated doing reference to equation [32] and [33]. Nevertheless, the proportional coefficients for manned habitat are different. In particular, k_{PVS} is equal to 20 Kg/m^2 and k_{OML} is equal to 11.6 Kg/m^2 . Alternatively, the mass of the primary structure of a pressurized module can be calculated as proportional only to the external surface of the module:

$$m_{\text{primary structure}} = k_{\text{primary structure}} S_e \quad [36]$$

In this case the proportional coefficient ($k_{\text{primary structure}}$ is equal to 24.4 kg/m^2 considering aluminum material structure) and the mass for the secondary structure is proportional to the number of equivalent racks for system, payloads and equipment accommodation (n_{rack}). The equation for secondary structure is:

$$m_{\text{secondarystructure}} = m_{\text{equivalentrack}} n_{\text{rack}} \quad [37]$$

Where $m_{\text{equivalent rack}}$ is equal to 190 kg.

For what concern the structural model of that modules such as propulsion stages, landers and so on with a shape similar to that of Figure 16. The mass of the primary structure and of the tank support can be calculated doing reference to equations [34] and [35]. In this case the surface to be considered is the surface of the platforms (SCP plat).

The Micrometeoroids and Debris Protection System (MDPS) protects the structures and internal components from the impact of micrometeoroids and debris. Generally, the MDPS consists of aluminum alloy sheets attached directly to the primary structure with a suspension scheme that reduces the interaction between the pressure shell and the MDPS. The thickness of the MDPS panels depends on the probability of impact. For the Low Earth Orbit (LEO) environment a thickness from 1.6 to 2.5 mm, pending the spacecraft lifetime in LEO, is sufficient as protection. The value are obtained doing reference to Columbus reference data, ref. [12]). The model of the MDPS assumes the mass of this component proportional to the surface of the spacecraft exposed to the space environments. Thus, the mass can be calculated according to equation [43] where k_{MDPS} is the mass proportional coefficient (equal to 2.25 kg/m^2 for 1 mm MDPS thickness) and S_{exp} is the exposed surface of the spacecraft.

$$m_{\text{MDPS}} = k_{\text{MDPS}} S_{\text{exp}} \quad [38]$$

4.6 Thermal Control System

The Thermal Control System (TCS) ensures the system thermal integrity. Mainly, it maintains the temperatures of inhabited volumes, systems and equipment within determinate operative ranges.

The Thermal Control System includes active and passive technologies. Thus, two main categories can be identified:

- Passive Thermal Control System (PTCS)
- Active Thermal Control System (ATCS)

Passive technologies are typical of small systems and dissipate heat through radiation from external surfaces. Passive thermal dissipation is obtained with careful geometrical design and layout, insulation, heaters and heat pipes. Instead, active technologies are typical of bigger spacecraft that require higher power levels. Active temperature control implies the movement of mass, usually fluids (liquids, gas or both) which allow convective heat transfer to augment conduction and radiation. Generally the active thermal control system includes both internal and external components such as pumped fluids loops collecting heat thank to cold plate and radiators that dissipate heat into the space.

Finally, part of the TCS is the thermal protection system (TPS) that shields the surface from heat sources and sinks such as the Sun, deep space and from the heat generated by the atmosphere during re-entry. In particular the re-entry is very demanding in terms of heat to be dissipated. Two main technologies can be identified to block, absorb and radiate heating: radiative systems reject heating by thermal radiation from high temperature surfaces;

absorptive systems absorb heat by heat sinks, ablation or transpiration. Ablation means that a material absorbs heat and then degrades. Transpiration means that a fluid collects heat from the surfaces and then dissipates.

The mass of the ablative thermal protection system (TPS-a) depends mainly on the re-entry velocity, trajectory and spacecraft shape. Nevertheless, as first approximation its mass can be estimated as proportional to the cross-sectional area of the re-entry vehicle during re-entry, equation [44]. In general, for a re-entry capsule of conical shape, the cross-sectional area is the lower surfaces ($S_{e\text{ lower}}$) of the truncated cone. The term $k_{\text{TPS-a}}$ is the mass proportional coefficient and it depends on the chosen material. Some of the materials for TPS may include carbon-carbon, carbon-phenolic, AVCO, Phenolic Impregnated Carbonaceous Ablator (PICA), PhenCarb-28, Alumina Enhanced Thermal Barrier-8 (AETB-8)/TUFI, Advanced Flexible Reusable Surface Insulation (AFRSI, LI-900 or LI-2200, CRI, SLA-561S, cork, and many others. For PICA, the mass proportional coefficient is equal to 20 kg/m^2 , ref. [11].

$$m_{\text{TPS-a}} = k_{\text{TPS-a}} \cdot S_{e\text{ lower}} \quad [39]$$

Generally, re-entry vehicles are also equipped with a reusable TPS that shields the surface from heat sources and sinks. The reusable TPS protects the spacecraft in the areas where the temperatures are less challenging. The mass of a reusable TPS can be scaled on the difference between the external lateral and upper surface and the windows and hatch area:

$$m_{\text{TPS-r}} = k_{\text{TPS-r}} \cdot (S_{e\text{ lateral}} + S_{e\text{ upper}} - S_{w-h}) \quad [40]$$

Where $k_{\text{TPS-r}}$ is the mass proportional coefficient and is equal to 4.3 kg/m^2 for a combination of LI-2200, LI-900, AFRSI, and Flexible Reusable Surface Insulation (FRSI), ref. [11].

Some spacecraft may use internal insulation to provide passive thermal control during all mission phases. The internal insulation consists of an insulating material layer between the pressurized structure and the OML. The mass of the component can be scaled on the value of the internal surface:

$$m_{ii} = k_{ii} S_i \quad [41]$$

Where m_{ii} is the mass of the internal TPS and k_{ii} is the mass proportional coefficient that assuming the utilization of Saffil high-temperature fibrous alumina is equal to 2 Kg/m^2 , ref. [11].

Other spacecraft makes use of Multi-Layer Insulation material (MLI). MLI provides protection of spacecraft surfaces directly exposed to space, not directly exposed to space because covered by the radiator panels and/or MDPS protections and to the surface not exposed to space but exposed to temperature impingement due to Engine and Thrusters. The mass of the MLI can be scaled through a mass proportional coefficient (k_{MLI}) on the value of the surfaces covered by MLI material (S_{MLI}) as equation [42] shows. A typical value for k_{MLI} ranges from 1 to 3 kg/m^2 , ref. [11].

$$m_{MLI} = k_{MLI} S_{MLI} \quad [42]$$

The design of the ATCS components depends by the amount of heat to be dissipated. The thermal load (Q_{ATCS}) is strongly related to the electrical power generated on board because virtually all electrical power generated will end up as waste heat to be removed. Thus, as first approximation, it could be considered that the thermal load to be dissipated is equal to the electrical power to be generated, plus the heat generated by the crew and excluding the heat necessary for heating internal components. The thermal load due to the presence of the crew is computed as follows:

$$Q_{crew} = k_{Qcrew} \cdot n_{crew} \quad [43]$$

The variable n_{crew} is the number of the crew members and k_{Qcrew} is the proportionality coefficient (140 W/person, ref. [11]).

More than one model exists for the determination of the ATCS mass. In some cases, it could be convenient, to estimate the mass of the ATCS on the basis of the total heat to be dissipated. Thus, the mass of the ATCS is calculated as:

$$m_{ATCS} = k_{ATCS} \cdot Q_{ATCS} \quad [44]$$

Where, m_{ATCS} is the mass of the active thermal control system components, k_{ATCS} is the mass proportional factor (kg/W) and Q_{ATCS} is the total thermal load that must to be dissipated. The value of k_{ATCS} depends on the TCS functionalities, architecture and technologies utilizes. In the case of a re-entry capsule, that collects heat and dissipates through the capsule resource module, a typical value for k_{ATCS} is 0.02125 kg/W, ref. [11]. Assuming that the capsule is equipped with a Fluid Evaporator System (FES) that utilizes water and Freon to dissipate heat during re-entry, the amount of fluids shall be also included. The consumable water for heat rejection can be estimated assuming a heat of vaporization of 2,260 kJ/kg (k_{heatH_2O}) while the mass of Freon can be estimated assuming a heat of vaporization of 216 kJ/kg ($k_{heatR134A}$).

$$m_{water-vap} = \frac{Q_{fesH_2O}}{k_{heatH_2O}} \quad [45]$$

$$m_{R134A} = \frac{Q_{fesR134A}}{k_{heatR134A}} \quad [46]$$

The mass of the radiators (m_{rad}) can be calculated assuming a mass penalty per unit area (k_{rad}), see equation [47]. Obviously, the mass penalty coefficient depends by the features (mainly technology and configuration) of the radiators. Table 1 provides reference values for mass proportional coefficient of some TCS components including radiators.

$$m_{rad} = k_{rad} A_{rad} \quad [47]$$

Component	Mass coefficient
Hardware for ATCS	
Heat acquisition	
Heat exchanger (>5 kW)	17 + 0.25 x capacity [kW]
Cold-plates	12 x capacity [kW]
Heat transport	
Pumps with accumulator	4.8 x loop capacity [kW]
Plumbing & valves	+15 %
Instruments & control	+5 %
Fluids	+5 %
Heat pumps	8 x capacity [kW]
Heat Rejection	
Deployable radiators (1 sided)	8.5 Kg/m²
Deployable radiators (2 sided)	17 Kg/m²
Fixed radiators (1 sided)	3.5-5.3 Kg/m²
Fixed radiators (2 sided)	10.6 Kg/m²
Hardware for PTCS	
Multi-layer insulation (MLI)	1-3 Kg/m²
Heaters	0.7 Kg/kW
Heat pipes	2,94 x 10⁻⁴ x capacity [W] x(length [m])²
Hardware for TPS	
Radiative type	4.3-10 Kg/m²
Absorptive type	20 Kg/m²

Table 1 TCS main components mass proportional coefficient (ref. [11], [4])

The area of the radiators (A_{rad}) can be preliminarily estimated on the basis of the amount of heat to be dissipated (Q), of the operative environment and radiator technology. With reference to Table 2, the appropriate value of heat-rejection per area for the desired average radiator temperature can be determined. Then, the required radiator area can be simply obtained by dividing the heat load to be rejected for the heat-rejection coefficient (k_{hr}) from the table. See equation [48].

$$A_{rad} = Q k_{hr} \quad [48]$$

Operative environment	Radiator type	Average radiator temperature	Approximate heat rejection (k_{hr})*
Near Earth orbit	Stationary radiator	270	50 (W/m ²)
		290	131 (W/m ²)
Near Earth orbit	Tracking radiator	270	104 (W/m ²)
		290	185 (W/m ²)
Moon-low altitude	Horiz. relative to surface	270	106 (W/m ²)**
		290	187 (W/m ²)**
Moon-poles orbit	Vert. or Horiz.	270	171 (W/m ²)
		290	251 (W/m ²)
Mars surface	Vert. or Horiz.	270	81 (W/m ²)
		290	162 (W/m ²)
Mars transit	-	270	171 (W/m ²)
		290	251 (W/m ²)

*often both sides of a radiator contribute to radiating area. May interpolate between the two values given depending on radiator temperature

**Significant degradation will occur over time. Not feasible for long duration missions

Table 2 TCS main components mass proportional coefficient (ref. [4])

If the radiator technology foresees a fluid loop for heat dissipation, a more accurate estimation of the radiators area is possible according to equation [49]. Where Q is the total heat load expressed in W, A_{rad} is the radiators area in m^2 , ε is the radiators surface emissivity, k is the Stefan-Boltzmann constant ($J/m^2/K^4/s$), V_F is the view factor, T_E is the radiator temperature at the equilibrium (K), T_{sink} is the temperature of the heat sink (K).

$$Q = A_{rad} \varepsilon k V_F (T_E^4 - T_{sink}^4) \quad [49]$$

First the radiator system architecture shall be chosen. Figure 17 shows an example of radiator system architecture. The system foresees four radiator panels in series so that the fluid outgoing from a radiator enters in the following one. T_0 represents the inlet temperature of the fluid in the radiator system and T_4 represents the outlet temperature of the fluid from the radiator system. A typical value for the inlet temperature (T_0) is 308 K (ref. [11]) while a typical value for the outlet temperature (T_4) is 275 K (ref. [11]). Nevertheless, this values depend by the chosen technology.

The methodology foresees to choose a value for the radiator area (A_{rad}) and then to increase or reduce it until the sizing of the radiator allows the dissipation of the necessary amount of heat. For each panel, an initial value for the outlet temperature shall be chosen and then the dissipated heat shall be calculated doing reference to equation [51]. The outlet temperature of the panels will be iteratively calculated doing reference to equation [52] until convergence. The iterative calculation is then performed for all the panels of the radiator systems. Finally, if the sum of the heat dissipated by each panel is less than the value of heat to be dissipated, the radiator area shall be increased. On the contrary, if the sum of the heat dissipated by each panel is bigger than the value of heat to be dissipated, the radiator area shall be decreased in order to reach optimization.

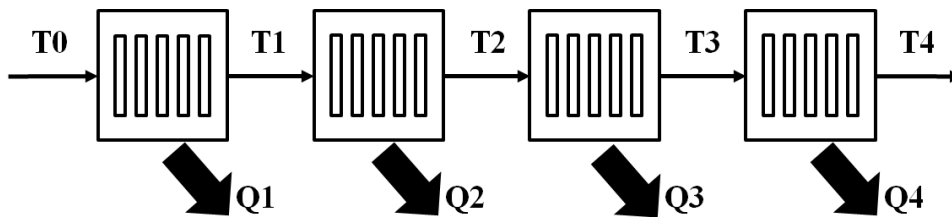


Figure 17 Example of radiator system architecture

$$A_{rad} = \sum A_i \quad [50]$$

$$Q_i = A_{rad} \varepsilon \sigma V_F \left(\left(\frac{T_{i-1} + T_i}{2} \right)^4 - T_{sink}^4 \right) \quad [51]$$

$$T_i = T_{i-1} - \frac{Q_i}{flow\ rate \cdot c_p} \quad [52]$$

$$Q = \sum Q_i \quad [53]$$

4.7 Power System

The electrical power system provides the primary electrical power generation, power management, distribution and storage. A power budget is necessary to design the power system. The power budget is the sum of the energy required by all the elements of the spacecraft in all the phases of the mission. The power budget can be computed in the modeling framework iteratively, by collecting the required information from all the elements of the system.

The selection of the primary power source can be performed according to the graph of Figure 18. The figure presents the power source generators against time and power load. Different technology solutions are possible but each of them results mass efficient only in determinate ranges of mission duration and load power, although overlaps are possible. For low power level and mission duration batteries results the most convenient technology. If the power level increases as well as the mission duration, battery are not convenient and chemical dynamic or fuel cell start to be the most effective. For very long mission duration, photovoltaic is preferable if the power level not exceed 10 kW. Nuclear source are preferable for very long mission duration and very high power loads.

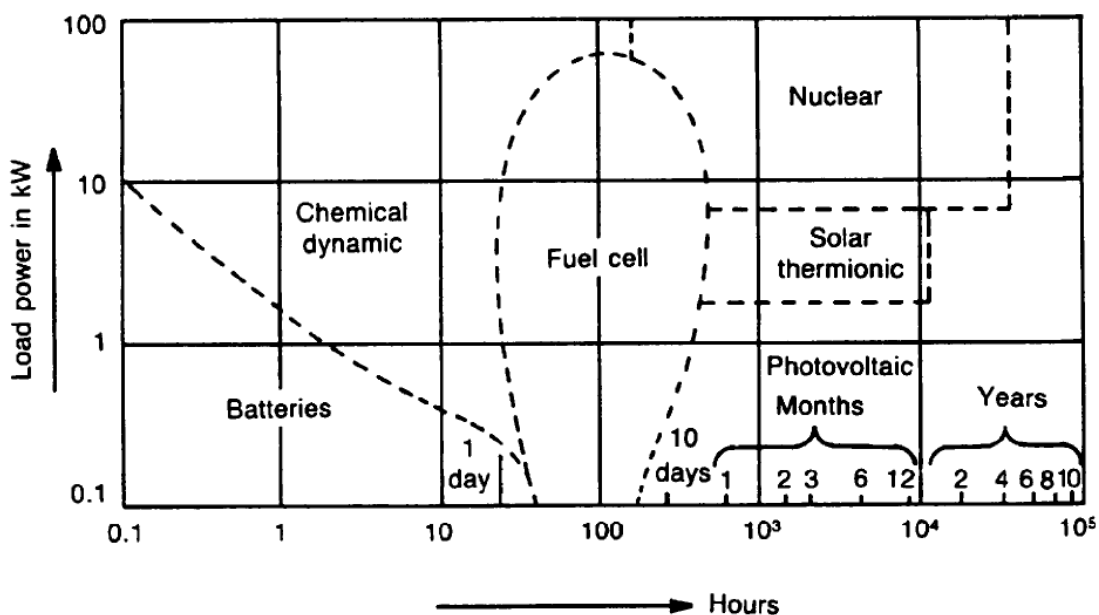


Figure 18 Primary electrical power generation technology Vs. mission duration and load power

For what concern the power storage, batteries turn out to be the most efficient storage system to supply power for low time duration. Regenerative fuel cells allows energy storage and are more efficient of batteries for long power demand periods and temporarily higher power needs. In fact, fuel cells imply increasing of the TCS loads, change the EPS requirements and impact on the logistic scenario.

The sizing of the solar arrays shall be performed considering that the system shall produce sufficient energy to power the spacecraft for the entire orbit. In fact, solar arrays produces energy only during sunlight periods while during eclipse periods they do not produce nothing. Thus, during sunlight periods, the solar arrays shall be able produce

sufficient energy to power the spacecraft systems and to recharge the batteries or fuel cells. The batteries or the fuel cells will supply energy during the eclipse periods.

Once the power budget has been performed, the average power required during eclipse (P_e) and the average power required during daylight (P_d) are known. The orbit characteristic allows to know the duration of eclipse period per orbit (t_e) and the duration of daylight period per orbit (t_d). Thus, the power that the solar array shall provide during daylight to power the spacecraft for the entire orbit (P_{sa}) can be calculated with equation [54].

$$P_{sa} = \frac{\frac{P_e \cdot t_e}{x_e} + \frac{P_d \cdot t_d}{x_d}}{t_d} \quad [54]$$

Where X_e is the efficiency of the paths from the solar arrays through the batteries to the loads and X_d is the efficiency of the paths from the solar arrays directly to the loads. A typical value for X_e ranges from 0.6 to 0.65 while a typical value for X_d ranges from 0.8 to 0.9, ref. [13].

The energy conversion efficiency of the solar cells (eff_{sc}) is the ratio between the power in input to the solar cells (i.e. the solar energy that the solar cells receive) and power in output that the solar cells produce (i.e. the electrical energy produced by the solar cells). Typical values for solar cell efficiency change according to the technology utilized. In general, silicon solar cells have an efficiency of about 0.14 and Gallium-Arsenide solar cells have an efficiency ranging from 0.18 to 0.26, ref. [13]. Once the energy conversion efficiency is known, doing reference to equation [55], is possible evaluate the ideal power per unit area produced by the solar cells at begin of life (P_0).

$$P_0 = eff_{sc} \text{ sun constant} \quad [55]$$

The sizing of the solar cells shall take into account the performance degradation due to design and assembly inefficiencies (I_{ass}), temperature inefficiencies (I_t) and shadowing of cells (I_s). Generally, a typical value for assembly inefficiencies ranges from 0.77 to 0.9, ref. [13]. The performance degradation due to the changing of the cells temperature increases with the temperature above the 28 °C. A degradation of about 0.5% per degree can be considered, ref. [13]. The degradation due to shadowing of cells depends by the spacecraft design and in general the value ranges from about 0.8 to 1, ref. [13]. The inherent degradation (I_d) takes into account of all these aspect and can be calculated doing reference to equation [56].

$$I_d = I_{ass} \cdot I_t \cdot I_s \quad [56]$$

Thus, the real power per unit area produced at the Begin of Life (BOL) can be calculated doing reference to equation [57] where the sun-incident is the angle between vector normal to the surface of the solar cells and the Sun line.

$$P_{BOL} = P_0 \cdot I_d \cdot \cos(\text{sun - incidence}) \quad [57]$$

It must be considered that the power produced by the solar arrays decreases over the time because of radiation, thermal cycling, micrometeoroids and thrusters plume. The value of the degradation per year (dpy) depends by the technology of the solar cells. Silicon cells have a dpy of about 3.75 % while Gallium-Arsenide cells have a dpy ranging from 2.5 to 2.75 %, ref. [13]. The values for other technology can be find in literature (ref. [13]). The equation [58] can be utilized to calculate the lifetime degradation (L_d).

$$L_d = (1 - dpy)^{lifetime} \quad [58]$$

Thus, the power per unit area produced at the end of life (P_{EOL}) can be calculated with equation [59].

$$P_{EOL} = P_{BOL} \cdot L_d \quad [59]$$

Finally the solar array area (A_{sa}) can be obtained by the ration between the power that the solar array must provide during daylight to power the spacecraft for the entire orbit and the power per unit area produced at the end of life, see equation [60].

$$A_{sa} = \frac{P_{sa}}{P_{EOL}} \quad [60]$$

Considering a mass of solar array per m^2 (k_{sa}) ranging from 3.6 to 5 kg/m^2 (ref. [13]) is possible to calculate the mass of all the solar array (m_{sa}) system thanks to equation [61].

$$m_{sa} = A_{sa} \cdot k_{sa} \quad [61]$$

As said before batteries can be utilized for energy storage. The batteries are called primary if they are not re-charged during the flight while they are called secondary if they are re-charged during the flight. In general, primary batteries are utilizes when power is required for short duration missions. Secondary batteries are utilizes mainly when photovoltaic power system have periods without sunlight and when there are peaks on the power demand that are greater than what the primary power source can produce.

The ideal energy capacity of the battery depends by the power (W_{bat}) that they shall provide and by the utilization time (t_{bat}). Nevertheless, part of this energy is lost due to the power management and distribution (losses) and part of the storage energy is not utilizable due to the depth-of-discharge (dod) which is the percent of total battery capacity removed during a discharge period. The dod depends by the number of re-charge/discharge cycles of the batteries and high dod percentages imply short cycle life. Thus the total energy that the batteries have to storage (E_{bat}) can be calculated doing reference to equation [62].

$$E_{bat} = \frac{W_{bat} \cdot t_{bat} \cdot (1 + losses)}{dod} \quad [62]$$

The mass of the batteries depends by their specific energy density (k_{bat}). The specific energy density is a ratio between the energy stored and the mass of the battery and depends by the technology of the battery. Typical values of energy density are proposed in Table 3

Technology	Specific energy density [W h/kg]	Rationale
Primary		
Silver-Zinc	60-130	High rate, short life (minutes)
Lithium Thionyl Chloride	175-440	Medium rate, moderate life (<4 hours)
Lithium Sulfur Dioxide	130-350	low/medium rate, long life (days)
Lithium Monofluoride	130-350	Low rate, long life (months)
Thermal	90-200	High rate, very short life (minutes)
Secondary		
Nickel-Cadmium	25-30	Space-qualified, extensive database
Nickel-Hydrogen (Individual pressure vessel design)	35-43	Space-qualified, good database
Nickel-Hydrogen (common pressure vessel design)	40-56	Space-qualified for GEO and planetary
Nickel-Hydrogen (single pressure vessel design)	43-57	Space-qualified
Lithium-Ion (LiSO ₂ , LiCF, LiSOCl ₂)	70-110	Under development
Sodium-Sulfur	140-210	Under development

Table 3 Characteristics of batteries (ref. [13])

Thus, knowing the battery specific energy density (k_{bat}), the mass of the batteries (m_{bat}) is calculable doing reference to equation [63] where the term *inst* takes into account the mass for battery installation (generally 10 %, ref. [11]).

$$m_{bat} = \frac{E_{bat}}{k_{bat}} \cdot (1 + inst) \quad [63]$$

Fuel cells can be also utilized for energy storage. They are devices that allow direct conversion of chemical energy into electricity like the batteries but with higher efficiency ($\eta_{fcs} \sim 63\%$). Power is generated from combination of an oxidizer and a fuel into a cell aided by the presence of a catalytic material. Generally, for space application, the fuel and the oxidizer consist of hydrogen and oxygen so that the product is energy and water. Thus, fuel cells require tankage to store the reactants and the water product.

The mass of a fuel cell system (m_{fcs}) is a function of energy to be provided and of the desired operating time, since the mass of the reactant must be included in the assessment. For a system of fixed mass, however, an energy density (k_{fcs}) of 500 – 700 Wh/kg at a power level of ~3 kW is reasonable, ref. [11].

$$m_{fcs} = E_{fc} \eta_{fcs} k_{fcs} \quad [64]$$

The power management and distribution consists of regulators, converters, charge controller and wiring. Generally, the mass of these components typically accounts for 20-30% of the power system total mass. More specifically, regulated systems have a specific mass of ~11.4 kg/kW excluding the wiring for distribution, ref. [11].

4.8 Propulsion System

The propulsion system provides orbit control, orbit maintenance, maneuvering and attitude control. Orbit control allows the spacecraft to move from an initial orbit to another, including escaping from a gravitational body. Orbit maintenance allows the spacecraft to keep a desired orbit. Attitude control allows the spacecraft to generate the torques necessary to keep the spacecraft pointed in a desired direction.

The propulsion system includes primary and secondary thrusters, tanks for propellant and the pressurization system.

The main engine mass can be estimated on the basis of statistical survey. Utilizing data from ref. [14], the following equation can be obtained:

$$m_{main-engine} = 0.0014 \cdot T + 65.5 \quad [65]$$

Where the variable T is the engine vacuum thrust and it is expressed in N .

Instead, the mass of the secondary thrusters can be estimated doing reference to equation [66]. Also in this case the mass of the thrusters has been considered proportional to the vacuum thrust:

$$m_{secondary-engine} = 0.004 \cdot T + 1.828 \quad [66]$$

The mass of the tanks is evaluated as a function of the external shape, the material, the liquid or gas pressure and its temperature, and the occupied volume. The tank wall thickness is computed by means of the thin-pipe theory, which is valid if the wall thickness, b , is small if compared to the pipe internal diameter, D_{it} . In particular the thin-pipe theory can be applied if the following is valid: $b < D_{it}/20$.

In case of cylindrical tank, the thickness of the tank is computed as follows:

$$b = \frac{P_t \cdot r}{\sigma_c} \quad [67]$$

In case of spherical tank, instead, the thickness of the tank (b) is computed as follows:

$$b = \frac{P_t \cdot r}{2 \cdot \sigma_c} \quad [68]$$

The variable p_i is the internal pressure of the tank, r is the tank mean radius, and σ_c is the yield strength of the tank material. The tank mass is computed as a function of the specific weight (ρ) of the tank material. The equations [69] and [70] can be used to calculate the mass of the spherical tank and cylindrical tank respectively.

$$m_{\text{tank}} = \frac{\pi}{6} (D_{\text{et}}^3 - D_{\text{it}}^3) \rho \quad [69]$$

$$m_{\text{tank}} = \frac{\pi}{4} (D_{\text{et}}^2 - D_{\text{it}}^2) l_{\text{tank}} \rho + \frac{\pi}{2} D_{\text{et}}^2 b \rho \quad [70]$$

Where m_{tank} is the tank mass, D_{et} is the external diameter of the tank, D_{it} is the internal diameter and l_{tank} is the length of the cylindrical tank. The dimension of the tank depends by the volume of propellant that must be stored into each tank (V_{prop}), see equations [82] and [83]. Thus, the internal dimension of the tank can be calculated with equation [71] for the spherical tank and [72] for the cylindrical tank.

$$D_{\text{it}} = \sqrt[3]{\frac{6}{\pi} V_{\text{prop}}} \quad [71]$$

$$D_{\text{it}} = \sqrt[3]{\frac{4}{\pi} \frac{V_{\text{prop}}}{k_{\text{tank}}}} \quad [72]$$

Where, k_{tank} is the ratio between the diameter of the cylindrical tank and its length.

The mass of the propellant (m_p) to be stored depends on the delta velocity (ΔV) to be obtained (the maximum change of speed of the rocket if no other external forces act), on the specific impulse of the propellant itself (I_{sp}) and on the overall mass of the spacecraft. The mass of the propellant necessary to obtain a ΔV can be calculated doing reference to the Tsiolkovsky rocket equation also called ideal rocket equation and to equation [74]. The equation relates the ΔV with the effective exhaust velocity and the initial and final mass of a spacecraft.

$$\Delta V = v_e \ln \frac{m_0}{m_1} \quad [73]$$

$$m_p = m_0 - m_1 \quad [74]$$

Where v_e is the effective exhaust velocity of the rocket, m_0 is the initial total mass of the spacecraft including the propellant and m_1 is the mass of the spacecraft after the manoeuvre.

Introducing the definition of the specific impulse, the equation can be re-written as [76].

$$I_{sp} = \frac{v_e}{g_0} \quad [75]$$

$$\Delta V = I_{sp} g_0 \ln \frac{m_0}{m_1} \quad [76]$$

Where, g_0 is the standard gravity (9.81 m/s^2).

The mass of propellant calculated with the rocket equation shall be increased to take into account of the residual propellant that remain inside the tanks and that cannot be utilized and, in case of cryogenic propellant system, of the propellant lost due to boil-off. Equations [77] and [78] can be utilized to calculate the amount of residual propellant and the amount of propellant that is lost due to the boil-off.

$$m_{rp} = k_{rp} m_p \quad [77]$$

$$m_{bo} = k_{bo} m_p \quad [78]$$

Where m_{rp} is the residual propellant, i.e. the amount of propellant trapped in the propulsion tanks after that the nominal ΔV maneuvers are completed. k_{rp} is the residual propellant proportional coefficient (2%, ref. [11]). m_p is the mass of required propellant to complete the maneuvers. m_{bo} is the mass of propellant lost due to the boil-off and k_{bo} is the boil-off proportional coefficient. In case of cryogenic propellant system it is possible to assume that the propellant is stored entirely and passively in the tanks. Therefore, as heat leaks into the propellant tanks, the cryogenic fluids will slowly vaporize (boil-off), and vented to maintain a nominal tank pressure. Assuming 60 layers of variable-density MLI per tank and SOFI, a 210 K external environment temperature, and the appropriate heats of vaporization for oxygen and methane, the k_{bo} , i.e. the boil-off proportional coefficient, can be assumed equal to 0.0265, ref. [11].

The mass of the insulation layer of the tank (m_{ii}) can be estimated as proportional to the numbers of insulation layers n_{ii} and to the amount of the tanks external surface S_t , expressed in m^3 . k_{ii} is the proportional coefficient (0.02 kg/m^2 , ref. [11]).

$$m_{ii} = k_{ii} S_t n_{ii} \quad [79]$$

To change the inclination of the orbital plane, the direction of the velocity vector must change as showed in Figure 19.

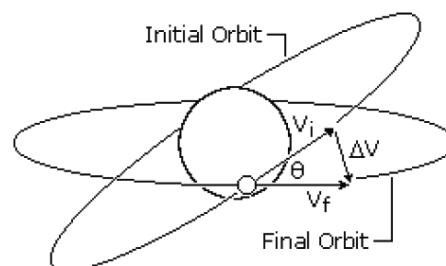


Figure 19 Change of orbital plane

This maneuver requires a component ΔV to be perpendicular to the orbital plane and, therefore, perpendicular to the initial velocity vector. If the altitude of the orbit remains constant, the maneuver is called “simple plane change”. The required change of velocity can be calculated using the following equation:

$$\Delta V = 2V_i \sin\left(\frac{\theta}{2}\right) \quad [80]$$

Where V_i is the velocity before and after the burn and θ is the angle change required.

If the angle of plane change is high the required change in velocity becomes very expensive. For example, if the angular change is equal to 60 degrees, the required change in velocity is equal to the current velocity of the spacecraft. Thus, some strategies can be implemented to minimize the ΔV required to change orbit. If the orbit is elliptical, the change of orbital plane can be performed in the point of the orbit where the velocity is the minimum (apogee for an elliptical orbit). In some cases, it may be cheaper to boost the spacecraft into a higher orbit, change the orbit plane at the apogee, and return the spacecraft to its original orbit. Figure 20 shows that for angle of plane change less than 38.94 deg the simple plane change is convenient while for angle of plane change amongst 38.94 deg and 60 deg the change of altitude strategy is better.

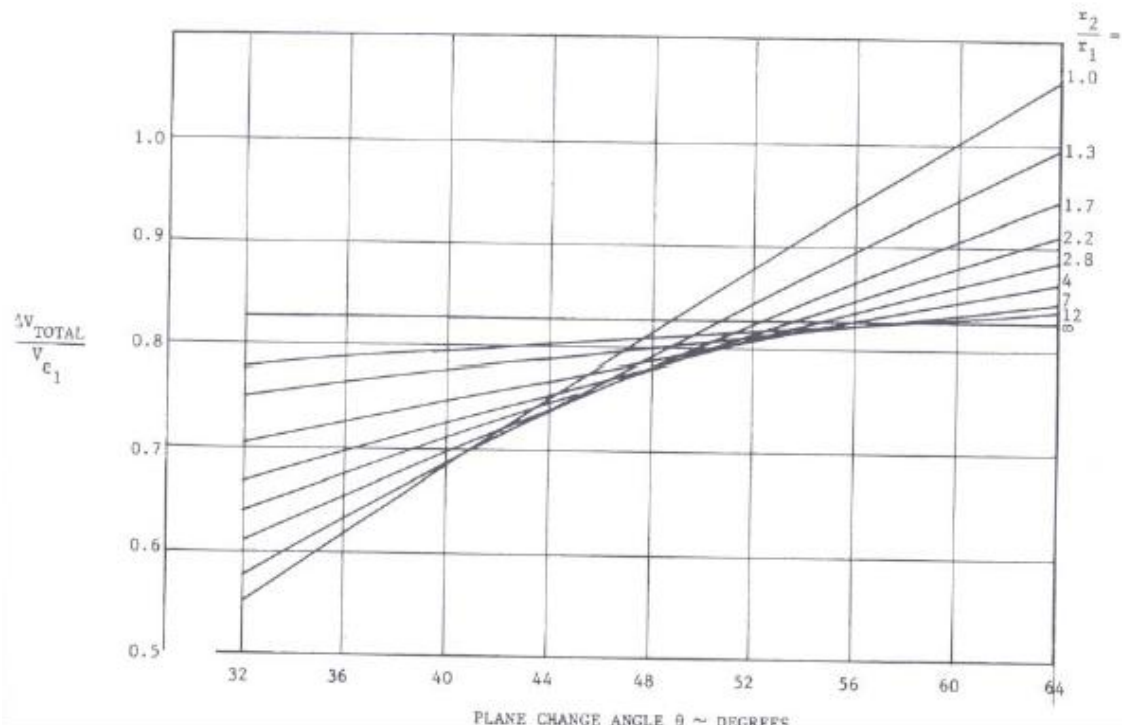


Figure 20 Plane change angle Vs ΔV

$$0^\circ < \theta < 38.94^\circ \Rightarrow \frac{r_2}{r_1} = 1$$

$$38.94^\circ < \theta < 60^\circ \Rightarrow \frac{r_2}{r_1} = \frac{\sin\left(\frac{\theta}{2}\right)}{1 - 2\sin\left(\frac{\theta}{2}\right)}$$

$$60^\circ < \theta < 180^\circ \Rightarrow \frac{r_2}{r_1} \rightarrow \infty$$

Where:

θ is the angle of orbit change

r_1 is the radius of the initial orbit

r_2 is the radius of the orbit where performs the change of orbit inclination

Once the mass of propellant has been calculated, the mass of fuel and oxidizer can be calculated knowing oxidizer-to-fuel mass ratio (O/F), equation [81].

$$O/F = \frac{\text{mass of oxidizer}}{\text{mass of fuel}} \quad [81]$$

Then, the volume of the fuel and oxidizer can be calculated knowing their density, respectively ρ_{fuel} and ρ_{oxidizer} expressed in kg/m^3 . Equations [82] and [83] can be utilized.

$$V_{\text{fuel}} = \frac{m_{\text{fuel}}}{\rho_{\text{fuel}}} \quad [82]$$

$$V_{\text{oxidizer}} = \frac{m_{\text{oxidizer}}}{\rho_{\text{oxidizer}}} \quad [83]$$

The pressurization system of the propulsion system utilizes an high-pressure inert gas to regulate the tank internal pressure that must be kept above a certain limit to allow the system to operate. The mass of the inert gas is computed as a function of the total internal volume of the tanks with the following relationship:

$$m_{\text{gas}} = \mu_{\text{gas}} \frac{P_{\text{min}} \cdot V_{\text{tank}}}{R \cdot T_{\text{gas}}} \quad [84]$$

The variable μ_{gas} is the molar mass of the inert gas, P_{min} is the minimum pressure to guarantee inside the tank expressed in Pa, V_{tank} is the volume of the tank in m^3 , R is the universal gas constant, and T_{gas} is the temperature of the inert gas expressed in K . The mass of the helium tank can be evaluated whit reference to the equation [69] or [70].

4.9 Life Support System Model & Consumables

The function of the Environmental Control and Life Support (ECLS) system is to keep the crew alive. Thus, it shall provide a physiologically acceptable environment within the spacecraft and all the resources that the crew requires and deal with its outputs. The human body can be assimilated to an open system that need of food, water and oxygen to survive and

produces heat and metabolic products such as sweat, urine, feces and carbon dioxide that must be removed.

Mainly, the ECLS system can be classified into two main categories: open and closed loop. The open loop ECLS system needs of external supply for consumables and produces waste. The closed loop ECLS system is able to recover resources from waste. Different closure levels are possible in function of how much the system is able to recycle. High closure level system need of less resupply and full closure level implies autonomous operation. The disadvantages of the closed loop ECLS system are higher costs of technology development, higher power demands, increased heat loads and more challenging maintenance requirements.

Figure 21 shows a trade-off between different ECLS closure level. Apart the open ECLS system, different closed loop levels have been considered. The lowest closure level foresees CO₂ removal but not water regeneration. Then, different technologies for water regeneration have been considered. The first option foresees water regeneration but not urine. The second one allows regeneration of the 92% of the urine produced. The third option allows completely regeneration of both water and urine. Then, the last two options foresee regeneration of both water and oxygen but utilizing different technologies, i.e. Sabatier and Bosch systems. The graph shows the cumulative launch mass (system mass, spares mass, delta mass of power/thermal system and delta mass due to system accommodation) for the different option as function of the mission duration. It appears clear that as the duration of the mission increases, the advantage of a closed loop system in terms of mass reduction becomes more and more significant.

The graph has been obtained on the base of the following assumptions:

- The assessment has been performed considering four crew members
- The food de-hydration is equal to 80%
- The contribution of EVA on consumables mass has been neglected
- A buffer of 1 week has been considered for air and water when regenerative technologies are considered. The assumption simplify the analysis because the buffer should be function of type of mission, distance from the Earth or from rescue systems
- Water availability for shower, hand wash, oral hygiene, drinking e food hydration has been considered
- Two redundancies have been considered for regeneration technologies
- The technologies considered derive from ISS

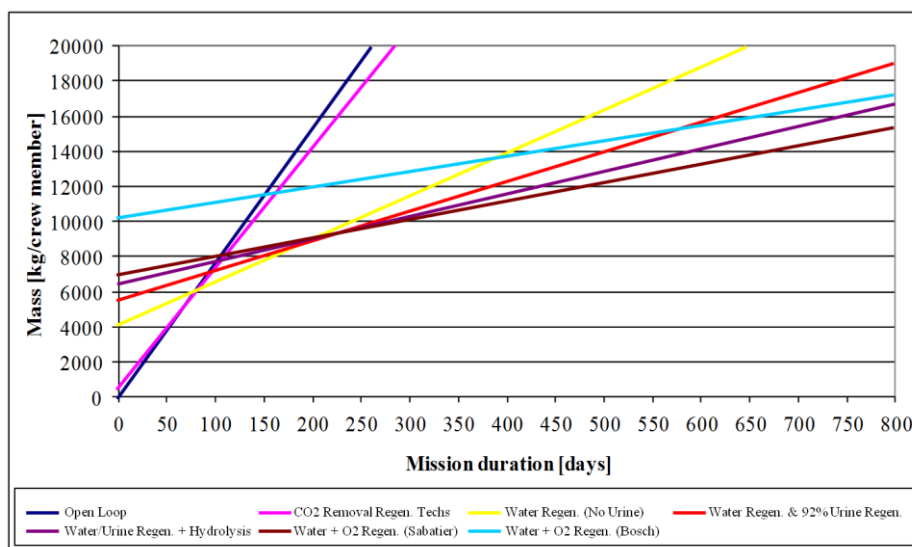


Figure 21 Different ECLSS closure level trade-off (TAS courtesy)

The ECLS system includes tanks for the nitrogen storage and oxygen storage, elements for atmosphere supply and control, fire detection and suppression, venting and thermal conditioning, Extra-Vehicular Activity (EVA) umbilical and support. Other elements for atmosphere contaminant control have a mass proportional to the number of crew members, ref. [4] and [15].

$$m_{atmcontrol} = 8 \text{ kg} \quad [85]$$

$$m_{ACC} = k_{ACC} \cdot n_{crew} \quad [86]$$

$$m_{smokedetector} = 3 \text{ kg} \quad [87]$$

$$m_{THC} = k_{THC} \cdot V_{pressurized} \quad [88]$$

$$m_{umbilicals} = 30 \text{ kg} \quad [89]$$

Where $m_{atmcontrol}$ is the mass of the atmosphere supply and control system, m_{ACC} is the mass of the atmosphere contaminant control system, k_{ACC} (25 kg/person) is the scalar factor on the number of crew members (n_{crew}) for the atmosphere contaminant control system, $m_{smokedetector}$ is the mass of the smoke detector system, m_{THC} is the mass of the venting and thermal conditioning system (kg), k_{THC} (3.5 kg/m³) is the scalar factor on this latter and $m_{umbilicals}$ is the mass of the EVA umbilical and support system (Kg), ref. [11].

For what concern the water management system, a linear proportion is usually assumed between the mass of the tank and the mass of the water to be stored.

$$m_{wt} = m_w \cdot k_{wt} \quad [90]$$

The variable m_{wt} is the mass of the water tank expressed in kg, m_w is the mass of the water stored in the tank expressed in kg, and k_{wt} is the proportionality coefficient. Doing reference the equivalent space shuttle subsystem (ref. [15]), the proportionality coefficient has been assumed equal to 0.24.

Closed loop ECLS systems utilize technologies for processing of the waste water. Amongst the main considered technologies, filtration of the water is relatively simple but it needs of expendables to regenerate filters. Distillation is mainly used for urine and solids. It foresees an evaporator and condenser that allow recovering of up to 96% of the water in the urine and up to 50% of the water in the solids. The water obtained after distillation shall be further treated to make potable the water. A process called Super Critical Waste Oxidation (SCWO) destroys waste using water in its supercritical state which changes its properties as a solvent. Organic compounds, normally insoluble in water at standard temperature and pressure, become soluble in supercritical water. If enough oxygen is available and the reactor temperature and pressure are high enough, organic compounds, along with process atmospheric and trace contaminant gases, completely oxidize to CO₂, H₂ and N₂. Inorganic salts are only slightly soluble in supercritical water so they separate by precipitating from the solution. The temperature and molecular densities allow the oxidation reactions to be rapid and essentially complete. In principle, the SCWO process can handle all types of spacecraft waste, plus condensate, wash and urine / flush waters. It creates an entirely drinkable water

supply from all waste waters. Nevertheless, the process needs post treatment to remove a few toxic product gases.

The Table 4 shows mass parameter and power requirements for the three technologies, ref. [4].

Parameter	Filtration	Distillation	SCWO
Hardware mass	10 kg/person	25 kg/person	150 kg/person
Expendables	3 kg/person/year	8 kg/person/year	N/A
Spares	10% of hardware mass per year		
Initial water charge	3 days water supply		
Power requirements	40 W/person	30 W/person	360 W/person

Table 4 Water management technologies

Also for what concerns oxygen, different technologies options are possible. The open loop system stores all the necessary oxygen into tanks. The mass of the tanks for oxygen storing can be estimated doing reference to equations [69] or [70] once the oxygen quantity as been calculated and the storing pressure and temperature have been assumed. Nevertheless, a more simple equation can be utilizes. Equation [91] assumes the mass of the oxygen tank ($m_{\text{ox tank}}$) proportional to the mass of the oxygen to be stored (m_{oxygen}).

$$m_{\text{ox tank}} = k_{\text{ot}} m_{\text{oxygen}} \quad [91]$$

Where k_{ot} is the proportional coefficient and it is equal to 0.9 for high pressure storage at 1 MPa and 297 K, ref. [13].

Several technologies option exists for oxygen regeneration. Partially closed loop foresees water re-supply but not foresees generation of waste water to be removed. Water can be provided by food that contains water or through the exceeding water produced by the fuel cells. Through electrolyzing of the water, oxygen and hydrogen are produced. An example of partially closed loop is the Oxygen Generation Assembly (OGA) developed by the Russian. Closed loop technologies recover the oxygen from the CO_2 . The reaction of hydrogen with the CO_2 under determinate condition produces water that allows generation of oxygen. The Sabatier process is a developed technology for the reduction of CO_2 . Table 5 shows mass parameter and power requirements for the two technologies, ref. [4].

Parameter	OGA	Sabatier
Mass	35 kg/person	38 kg/person
Power requirements	350 W/person	20 W/person

Table 5 Oxygen regeneration technologies

A list of required resources for the crew accommodation can be found in ref. [11], [4] or [16]. In particular the galley and food system, the Waste Collection System (WCS) and sleep accommodations are required to provide crew accommodation.

The galley and food system includes conventional ovens, microwave ovens, kitchen/oven cleaning supplies, sink & spigot for hydration of food and drinking water, cooking/eating supplies. Data from ref. [11] and [4]:

$$m_{conventionalovens} = 50 \text{ kg} \quad [92]$$

$$m_{microwaveovens} = 70 \text{ kg} \quad [93]$$

$$k_{k/o\ cleansupp} = 0.25 \frac{\text{kg}}{\text{day}} \quad [94]$$

$$m_{k/o\ cleansupp} = k_{k/o\ cleansupp} \cdot n_{daymission} \quad [95]$$

$$m_{sink} = 15 \text{ kg} \quad [96]$$

$$k_{c/e\ supp} = 0.5 \frac{\text{kg}}{\text{person}} \quad [97]$$

$$m_{c/e\ supp} = k_{c/e\ supp} \cdot n_{crew} \quad [98]$$

The waste-collection system includes toilets, WCS supplies, contingency fecal and urine collection mittens and bags.

$$m_{toilet} = 45 \text{ kg} \quad [99]$$

$$k_{WCSsupp} = 0.05 \frac{\text{kg}}{\text{person days}} \quad [100]$$

$$m_{WCSsupp} = k_{WCSsupp} \cdot n_{crew} \cdot n_{daymission} \quad [101]$$

$$k_{waste\ collection\ bags} = 0.23 \frac{\text{kg}}{\text{person days}} \quad [102]$$

$$m_{w.c.b.} = k_{wastecollectionbags} \cdot n_{crew} \cdot n_{daymission} \quad [103]$$

The sleep accommodations include sleep provisions (sleep restrain only), ref. [11] and [4].

$$k_{SA} = 9 \frac{\text{kg}}{\text{person days}} \quad [104]$$

$$m_{SA} = k_{SA} \cdot n_{crew} \cdot n_{daymission} \quad [105]$$

There are other systems that determine the mass of a capsule, that have not been mentioned so far. We put these elements in the category named “*other*”. In this category there is the parachute system, landing airbags, a water flotation system, doors, hatches and docking

mechanism. At this stage of development, the masses of these elements are considered to be constant in the mathematical model, equal to 1167 kg, ref. [11].

$$m_{other} = 1167 \text{ kg} \quad [106]$$

Non-cargo elements include crew and personnel provisions. The personnel provisions depend on the number of crew members and on the mission duration.

$$m_{recreational\ item} = k_{recreational\ item} \cdot n_{crew} \quad [107]$$

$$m_{hygienekit} = k_{hygienekit} \cdot n_{crew} \cdot t_{mission} \quad [108]$$

$$m_{closet} = k_{closet} \cdot n_{crew} \cdot t_{mission} \quad [109]$$

$$m_{vacumtrashbag} = 13 \text{ kg} \quad [110]$$

$$m_{dispensewipes} = k_{dispensewipes} \cdot n_{crew} \cdot t_{mission} \quad [111]$$

$$m_{trashbag} = k_{trashbag} \cdot n_{crew} \cdot t_{mission} \quad [112]$$

$$m_{basicsupply} = 5 \text{ kg} \quad [113]$$

$$m_{lighting} = 10 \text{ Kg} \quad [114]$$

$$m_{restrains} = 12 \text{ Kg} \quad [115]$$

$$m_{emergencykit} = 2.3 \text{ Kg} \quad [116]$$

$$m_{COAS} = 13 \text{ Kg} \quad [117]$$

$$m_{survaivalkit} = 44 \text{ Kg} \quad [118]$$

$$m_{accessoris} = 100 \text{ Kg} \quad [119]$$

$$m_{test\ equipment} = 50 \text{ Kg} \quad [120]$$

$$m_{generictools} = 50 \text{ Kg} \quad [121]$$

$$m_{sleep\ accomodat\text{ion}} = k_{sleep\ accomodat\text{ion}} \cdot n_{crew} \quad [122]$$

$$m_{suit} = k_{suit} \cdot n_{crew} \quad [123]$$

$$m_{food} = k_{food} \cdot n_{crew} \cdot t_{mission} \quad [124]$$

Where $k_{recreational\ item}$ is equal to 5 Kg/person, $k_{hygiene\ kit}$ is 1.17 Kg/person/day, k_{closet} is 0.46 Kg/person/day, $k_{dispensewipes}$ is 0.15 Kg/person/day, $k_{trashbag}$ is 0.05 Kg/person/day, $k_{sleep\ accommodation}$ is 2.3 Kg/person, k_{suit} is 20 Kg/person and k_{food} is 1.8 Kg/person/day, ref. [11] and [4].

Table 6 provides further consumables and waste mass coefficient to be considered for crew support and habitation. The values have been proposed by ESA as a reference in the final stages of the architecture study.

Resource Requirements

	μg	Moon	Mars	Units
Food Dry mass	0,67	0,67	0,67	kg/person/day
Freeze Dried Food	0,45	0,45	0,45	kg/person/day
Packaging	0,26	0,26	0,26	kg/person/day
Canned Food	0,75	0,75	0,75	kg/person/day
Containers	0,35	0,35	0,35	kg/person/day
Metabolic Water				
Drinking Water	2	2	2	kg/person/day
Food Hydration Water	0,8	0,8	0,8	kg/person/day
Equipment Water				
EVA Suit Evaporator Water	5	5	5	kg/person/EVA
Sanitary Water				
Urine Flush	0,3	0,5	0,5	kg/person/day
Hand Wash	0	0	0	kg/person/day
Oral Hygiene	0	0,37	0,37	kg/person/day
Shower	0	2,72	2,72	kg/person/day
Laundry	0	6	6	kg/person/day
Dish Wash	0	2.5	2.5	kg/person/day
Food Preparation and Processing	TBD	TBD	TBD	kg/person/day
Air				
Oxygen	1,02	1,02	1,02	kg/CM-d
Waste				
Food and Food Packaging Maximum Absorption	0,324	0,324	0,324	kg/person/day
Garments (EVA)	0,173	0,173	0,173	kg/person/EVA
Feminine Wastes	0,113	0,113	0,113	kg/female/cycle
Feminine Products	0,104	0,104	0,104	kg/female/cycle
Gloves	0,007	0,007	0,007	kg/person/day
Duct Tape	0,033	0,033	0,033	kg/person/day
Human Detritus	0,016	0,016	0,016	kg/person/day
Paper	0,025	0,025	0,025	kg/person/day
Toilet Paper	0,03	0,03	0,03	kg/person/day
Wipes, Detergent	0,05	0,05	0,05	kg/person/day
Wipes, Disinfectant	0,05	0,05	0,05	kg/person/day
Wipes, Dry	0,01	0,01	0,01	kg/person/day

	Wipes, Wet	0,05	0,05	0,05	kg/person/day
	Wipes, Hygiene	0,23	0,2	0,2	kg/person/day
	Urinal Pretreatment	0,01	0,01	0,01	kg/person/day
Metabolic Wastes					
Urine	Total	1,562	1,562	1,562	kg/person/day
	Solids	0,059	0,059	0,059	kg/person/day
	Liquid	1,503	1,503	1,503	kg/person/day
Feces	Total	0,123	0,123	0,123	kg/person/day
	Solids	0,032	0,032	0,032	kg/person/day
	Liquid	0,091	0,091	0,091	kg/person/day
Air	CO2	1,219	1,219	1,219	kg/person/day
	Leakage Rate	0,0014	0,0014	0,0014	% of habitat air volume (1.00 is 100%)
Spare Parts					
	Thermal System	0,03	0,03	0,03	kg/person/day
	Air Evaporator Wicks	0	0,08	0,04	kg/person/day
	Air Subsystem	0,13	0,13	0,13	kg/person/day
	Misc.	0,89	0,89	0,89	kg/person/day
Clothing		0,0373	0,0373	0,0373	kg/person/day
EVA					
	Cooling Water Losses	0,57	0,19	0,19	kg/person/EVA/h
	Oxygen Losses	0,15	0,15	0,15	kg/person/EVA/h
	Oxygen Consumption	0,075	0,075	0,075	kg/person/EVA/h
	Potable Water Consumption	0,24	0,24	0,24	kg/person/EVA/h
	Food Consumption	0,029	0,029	0,029	kg/person/EVA/h
	Total Food mass w/ packaging & containers	0,078	0,078	0,078	kg/person/EVA/h
Additional waste material					
	Carbon Dioxide Production	0,093	0,093	0,093	kg/person/EVA/h
	Respiration and Perspiration	0,0568	0,0568	0,0568	kg/person/EVA/h
	Water Production				kg/person/EVA/h
	Urine Production	0,1782	0,1782	0,1782	kg/person/EVA/h
	Feces	0,014	0,014	0,014	kg/person/EVA/h
	Airlock gas losses per cycle	0,1	0,1	0,1	% of airlock gas mass (1.00 is 100%)

Table 6 Crew and life support consumables, ref. [16]

4.10 Communication

The communication system shall allow transmission of voice, video and data to and from a spacecraft. The communication system of a spacecraft shall be able to provide connection with another space vehicle, with the astronaut during EVA and with the ground or in general with the surface of a planet. If a straight line connects the transmitting and the receiver, direct communication link is possible, otherwise, a relay platform is necessary.

Figure 22 shows an example of communication architecture. The communication architecture represents schematically how the connection between a spacecraft and the other systems is organized giving information about the operating frequency of each channel. In the example of Figure 22, a communication architecture for an hypothetical Cis-lunar Free-Flyer orbiting around the Earth-Moon Lagrangian point 2 is shown. The Free-Flyer shall be able to

communicate with the visiting vehicles, with crew during EVA, with the Moon surface and with the ground station. Direct link is possible with the crew during EVA, with the Moon surface and with the visiting vehicle when they are visible. A data relay system is necessary to allow communication with the Earth and with visiting vehicles when they are not visible from the Free-Flyer. The communication architecture shall also take into account of existing communication system to be cost efficient. In the example proposed, the existing Tracking and Data Relay Satellite System (TDRSS) allows continuous communication link with the ground station. The scheme shows also the frequency considered for each link. Thus, S-band communication link is utilized to allow communication with visiting vehicle and Moon surface while Ka-band is utilized for the other links. Finally, VHF or UHF are considered to provide communication with EVA crewmembers.

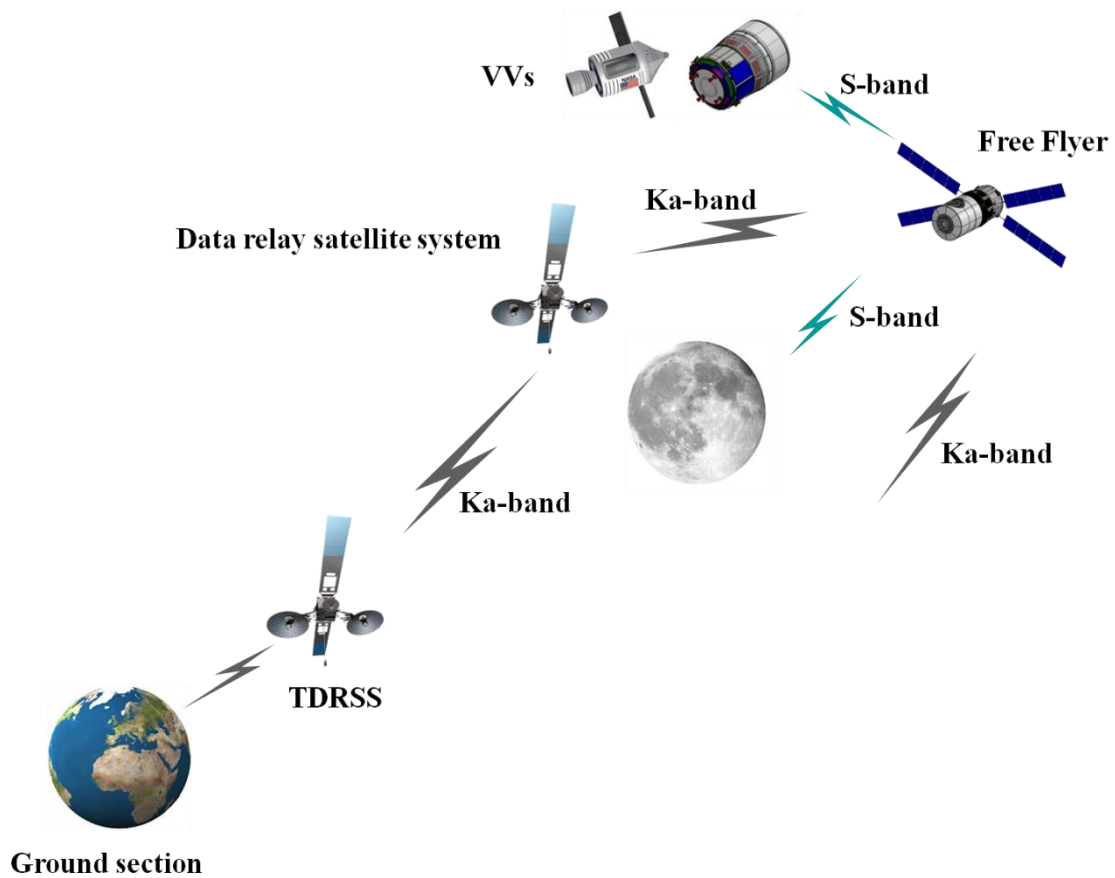


Figure 22 Communication architecture for Cis-lunar Free Flyer

The main performance parameters that characterize the communication architecture are data-rate (R_d), bit error rate (BER), end to end (E/E) delay and the link availability.

The data rate is the quantity of information that is transferred per unit time. The data-rate can be derived according to equation [125]. Where x is the messages per second that shall be transmitted, y is the number of bytes per message and df is the duty factor.

$$R_d [bps] = \frac{x[messages / s] \cdot y[bytes / message] \cdot 8[bits / byte]}{df} \quad [125]$$

The duty factor is the fraction of time that the communication link is effectively transmits the information. Thus, if the duty factor is 10%, it means that only for the 10% of the visibility time the information is effectively transmitted to the receiver.

The bit error rate is the probability of bit error. This means that if the BER is 10^{-5} , one bit in 100000 will be in error.

The end to end delay (t_{delay}) is the sum of the delay due to transmission ($t_{\text{transmission}}$), propagation ($t_{\text{propagation}}$), queuing and processing of the information. Queuing is the amount of time that transpires before a packet is processed and as well as the processing delay, it depends from the communication equipment. Considering that the queuing and processing delay are quite small with respect to the transmission and propagation time, they can be neglected and the total delay time can be calculated doing reference to equation [126].

$$t_{\text{delay}} = t_{\text{transmission}} + t_{\text{propagation}} \quad [126]$$

The transmission delay is the time necessary to the transmission of a packet of data. The transmission delay is proportional to the block of data size (z) and to the data rate. Equation [127] can be utilized to evaluate the transmission delay.

$$t_{\text{transmission}} = \frac{z[\text{bytes}] \cdot 8[\text{bits / byte}]}{x[\text{messages / s}]} \quad [127]$$

The propagation delay is the time necessary to the signal to reach the receiver. Considering that the signal is an electromagnetic wave, it travel at the speed of light (c) which is 3×10^8 m/s.

$$t_{\text{propagation}} = \frac{\text{distance}}{c} \quad [128]$$

The link availability takes into account the environment effects on the transmission channel. Thus, a link margin shall be considered for attenuation due to atmospheric absorption or free space losses. For what concern the attenuation due to atmospheric absorption, rain and dust attenuation shall be considered. The attenuation for both phenomena depends mainly on the operating frequency and for what concern the atmospheric loss on the antenna elevation angle. While for the attenuation due to dust 0.5 dB/km at 45 GHz and 0.2 dB/km at 20 GHz can be considered, for attenuation due to atmospheric absorption the values in Table 7 can be considered.

f	Elevation angle			
	90°	30°	20°	10°
20	0.25	0.5	0.73	1.44
30	0.2	0.4	0.58	1.15
40	0.3	0.6	0.88	1.73
44	0.6	1.2	1.75	3.46
50	1.79	3.58	5.23	10.31

Table 7 Atmospheric absorption (dB) as function of frequency and antenna elevation angle

Especially for space systems, because of the very large distances amongst the transmitter and the receiver, propagation losses are not negligible. The propagation loss can be calculated according to equation [129], where f_c is the carrier frequency and s is the slant range. Constant depends by the units of measurement of the slant range. Considering km, constant is equal to 92.45 for GHz and 32.45 for MHz.

$$L_{fs}(dB) = \text{constant} + 20\log(f_c) + 20\log(s) \quad [129]$$

Also the geometry of the source and the target platform shall be taken into account. Thus, the coverage area, the slant range and the viewing time shall be taken into account. The coverage area is the part of the target surface the effectively receive the signal. The slant range is the distance from the receiver and the transmitter. The viewing time is the duration of visibility of the ground station from the transmitter.

Table 8 shows typical requirements for voice, video and data information transmission, ref. [4]. In general, voice communication are characterized by low data rate and accept less stringent BER but requires low delay. Video communications have stringent requirements on delay and BER and require high bandwidth (up to 10s of MHz). Data information have not requirement on delay but their data rata need can be more challenging and have stringent requirements on BER.

Source	Data rate	Delay	BER
Voice	Low (10s of kbps)	Low (<0.1 s)	10-2 to 10-3
Video	High (10s of Mbps)	Medium (0.5 to 1.5 s)	10-5 to 10-7
Data	Variable (kbps to Mbps)	Variable (up to minutes)	10-5 to 10-7 (and higher)

Table 8 Requirements for voice, video and data information transmission

A link supports a determinate data rate if the link margin (M) is equal or bigger than zero. Thus, as equation [130] shows, the signal to noise ratio received (SNR_{avail}) shall be compared to the signal to noise ratio required to achieve a required BER ($SNR_{required}$).

$$M = SNR_{avail} - SNR_{required} \begin{cases} \text{if } M > 0 \text{ comm. link supported (e.g. 2 dB)} \\ \text{if } M = 0 \text{ comm. link just enough supported} \\ \text{if } M < 0 \text{ comm. link does not supported} \end{cases} \quad [130]$$

The link budget equation for the signal to noise ratio received is:

$$SNR_{avail} = EIRP + G/T_n - L_{fs} - L_{other} - k - R_d \quad [131]$$

Where EIRP is the effective isotropic radiated power of the transmit terminal, G is the receive antenna gain, T_n is the system noise temperature of the receive terminal, L_{fs} is the free

space signal loss, L_{other} is the term that accounts for the other link loss terms, k is the Boltzmann constant (-228.6 dBW/K/Hz) and R_d is the link data rate.

The EIRP can be calculated doing reference to equation [132]. EIRP is simply the sum of the transmitted power (P_t) and antenna gain (G_t) expressed in dB.

$$EIRP = 10 \log(P_t) + G_t \quad [132]$$

Where generically, the antenna gain (G) for a directional antenna is:

$$G = \text{constant} + \log(\eta) + 20 \log(f_c) + 20 \log(D) \quad [133]$$

Where η is the antenna efficiency (0.55 for parabolic dish antennas, ref. [4]), f_c is the frequency and D is the antenna diameter. if the antenna diameter is expressed in meters, constant is equal to -159.6 for Hz and 20.4 for GHz.

G/T is the ratio between the receiver antenna gain (G_r) and the receiver system temperature (T_r). G/T is in general given by the ground terminal features and can be calculated as equation [134].

$$G/T = G_r [dB] - T_r [dB] \quad [134]$$

Finally, the SNR_{required} can be estimated doing reference to Figure 23. Assuming the BER and the modulation (generally BPSK for space application), it is possible the definition of E_b/N_o ($=SNR_{\text{required}}$)

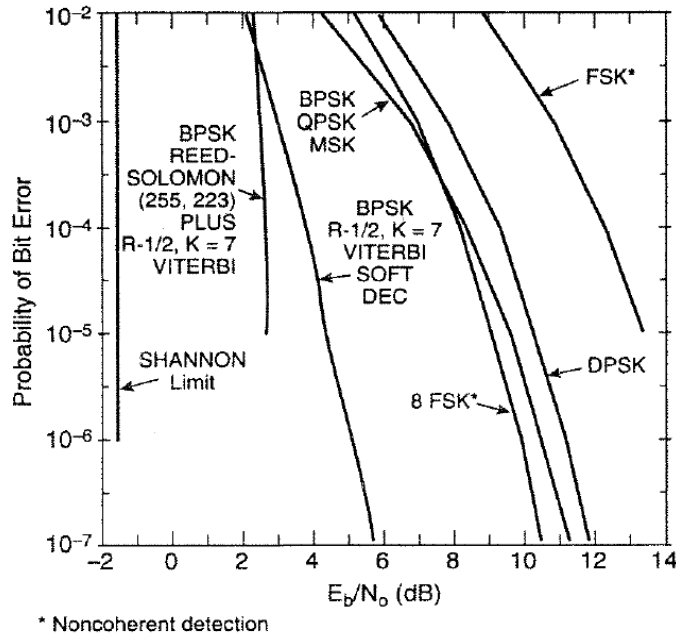


Figure 23 BER as function of noise to power density ratio (E_b/N_o), ref. [4]

The database provided by ref. [13] can be utilized to determinate the mass of the antenna. Several antenna design are considered: quad helix, horn and parabola. The mass of the antenna (including the installation mass) is considered proportional to the main

dimensions. For Quad Helix and horn design, the mass of the antenna can be assumed proportional to the length of the antenna (L_{antenna}) and its diameter (D_{antenna}). The mass proportional coefficients (k_{antenna}) are equal to 10 for the quad helix design and 16 for the horn antenna design.

$$m_{\text{antenna}} = k_{\text{antenna}} L_{\text{antenna}} D_{\text{antenna}} \quad [135]$$

Several design solution are available for parabolic antennas. The antenna can be fixed, with feed array or steerable. For all these configurations, the mass of the antenna can be considered proportional to the reflector area. The mass proportional coefficient (k_{antenna}) are equal to 10.2 for the fixed parabola, 7.2 for the parabola with feed array and 6.1 for the steerable parabola.

$$m_{\text{antenna}} = k_{\text{antenna}} \pi \frac{D_{\text{antenna}}^2}{4} \quad [136]$$

Ref. [13] shows how the transmitter mass varies with the output power (P_t) for two different technologies. Solid-state transmitter technology weights less than the Traveling Wave Tube Amplifier (TWTA) technology and is more reliable but requires more input power. For these reasons, that solid-state transmitters are preferred for power outputs up to 5 or 10 W, except at frequencies below 2 GHz, where power outputs up to 80 W are achievable. Interpolating the available data, the following equations have been obtained for estimation of the transmitter mass:

$$m_{\text{SS transmitter}} = (0.0004P_t^2 - 0.00031P_t + 1.2945) \left(1 + \frac{M}{100}\right) \quad [137]$$

$$m_{\text{TWTA transmitter}} = (-0.0005P_t^2 + 0.1099P_t + 2.0838) \left(1 + \frac{M}{100}\right) \quad [138]$$

4.11 Locomotion and mechanisms

Surface mobility systems shall ensure an efficient and safe surface exploration. A large number of possible system configuration and options have been proposed for surface mobility. Nevertheless, the most important include wheels, tracks, screw drives and legs. In the past, only wheel have been utilized in space missions, both manned and unmanned. The Lunar Roving Vehicle (LRV) is the only manned rover, which has so far been launched and used on the Moon surface. Its mobility system included four flexible wheels, constituted by a wire mesh carcass with a stiff inner frame, powered by a traction drive attached to each wheel through a motor harmonic drive gear unit, and a brake assembly. Apart from the LRV, so far only two other rover systems have landed on the Moon surface: the Lunokhod and the Mobile Equipment Transporter (MET). The Lunokhod had eight rigid wheels constituted by a wire carcass, each with an independent suspension, motor and brake. The MET had not propulsion and its wheels were made of rubber. No other systems have been delivered on the Moon surface so far. Also on Mars several rovers have been landed. The first rover landed on the surface of Mars was the Rover Sojourner in the 1997 and then in the 2004 was the turn of

Spirit and Opportunity. The last rover landed was Curiosity in the 2012. The locomotion system of the entire three rovers consists of a rocker-bogie suspension system equipped with six rigid wheels each of them with its own motor.

Wheels have demonstrated very good performances on the Moon and Mars surface but, basically because the soil characteristics, only for small and medium loads. Tracked locomotion systems are in general heavier than wheeled system but there are able to generate a propelling force considerably bigger. Legs and screw drives are slower than wheel and tracks, consume more energy and are more complicated systems.

A comparative evaluation of the most important architecture of lunar rover wheels, that have so far been studied, is shown in ref. [17]. The document does not recommend rigid or pneumatic wheels. Pneumatic wheels are not compatible with the lunar environment because of the rubber degradation due to the solar radiation. Rigid wheels, as the rigid rim wheel, have not ride comfort, especially for manned vehicle. As far as the wire mesh wheels (see the LRV's wheels of the Apollo missions) are concerned, they cannot be scaled to heavier and longer range vehicles. The elliptical wheel and the hub-less system (tracked system) have reliability problems and high specific weight. Taking into account the above considerations, only two wheel configurations match the lunar rover requirements: the hoop spring wheel and the spiral spring wheel. Both these two wheel configurations ensure soft ground performance, i.e. low motion resistances, adequate thrust generation and good wear resistance. In particular, however, the hoop spring wheel seems to be lighter, more comfortable and more stable than the spiral spring wheel.

Because of their highest efficiency in locomotion, only wheels have been modeled. In particular the equation [139] can be considered.

$$m_{wheels} = k_w m_{suspended} \quad [139]$$

Where, m_{wheels} is the mass of the wheels of a rover. $m_{suspended}$ is the suspended mass, i.e. the suspended mass of a vehicle is the mass of that set of elements that can have a variation of their distance from the ground. The proportional coefficient is k_w and it is equal to 0.1, ref. [4].

In order to predict the performances of a vehicle locomotion system, the semi-empirical equations developed by Bekker have been considered, ref. [18] and [19]. This theory allows estimation of the motion resistances and of the ability of the system to generate the horizontal propelling force (thrust).

The energy consumed by a wheeled vehicle operating on the sandy surface can be divided into three components: soil compaction, bulldozing and dragging, rolling resistance, ref. [20] and [21]. These components depend on the ground consistency and on the wheel deformability. In fact, the wheels can be classified as rigid or deformable: the rigid wheels have a constant rolling diameter, while the deformable wheels can decrease their rolling diameter up to 10%, ref. [21].

When a wheel moves on the soft ground, it is subjected to sinkage. The maximum sinkage (z_w) depends on the ground contact pressure (p_w), on the wheel width (b_w) and on the soil geophysical properties, namely the modulus of the soil deformation due to the soil cohesive ingredients (k_c), the modulus of the soil deformation due to the soil frictional ingredients (k_ϕ) and the exponent of soil deformation (n), (reference values for Moon and Mars are reported in Table 9).

$$z_w = \left(\frac{P_w}{\left(\frac{k_c}{b_w} + k_\phi \right)} \right)^{\frac{1}{n}} \quad [140]$$

Symbol	Moon	Mars	
g	1.635	3.688	[m/s ²]
φ	40	20	[°]
c _c	170	4800	[N/m ²]
γ	1680	1250	[kg/m ³]
n	1	1	[-]
k _c	1400	28000	[N/m ⁿ⁺¹]
k _φ	820000	7600000	[N/m ⁿ⁺²]
f _r	0.025	0.025	-

Table 9 Lunar and Mars soil parameters. Ref. [22], [23]

The wheel work done to compact the soil is proportional to the maximum sinkage, ref. [18]. The equation proposed by Bekker to evaluate the compaction resistance (R_{cf}) for deformable wheel is:

$$R_{cf} = \frac{(b_w \cdot p_w)^{\frac{n+1}{n}}}{(k_c + b \cdot k_\phi)^{\frac{1}{n}} (n+1)} \quad [141]$$

While the equation to evaluate the compaction resistance for rigid wheels (R_{cr}) is:

$$R_{cr} = \frac{\left(\frac{3W \cos \theta}{\sqrt{D}} \right)^{\frac{2n+2}{2n+1}}}{(k_c + bk_\phi)^{\frac{1}{2n+1}} (n+1) (3-n)^{\frac{2n+2}{2n+1}}} \quad [142]$$

The equation assumes that the compaction resistance (R_{cf} or R_{cr}) depends on the ground contact pressure (p_w), the wheel width (b_w), on the slope angle (θ), on the wheel diameter (D_w) and on the soil geophysical properties.

In case of a wide wheel and very soft ground, the bulldozing resistance cannot be neglected. The bulldozing resistance (R_b) is due to a substantial soil mass that it is pushed in front of the wheel. The bulldozing resistance is particularly evident when a wheel moves on a soft soil upon a stronger bottom layer. The equation proposed is:

$$R_b = \frac{b_w \sin(\alpha_a + \phi)}{2 \sin \alpha_a \cos \phi} \left(2z_w c_c K_c + \gamma z_w^2 K_\gamma \right) + \frac{\pi^3 \gamma (90 - \phi)}{540} + \frac{c_c \pi^2}{180} + c_c t^2 \tan \left(45 + \frac{\phi}{2} \right) \quad [143]$$

Where, K_c , K_γ , t and α_a are:

$$K_c = (N_c - \tan \phi) \cos^2 \phi \quad [144]$$

$$K_\gamma = \left(\frac{2N_\gamma}{\tan \phi} + 1 \right) \cos^2 \phi \quad [145]$$

$$t = z_w \tan^2 \left(45 - \frac{\phi}{2} \right) \quad [146]$$

$$\alpha_a = \cos^{-1} \left(1 - \frac{2z_w}{D_w} \right) \quad [147]$$

Where, b_w is the wheel width, z_w is the sinkage of the wheel, γ is the specific weight of soil, c_c and ϕ are respectively the Coulombian coefficient of cohesion and the Coulombian angle of internal friction of the soil. The symbol α_a is the angle of approach and can be calculated from the equation [147], t (equation [146]) is the distance of rupture and K_c and K_γ are the modulus of cohesion and the modulus of density of soil deformation respectively and can be calculated from equations [144] and [145]. Finally, N_c and N_γ are the Terzaghi's bearing capacity factors in general shear failure and can be calculated as reported in ref. [24].

The rolling resistance (R_r) is due to the wheel deformation, wheel slip and scrubbing, ref. [21]. If the wheel slip and scrubbing are negligible, the rolling resistance is associated to the energy dissipation due only to the wheel deformation and can be modeled as:

$$R_r = f_r W \quad [148]$$

where W is the vertical load acting on the wheel and f_r is the coefficient of rolling resistance.

The motion of a system is possible if the maximum thrust (F), which can be generated by the motor-wheel, is bigger than the sum of the motion resistances (R). However, this is not satisfactory, as it has also to be ensured that the drawbar pull (DP), equation [149] is sufficient to provide the system with the necessary acceleration, in order to cope with the slopes and the obstacles, which the system shall be able to clear. The maximum thrust (F) that can be generated depends obviously on the power of the wheel motor but cannot exceed the maximum horizontal propelling force that can be generated on a sandy surface (H). This force depends on its turn on the ground contact area (A), on the vertical load (W), on the Coulombian coefficient of cohesion (c_c), and on the Coulombian angle of internal friction of the soil (ϕ). Neglecting the tire treads effect and the wheel slip, H can be expressed as equation [150].

$$DP = F - R \quad [149]$$

where F is the thrust developed by the mobility system

$$H = A c_c + W \tan \phi \quad [150]$$

In order to provide the necessary thrust, the mobility system shall be able to develop a torque (T), given by the equation [151]:

$$T = (R_c + R_b + R_r + R_g + I) \left(\frac{D_w}{2} - \delta_w \right) \quad [151]$$

where R_c and R_b are the resistances due to soil compaction and bulldozing, R_r is the rolling resistance, R_g is the gravitational resistance ($R_g = W \cos \theta$, θ is the slope angle), I is the inertial force generated by the acceleration and D_w and δ_w are the wheel diameter and the wheel deflection respectively.

Finally, assuming that each wheel has been equipped the an electric motor, the power to be generated by each motor (P_w) is proportional to the torque to be developed by the motor (T) and to the rotation velocity of the wheel (ω):

$$P_w = T\omega \quad [152]$$

Thus, once the power to be developed (P_w) is known, it is possible the characterization of the wheel motor. The equation for the model of the drive motor considers the mass of the motor (m_{wm}) proportional to the power to be generated. The proportional coefficient id k_{wm} and it is equal to 10 kg/Kw, ref. [4].

$$m_{wm} = k_{wm} P_w \quad [153]$$

The mass for suspension and steering system ($m_{susp/steering}$) of the rover can be considered proportional to the suspended mass. Equation [154] can be considered.

$$m_{susp/steering} = k_{susp/stering} m_{suspended} \quad [154]$$

Where, $m_{suspended}$ is the suspended mass, and $k_{susp/steering}$ is the mass proportional coefficient equal to 0.05, ref. [4].

The landing system shall allow landing of a spacecraft on the surface of a planet. The landing system has to satisfy mass budget constraints, feasibility, landing performance and stability. Many landing concept can be found in literature and different solution have been utilized on Moon and Mars.

The landing system concept proposed refers to an Apollo-like concept thus for Moon application. The concept is based on a cantilever design solution. The four legs are attached to the lander chassis, the design guarantee the ability to overtake obstacles and dampers allow absorption of the residual vertical energy at the touch down.

The mass of the landing system ($m_{landingsys}$) can be calculated as proportional to the mass of the structure of the spacecraft (m_{lander}). Equation obtained through elaboration of data from ref. [11].

$$m_{landingsys} = 0.05m_{lander} \quad [155]$$

Finally, there are subsystems elements that cannot be well classified in a determinate subsystem. These elements are a part of “other”. In this category we consider spacecraft attachment system, pyrotechnic separation mechanisms, doors and hatches.

The mass of the pyrotechnic mechanisms ($m_{pyrotechnic}$) can be assumed independent from dimensions, ref. [11].

$$m_{pyrotechnic} = 100kg \quad [156]$$

The mass of the windows ($m_{windows}$), mainly used by the astronauts for rendezvous and docking operations, observation, and photography, can be considered constant (ref. [11]) and equal to:

$$m_{windows} = 37.15 Kg \quad [157]$$

Also the mass of the hatches can be considered constant (ref. [11]) and equal to:

$$m_{hatches} = 102 Kg \quad [158]$$

4.12 Launcher

The launcher is a system that puts a payload (a spacecraft) into a desired orbit. A detailed model of the launcher system is beyond the scope of this document. The model of the launcher consists of a mathematical relation between the payload mass and the launch cost and the launch probability of success (also called reliability). The launcher model is based on a database of sixty-four launch vehicles, Table 10 and Table 11.

Table 10 lists all the considered launch vehicles and characterizes each of them with information about the payload mass capability into Low Earth Orbit (LEO), Polar Orbit and Geosynchronous Transfer Orbit (GTO). Additional information concerning the launch cost and reliability have been provided. The reliability is estimated on the base of the ratio between the number of successful launches and total number of launches. Where information was not available (N/A), these have been omitted.

Launcher	Payload to LEO [kg]	Payload to Polar Orbit [kg]	Payload to GTO [kg]	Cost [M\$]	Reliability [%]
AR40	4900	3900	1900	65	92.8
AR42L	7400	5900	3200	90	92.8
AR42P	6100	4800	2600	67	92.8
AR44L	9600	7700	4200	115	92.8
AR44LP	8300	6600	3700	95	92.8
AR44P	7725	5500	3000	70	92.8
AR5	18000	12000	6920	105	92.8
ASLV	150	N/A	N/A	N/A	N/A
Athena-1	800	520	N/A	N/A	N/A

Launcher	Payload to LEO [kg]	Payload to Polar Orbit [kg]	Payload to GTO [kg]	Cost [M\$]	Reliability [%]
Athena-2	1990	1490	N/A	N/A	N/A
Athena-3	3655	2855	N/A	N/A	N/A
Atlas I	5580	4670	2250	70	86.5
Atlas II	6395	5400	2680	75	86.5
Atlas IIA	6760	5715	2810	85	86.5
Atlas IIAS	8390	6805	3490	115	86.5
Conestoga 1229	665	500	N/A	15,5	N/A
Conestoga 1620	1980	N/A	960	18	N/A
Conestoga 1679	1500	1250	N/A	N/A	N/A
Delta 6925	3990	2950	1450	N/A	N/A
Delta 7326	2865	2095	950	N/A	98
Delta 7925	5045	3830	1820	50	98
Delta III	N/A	N/A	3800	N/A	98
Delta Lite	1985	1510	660	25	98
Delta Lite	2610	2030	860	25	98
Energia	88000	80000	22000	N/A	N/A
GSLV	5000	N/A	2500	N/A	N/A
H-2	10500	6600	4000	160	1
Ikar-1 (SS-18)	4200	2800	N/A	N/A	N/A
Ikar-2 (SS-18)	4050	3600	N/A	N/A	N/A
J-1	900	N/A	N/A	43	N/A
Kosmos (SS-5)	1400	1100	N/A	N/A	98.4
LLV-1	795	515	N/A	16	N/A
LLV-2	1985	1490	593	22	N/A
LLV-3	3655	2855	1136	N/A	N/A
Long March (CZ-1D)	720	N/A	200	10	N/A
Long March (CZ-2C)	2800	1750	1000	20	1
Long March (CZ-2E)	9200	N/A	3370	40	N/A
Long March (CZ-3)	5050	4800	1500	33	N/A
Long March (CZ-3A)	N/A	7200	2500	N/A	1
Long March (CZ-3B)	13600	N/A	4800	N/A	N/A
Long March (CZ-4)	4000	2500	1100	N/A	1
M-3SII	880	680	517	N/A	N/A
Molniya	1500	N/A	2000 to Molniya	N/A	N/A
M-V	1950	1300	1215	N/A	N/A
Pegasus	375	N/A	N/A	N/A	N/A
Pegasus XL	455	365	125	13,5	N/A
Proton D-1	20900	N/A	N/A	65	93.2
Proton D-1e	N/A	N/A	20900	N/A	N/A
PSLV	3000	1000	450	N/A	N/A
Roskot (SS-19)	1850	N/A	N/A	N/A	N/A
Shavit	160	N/A	N/A	22	1
Shuttle/RSRM	24400	N/A	5900	N/A	98,6
Soyuz	7000	N/A	N/A	N/A	93
Start-1	N/A	600	N/A	7	N/A
Taurus	1450	1180	375	15	N/A
Titan II	N/A	1905	N/A	43	1
Titan III	14515	N/A	5000	N/A	N/A

Launcher	Payload to LEO [kg]	Payload to Polar Orbit [kg]	Payload to GTO [kg]	Cost [M\$]	Reliability [%]
Titan IV /SRMU	21640	18600	8620	300	N/A
Titan IV/SRM	17700	14100	6350	340	90
Tsyklon (SL-11)	2800	N/A	N/A	N/A	N/A
Tsyklon (SL-14)	3600	N/A	N/A	N/A	N/A
Vostok	4730	1840	N/A	N/A	N/A
Zenit-2	13740	11380	4300	65	88
Zenit-3	N/A	N/A	5180	N/A	N/A

Table 10 Launcher data base: payload mass to orbit, cost and reliability, ref. [4], [25]

Figure 24 and Figure 25 graphically show the information provided in Table 10. In particular, Figure 24 puts in relation the payload mass into LEO orbit and the launcher cost. Figure 25 puts in relation the payload mass into LEO orbit and the launch probability of success. A mathematical relation has been then obtained with interpolation of the data points. The obtained equations, [159] and [160] are valid for LEO insertion.

$$C_{launch} = 0.1196m_{payload}^{0.7193} \quad [159]$$

$$P_{launch} = -2 \cdot 10^{-6} \cdot m_{payload} + 0.9498 \quad [160]$$

Where C_{launch} is the launch cost expressed in millions of Dollars, $m_{payload}$ is the payload mass expressed in kilograms and P_{launch} is the launch probability of success.

The statistical survey shows that the higher is the launcher payload mass, the higher is the launch costs and the lower is the probability of mission success.

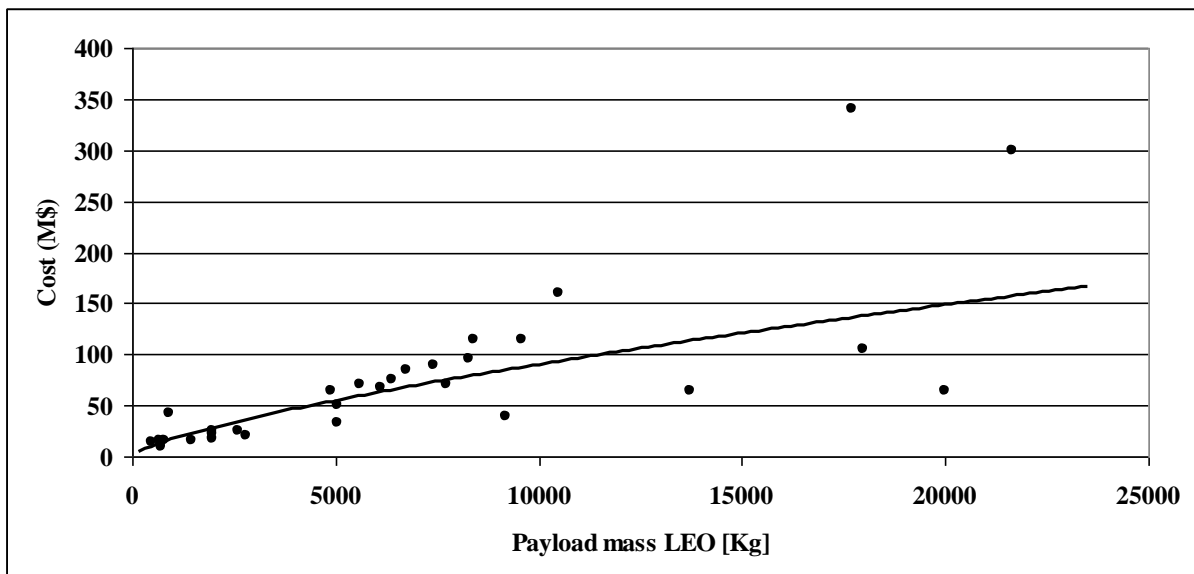


Figure 24 Launch cost as function of payload mass to LEO

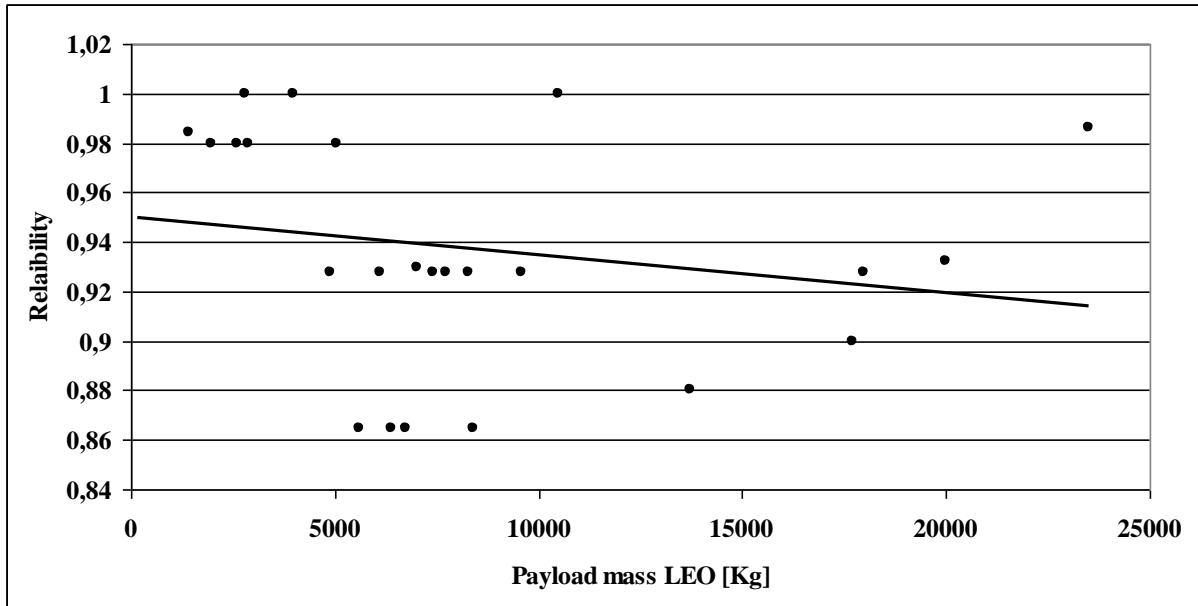


Figure 25 Launch reliability as function of payload mass to LEO

Table 11 shows the fairing dimensions for the considered launchers. The fairing of the launcher is not always characterized by a constant section. For this reason it has been schematically assumed as a combination of a cylindrical of constant diameter (Φ) and a tapered section, as Figure 26 shows. Obviously, where information are not available, these have been omitted.

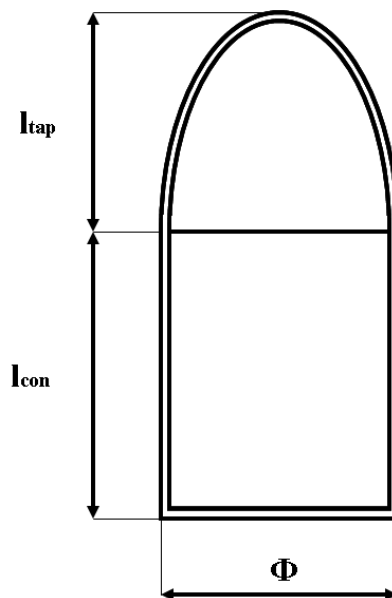


Figure 26 Fairing envelop definition, Φ : diameter of the cylindrical section; l_{con} : length of the cylindrical section; l_{tap} : length of the tapered section

Launcher	Φ [m]	l [m]	Launcher	Φ [m]	l [m]
AR40			LLV-2		
AR42L			LLV-3		
AR42P	3.65	6.52 con, 4.52 tap	Long March (CZ-1D)	1.56	1 con, 1 tap
AR44L			Long March (CZ-2C)	3.07	2 con, 3 tap
AR44LP			Long March (CZ-2E)	3.8	6 con, 4 tap
AR44P			Long March (CZ-3)	2.7	2.6 con, 2.5 tap
AR5			4.57	10.35	Long March (CZ-3A)
ASLV	1	3.2	Long March (CZ-3B)	3.8	6 con, 4 tap
Athena-1	1.98	2.3 con, 2 tap	Long March (CZ-4)	3	3.9 con, 2.6 tap
Athena-2			M-3SII	1.4	2.06 con, 1.4 tap
Athena-3	3.28	5.5 con, 3.2 tap	Molniya	2.65	1.65 con, 2.05 tap
Atlas I			M-V	2.2	3.5 con, 2.6 tap
Atlas II			Pegasus	1.12	1.11 con, 1.02 tap
Atlas IIA	2.92	4.19 con, 5.55 tap	Pegasus XL	1.12	1.11 con, 1.02 tap
Atlas IIAS			Proton D-1	4.1	10.8 con, 3 tap
Conestoga 1229			Proton D-1e	4.35	3.5 con, 4.3 tap
Conestoga 1620			PSLV	3.2	8.3
Conestoga 1679			Roskot (SS-19)	2.5	
Delta II 6925			Shavit		1.2
Delta II 7326	2.79	3.7 con, 2.4 tap	Shuttle/RSRM	4.7	18.6
Delta II 7925			Soyuz	2.85	6.72 con, 2.28 tap
Delta III			Start-1	1.45	2.2 con, 0.62 tap
Delta Lite			Taurus	1.37	2.8 con, 0.51 tap
Delta Lite			Titan II	2.84	5.1 con, 1.6 tap
Energia	5.5	37	Titan III	3.65	11 dual
GSLV	3.4	7.8	Titan IV /SRMU	4.57	12.2 con, 4 tap
H-2	4.6	9.2	Titan IV/SRM		
Ikar-1 (SS-18)	2.7	1.88 con, 2.78 tap	Tsyklon (SL-11)	2.13	14.1
Ikar-2 (SS-18)	2.38	3.84 con, 2.5 tap	Tsyklon (SL-14)	2.42	3.4 con, 2.5 tap
J-1			Vostok		
Kosmos (SS-5)	2.4	1.8 con, 2.9 tap	Zenit-2	3.3	8.4 con, 3.8 tap
LLV-1			Zenit-3	3.7	6 con, 5 tap

Table 11 Launcher data base: fairing dimensions (con: fairing conical section, tap: fairing tapered section), ref. [4]

4.13 Cost

Space system costs cannot be estimated with a high level of confidence, especially in the early design phases. This is because in the aerospace field a mass-production does not exist and because the knowledge of the production costs of the existing products is not public, at all. As a consequence, the traditional cost models assume costs proportional to mass and system complexity. The method implemented and adopted to estimate the building-blocks cost is based on the advanced missions cost model (AMCM) proposed by NASA, ref., [4] and [26]. This is a parametric cost model that can be applied in the first phases (A and B) of the design of a spacecraft where not detailed information about the system design is available. Other methods useful for estimation of cost exist. These methods estimate the cost of a spacecraft for analogy, grassroots and again on system parameters (generally the mass). Grass roots cost model estimate the cost of a spacecraft with a bottom-up approach. Basically, the cost is obtained by the sum of the cost of each component of the spacecraft itself. Thus, very detailed information of the spacecraft design is necessary because the cost of each component

is estimated considering the cost of the material and labor to develop and produce the component itself. Analogy cost model is a method to estimate the cost of a system based on the analogy with other systems (of known cost) with similar performances and characteristics. Considering the main differences amongst the two systems and engineering judgment the cost of the new spacecraft is estimated. The problem of these methods is that, often, spacecraft are unique systems and the cost is not available. Parametric cost models assume the cost of a spacecraft as proportional to the system characteristics, performances and functionalities. In aerospace, the main cost models, for estimation of the cost of a manned or unmanned spacecraft, are the AMCM, the NASA-Air Force Cost Model (NAFCOM) and PRICE.

NAFCOM cost model has been developed by NASA and it is based on data from the Mercury, Gemini, Apollo, Skylab, Shuttle Orbiter and Spacelab programs. The cost model estimates the cost of each spacecraft subsystem on the base of mass, power and number of devices and then, to this, sums the costs for design, development, test and evaluation which can not be attributed to a single subsystem.

PRICE cost model is a commercial tool that allows estimation of development and production costs for hardware and software. It is a parametric cost model and requires a lot of information (that sometimes in the first phases can be not available) and it is very sensible to the design. This means that a little variation on an input parameter can change a lot the cost of the system/subsystem.

The AMCM (the reference cost model) is a parametric model suitable for manned and unmanned space systems and useful to estimate development and production costs of the spacecraft. The AMCM is not only based on the mass, but it takes into accounts also the type of system (manned habitat, manned re-entry, planetary lander, etc.), the level of design inheritance of the system, the level of programmatic and technical difficulty anticipated for the new system, and the total number of units that will be produced. The cost model is based on a database of more than 260 programs, ref. [26]. The equation used to estimate the cost is the following:

$$C = \alpha Q_e^\beta M_d^\Xi \delta^{S_p} \varepsilon^{(1/(IOC-1900))} B_n^\phi \gamma^{D_c} \quad [161]$$

where the cost regression coefficient α is equal to 5.04839×10^{-4} , β is equal to 0.594183076, Ξ is equal to 0.653947922, δ is equal to 76.99939424, ε is equal to 1.68051×10^{-52} , Φ is equal to -0.355322218 and γ is equal to 1.554982942. The IOC is the year of Initial Operating Capability and for space systems. This is the year in which the spacecraft or vehicle is first launched. Q_e is the development and production quantities of the system expressed in equivalent unit, while M_d is the dry mass of the system in Pounds. The parameter S_p is the *Specification*. It designates the type of mission that is going to be flown (e.g., planetary, physics and astronomy, Earth observation). The parameter B_n is the system's block number, which represents the level of design inheritance. It is equal to 1 if the design is completely new while it is equal to 2 or more if the design is derived by an existing one. Finally, D_c is a qualitative assessment of the relative programmatic and technical development and production complexity of the element. It may range between -2.5 (design extremely easy) to 2.5 (design extremely complex).

5 Analysis methods

5.1 Value Analysis

A standard formula to evaluate a space mission does not exist. As reported in ref. [4], if the possible mission options have equal or similar performances the selection of the best one can be based on the mission cost. On the other hand, if the mission options imply different performances and success ratio, the comparison of the alternative mission concepts becomes more challenging. Nevertheless, the space-mission value-analysis creates the basis to compare different architectures. Once the necessary system functions have been established, the value analysis allows the definition of the cost-effectiveness (or value, V) of a mission by dividing the system global functionality (f) by its cost (C) and multiplying per the mission success ratio (p).

$$V = \frac{f}{C} p \quad [162]$$

The system global functionality (f) can be obtained by the sum of each system performance (P_n) multiplied by a weighting factor. The system performances include all that functions performed by a system and that have been considered important and representative of the mission capabilities. The performance can be expressed in term of capabilities of the system. The weighting factors ($\alpha_1, \alpha_2, \dots, \alpha_n$) indicate the relative importance of the system performances.

$$f = \alpha_1 P_1 + \dots + \alpha_n P_n \quad [163]$$

The mission success ratio is an indicator proportional to the probability of mission success. It strongly depends by the mission and a general equation representative of the parameter does not exist. Nevertheless, for general exploration missions, it can be considered proportional to the number of launches and docking/undocking maneuvers.

The value of a mission can be increased if variations of global functionality and/or cost are possible. Table 12 shows how the variation of the global functionality coupled with the variation of the cost affect the value of a system. The variation of the global functionality and/or cost shall be performed when the impact on the value is positive. When the impact is uncertain, it is necessary to assess the relative variation of cost and benefits. Obviously if the value decreases, the system configuration shall not be changed in that direction.

Value variation	Impact
$V = \frac{f \uparrow}{C \downarrow}$	Positive
$V = \frac{f \uparrow}{C \uparrow}$	Uncertain
$V = \frac{f \downarrow}{C \uparrow}$	Negative
$V = \frac{f \downarrow}{C \downarrow}$	Uncertain

$V = \frac{f \rightarrow}{C \downarrow}$	Positive
$V = \frac{f \uparrow}{C \rightarrow}$	Positive
$V = \frac{f \rightarrow}{C \uparrow}$	Negative
$V = \frac{f \downarrow}{C \rightarrow}$	Negative

Table 12 Variation of the value

The value analysis is a method utilized by the value engineering. This is a creative, structures approach, function oriented, based on the identification of the functions to be implemented by a system and their cost. The scope of the value engineering is the identification of all the basic and secondary functions and the attribution of the cost to each of them to eventually adopts measures useful to reduce costs.

The functional analysis methodology allows decomposition of the system functions and organization of them into a logic diagram called functional diagram, Figure 27. A functional diagram graphically displays the functions dependency and supports the study of the functions links. The functional diagram has two main directions, one vertical and one horizontal. The vertical direction is also called “how-why”. The top-down direction starts with the basic functions and for each ask “how” it is performed. The question is repeated until the lowest function. The bottom-up direction starts with the lowest level functions and crosses the diagram answering the question “why”, so expressing the goal of the functions. The horizontal direction is also called “when”. It is not a time orientation but shall be intended as a “as well as” orientation.

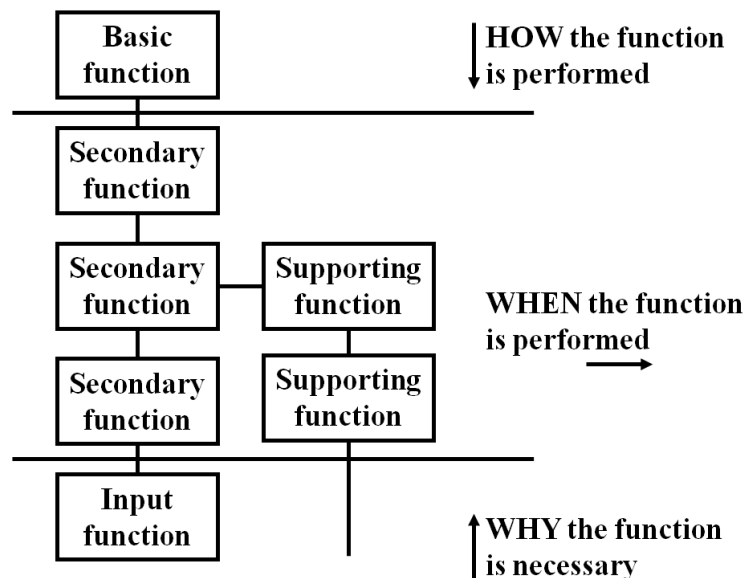


Figure 27 Functional diagram

Once the functions of a system have been identified, it is necessary to identify their cost. The method to assess the function cost foresees three main steps. The first step foresees to create a matrix with all the functions on the rows and all the components on the columns as Table 13 shows. The second step foresees to identify the components that perform a certain function. There could be components that perform a single function, components that perform

more than one function and functions that are performed by more than one component. The third step foresees the identification of the cost of each function. If the function is performed by a component only, the cost of the function is equal to the cost of the component. If a function is performed by more than one component, the cost of the function is the sum of the cost of the components. If a component performs more than one function, the cost of the component shall be distributed between the functions performed. There are more than one method to perform cost allocation:

- The proportional method foresees to make a specific analysis to assess how much a component is dedicated to a certain function and then to attribute proportionally the component cost to that function.
- The marginal method foresees to identify the less important function performed by a component and then to assess the cost of the component in the case it not perform that function. The cost to be attributed to the function is equal to the difference of the component cost.
-

	Component 1	Component 2	Component ...	Component ...	Component ...	Component ...	Component n	
	C1	C2	C...	C...	C...	C...	Cn	
Function 1	α_{11}							$F_1=C_1$
Function 2		α_{22}	α_{23}					$F_2=C_1+C_2$
Function ...				$\alpha_{...}$				$F_{...} = \alpha_{...} \times C_{...}$
Function ...				$\alpha_{...}$				$F_{...} = \alpha_{...} \times C_{...}$
Function ...					$\alpha_{...}$	$\alpha_{...}$	$\alpha_{...n}$	$F_{...} = \sum(\alpha_{...} \times C_{...})$
Function n					$\alpha_{n...}$	$\alpha_{n...}$	α_{nn}	$F_{ij} = \sum(\alpha_{ij} \times C_{ij})$

Table 13 Function-components matrix

As example of application of the value analysis, a study about an hypothetical mission for ISS logistic support is performed. The mission need is to transport six crew members to the ISS and return them safely on the Earth at any time during the mission. Figure 28 shows the mission concept: the capsule and the service module are launched in LEO. The service module performs a series of burns that put the two systems into ISS orbit. The two systems perform rendezvous and docking (RvD) with the ISS. Once the activities on the ISS have been completed, the crew returns on the capsule. The service module and the capsule perform ISS undocking and de-orbit burns. After burn completion, the service module is discarded. The capsule performs re-entry and landing.

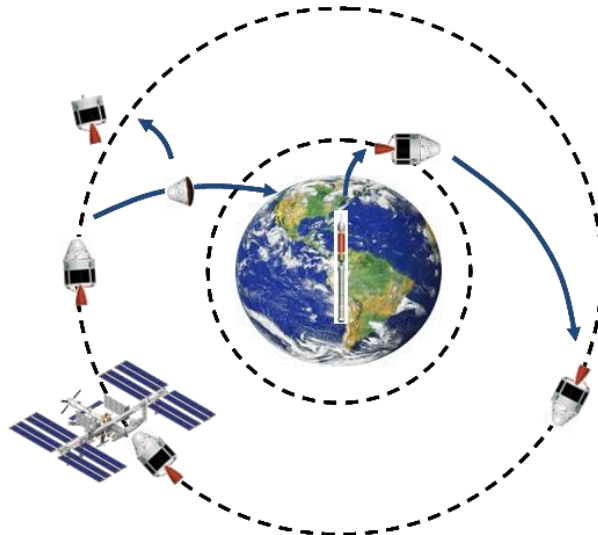


Figure 28 Mission architecture for ISS logistic support

Figure 29 shows a top level functional diagram for the ISS facility. The first level of the functional tree includes three voices: in order to have a research facility in LEO is necessary to provide transport, payload support and operation support. The second level functions explain how the first level functions must be performed. Each second level function includes a very large number of sub-levels until the definition of the components. In this example only the “provide space logistics” function will be implemented until the seventh sublevel for simplicity.

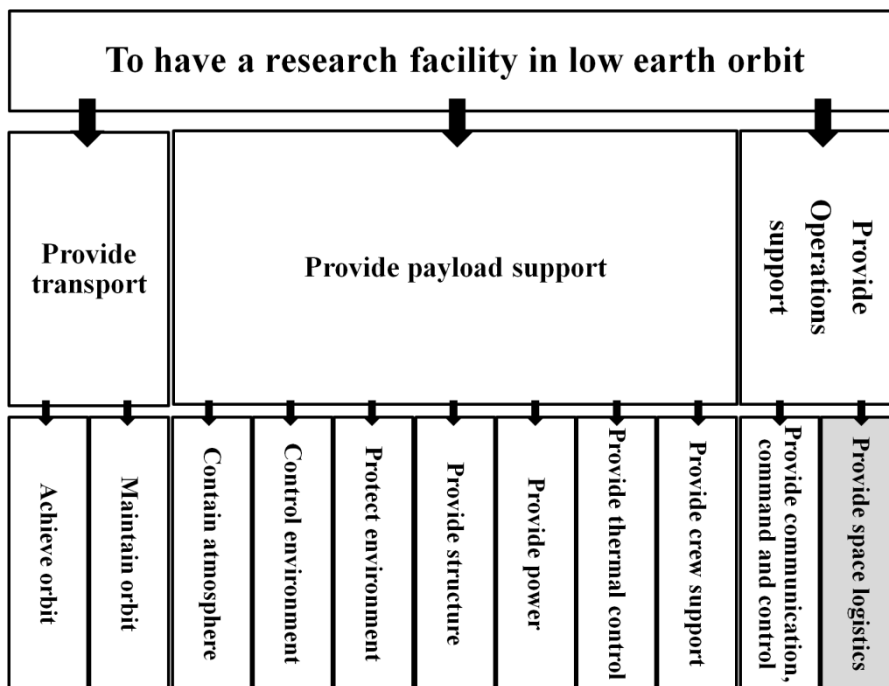


Figure 29 Top level functional diagram for the ISS facility

Logistics is the “art and science of management, engineering, and technical activities concerned with requirements, design supply, and maintaining resources to support objectives, plans and operations”, ref. [27]. The definition of logistic allows to identify the sublevel functions to provide logistic: in order to provide space logistic, it is necessary to provide software support, logistic facilities, support equipment, technical data and documentation,

packaging and transporting, maintenance and supply. Provide supplies includes all the activities useful to provisioning, buying, inventorying, warehousing, and distributing all pieces of equipment, spares, repair parts, consumables, special supplies and associated documents, schedule or resources. Crew members can be considered as resources that must be managed. Crew rotation ensures that the astronaut health is ensured.

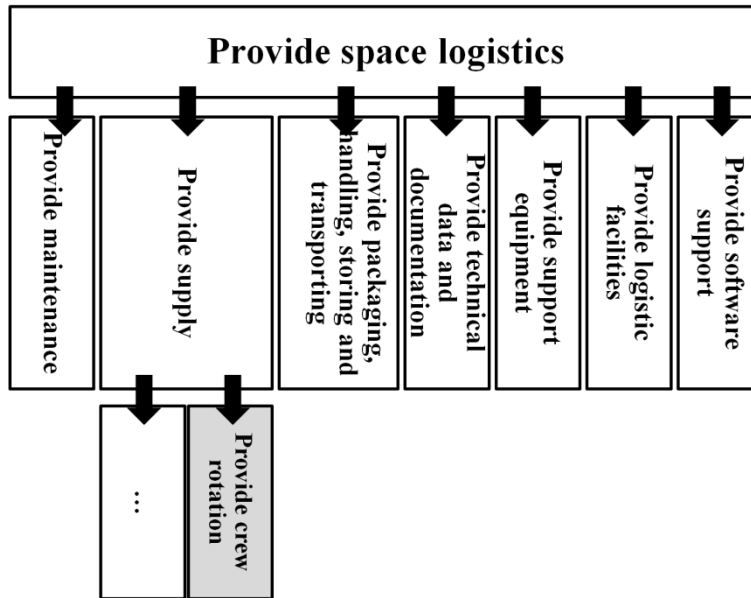


Figure 30 Functional diagram for supply function

In order to provide crew rotation is necessary to provide transport from Earth surface to LEO. At the same time it is necessary to provide payload support (in this case only the astronauts as hypothesis) and operations support. The sublevel functions are sufficiently detailed to define the components (as space elements) that perform such functions.

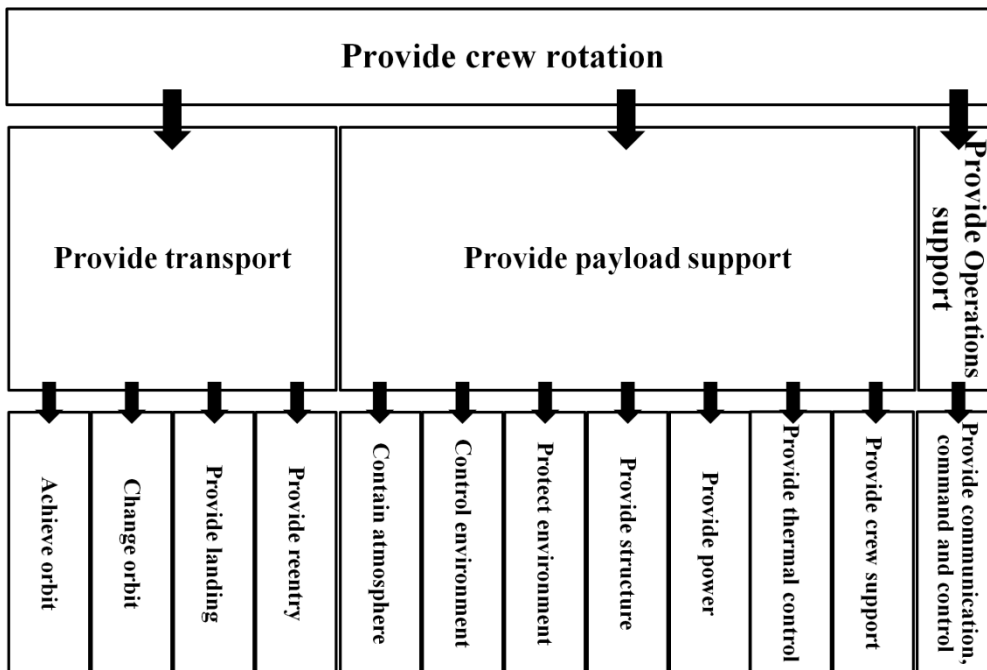


Figure 31 Functional diagram for crew rotation function

The identified space elements are the launcher, the capsule and the capsule service module. In Figure 32, all the low level functions, that have been identified, are listed on the first line of the table. The components have been listed in the first column. Then, the functional allocation has been performed. The result shows that a component performs more than a function and that some functions are performed by more than a component.

At so high level of design a mark in this matrix is very important because it influences the design of the corresponding space element. To put or not to put a mark in a determinate cell could involve into two completely different components. For example, the NASA STS (or Space shuttle system) is a particular system that performs all the functions (and more) listed.

	Achieve orbit	Change orbit	Provide landing	Provide reentry	Contain atmosphere	Control environment	Control environment	Control environment	Control environment	Control environment	Control environment	Provide crew support	Provide communication, command and control
Capsule			X	X	X	X	X	X	X	X	X	X	X
Service module		X						X	X	X	X	X	X
Launcher	X												

Figure 32 Matrix functions-components

Figure 33 and Figure 34 show the costs allocation to each function for the capsule and the service module respectively. The cost allocation has been performed on the base of the mass of each subsystem, utilizing the proportional method previously presented and assuming that the total system cost is 100. The cells of the matrixes report the percentage of the subsystem cost associated to the function and last column shows the cost of each function.

CAPSULE	Structure sys	Protection sys	Propulsion sys	Power sys	Avionics sys	Environment sys	Other sys	
Provide landing							100%	15
Provide reentry		88%	100%		50%			24,8
Contain atmosphere	40%							10
Control environment						38%		6,84
Protect environment	40%	12%						11,7
Provide structure	20%							5
Provide power				100%				12
Provide thermal control						14%		2,52
Provide crew support						48%		8,64
Provide communication, command and control					50%			3,5
TOT SYS COST	25	14	9	12	7	18	15	100

Figure 33 Cost assessment for the capsule

SERVICE MODULE	Structure sys	Protection sys	Propulsion sys	Power sys	Avionics sys	Environment sys	
Change orbit			100%				51
Provide structure	100%						14
Provide power				100%			7
Provide thermal control		100%				100%	24
Provide communication, command and control					100%		18
TOTSYS COST	22	6	51	12	5	4	100

Figure 34 Cost assessment for the service module

For what concerns the capsule, the functional costs allocation is reasonable because the main functions of the capsule (ensure crew life and re-entry) are the most costly. Figure 33 shows that the most costly function is “provide re-entry” that imply the 24 percent of the total cost. Provide power, landing and protect environment imply the 30 percent of the total cost (about 10% each).

For what concerns the service module, the most costly function is “change orbit”. Also for the capsule service module, the most costly function is also the main function of the space element.

The cost model so implemented cannot give information on the space elements relative cost. However considerations can be done to find a way to reduce costs.

5.2 Sensitivity and Optimization Analysis

The sensitivity and optimization analyses introduced and described in this section have been implemented by Guido Ridolfi in the framework of his PhD studies at the Politecnico di Torino. The natural collaboration that is born allowed us to obtain synergisms with benefic effects on the results of the research activities. Thus, the integration of the sensitivity and optimization analyses with the modeling framework described in the previously sections allowed to find application of the analysis techniques and at the same time testing and debugging of the SoS models.

The final result of the collaboration has been the integration of the sensitivity and optimization analyses in the simulation software tool that is one of the results of this research activity.

For completeness, the analysis techniques have been introduced and described in this section. Nevertheless, a more detailed discussion is reported in ref. [28].

A schematic representation of the analysis methodology applied to the modeling framework is shown in Figure 35. The objective is to select the best combination of the levels of the design parameters to optimize the performances while satisfying boundaries and constraints. Typically, continuous and discrete, or architectural, variables are of interest for the analysis. At first, a sensitivity analysis is carried out to have a first impression on the relative importance of the design parameters on the performances. The sensitivity analysis is performed utilizing the factorial technique to speed up the process reducing the number of model runs. Then, a multi-objective optimization process is executed considering the most

relevant factors only, fixing the others. This allows, reducing the design space dimensionality, to facilitate and speed up the optimization process.

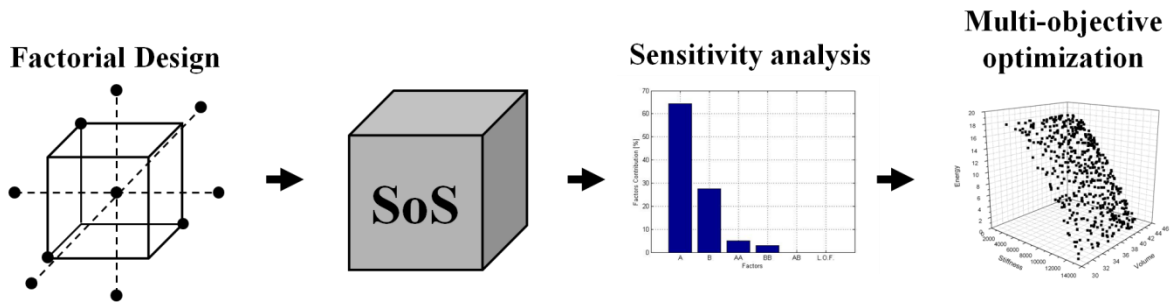


Figure 35 Design methodology

5.2.1 Sensitivity analysis: the method of Morris

The method of Morris was introduced to solve the problem of designing computational experiments to determine the subset of input factors having important effects on the model output, ref. [27]. The method is based on the so-called *elementary effect*, which is a measure of the sensitivity in the form of incremental ratios, i.e., an approximation of a local derivative within a finite interval of variation of the variable:

$$d_i(\mathbf{x}) = \frac{[y(x_1, \dots, x_{i-1}, x_i + \Delta, x_{i+1}, \dots, x_k) - y(\mathbf{x})]}{\Delta} \quad [164]$$

As such, the elementary effect is a local measure of sensitivity. However, in the method of Morris, the final value attributed to the sensitivity of each design variable is obtained by averaging several elementary effects and their absolute values computed at different points of the input space, ref. [29]. In Eq. [164], Δ is the width of the step in the i^{th} dimension of the design region needed to compute the incremental ratio. To compute the sensitivity measures for all the factors the design region is fractioned into a grid of dimensions $k_f \times P$, where k_f is the number of factors and P is the number of levels in which every dimension is subdivided. The influence of a factor is determined by computing several elementary effects (the number of elementary effects is indicated by R_e) at points randomly selected from the grid. The value of Δ is defined as a multiple of $1/(1-P)$.

The method of Morris provides two qualitative measures of sensitivity, namely the mean μ and the standard deviation σ of the elementary effects.

$$\mu = \sum_{i=1}^{R_e} \frac{d_i}{R_e} \quad \sigma = \sqrt{\sum_{i=1}^{R_e} \frac{(d_i - \mu)^2}{R_e}} \quad [165]$$

Large values of μ indicate that a factor has a prominent overall influence on the output. Large values of σ , instead, are the result of interactions of the factors with other factors or non-linear effects on the output. An alternative measure of the parameter μ was introduced by Campolongo et al. in ref. [30] to avoid misleading results with non-monotonic models. Indeed, computing the mean of the elementary-effect distribution in a non-monotonic model may cause some effects to cancel each other out. The alternative figure μ^* , computed as the mean of the distribution of the absolute values of the elementary effects, provides a more reliable

measure for ranking the factors. This measure presents the drawback of losing the sign of the effect. However this information is available by the analysis of μ , which comes at no extra computational effort.

$$\mu^* = \sum_{i=1}^{R_e} \frac{|d_i|}{R_e} \quad [166]$$

The computational cost of the method of Morris is linear with the number of factors, equal to $R_e \times (k_f + 1)$. A thorough description of the method of Morris and its implementation is provided in the original work of the author, ref. [27]. Saltelli et al. and Campolongo et al, respectively in ref. [29] and [30], describe instead the implementation of the method with the alternative measure of the mean. This method is very effective and computationally cheap in identifying factors with an overall contribution to the determination of the variability of the results obtained with the simulations.

The output of the sensitivity analysis is one or more graphs, one for each performance parameter object of the study. The sensitivity indicators μ^* and σ are plotted on the horizontal and vertical axis respectively as it can be seen in Figure 36. The most relevant design variables will have high values of σ and μ^* . The other variables with limited influence will have lower value. Thus, in the example of Figure 36, the variable A has a strong influence on the performance and none interactions with other factors or non-linear effects occur. The variable B has a strong effect on the performance of the system by interactions with other factors or by non-linear effects. The direct effect of B is very limited. The variable C has both a prominent direct influence on the performance and by interactions with other factors or by non-linear effects. The variable D has no effect on the performance of the system.

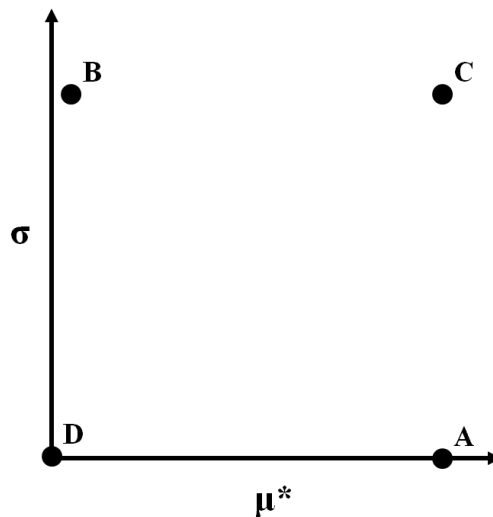


Figure 36 Example of screening analysis results

5.2.2 Multi-objective Optimization

Multi-objective optimization techniques aim at finding a set of good compromises, i.e., trade-offs, rather than a single optimal solution, by optimizing all the objectives of a given problem simultaneously. The set of solutions is usually found using the Pareto-optimality concept. A solution is defined to be Pareto-optimal or *non-dominated* if there is no feasible solution for which one cannot improve a single objective without causing a degradation of at least one other objective. According to the Pareto-optimality concept, a variables vector a is

said to dominate another vector \mathbf{b} in a maximization problem with N objectives, also written as $\mathbf{a} \prec \mathbf{b}$, if and only if the following relationship holds:

$$\forall i \in \{1, \dots, N\}: f_i(\mathbf{a}) \geq f_i(\mathbf{b}) \wedge \exists j \in \{1, \dots, N\}: f_j(\mathbf{a}) > f_j(\mathbf{b}) \quad [167]$$

The set of *non-dominated* vectors, plotted in the objective space is defined as the Pareto front.

Many multi-objective optimization techniques and algorithms have been developed and implemented to date, to solve *ad-hoc* mathematical problems. Examples include genetic algorithms, evolutionary algorithms based on swarm intelligence and tabu-search based algorithms. These are described in detail and compared in many publications, such as ref. [31] and [32].

Each one has specific advantages and disadvantages, mostly related to the problem to be solved. The Non-dominated Sorting Genetic Algorithm II (NSGAI), ref. [33], is a population-based evolutionary algorithm. It was developed as an improved version of the NSGA proposed earlier, ref. [32]. As in the original concept of genetic algorithms (developed for single-objective implementations), NSGAI uses techniques inspired by the natural evolutions, e.g., crossover, mutation, and individuals selection. The Multiple Objectives Particle Swarm Optimization, ref. [34], is an extension of the Particle Swarm Optimization (PSO) approach proposed in ref. [35]. The PSO is a distributed behavioral algorithm, also classified as an agent-based algorithm, inspired by the social dynamics of groups of individuals (e.g., flocks of birds or fish schoolings).

Zhang and Li, ref. [36], present an alternative method for computing the Pareto front of multi-objective problems. The Multi-objective Evolutionary Algorithm Based on Decomposition (MOEA/D) method is based on the decomposition of the multi-objective problem into a number of scalar sub-problems and on their simultaneous optimization. Consider for instance a two-objectives (f_1 and f_2) problem. The transformed scalar optimization problem can be formulated as the optimization of the functional $F = \lambda_1 f_1(\mathbf{x}) + \lambda_2 f_2(\mathbf{x})$, where the λ_i are coefficients subject to $\sum \lambda_i = 1$, and \mathbf{x} is the vector of the variables. This weighted-sum approach allows generating a set of N different Pareto optimal vectors by using N different weights combinations. In ref. [36], the Tchebycheff approach and the boundary-intersection approach for the decomposition of the multi-objective problem are discussed and compared as well.

For comparison purposes, in ref. [28] the NSGAI, the MOPSO, and the MOEA/D have been tested on most of the constrained and un-constrained problems proposed in ref. [37], [38], [39] and [40].

As a result of the testing process, the author conclude that MOEA/D reaches the Pareto front quickly when compared to MOPSO and NSGAI, and it is more accurate in the determination of the Pareto-front maintaining a higher level of diversity of the solutions. This means that using the MOEA/D there are high chances of getting solutions close to the true Pareto front and that the solutions presented at the end of the process are *more diverse* from each other, giving more degrees-of-freedom for the final decision process as will be demonstrated later in this section. Due to its capability to deal with constrained multi-objective problems, in the presence of different types of Pareto fronts, and due to its convergence speed, accuracy and solution diversity characteristic, the MOEA/D algorithm has been utilized for the optimization analyses.

A detailed description of the optimization methodology introduced in this section is reported in ref. [28].

The output of the optimization analysis is a graph on which two of the performance parameter object of the optimization analysis can be plotted. The Pareto front obtained shows that combination of variables for which is not possible to improve one objective without worsening the other. Therefore, all the solutions are optimal solutions. The choice of the most suitable design is then delegated to the engineering team on the base of its engineering judgment.

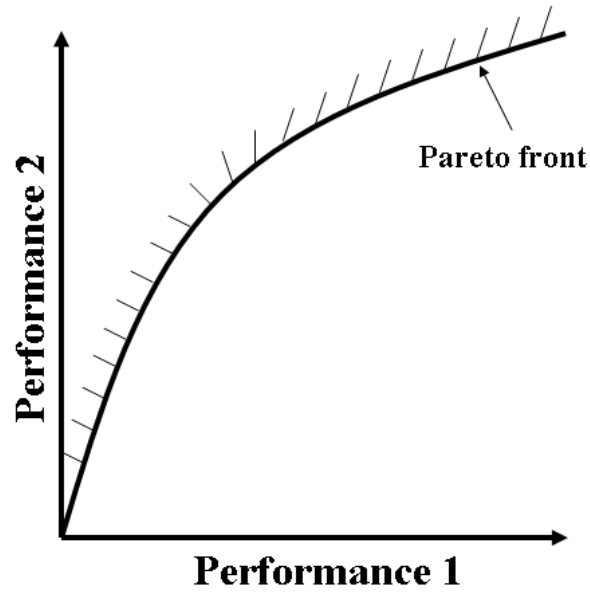


Figure 37 Example of optimization analysis results

6 Scenario Evaluator Tool

6.1 Tool scope

The concept of the Scenario Evaluator Tool (SET) derives from putting together the modeling strategies and the design methodologies developed in the framework of the research presented, with a functional graphical user interface.

SET supports the design team in the framework of the space mission design process, allowing mission architecture definition and building block engineering with a significantly reduction of time and computational effort. The software allows the characterization, comparison and optimization of exploration scenarios and building blocks. The characterization of a particular mission architecture is provided by evaluation and definition of the mass budget of the space elements present in the mission scenario, cost index and exploration capabilities. These information are then useful to perform trade-off of the different possible solutions to the same problem.

SET is implemented in Matlab and shows the results directly to the user through Graphical User Interface (GUI) and exports them through an Excel file that can be used for post-processing analyses. SET is conceived in order to be applicable at several space exploration scenarios for Gap-analysis studies and allows introduction/customization of the models libraries to introduce new space elements or to modify the existents.

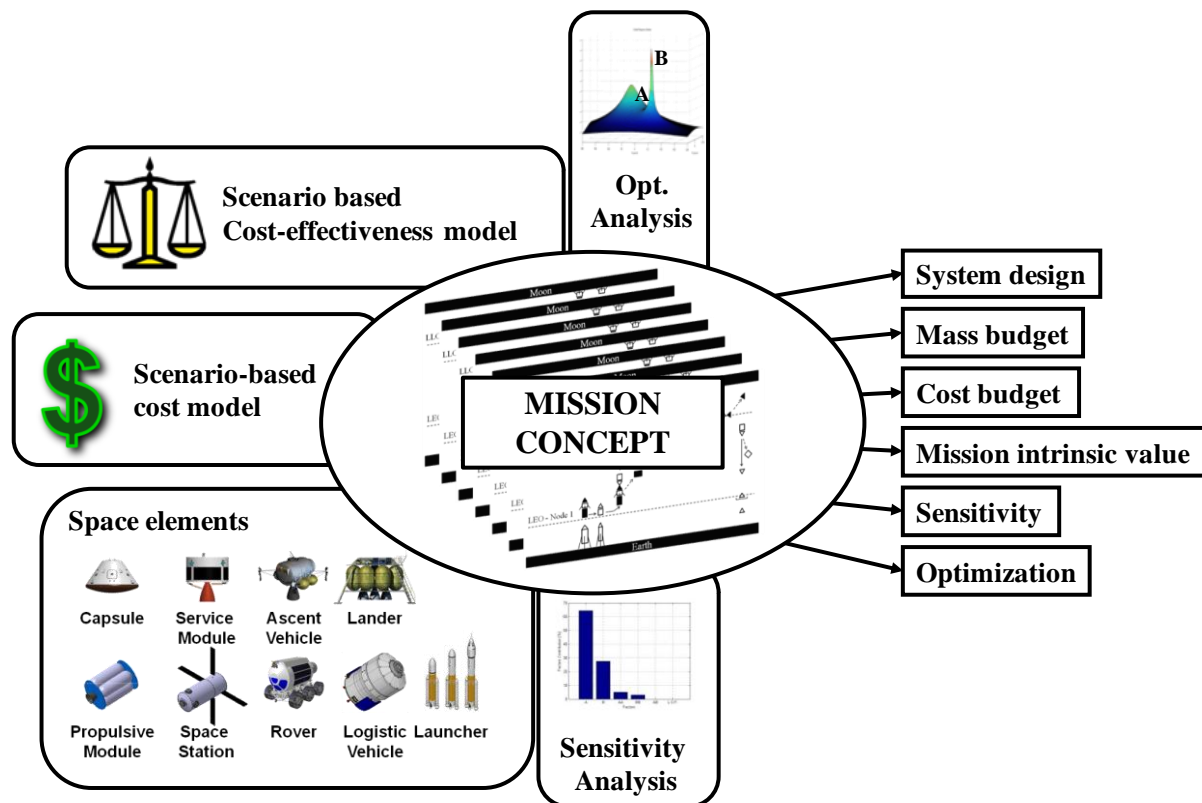


Figure 38 Scenario Evaluator Tool (SET)

6.2 Tool description

6.2.1 Tool general description

The Graphical User Interface is organized in four main tabs, through which the user provides inputs and access to the results, see Figure 39. The SET tabs are the scenario tab, the building blocks tab, the results tab and analysis tab. The scenario tab allows the user to

specify the mission scenario and the mission architecture. Thus, the user selects the number of mission phases and the number and typology of building blocks that take part actively (the space element that performs an action during a mission phase) or passively (the space elements acting as a payload) to the maneuvers. The scenario description is completed by the selection of the starting and destination nodes. The nodes are positions in space intended as orbits around celestial body or surface locations. SET is provided with a database of nodes to which the corresponding values of ΔV is associated. In any case, the user can set-up the ΔV at via graphical interface.

Once the mission scenario has been described, the user shall provide the design input of the space elements (or building blocks) present in the mission scenario. The space elements available in the SET database are the Capsule, the Capsule Service Module, the Propulsion module #1, the Propulsion module #2, the Ascent module, the Descent Module, the Space Station Service module, the Space Station Node and the Space Station Integrated module. Moreover, SET is provided with seven generic space elements and two simple mass elements. Generic space elements are characterized by the ratio between the inert mass and the total mass, by the specific impulse (I_{sp}) and by the spacecraft typology. Mass elements are building blocks characterized by the mass and spacecraft typology. Both for generic modules and mass elements the typology of spacecraft that can be chosen includes Planetary Lander, Planetary, Manned Re-entry, Communication, Weather, Physics & Astronomy, Earth Observation, Lunar Rover, Manned Habitat, Unmanned Re-entry, Launch Vehicle Stage, Upper Stage, Liquid Rocket Engine - Lox/Lh, Liquid Rocket Engine - Lox/RP-1, Payload Fairing, Centaur Fairing. The typology of spacecraft is useful for the estimation of the building block cost.

The building blocks tab allows the user to specify the main building block design parameters. Once the user has selected the building block, he is free to change the default design parameters. Since the software is integrated with concurrent design methodologies that allow the tool to perform sensitivity analyses and optimization processes, in the building blocks tab, the user can also consider ranges of possible variation of the design parameters and the weighting factor necessary for the mission capability index definition. The weighting factor can be defined both for design parameters and performance parameters.

Once all the inputs concerning the mission scenario and the space elements have been provided, the user access to the results through the results tab and analysis tab. Although the results tab is an output tab, the user can still select some mission scenario features. In particular, the user can select the number of launches and which space element is launched with the launcher #1 or #2. Once all the inputs have been provided the tool shows all the results. The results tab provides the user with information about the mass budget of each space element, the total mass launched in orbit, and eventually the cost of the space element, of the launch and of global of the mission. Finally, the software provides the user with information about the mission capability index and mission cost-effectiveness (or value). All the mass results are provided in kilograms and all the cost information are provided in millions of dollars. Obviously the mission capability index and the mission value are dimensionless entities.

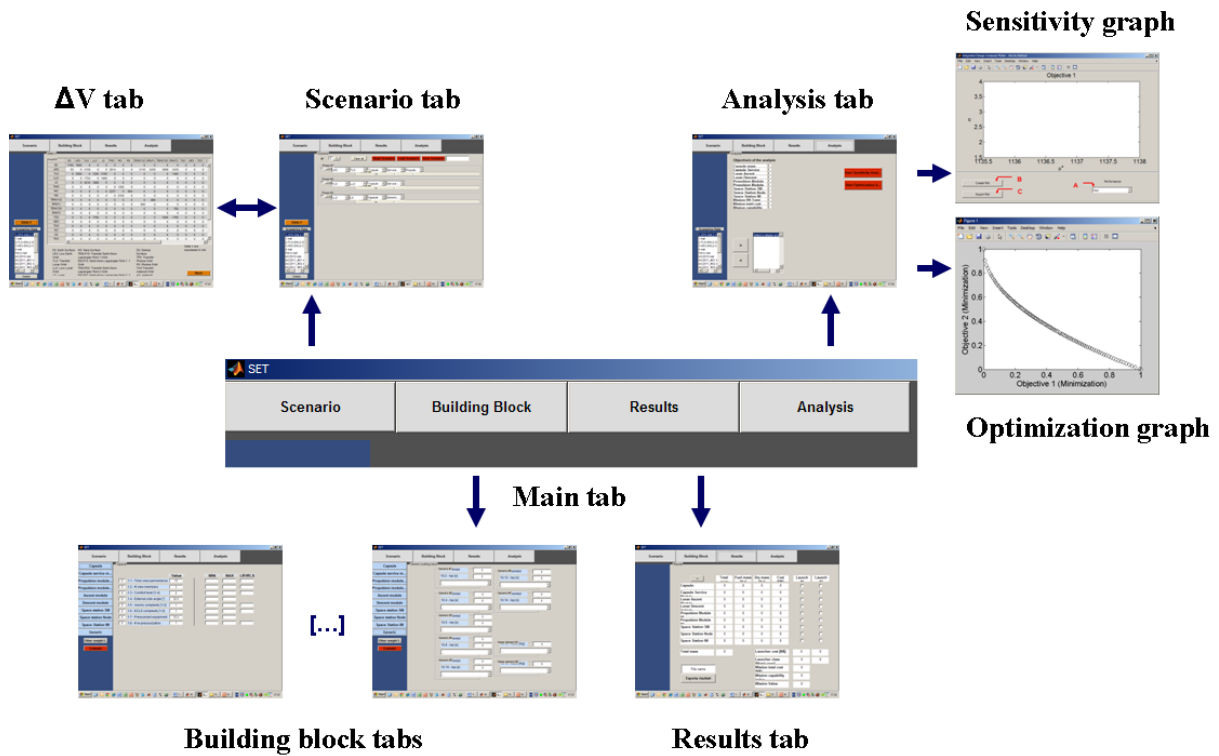


Figure 39 SET Graphical User Interface organization

The main screen of SET is shown in Figure 40. Mainly there are for tabs each of them allow specific actions. The SET tabs are the scenario tab, the building block tab, the results tab and analysis tab. The user has access to each of them by clicking on the corresponding push-button.

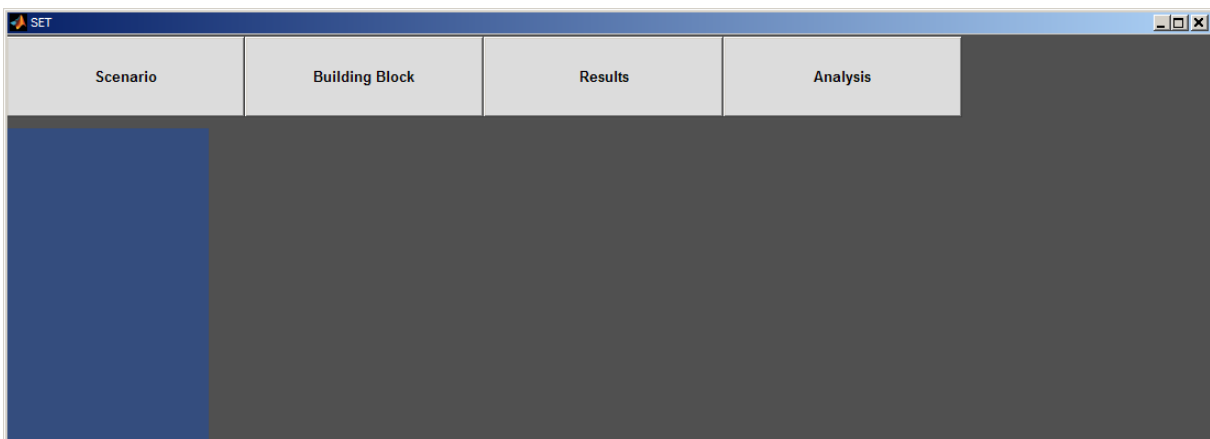


Figure 40 SET main interface

6.2.2 Scenario tab

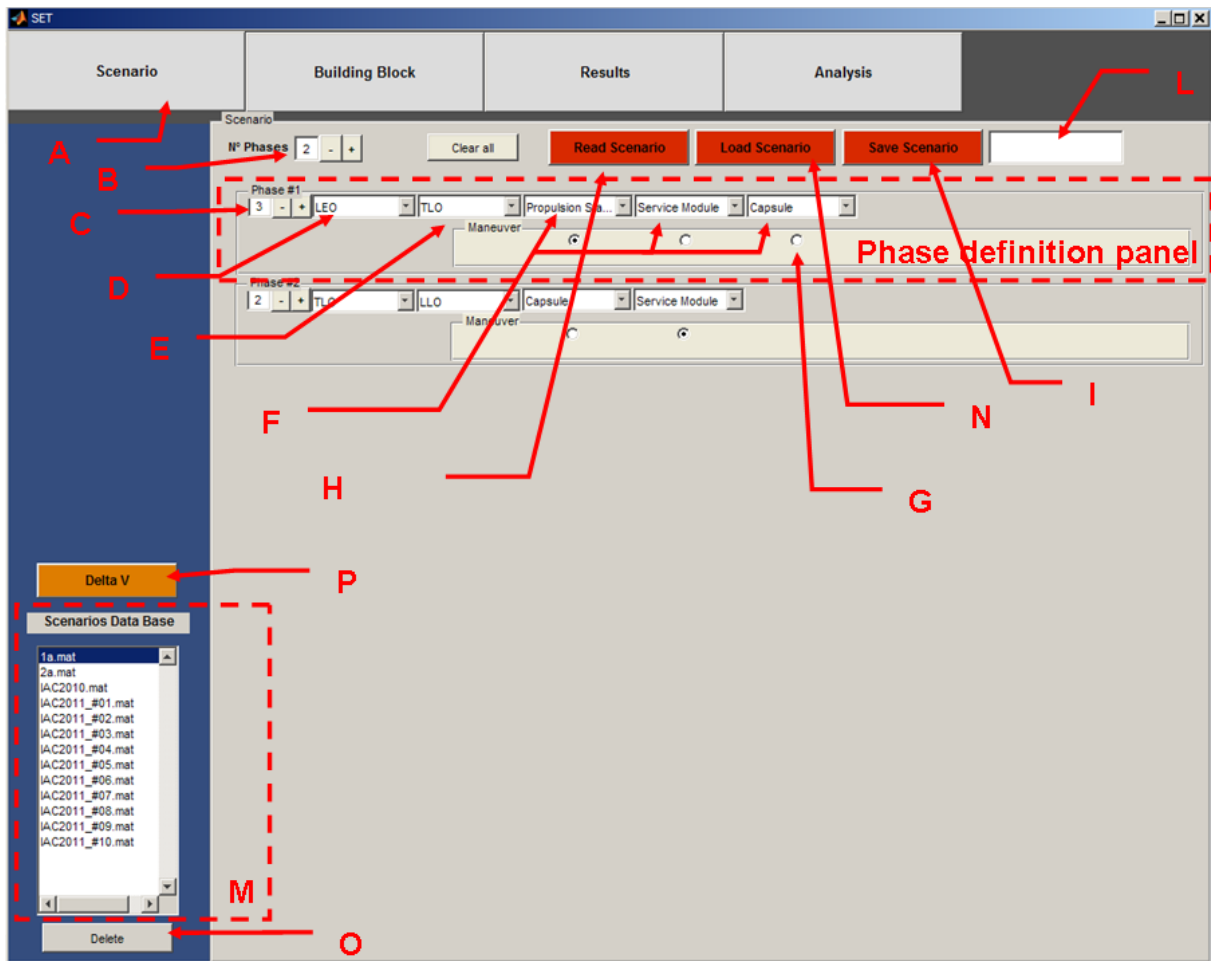


Figure 41 Scenario tab

The user accesses to the scenario tab clicking on the push-button A “Scenario”. The screen visualized is shown in Figure 41. This is an input tab that allows the user to specify the mission architecture. The input process is quite simple and starts by the definitions of the number of mission phases. The number of mission phases is indicated in the textbox B and can be increased or decreased clicking respectively on the adjacent push-button + and -. Once the number of phases is chosen the related phase definition panels appears. For each mission phase, the user can select the number of building blocks that are activated in the mission phase clicking on the push-button + and - located near the textbox C. The building block is considered activated if it takes part actively or passively at the maneuver phase. The textbox B shows the number of building blocks considered in the mission phase. Once the number of building block is selected, the user can select the starting node and the destination node clicking respectively on the list-box D and E. The nodes into the SET database are listed in Table 14.

Acronyms	Description
ES	Earth Surface
LEO	Low Earth Orbit
LTO	Lunar Transfer Orbit
LLO	Low Lunar Orbit
LS	Lunar Surface
MTO	Mars Transfer Orbit
MO	Mars Orbit
MS	Mars Surface
EMLP1TO	Earth-Moon Lagrangian Point 1 Transfer Orbit
EMLP1O	Earth-Moon Lagrangian Point 1 Orbit
EMLP2TO	Earth-Moon Lagrangian Point 2 Transfer Orbit
EMLP2O	Earth-Moon Lagrangian Point 2 Orbit
GTO	Geostationary Transfer orbit
GEO	Geostationary orbit
DTO	Deimos Transfer Orbit
DO	Deimos Orbit
DS	Deimos Surface
PTO	Phobos Transfer Orbit
PO	Phobos Orbit
ATO	Asteroid Transfer Orbit
AO	Asteroid Orbit
AS	Asteroid Surface

Table 14 Database of the node of SET

Figure 42 and Table 15 show the ΔV needed for various orbital maneuvers using conventional rockets and included into SET. In particular, Figure 42 graphically shows the ΔV map for the Earth-Moon and Earth-Mars systems as well as for a hypothetical asteroid. Black arrows indicate that an orbital maneuver is necessary to go from one location to the other and red arrow shows that direct re-entry is possible. Each orbital maneuver is associated to a number that is reported in Table 15 with the related ΔV necessary to perform the maneuver. The values of Table 15 have been obtained by literature survey on Moon and Mars missions and they have been included in the initial SET ΔV database. The SET ΔV database can be reached clicking on the push-button P. The panel visualized is shown in Figure 43. Mainly, the ΔV panel shows the ΔV table and allows the user to update the database values. The rows of the table indicate the starting point and the column of the table indicate the destination point. Once the new input has been provided, SET saves the new values autonomously. The user returns to the scenario tab clicking on the pushbutton A.

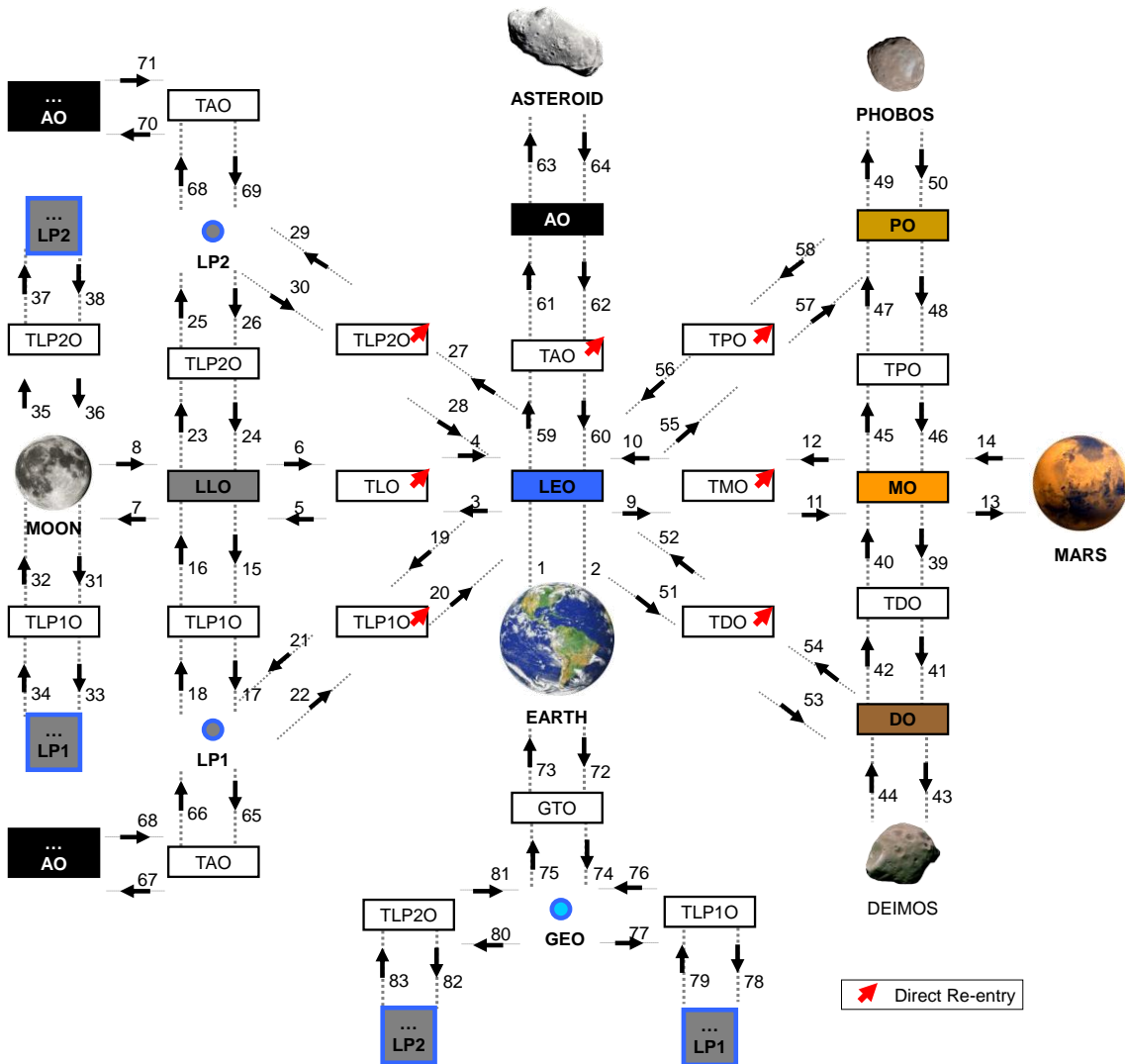


Figure 42 ΔV map

ΔV	Value [m/s]	ΔV	Value [m/s]	ΔV	Value [m/s]	ΔV	Value [m/s]	ΔV	Value [m/s]	ΔV	Value [m/s]
1	7900	16	N/A	31	N/A	46	N/A	61	1300	76	772
2	50	17	N/A	32	N/A	47	664	62	1600	77	N/A
3	3120	18	N/A	33	N/A	48	N/A	63	100	78	4
4	3000	19	3085	34	2750	49	N/A	64	200	79	N/A
5	1390	20	3085	35	N/A	50	N/A	65	N/A	80	N/A
6	1724	21	740	36	N/A	51	N/A	66	N/A	81	N/A
7	1900	22	740	37	N/A	52	N/A	67	N/A	82	N/A
8	1888	23	N/A	38	N/A	53	N/A	68	N/A	83	N/A
9	3614	24	N/A	39	N/A	54	N/A	69	N/A		
10	1365	25	N/A	40	N/A	55	N/A	70	N/A		
11	1285	26	N/A	41	N/A	56	N/A	71	N/A		
12	1419	27	3120	42	N/A	57	N/A	72	N/A		
13	694	28	3120	43	N/A	58	N/A	73	N/A		
14	5700	29	1160	44	N/A	59	4600	74	N/A		
15	N/A	30	1160	45	440	60	N/A	75	N/A		

Table 15 Maneuver ΔV database value

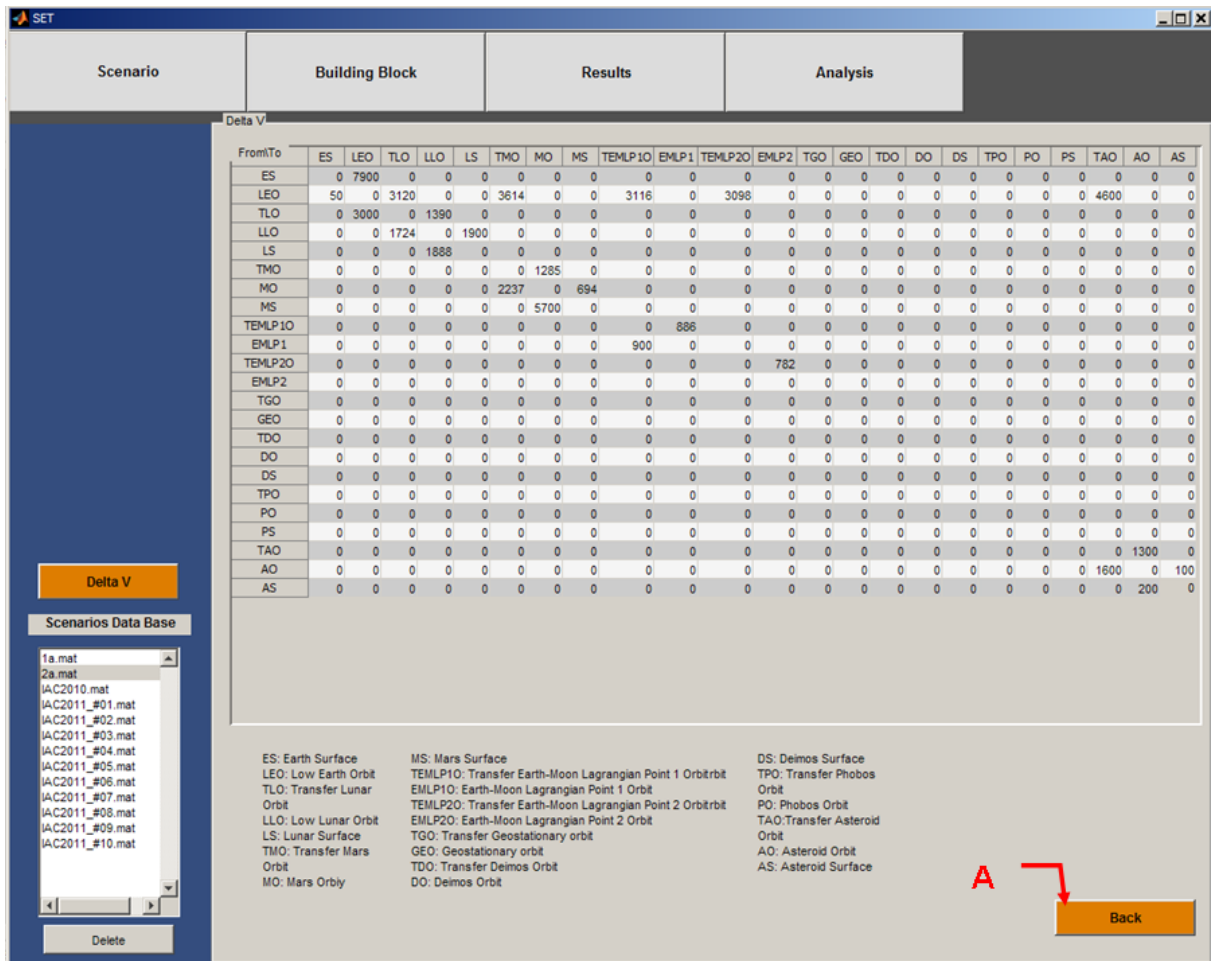


Figure 43 ΔV database tab

In the scenario tab (Figure 41), the list-boxes F allows to select the building blocks that are activated in the mission phase. The building block available in the SET database are the Capsule, the Capsule Service Module, the Propulsion module #1, the Propulsion module #2, the Ascent module, the Descent Module, the Space Station Service module, the Space Station Node and the Space Station Integrated module. Moreover, SET allows to select seven generic module and two mass elements. Generic modules are space elements characterized by the ratio between the inert mass and the total mass, by the specific impulse (I_{sp}) and by the spacecraft typology. Mass elements are space elements characterized by the mass and spacecraft typology (see next section for a detailed description).

In order to complete the definition of the mission phases, the user had to select the space element that provides the acceleration for the maneuver. This can be performed selecting one of the radio button G under the corresponding space element. The definition of the mission architecture can be considered completed when all the mission phases have been implemented.

Once the mission concept has been defined, the user had to click on the push-button H “read Scenario” so that the tool processes the information. Once the mission scenario has been processed, the user can save it into the database. This is possible clicking on the push-button I “Save Scenario”. The scenario is saved in the database with the name written in the text-box L. The accepted name cannot contain any of the following characters \ / : * ? “ < > |, the file extension must not be provided and the file name must be shorter than 207 characters. Once the mission scenario has been saved into the database, its name appears into the list-box M “Scenarios Data Base”. The user can load one of the scenarios saved into the database

selecting it into the list-box M and clicking on the push button N. Every time that a scenario has been read or saved, a text message appears on the screen to confirm it. Every time a scenario has been loaded it is displayed in the scenario tab.

Finally, the user can delete a scenario stored into the database clicking on it into the list-box M and then clicking on the push button O “Delete”

For what concerns the mission scenario definition, SET has some limitations that have been considered sufficient to the description of the most mission scenarios:

- a maximum of six building block can be selected for each mission phase
- each building block cannot be selected more than one time otherwise numerical error occurs
- the maximum number of mission phases has been limited to 8

6.2.3 Building Block tab

Building Block	Value	MIN	MAX	LEVELS
0 1.1 - Time crew permanence [days]	15			
0 1.2 - # crew members	3			
0 1.3 - Comfort level [1-4]	2			
0 1.4 - External side angle [°]	32.5			
0 1.5 - Avionic complexity [1-2]	1			
0 1.6 - ECLS complexity [1-2]	1			
0 1.7 - Pressurized equipment volume [m3]	15.4			
0 1.8 - # re-pressurization	1			

Figure 44 Building Block tab

The user accesses to the building block tab clicking on the push-button A “Building Block”. The screen visualized is shown in Figure 44. This is an input tab that allows the user to specify the main space elements design parameters. The user selects the building block clicking on the consistent push-button B. The screen example of Figure 44 shows the Capsule input panel. The name of the panel is reported in the text-box C. The panel is divided into two main parts. The first one, on the left of the panel, allows inserting of the value of the main design parameters of the space element. These inputs can be provided setting the relative numeric value into the text-box D. The tool suggests reference numeric values. The text-box E allows to specify the weighting factor associated to each design parameter and necessary for the mission capability index calculation. In this case, the default parameters are set to 0.

The software is integrated with concurrent design methodologies that allow the tool to perform sensitivity analyses and optimization processes. These analyses require additional information to be performed. In particular, it is necessary to provide information about the

ranges of possible variation of the design parameters. This operation can be performed providing the necessary numeric input into the text-boxes F, G and H on the right of the panel. The text-box F sets the minimum value of the range of variation, the text-box G sets the maximum value of the range of variation and finally, for the design parameters that does not allow continuous variations (such as the number of crew members on the capsule that must be an integer), the text-box H allows to set the number of levels (or intervals) between the minimum and maximum of the range of variation.

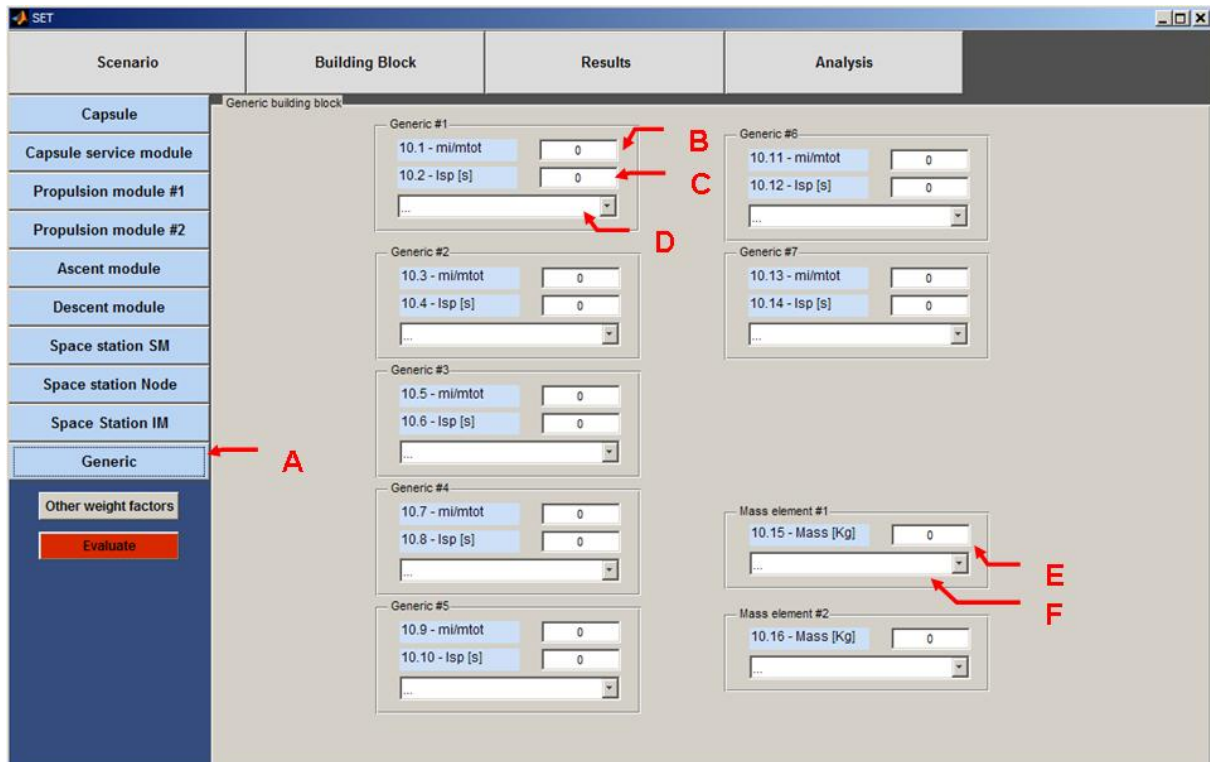


Figure 45 Building Block tab – generic modules

The user accesses to the building block tab for generic modules clicking on the push-button A. The screen visualized is shown in Figure 45. This is quite different by the other space elements input tabs mainly because only few inputs are necessary for the characterization of these kinds of space elements. For what concerns the seven generic modules, the user can provide the ratio (δ) between the inert (m_i) and total system mass (m_{tot}), that can be provided in the text-box B, the specific impulse (I_{sp}) that can be provided in text-box C, and the typology of spacecraft that can be provided in text-box D.

Considering that the module total mass is the sum of the inert mass, the fuel mass (m_{fuel}) and of the payload mass ($m_{payload}$), the equation for the calculation of δ is:

$$\delta = \frac{m_i}{m_i + m_{fuel} + m_{payload}} \quad [168]$$

The mass of fuel is calculated using the rocket equation, equation [76].

For what concern the two mass elements, the mass can be provided through the text-box E and the typology of spacecraft through the text-box F. Both for generic module and mass elements the typology of spacecraft that can be chosen includes Planetary Lander, Planetary, Manned Reentry, Communication, Weather, Physics & Astronomy, Earth Observation, Lunar Rover, Manned Habitat, Unmanned Reentry, Launch Vehicle Stage,

Upper Stage, Liquid Rocket Engine - Lox/Lh, Liquid Rocket Engine - Lox/RP-1, Payload Fairing, Centaur Fairing. No concurrent design methodologies can be applied to these kinds of building blocks.

Once the all design parameters have been set, the user starts the mission analysis clicking on the push-button I “Evaluate” of the Figure 44. The software starts the mission architecture analysis and shows the results screen (Figure 46).

Eventually, if the user want to re-set some design parameters, this is possible clicking on the Building block push-button to return to the input tabs.

6.2.4 Results tab

	Total mass [Kg]	Fuel mass [Kg]	Dry mass [Kg]	Cost [M\$]	Launch #1	Launch #2
Capsule	0	0	0	0	<input type="checkbox"/>	<input type="checkbox"/>
Capsule Service Module	0	0	0	0	<input type="checkbox"/>	<input type="checkbox"/>
Lunar Ascent Module	0	0	0	0	<input type="checkbox"/>	<input type="checkbox"/>
Lunar Descent Vehicle	0	0	0	0	<input type="checkbox"/>	<input type="checkbox"/>
Propulsion Module #1	0	0	0	0	<input type="checkbox"/>	<input type="checkbox"/>
Propulsion Module #2	0	0	0	0	<input type="checkbox"/>	<input type="checkbox"/>
Space Station SM	0	0	0	0	<input type="checkbox"/>	<input type="checkbox"/>
Space Station Node	0	0	0	0	<input type="checkbox"/>	<input type="checkbox"/>
Space Station IM	0	0	0	0	<input type="checkbox"/>	<input type="checkbox"/>

Total mass	0	Launcher cost [M\$]	0	0
		Launcher class [Metric tons]	0	0
		Mission total cost [M\$]	0	
		Mission capability index	0	
		Mission Value	0	

File name: _____

Esporta risultati

Figure 46 Results tab

The user accesses to the results tab clicking on the Evaluate button of the Building Block tab or clicking on the push-button A (Figure 46 - Results tab). Mainly, the results tab is an output tab but the user can still select some mission scenario features. In particular, the user can select the number of launches and which space elements are launched in the launch #1 or #2. These information are provided checking the consistent check-box B. Once all the inputs have been provided the tool shows all the basic information.

The text-boxes C provides information about the mass budget of each space element. The text-box D provides the value of the total mass launched in orbit. The text-boxes E shows information about the space element cost. The cost model implemented is well described in the section 4.13. Finally, the text-boxes F shows the launcher cost and the launcher class. The text-boxes G provides information about the mission total cost, the mission capability index and mission cost-effectiveness (or value). All the mass results are provided in kilograms and

all the cost information are provided in millions of dollars. Obviously the mission capability index and the mission value are dimensionless entities.

The user can export the results into a file Excel for post processing operations or simply for exchanging. This operation can be performed clicking on the push-button H “Export Results”. The results are saved in the file Excel with the name written in the text-box I. The accepted name cannot contain any of the following characters \ / : * ? “ < > |, the file extension must not be provided and the file name must be shorter than 207 characters. A screen of the generated file Excel is shown in the Figure 47. The table reports the name of the considered building block with the relative mass budget (total mass, fuel mass and inert mass) and cost. Moreover, the file presents information about the systems total mass, the cost and class of the launchers, the mission total cost and value. Also in this file the mass results are presented in kilograms and the cost mass in millions of Dollars.

	A	B	C	D	E
1	BLOCCO	M TOT	M FUEL	M INERTE	COSTO
2	Capsula	9678	0	9041	2786
3	Departure stage	91927	73598	18304	1428
4	Service module	14202	9152	5049	3205
5	Lander	20786	14867	5737	4723
6	Ascent module	8995	3685	5282	3301
7					
8	Systems total mass	145591			
9	Launcher 1 class	0			
10	Launcher 1 cost	0			
11	Launcher 2 class	0			
12	Launcher 2 cost	0			
13	Mission total cost	0			
14	Mission value	0			

Figure 47 SET generated file Excel

6.2.5 Analysis tab

SET is provided with the ability to simulate and evaluate various scenarios as well as the application of optimization techniques. The optimization activity can be performed having access to the Analysis tab (push-button A “Analysis”). To perform the sensitivity or optimization analyses the user had to select the objectives of the (both sensitivity and optimization) analysis. The objectives include minimizing of the Capsule mass, the Capsule Service Module mass, the Propulsion module #1 mass, the Propulsion module #2 mass, the Ascent module mass, the Descent Module mass, the Space Station Service module mass, the Space Station Node mass and the Space Station Integrated module mass as well as the Building block total mass and mission total cost. Moreover, the mission capability index can be selected to be maximized. This operation is performed checking the consistent check-box B. Once the objectives have been selected, the user has to select the mission architecture that shall be considered for the sensitivity or optimization processes. This operation is performed selecting it from the list-box C and then clicking on the push-button D >. Thus, in order to be selected, the mission architecture must be saved into the SET database. When a mission architecture is selected it is listed in the list-box E. More than one mission architecture can be selected. In this case, the analyses are performed considering the mission architecture as a design parameter. The user unselects mission architectures by the push-button F <.

The sensitivity analysis can be started by the push-button G as well as the optimization analysis can be started by the push-button H. At the end of the analysis, the panel showed in

Figure 49 and Figure 50 are presented as output of the sensitivity and the optimization analysis respectively.

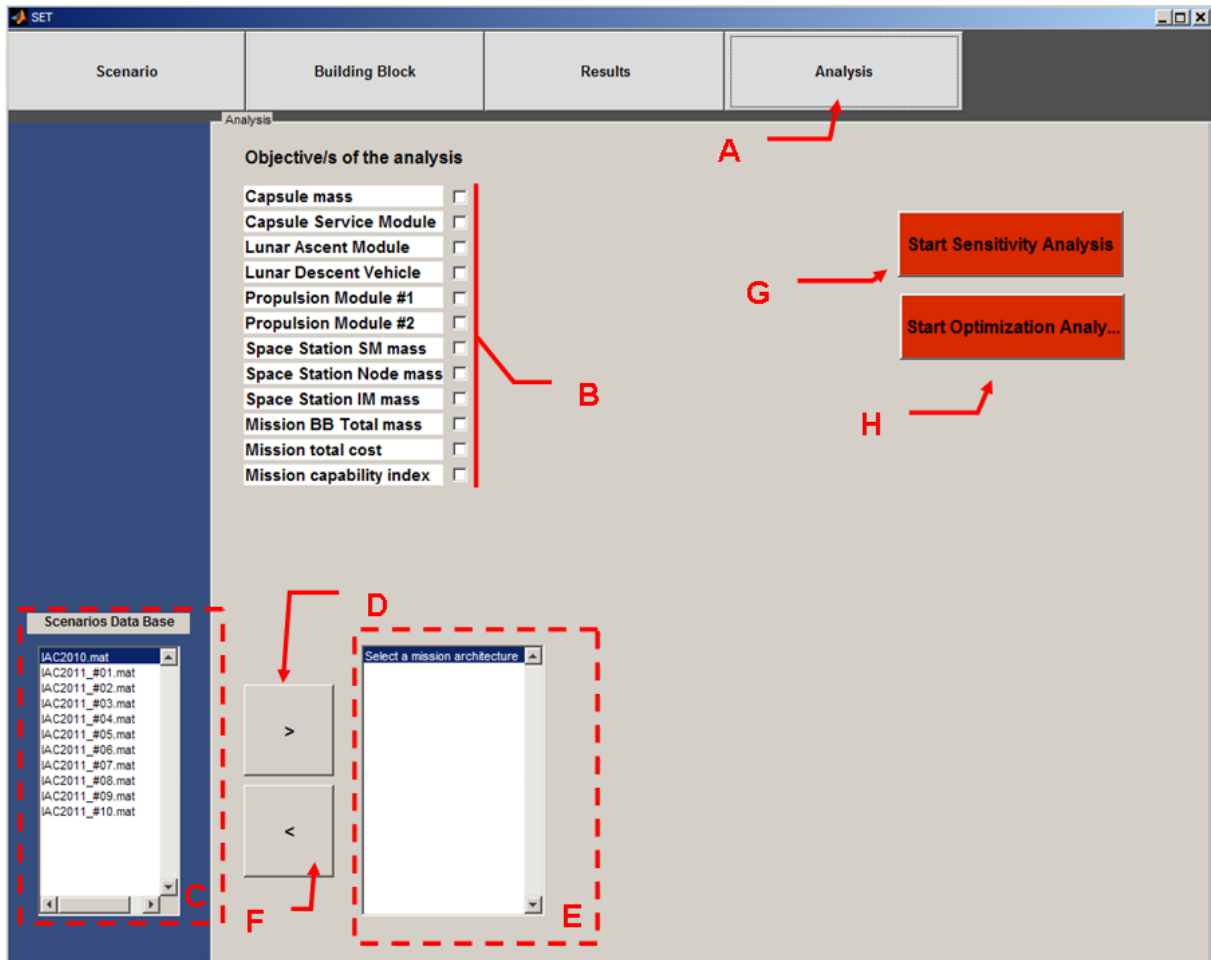


Figure 48 Analysis tab

The sensitivity panel allows the user to plot the results of the sensitivity analysis. The detailed description of the results is provided in the section 5.2.1 Sensitivity analysis: the method of Morris. Nevertheless, μ indicates that a design factor has a prominent overall influence on the output and σ indicates that the influence of a design factor results by the interactions of the factors with other factors or by non-linear effects on the output. In order to create the plot the user has to select the performance objective to plot by the box-list A and click on the push-button B. Finally, the user is able to export the graph as jpeg clicking on the push-button C.

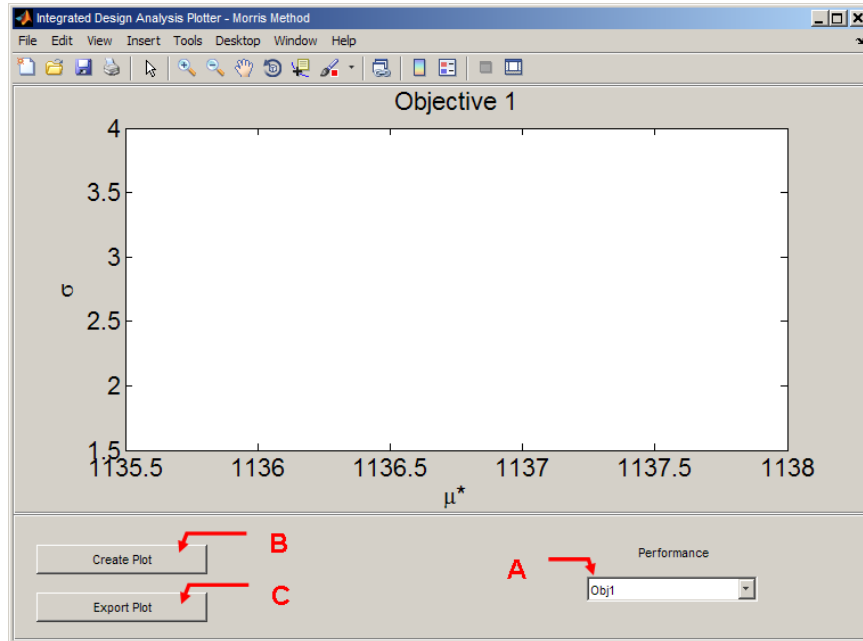


Figure 49 Sensitivity panel

The optimization panel allows to plot the results of the optimization analysis. The graph shows the Pareto front calculated by means of the analysis. The detailed description of the results is provided in the section 5.2.2 Multi-objective Optimization.

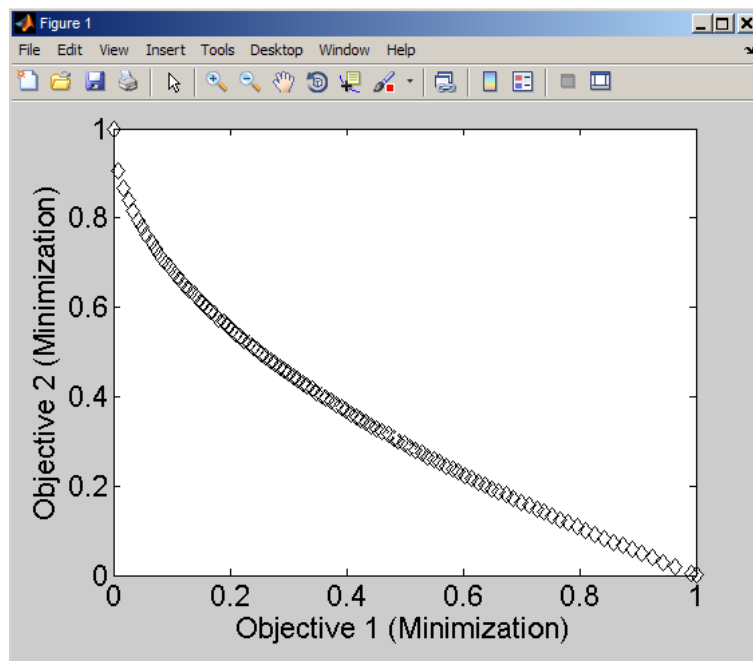


Figure 50 Optimization panel

7 System design

The section provides description of the main analyses and results obtained through application of the design methodology and mathematical models developed and presented in the previous sections on systems for space exploration.

The studies concern the analysis of mission objectives and main high level requirements, the identification and development of high level system trade-offs, the mission profile definition and finally the system concept definition as result of the analyses and trade-offs performed.

The design methodology will be applied to perform the design of a Free Flyer for LEO, a Cargo Logistic Vehicle for supporting of a Cis-lunar orbiting infrastructure and a pressurized rover for Moon surface exploration.

7.1 Free-Flyer

7.1.1 Mission objectives

The Free Flyer allows extended autonomous free-flying durations enabling microgravity research and/or exploration technology demonstration. The mission objectives of the system are:

- allow scientific research (μ g and vacuum experiments) in LEO environment
- provide test and validation of new technologies for space exploration

7.1.2 System requirements

The main high level system requirements include functional, interface, lifecycle and mission requirements.

Functional Requirements

Host and support payloads/experiments

- provide up to 4 racks equivalent volume for the accommodation of the payloads and experiments (up to 2500 kg)
- provide interface for external payload platforms
- support payloads with power and thermal dissipation capabilities (up to 2.5 kW for both)
- allow bidirectional data communication

Support visiting crew

- 3 crew for up to 2 weeks (4 weeks worst case)
- 2 visiting crew rotation per year
- provide at least 33 m³ of habitable volume (shirt-sleeve condition)
- shall protect the crew from the LEO environment

Perform as autonomous system

- generate/store/distribute electrical power
- maintain temperature of all equipment inside the allowable range
- collect/reject waste thermal power
- determine/control attitude and orbit
- monitor and control all equipment on the basis of system software
- provide up to 4 racks equivalent volume for the accommodation of the system equipment

Allow for autonomous operation while un-crewed

- allow remote monitoring and control capabilities

Interface Requirements

RvD with Visiting Vehicles (VVs)

- provide 3 docking ports to allow concurrent docking with 2 VVs (crew VV and cargo VV)
- act as collaborative target

RvD and Docking capabilities with LEO infrastructure

- Free Flyer shall be the chaser
- Free Flyer shall allow up to 1 RvD maneuvers (+1 backup attempt) with the LEO infrastructure

Reference Launcher

- compatible with Ariane 5 midlife evolution (A5ME)

Mission Requirements

Operations

- Lifetime of at least 10 years in LEO environment

7.1.3 Mission Reference Scenario

The Free Flyer is launched in LEO orbit by A5ME. Then, Free Flyer reaches the ISS where it performs RvD. After the Free Flyer outfitting is completed by the ISS crew, the Free Flyer undocks and starts the autonomous phase, during which periodic visits are foreseen by visiting vehicles (crew and logistic). After 10 years, the Free Flyer is disposed with destructive re-entry.

The mission scenario is constituted by three main phases, i.e. Launch and Outfitting, Free-flyer and End of Life disposal.

Launch & Outfitting Phase

- The Free Flyer is launched by A5ME in LEO orbit @ 51.6° inclination, 260 km altitude orbit (max A5ME payload mass 20 t)
- A5ME performs Circularization
- After separation from the launcher, the Free Flyer performs transfer orbit insertion maneuvers to reach ISS @ 51.6° inclination, 350 ÷ 500 km altitude orbit
- The Free Flyer performs ISS orbit insertion maneuvers @ ISS at 51.6° inclination, 350 ÷ 500 km altitude orbit
- The Free Flyer perform RvD with ISS
 - The Free Flyer is the chaser during RvD
 - Up to 2 RvD attempt are considered
 - The Free Flyer receives from the station the same services as Automated Transfer Vehicle (ATV)
 - ISS crew performs payloads exchange compatible with International Berthing and Docking Mechanism (IBDM) and internal pressurized compartment operations

Free-flyer Phase

- When the Free Flyer outfitting is completed, it undocks and starts the autonomous flight in LEO up to 10 years
- cVV provides Free Flyer access (up to 2 weeks; minimum one every 2 years)
 - cVV provides rescue functionalities
 - cVV provides safe Heaven
 - cVV return crew and cargo
- Logistic Vehicle (LV) (until unloading operation completed; minimum one every 2 years)
 - LV provides large cargo delivering
 - LV performs self-disposal maneuvers with Free Flyer waste

Disposal

- After 10 years lifetime, the Free Flyer is disposed with destructive re-entry
 - The Free Flyer performs the necessary maneuvers

A schematic of the above mission scenario is provided in Figure 51.

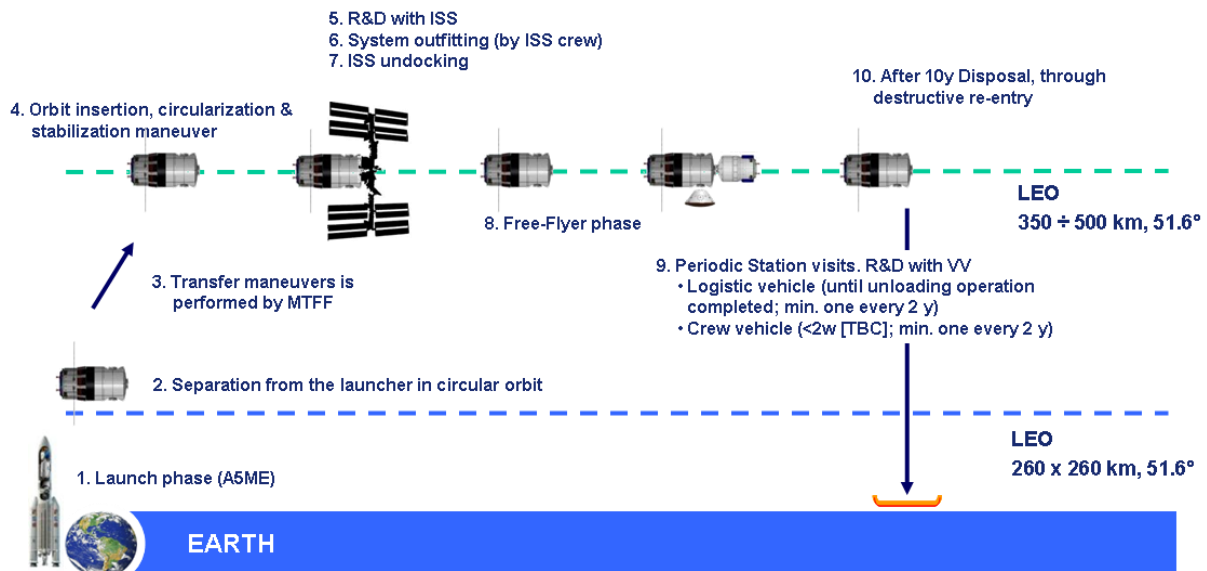


Figure 51 Free Flyer mission profile

7.1.4 Operation Concept

7.1.4.1 Deployment location and flight mode

The objective is to select the most favorable orbit features. In particular:

- the most favorable orbit altitude
- the free flyer flight mode

The selection will be performed pursuing the minimization of the re-boost frequency necessary to maintain the orbit, the minimization of the accessibility cost. For what concerns the orbit inclination, the ISS orbit inclination has been chosen to minimize ΔV after ISS departure.

The low Earth orbits are characterized by the presence of a non-ionized atmosphere mainly composed of atomic oxygen (AO) up to 650 km. Then the Helium dominates until hydrogen takes over above 2000 km. Because a spacecraft's orbital velocities are about 8

km/s for circular orbit near the Earth, molecules striking it will cause drag, which slows the spacecraft down and decays the orbit if periodic re-boost are not provided. The drag force (D) acting on a spacecraft can be expressed by equation [169]:

$$D = \frac{1}{2} \rho v^2 C_d A_n \quad [169]$$

Where ρ (kg/m^3) is the atmospheric mass density, v (km/s) is the spacecraft's orbital velocity, C_d is drag coefficient, and A_n (m^2) is the spacecraft's cross-section area normal to its velocity. In general, the drag coefficient ranges between 1.9 for small spacecraft and 2.6 for very large spacecraft, ref. [4]. Figure 52 shows the decay time (years) for orbits near Earth ranging from 300 km to 700 km in function of the Solar Cycle (F10.7) and assuming a drag coefficient of 2.1. The solar cycle (or solar magnetic activity cycle) has a period of 10.7 years and essentially is a periodic change in the amount of irradiation from the Sun that is expected on Earth. The next solar cycle will begin in the 2023 and will end about in the 2033.

In order to minimize the frequency of the periodic re-boost, the orbit altitude should be as high as possible. On the contrary, however, if free flyer access costs are considered, lower orbits are better.

Considering that, the most favorable orbit is circular with altitude amongst 350 and 450 km. More precisely, in the initial phases of the free flyer operational lifetime, lower altitude are allowed because the decay time is about 1.1 year at 350 km, sufficiently to provide periodic re-boost missions. Around the year 2033, higher altitude are preferred because the minimum decay time decrease to 0.3 years, that is more challenging by the point of view of orbit keeping.

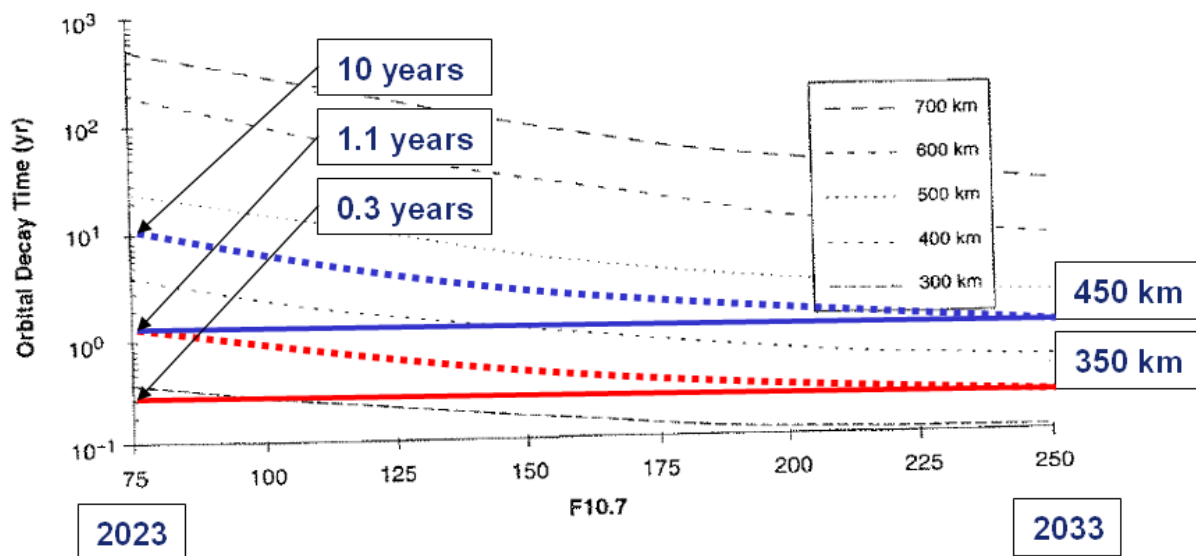


Figure 52 Decay time for orbits near Earth

There are two basic flight modes for Earth orbiting systems: Earth-oriented and Inertial. The Earth-oriented flight mode foresees that the spacecraft shows always the same side to the Earth while the inertial flight mode foresees that the reference point is the Sun or another fixed point in the space. The selection of the flight mode must take into account various aspects regarding safety, operations and utilization issues. In particular:

- Astronomical observations, which need of inertial orientation, are favored by the inertial flight mode because astronomy payloads pointing and operations are greatly simplified. On the other hand, Earth observations, telecommunication and all the experiments affected by the changes in the direction of microgravity are disadvantaged
- By the point of view of the power and electrical systems, the inertial flight mode allows more efficient solutions because solar panels and radiators can be correctly oriented without utilization of complex dedicated mechanisms
- In case of Earth oriented flight mode, if the axis with the smallest moment of inertia is oriented towards the Earth, the gravity gradient stabilizes the station and attitude maneuvers are not necessary to control the Free Flyer. On the contrary, in case of inertial flight mode, the gravity gradient is always a perturbation on the attitude. However, if the two Free Flyer main axes of inertia are oriented in the orbital plane, the gravity gradient causes only a cyclic perturbation that is easily controllable without the use of propellant and momentum wheels or gyros are sufficient
- The effects of the aerodynamic drag are important especially for low orbits. Drag causes spacecraft deceleration and decay of the orbit. In order to minimize drag, the station's area in the velocity direction must be kept as small as possible. This means that the longitudinal axis of the Free Flyer must be parallel to the velocity vector and that the normal vectors of solar panels and radiators must be perpendicular to the velocity. Considering that, the Earth oriented flight mode seems the best solution. However, considering that the Free Flyer is very small and that, also in case of Earth oriented flight mode, it is not always possible to maintain the correct alignment of the axes, the advantages deriving from the Earth oriented flight mode are negligible
- Considering the Free Flyer accessibility, the Earth oriented flight mode allows easier RvD because the corridors used for these maneuvers correspond to the reference axes of the station. On the contrary, if the station adopts inertial flight mode, special attitude maneuvers are necessary to get the docking adapters in the right position.

Table 16 summarizes pros and cons of the two flight modes. In general, both the flight modes are possible for small space stations without any particular impact on the design because characterized by a relatively homogeneous mass distribution. On the contrary, bigger space stations, as the Mir or the International space station (ISS), require more stable attitudes because the control becomes more challenging. These systems require too much propellant to keep an attitude that is continually acting against gravity gradient or aerodynamic torque so they need to fly Earth-oriented in a torque-equilibrium attitude, meaning no momentum accumulates in the attitude-control system over an orbital revolution.

	Pros	Cons
<u>Earth-oriented flight mode</u>	<ul style="list-style-type: none"> • Advantages on Earth observation and telecommunication • Gravity gradient stabilizes attitude • Earth allows crew orientation during EVA • Easier rendezvous and docking • More flexible mass distribution during assembly • More flexibility for microgravity experiments 	<ul style="list-style-type: none"> • More complicated solar array and radiator systems • Variable light conditions
<u>Inertial flight mode</u>	<ul style="list-style-type: none"> • Advantages for astronomy observations • Simpler solar array and radiator systems • Constant light conditions • Constant thermal control conditions 	<ul style="list-style-type: none"> • Gravity gradient always a perturbation • Problems on mass distribution during assembly • Disadvantages on Earth observation for tourism

Table 16 Pros and cons of Earth-oriented and Inertial flight mode

Considering pros and cons of the two possible flight modes, the inertial flight mode results the best option for the Free Flyer. The inertial flight mode allows a simpler Free Flyer from the power and thermal control systems point of view. The solar arrays and radiators, in general, need two rotary joints actuation to avoid losses of efficiency caused by non-optimized Sun incidences. In the inertial flight mode, if we orient one spacecraft axis with respect to the Sun, we can get perfect solar tracking using only one rotating joint for the solar arrays or radiators. By the point of view of the space station control, the Free Flyer has limited problems on mass distribution and does not require a significant amount of fuel to keep attitude. However, it must be considered that the flight mode affects the kind of experiments or astronomical observations that can be done. In fact, the Earth-oriented flight mode is preferred for Earth observation, telecommunications as well as for microgravity missions because tidal forces perturbations are steady and indifferent in the direction of the velocity vector. For these reasons, it must be considered that the Free Flyer flight mode could be switched from inertial flight mode to Earth-oriented flight mode during mission.

7.1.4.2 Flight Autonomy

An assessment about the possibility that the Free Flyer performs periodical dockings to a LEO infrastructure to complete servicing operations has been performed. The identified possible LEO infrastructures are the International Space Station (ISS) and the Chinese Space Station.

The ISS is assumed as reference because no major differences are expected in principle and in case, switching to Chinese station is possible pending station interfaces check/understanding. Table 17 provides some details about the orbit of the two space stations.

	ISS	Chinese Space Station
Apogee	398	340 to 450 km
Perigee	376	340 to 450 km
Orbit Inclination	51.6 deg	42-43 deg

Table 17 ISS and Chinese Space Station orbit features

The operation concept traded options are ISS-serviced, autonomous free flyer and mixed solution:

- **ISS-serviced:** the Free Flyer is normally attached to ISS and periodically detached for limited time periods to perform experiments/demonstrations
- **Autonomous free flyer:** the Free Flyer performs free-flyer without ISS dockings
- **Mixed solution:** the Free Flyer operated as ISS-serviced until ISS availability. Then, when ISS no more available, the Free Flyer operates as autonomous system

The trade assessment has been performed considering:

- The Free Flyer Propulsion system impact (mainly fuel consumption) of number and frequency of orbital maneuvers to be performed
- The effect of the ISS availability. Considering that ISS will be dismissed in near future, the figure of merit assess the effect on the Free Flyer operations
- The needing of dedicated crewed mission to take into account of the possibility to exploit synergism with ISS, i.e. to take advantage of the crew already aboard the ISS. If the ISS crew performs the operations, no dedicated crew mission are necessary to support the Free Flyer
- The needing of dedicated logistic mission to take into account of the possibility to exploit logistic synergism with ISS. The figures of merit does not take into account of fuel refurbishment which is yet considered in propulsion system impact
- The impact on ISS operations to takes into account of docking ports occupation, resource allocated
- The impact on the Free Flyer design in terms of complexity
- The scientific and research opportunity that different operation concept allow
- The risk deriving from orbital maneuvers

The ISS-serviced configuration requires frequent docking and undocking maneuvers with ISS. This implies high fuel consumption and consequently more refurbishment missions. Autonomous free flyer and mixed configuration reduce the needing of refurbishment although the mixed configuration implies more fuel consumption when ISS serviced.

The ISS availability is mandatory for operation of the Free Flyer ISS-serviced configuration. Mixed configuration needs of ISS for only a part of the operational life. Thus, ISS availability does not limit the research and demonstration capabilities.

The ISS-serviced configuration does not need of dedicated crew missions. In nominal conditions (i.e. if there are not failures or other critical events), crew missions are performed when the Free Flyer is attached to the ISS. On the contrary, autonomous and mixed (when autonomous) configurations require dedicated crewed mission to allow operations.

Considering logistic, ISS-Serviced and mixed (when attached to ISS) configurations take advantage of synergisms with ISS logistic operations thus reducing general costs. On the contrary, autonomous and mixed (when autonomous) configurations require dedicated logistic missions.

The impact on ISS operations figure of merit takes into account of resources and servicing that the ISS shall provide to the Free Flyer. Since the ISS-serviced configuration foresees the Free Flyer frequently docked, the impact is severe because a permanent occupation of a docking port with associated resources. The same considerations can be performed for the mixed configuration that is serviced until ISS dismissing.

The system complexity (mainly ECLS considerations have been performed) is certainly affected by the operation concept. In fact, since crew missions are not expected during autonomous flight, the ECLS for the ISS-serviced configuration has been assumed to be simpler (open loop instead of closed loop). On the contrary, since the autonomous and the mixed configurations shall support crew life for longer periods of time, the ECLSS has been considered more complex.

The scientific and demonstration opportunities depend by the operation concept. The ISS-serviced configuration provides poor additional value to ISS research capabilities and does not allow testing of a completely autonomous exploration system. In fact, although the Free Flyer would be an alternative LEO destination to ISS research environment, it does not provide significant different environmental conditions. Moreover, since the Free Flyer docks periodically to ISS, there are not reasons to increase the autonomy level of the system which shall not support crew during free fly thus limiting the demonstration capabilities of exploration technologies. The Autonomous operation concept has been considered the best option because the system allows demonstration of a completely autonomous exploration system for long periods of time and allows scientific research. The mixed configuration has been considered less rewarding than the autonomous configuration because although it has the capabilities to operate for extended periods of time in autonomous conditions, it does not exploit its potentialities for a long part of its operational life.

The risk level has been assumed proportional to the number and frequency of orbital maneuvers to be performed. Thus, the autonomous free flyer has the lower risk. The mixed and ISS-serviced configurations have higher score because the higher is the number of maneuvers. The table summarizes the main consideration performed.

Options	ISS-serviced	Autonomous FF	Mixed
Prop. Sys impact	Frequent dock/undock maneuvers w/ ISS	Re-boost	Frequent dock/undock w/ ISS (beginning) Re-boost (if to be performed by Free Flyer)
ISS availability	Mandatory for entire life	Not necessary	Switch to autonomous FF when needed
Need for dedicated crew missions	No	Yes	No (when ISS-serviced) Yes (when autonomous)
Need for dedicated logistic missions	No	Yes	No (when ISS-serviced) Yes (when autonomous)
Impact on ISS ops	Severe (i.e. almost permanent occupation of a docking port with associated resources demand)	None	High (i.e. almost permanent occupation of a docking port with associated resources demand)
Impact on Free Flyer design	Simple ECLSS	More complex ECLSS	More complex ECLSS
Research and demonstration opportunities	<ul style="list-style-type: none"> Poor additional value to ISS research capabilities Test of non-completely autonomous exploration system 	<ul style="list-style-type: none"> Potentially higher additional value to ISS research capabilities Test of autonomous exploration system 	<ul style="list-style-type: none"> Poor additional value to ISS research capabilities (when ISS-serviced) Potentially higher additional value to ISS research capabilities (when autonomous) Test of autonomous exploration system only for the second part of lifetime.
Risk level	Higher	Lower	Mid

Table 18 Autonomy level trade off

At the end of the trade-off the Autonomous Free Flyer configuration results to be the best option. Nevertheless, an initial outfitting and set up is foreseen at ISS. On orbit set-up can be performed by the crew already on the ISS. The experiments and consumables can be carried on the station with a different cargo mission and re-use of LEO station payload is possible.

7.1.4.3 Lifetime Approach

An analysis of different approaches for increasing the lifetime of the Free Flyer has been performed. The traded options are refueling by a servicing vehicle, re-boost by a servicing vehicle, replacement of the propulsion module. The options have been analyzed taking into account of the following figures of merit:

- opportunity to provide a demonstration of new technologies that could be relevant in the framework of the future human exploration of Moon, Mars and Deep space
- Free Flyer system complexity to take into account of the Free Flyer increasing complexity due to the presence of additional onboard equipment
- servicing vehicle systems complexity
- impact on operations frequency and flexibility
- operations complexity to take into account of autonomous orbit maneuvers or advanced robotic operations
- system development costs

Table 19 summarizes the consideration performed:

- the refueling option allows demonstrating refueling technologies that could be useful in the future to provide servicing of exploration spacecraft or of on-orbit satellites (e.g. for life time extension). Also the replacement of the Free Flyer propulsion module would allow demonstrating of docking and undocking systems that could be useful for future exploration spacecraft. Re-boost operation are sufficiently demonstrated at ISS by servicing vehicles
- concerning the system architecture complexity, the replacement option implies the increasing of the Free Flyer complexity:
 - the pressurized module shall be provided with ACS to allows control during propulsion module docking and undocking
 - a complex dock/undock system must be provided to allow separation of the resource module by Free Flyer
 - the propulsion module must be able of flying without payload (pressurized module) to de-orbit

Nevertheless, the refueling option requires a robotic refueling system and the re-boost option requires a docking system at nadir side which allows docking of the servicing vehicle

- The refuel and replacement options imply servicing systems more complex than re-boost. The system which allows refuel shall be provided with a complex robotic refueling system. The system which allows propulsion module replacement shall be provided with a complex dock/undock system. The re-boosting vehicle can be fully derived from ATV.
- Although the operation complexity of the refueling and replacement option is high, the refueling option has been evaluated less challenging than the propulsion module replacement. In fact, even though advanced robotic operations must be performed, these are performed on suitable refueling system interfaces

- Refueling or replacement options have been considered less critical than re-boost option by the point of view of the servicing operation frequency and flexibility. In fact, assuming sufficient storage capabilities, the servicing frequency decreases and any delay in the servicing operations is less critical
- The costs have been considered proportional to the system complexity, to the available heritage from existing vehicle and to servicing frequency

Options	Refueling	Re-boost	Replacement
Technology demo opportunity	Yes (Robotic Refueling system)	Not particularly relevant (yet demonstrated in LEO - ISS)	Yes (Dock/undock system)
Impact on Free Flyer complexity	Robotic refueling system	Mandatory dock system @ nadir side	<ul style="list-style-type: none"> • Need for AOCS on the pressurized module of the Free Flyer • Need for complex dock/undock systems • SM must be capable of flying w/o P/L (to de-orbit)
Impact on servicing vehicle complexity	Need of complex refueling system	Not particularly relevant.	Need for complex dock/undock system
Operations complexity	Complex robotic operations	Not critical (only docking operation sufficiently tested at ISS)	Very complex
Impact on operations frequency/flexibility	<ul style="list-style-type: none"> • Possible lower frequency (assuming Free Flyer tanks sufficiently capable) • Higher operation flexibility (less constrained by schedule) 	More rigid schedule for servicing missions	<ul style="list-style-type: none"> • Possible lower frequency (assuming resource module sufficiently capable) • Higher operation flexibility (less constrained by schedule)
Costs	Mid development cost (manly due to refueling system)	Lower (possible reutilize existing technologies)	Very high

Table 19 Lifetime Approach trade off - rationale

As result of the trade-off, the refueling option is the best one. Nevertheless, the option to have re-boost by the servicing vehicle at the end of refueling operations has not been discarded.

	Technology demo opp.	Impact on Free Flyer comp.	Impact on SV comp.	Operations complexity	Impact on ops frequency/flexibility	Cost	
Weighting factor	20	15	15	15	15	20	100
Refueling	1	0	0	0	1	0	35
Re-boost	-1	0	1	1	0	1	30
Replacement	1	-1	0	-1	1	-1	-15

Table 20 Lifetime Approach trade off - results

The refueling mission could be performed by an ATV derived servicing vehicle. The Free Flyer allows storing of up to 3000 kg of fuel which are sufficient to provide control up to 5 years in accordance with mission scenario. At midlife, the servicing vehicle provides 3000 kg of propellant to complete other 5 years lifetime (the propellant estimates have been

performed considering I_{sp} 270 s which is the specific impulse of current ATV secondary thrusters).

7.1.5 System Configuration Definition

7.1.5.1 Crew approach

Two crew approaches are possible for the Free Flyer. The first one is permanent crew which implies a continuative human presence during all the mission phases. The second one is crew-tended. This means that, on the Free Flyer, the human presence is not continuative and that humans will be on the space station for short periods of time.

In order to choose the best compromise amongst these two options, a trade-off has been performed. The trade-off takes into account of parameters concerning system design, operations, logistic needs and research capabilities. Table 21 shows the trade-off results.

More in detail, the figures of merit considered for the trade-off are:

- habitat sizing to take into account that a continuative human presence requires larger habitable volumes to ensure adequate comfort performances
- complexity of the life support system because it must be considered that a permanently habited Free Flyer requires almost certainly a closed loop life support system (high complexity) while a crew tended Free Flyer should allow an open loop life support system (lower complexity)
- shielding requirements to take into account that if the crew is exposed to space radiation for short periods of time, the shielding requirements are less challenging whit benefits on mass
- maintenance level to take into account that a crew tended space station requires higher reliability systems
- logistic needs of the Free Flyer because the logistic support of a crew tended space station is less challenging of a permanently inhabited space station
- orbit perturbations because the human presence is cause of attitude perturbations that could have effect on the research activities
- research capabilities because the continuative presence of a crew allows to extend the research fields

	Habitat sizing	Life support system	Shielding required	Maintenance level	Logistic needs	Orbit perturbations	Research capabilities	TOT
Weighting factor	20	15	5	20	15	5	20	100
Permanent crew	-1	-1	-1	1	-1	-1	1	-20
Crew tended	1	1	1	-1	1	1	-1	20

Table 21 Permanent-crew vs. crew-tended space station trade-off

The trade-off shows that the crew-tended space station is the best option. In fact, a crew tended space station is less challenging from the subsystems point of view, the reduced crew comfort is acceptable for short missions (i.e. less impact on Free Flyer size), the logistic needs are limited to short periods of time and because experiments are less perturbed by the human presence although research potential is limited.

Some considerations on the compatibility of the human absence with some research fields have been performed. In particular for what concern:

- **Material science** Research activities can be performed to study the crystal growth in absence of gravity. The material science requires long periods of execution and perturbations are very influent on the experimental results. A very small and crew-tended space station minimizes external perturbations and maximizes the research value. Other research activities can be performed to study the material response to the space environment, e.g. degradation phenomena due to the presence of the atomic oxygen
- **Fluid Dynamics** Research activities can be performed to study liquid mixing and turbulence effects in micro-gravity environment. Also in this research field, the absence of external perturbations is very important and maximizes the research value
- **Biology** In general, biology research activities are incompatible with the absence of humans. However, research activities can be performed to study the effects of the space environment bacterial contamination. In this case, the presence of humans limits the research capabilities for safety reasons
- **Radiation** Research activities can be performed to study the radiation field in the space environment. The radiation shielding requirements on a crew-tended space station are less restrictive and the research activity results less constrained
- **Earth observation** Effects of climate change can be observed by an on-orbit space station. The absence of a permanent crew is not limiting.
-

7.1.5.2 Crew size

The number of crew members has been chosen after assessment of the crew size effect on research capabilities, payloads, experiments, required autonomy level, system maintenance capabilities, visiting vehicle logistic and safety issues. Table 22 summarizes the main considerations performed. The crew size considered ranges from 2 to 4. One crew member has been discarded mainly because the safety problems and EVA impracticability. Five or more crew members have been discarded because:

- Higher crew size implies excessive Free Flyer complexity that, considering system requirements and constraints, is not justifiable
- The set of visiting vehicles able to provide Free Flyer full occupation would be considerably reduced: the crew visiting vehicles considered are Soyuz, MPCV, Shenzhou, Dragon, CST-100, PTK, and Dream Chaser and only the last four are able to provide accessibility to more than 4 crew members

The number of crew members has been chosen considering that two astronauts implies limited research capabilities mainly because the excessive crew workload: higher system reliability and higher payload autonomy level requirements are necessary to contain workload. At the same time, two astronauts imply limited EVA capabilities and critical safety problems. The increasing of the crew size allows higher research capabilities and less challenging payload autonomy and maintenance requirements. Nevertheless, the increasing of the crew number reduces the set of potential visiting vehicles (Soyuz and Shenzhou transport up to 3 crew members) and/or the available volume for logistic provided by the capsule.

Options	Number of crewmembers		
	2	3	4
Research capabilities and P/L-experiments autonomy level	<ul style="list-style-type: none"> Limited research capability, high autonomy level of P/L & experiments required (even when crewed) 	<ul style="list-style-type: none"> good research capability, medium autonomy level of P/L & experiments required when crewed 	<ul style="list-style-type: none"> Good research capability, low autonomy level of P/L & experiments required when crewed
System maintenance capabilities	<ul style="list-style-type: none"> Maintenance capability very limited Limited EVA capability 	<ul style="list-style-type: none"> Medium maintenance capability good EVA capability 	<ul style="list-style-type: none"> High maintenance capability good EVA capability
Visiting vehicle logistic	Low impact (high volume for logistics and P/L)	Medium impact (volume available for logistics and P/L)	<ul style="list-style-type: none"> High impact (limited volume for logistics and P/L) Soyuz and Shenzhou cannot transport 4 astronauts
Safety	Critical	Good	Good

Table 22 Crew size trade-off - rationale

The crew size assessment has been performed giving higher weight to Research capabilities, P/L-experiments autonomy level and to the VV logistic. The intention is to maximize the Free Flyer utilization benefits without impacting negatively the logistic scenario.

	P/L & exp capabilities	Sys maintenance capabilities	Visiting vehicle	Safety	
Weighting factor	30	25	30	15	
2 CM	-1	-1	1	-1	-40
3 CM	1	1	0	1	70
4 CM	1	1	-1	1	40

Table 23 Crew size trade-off - results

Table 24 provides a further assessment about the impact of the crew size on system complexity, logistics, operations and workload. The Workload is a measure of how effort a person must exert to do a task. It can be mental, physical, or a combination of them. Workload can be defined by timelines, i.e. the activities scheduled in a certain period. Excessive workload results in fatigue stress, and decreasing concentration. Too little workload results in boredom, loss of attentiveness and alertness, poor morale, and lack of readiness to deal with contingencies. Logistic & Operations includes the activities concerned with crew and systems support. Logistic needs are those elements of mission hardware and software that most necessarily serve human needs. They depend on the mission's envisioned functions, activities, and duration, as well as the physical, psychological and physiological characteristics of the human beings. Logistic needs can be re-supplied during the mission or stored entirely on board and can be regenerated or not. System complexity is a judgment about the technological complexity required to meet the crew size constraint. The system complexity includes issues about systems reliability, scale, level of maintenance and resources loop closure level. Table 24 summarizes these considerations in function of the crew size that ranges from one to six.

Crew size	Workload	Logistic & Operations	System complexity
1	<ul style="list-style-type: none"> • Very limited research capabilities • Excessive workload problems • Psychological problems • Safety problems • EVA activities not possible 	<ul style="list-style-type: none"> • Logistic needs for all mission duration could be stored entirely on board • Maintenance capability very limited • Completely automated experiments 	<ul style="list-style-type: none"> • Use of safe/fail, reconfigurable, robotic compatible systems design • Low level of ECLSS closure possible • Small ECLSS scale possible • Robotic system required
2	<ul style="list-style-type: none"> • Limited research capabilities • Sustainable but high workload level • Crew tasks rotation possible but limited • EVA are limited 	<ul style="list-style-type: none"> • Logistic needs for all mission duration could be stored entirely on board • Maintenance capability limited • Mostly automated for experiment 	<ul style="list-style-type: none"> • Use of safe/fail, reconfigurable, robotic compatible systems design • Low level of ECLSS closure possible • Small ECLSS scale • Robotic system maybe required
3	<ul style="list-style-type: none"> • Good research capabilities • Sustainable workload level • Crew tasks rotation possible • EVA excursions are possible 	<ul style="list-style-type: none"> • Depending by mission duration, logistic needs could be stored on board or re-supplied. • Moderate maintenance possible • Mostly automated for experiment 	<ul style="list-style-type: none"> • Use of safe/fail, reconfigurable systems design • Increased level of ECLSS closure necessary
4	<ul style="list-style-type: none"> • Good research capabilities • Usual EVA excursions are possible 	<ul style="list-style-type: none"> • Depending by mission duration, logistic needs could be stored on board or re-supplied. • Ordinary maintenance possible • Semi-automated experimental activities are possible 	<ul style="list-style-type: none"> • Increased level of ECLSS closure necessary
5	<ul style="list-style-type: none"> • Very good research capabilities • No workload problems • Frequently and usual EVA excursions are possible 	<ul style="list-style-type: none"> • Depending by mission duration, logistic needs could be re-supplied or a regenerative life support systems could be necessary • Ordinary maintenance possible • Manual experimental activities possible 	<ul style="list-style-type: none"> • High level of ECLSS closure required • Large ECLSS scale required
6	<ul style="list-style-type: none"> • Very good research capabilities • No workload problems • Frequently and usual EVA excursions are possible 	<ul style="list-style-type: none"> • Depending by mission duration, logistic needs can be re-supplied or a regenerative life support systems could be necessary • Ordinary maintenance possible • Mostly scientists possible for crew composition 	<ul style="list-style-type: none"> • High level of ECLSS closure required • Large ECLSS scale required

Table 24 Crew size trade-off - rationale on workload, logistics & operations and system complexity

As result of the considerations performed, 3 crew members results to be the best option mainly because allow good research and maintenance capabilities (with sustainable workload for the crew) without limiting the number of possible crew transportation vehicle or their logistic potentialities.

7.1.5.3 Docking Ports Number and Location Assessment

The number of docking ports is assessed considering issues about EVA capabilities, risks in case of system failure, flexibility and expandability of the Free Flyer concept, Free Flyer mass and volume. Table 25 summarizes the considerations that have been performed.

Options	Number of docking ports		
	1	2	3
EVA capability	Total depressurization or through VV	Possibility to attach an airlock	Possibility to attach an airlock
Risks	High	Low	Low
Flexibility / Expandability	Critical	Limited (but possibility to attach a node or a hub)	High
Mass/Volume impact	Low	Medium	High

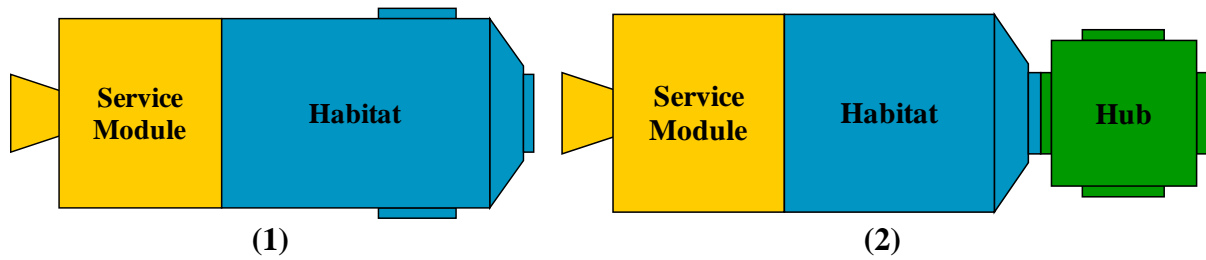
Table 25 Number of docking port trade-off

As result of the trade-off the 3 docking ports results the best one option. In fact, having only one docking port would not allow performing EVA, unless performing EVA through total or partial (in case only visiting vehicle) system depressurization, or through a possible dedicated airlock provided by the visiting vehicle. The risks in case of failure are very high because the impossibility to have a safe haven or alternative docking capabilities. It must be considered that having the possibility to perform EVA shall be considered for external maintenance reasons (unless very advanced robotics is considered, able to accomplish those tasks autonomously).

Two or more docking ports allow the addition of an airlock without the needing to add a further hub module. Moreover, inserting additional docking ports would allow a higher flexibility, leaving the possibility, in case, to expand the Free Flyer (by adding additional modules) and, in particular, an airlock to perform EVA. Having only one docking port does not allow the possibility to add an airlock without also add a hub module (the resulting system would be characterized by a more constrained expansion strategy). Moreover, more than one docking port allow the launch of the Free Flyer provided with the airlock at the beginning of the mission pending launcher constraints and the contemporary access to more than one visiting vehicle. Considering a minimum of 2 visiting vehicles (cargo and crew vehicles) 3 docking ports is the minimum number.

Two docking ports accommodation alternatives have been considered:

1. Integrated whit the resource/pressurized module
2. Provided by addition of a module (Hub)



The integrated configuration is chosen mainly because:

- the integrated configuration allows system mass reduction with respect to the double module configuration (resource/pressurized module + docking hub).
- general development and deployment costs decreasing:
 - the development of two modules implies higher cost than the development of an integrated module
 - the launch costs increase if a 2 launch mission is necessary
 - there is not needing of a further tug that allows Hub transfer and assembling
- lower deployment risks since docking/berthing phase of the hub module is not needed
- also if the docking hub allows additional habitable volume, no further research and technological demonstration potentialities are provided because it does not house additional research equipment

Options	Integrated	Hub
Mass	Lower	Higher
Habitable Free Volume	Limited by launch constraints	Potentially higher
Cost	Lower	Higher (2 module to develop, 2 launch need)
Deployment complexity	Lower	Higher (more launch, dock ops)

Table 26 Docking ports location trade-off – rationale

	Mass	Free Volume	Cost	Deployment complexity	
Weighting factor	25	20	30	25	
Integrated	1	-1	1	1	60
Hub	-1	1	-1	-1	-60

Table 27 Docking ports location trade-off – result

7.1.5.4 Habitable volume assessment

The habitable volume of the Free Flyer is estimated on the base of the following assumptions:

- Nominal crew stay 2 weeks
- Contingency crew stay 4 weeks
- Nominal crew up to 3
- Optimal comfort conditions

Doing reference to the NASA-STD-3000 (ref. [9]), the minimum habitable volume has been estimated. Figure 53 shows how much habitable volume [m³] shall be assured to each crew member. Considering 3 crew members for a total crew stay of up to 4 week the minimum necessary volume is 33 m³ (which provides 11 m³ for each astronaut).

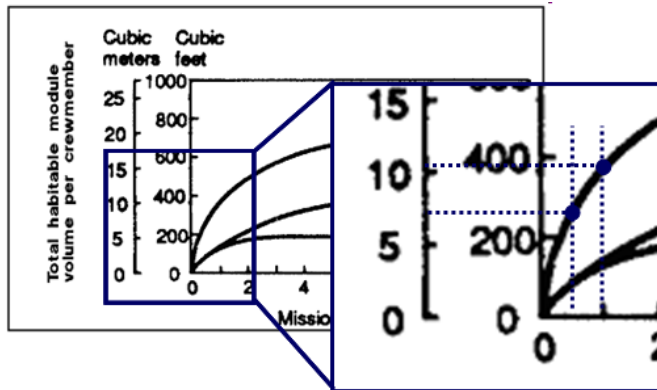


Figure 53 Free Flyer habitable volume assessment

	Habitable Volume requirement
Total 2w	> 22 m ³
Total 4w	> 33 m ³

Table 28 Free Flyer habitable volume assessment result

7.1.5.5 ECLSS closure level

Different ECLSS closure levels are possible. The considered options are:

- completely open loop
- water regeneration
- air and water regeneration

Figure 54 shows a graph of the cumulative launch mass (system mass, spares mass, delta mass of power/thermal system and delta mass due to system accommodation) for different ECLS technologies as function of the mission duration. It is clear that as the duration of the mission increases, the advantage of a closed loop system in terms of mass reduction becomes more and more significant, even though the operations and the hardware required for the maintenance are more demanding.

The analyses are performed on the base of data available in literature. The analysis takes into account chemical and physical proprieties of the different technologies considered. Figure 54 is obtained on the base of the following assumptions:

- the assessment has been performed considering four crew members
- the food de-hydration is equal to 80%
- the contribution of EVA on consumables mass has been neglected
- the mass of the tanks has been derived from experiences on ATV
- a buffer of 1 week is considered for air and water when regenerative technologies are considered. The assumption simplify the analysis because the buffer should be function of type of mission, distance from the Earth or from rescue systems
- water availability for shower, hand wash, oral hygiene, drinking e food hydration is considered
- two redundancies are considered for regenerative technologies
- the technologies considered derive from ISS

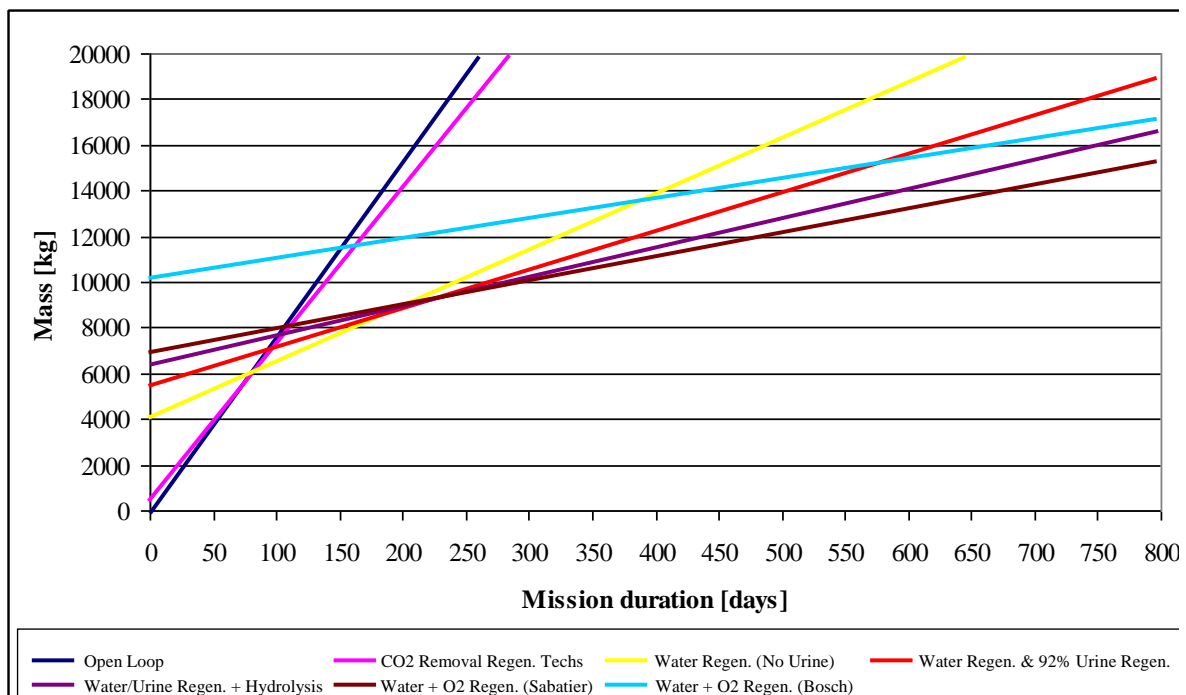


Figure 54 ECLSS - open Vs closed loop

The Free Flyer shall support 3 astronauts for the nominal mission duration of 2 weeks and for up to 4 weeks as worst case. The crew missions are foreseen 2 time per years and the Free flyer life-time in 10 years. The trade-off concerning the ECLS closure level shall be performed considering the cumulative crew presence over the lifetime which amount to 560 days. Doing reference to Figure 54, for the reference crew mission duration, water+O2 regeneration technology allows saving of mass with respect to the other ECLS technology options.

7.1.6 System description

The Free Flyer concept consists of an integrated system composed of two main modules able to provide support to 3 crew members for up to 4 weeks. Free Flyer provides 3 docking ports (1 axial and 2 radial) where visiting vehicles can dock and get servicing. The two main modules are the Laboratory module (LM) and the Resource Module (RM), see Figure 55:

Laboratory Module provides:

- Pressurized human rated environment
- Laboratory for scientific research
- Logistic storage
- Docking/berthing capabilities
- ECLS consumables storing [TBC]
- GNC (only sensors required for RvD)
- Active and Passive Thermal Control System

Resource Module provides:

- Propulsion capabilities
- Avionic/ power/ GNC
- Communication capabilities
- Active and Passive Thermal Control System

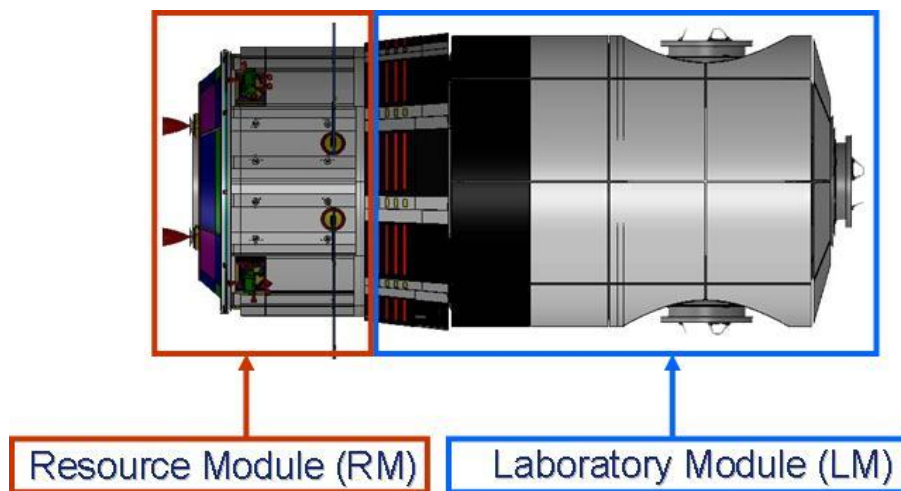


Figure 55 Free Flyer preliminary concept

7.1.6.1 Pressurized module design

The total pressurized volume provided by Free Flyer is 79 m^3 . Part of the pressurized volume is occupied by internal systems: 16 m^3 are necessary to provide 8 racks accommodation (circumferentially disposed in 2 sections of 4 racks each), 7.5 m^3 are necessary to 3 IBDM and related systems accommodation, 10 m^3 are provided to stand offs and other equipment accommodation. Thus, the total habitable volume is 45 m^3 . Figure 56 and Figure 57 show LM external layout and racks accommodation.

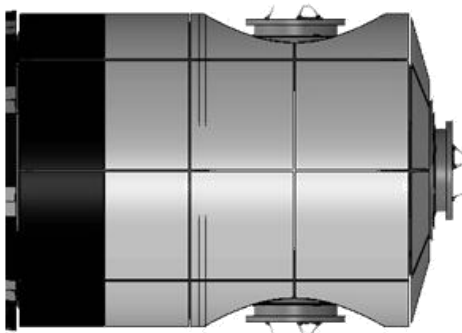


Figure 56 Pressurized module external layout

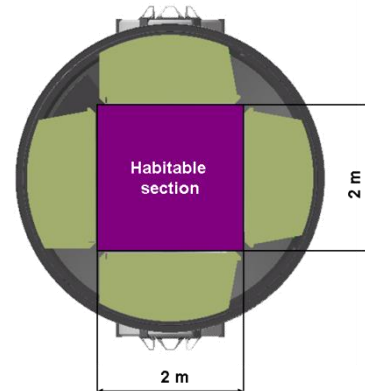


Figure 57 Racks disposition

LM is conceived as a pressurized module made of a cylindrical segment core closed at the ends by two conical segments:

- an aft closure cone with Resource Module interfaces
 - the mechanical interface allows rigid connection of RM with LM. The mechanical interface consists of a cylindrical segment which interfaces wide the sidewall cylindrical structures of the LM. No separation mechanisms are foreseen
 - electrical and fluidic connections are envisaged on the aft closure panels
 - electrical power connections allow power supply to the pressurized module equipment
- data interface allows connection of onboard equipment with the resource module avionic systems

- an heat exchanger allows transfer of exceeding heat to the RM TCS
- consumables (water and oxygen) are distribute through dedicated interfaces
- a front cone with adapter and IBDM

Apart from the racks, the Free Flyer habitable compartment houses the main additional following systems such as:

- Environmental Control and Life Support (ECLS)
- Docking system (IBDM)

7.1.6.2 Resource Module design

The Resource Module design is derived from ATV. It provides propulsion capability for orbit and attitude control, housing of GNC components, power generation and active thermal control, avionic and communication systems and finally accommodation of ECLS consumables.

The Resource Module consists of three bays:

- The Propulsion Bay
- The Avionic Bay
- The Resource Bay

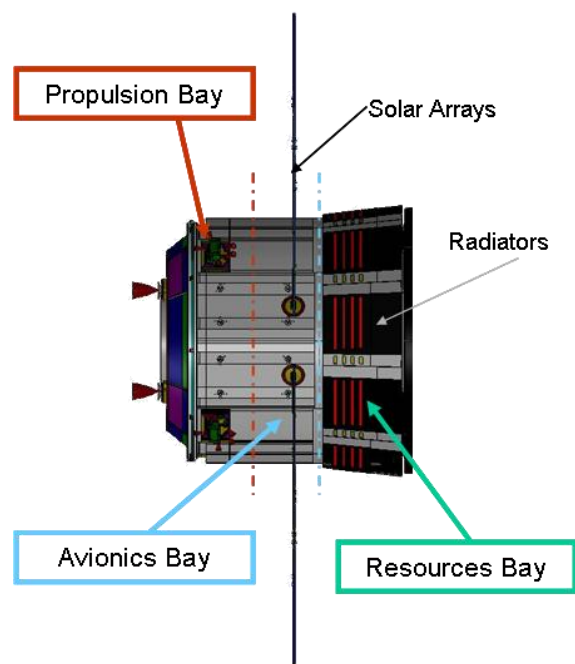


Figure 58 Resource module design

Propulsion

The propulsion bay provides the Free Flyer with the capability for the orbit station. In particular the propulsion system allows to:

- execute orbital maneuvers for re-boost operations
- maintain attitude for the entire mission
- execute maneuvers to perform RvD with the ISS. The ISS is the target and the Free Flyer is the chaser

The propulsion system stores up to 3000 kg of propellant. The ΔV capabilities are not sufficient for Free Flyer entire lifetime in LEO orbit thus refueling mission shall be performed.

The proposed equipment are:

- OCS: 4 Main Engines thrust level 490N; I_{sp} 315s
- ACS: 28 Secondary thrusters thrust level 220N, I_{sp} 270s
- Propellant tanks (Propellant type: MON/MMH)

- Pressurant tanks, Valves & Pipes

Electrical Power System

The EPS supplies power to the Free Flyer (resource and laboratory module) during all mission phases and to the other vehicles docked to the Free Flyer during its mission life time.

The main high level requirements are:

- Free Flyer shall provide electrical power to its subsystems during all mission phases and for all the mission duration:
 - Up to 3.7 kW to internal equipment
 - Up to 2.5 kW to the experiments during unmanned phases
 - Up to 1 kW to the experiments during manned phases: part of the experiments operate for extended periods of time while other operate between two crew rotations. The astronauts, during manned phases, collect research material and perform new experiments setting. In case Cargo Logistic Vehicle is not attached additional power can be reallocated to experiments (+1 kW)
- Free Flyer shall provide vital power to the vehicles docked
 - 2 kW to Crew Transportation Vehicle
 - 1 kW to the Cargo Logistic Vehicle
- Free Flyer shall store electrical power
- Free Flyer shall provide energy by a storage system during shadow

Figure 59 presents graphically the power source generators against time and power load. The solution that best fits the electrical power needs is photovoltaic.

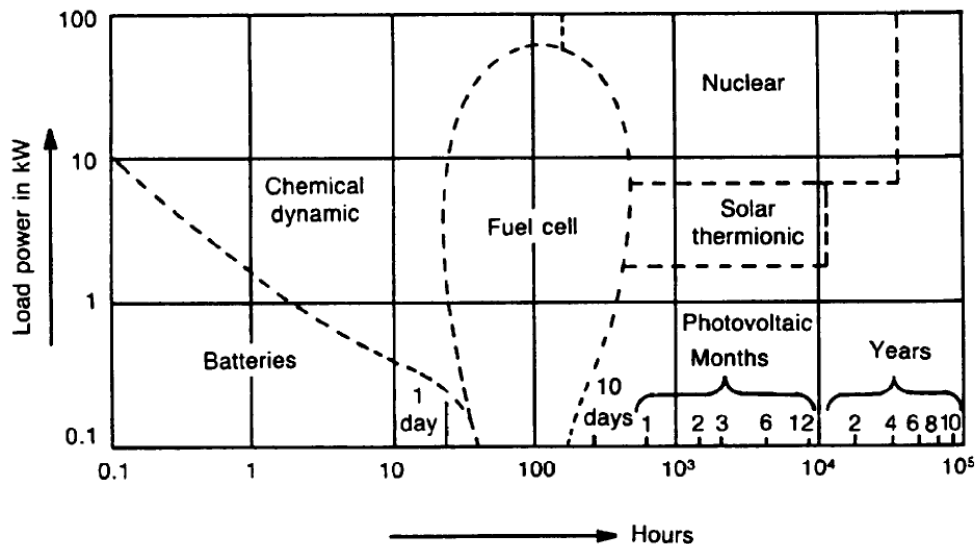


Figure 59 Power source generators against time and power load, ref. [4]

Batteries turn out to be the most efficient storage system to supply power during the Free Flyer eclipse periods. Regenerative fuel cells allow energy storage and are more efficient of batteries for long power demand periods and temporarily higher power needs. Fuel cells are able to provide oxygen, prepare propellant and produce water. Nevertheless, fuel cells imply higher TCS loads, change the EPS requirements and require other subsystem adaption and impact on the logistic scenario. Space Shuttle was equipped with fuel cells to provide power from launch through landing rollout. The fuel cells generate heat and water as products of electrical power generation and was coupled with crew support system and thermal system

to allows synergisms. Fuel cells are considered less efficient in terms of “integrated” mass than batteries for the Free Flyer

The Resource Module solar arrays configuration is shown in Figure 60. Mainly it consists of four wings (GaAs cell) deployable with orientation mechanisms for sun tracking. The total solar array area is 75 m².

The solar arrays provide 17.2 kW (at the end of life) during daylight to power the spacecraft for the entire orbit. Thus, the power generated during daylight support the Free Flyer systems including recharging of batteries. The average power to be generated during daylight is calculated considering an efficiency of the paths from the solar arrays through the batteries to the loads of 0.65 and an efficiency of the paths from the solar arrays directly to the loads of 0.9. The duration of the daylight (55 minutes) and eclipse (37 minutes) periods are assumed doing reference to ISS orbit. The design takes into account design and assembly inefficiencies, temperature inefficiencies and shadowing of cells. The efficiency factor takes into account of these inefficiencies and it is equal to 0.85. Finally, considering a lifetime of 10 years and related degradation, 75 m² of solar arrays are necessary.

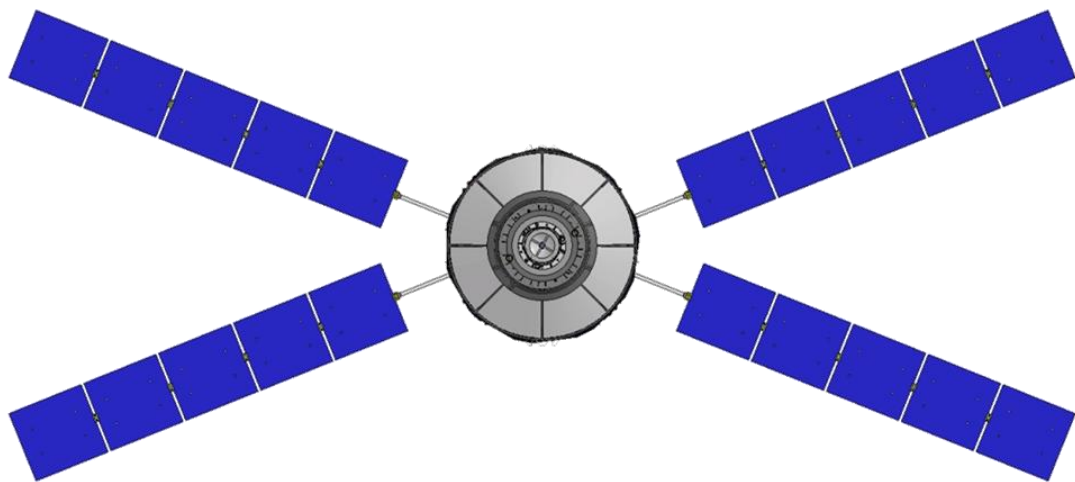


Figure 60 Solar arrays design

Other than solar arrays and batteries, the proposed components are:

- PCDU: performs the power conversion capability
- Remote Powered Control Modules: performs the power distribution capability
- Utility Outlet Panels (UOPs): performs the power distribution capability
- Remote Control Assemblies: allows illumination control
- General Lights Assemblies: supports crew operations activities
- Emergency Lights System: turns autonomously on in case of primary illumination loss
- Harness: performs the power distribution capability

Thermal Control

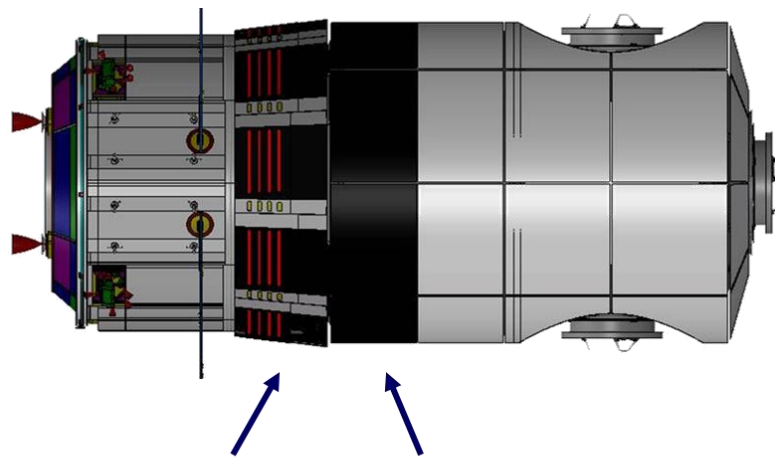
The thermal system provides active and passive temperature control for the entire Free Flyer through heaters, fluidic loop systems, radiators, MLI. The following set of requirements has been considered in the thermal design:

- The Resource Module shall have an operational life of 10 years
- The Resource Module shall be located in Earth orbit
- The Resource Module shall provide heat rejection for the whole Free Flyer

- The Resource Module shall support an overall electrical power of 5.2 kW (during manned phases and assuming self-thermal dissipation of visiting vehicles)
- The Resource Module shall support crew presence (0.5 kW)

To reject the maximum heat load of 5.7 kW a total surface area of $\sim 30 \text{ m}^2$ is requested if 190 W/m^2 are assumed.

The radiators are body mounted: the radiators are located partially on the resource module and partially on the pressurized module. The proposed solution is aimed to provide as much as possible the reutilizing of ATV derived components, eventually resized to higher heat rejection requirements.



Radiators (Body mounted)

Figure 61 Body mounted radiators

ECLS

The Free Flyer shall provide a pressurized environment in accordance with the applicable human habitability requirements, shall ensure a safety environment and shall support the crew during their presence onboard also providing, consumables and facilities.

The ECLS system foresees regenerative technologies

- To provide oxygen recovery
- To recover water

Food production capabilities have been considered not necessary for the Free Flyer. In fact for what concerns the regenerative processes are not mass-efficient for such mission duration. The choice is to store food.

Although, Free Flyer provides ECLS capabilities (FDS, pressurization, ventilation, consumables storing, CO_2 removal and water regeneration and management) for all the on orbit assembly, the choice is to allocate functional volume (such as sleep accommodations and food production) to the crew visiting vehicle because, however, it shall provide such capabilities during the transfer phase.

The detail break down of the necessary consumables is reported in Table 29. The mass coefficient are provided in section 4.9.

Consumable*	Mass	
Water**	120	kg
Oxygen**	10	kg
Food	195	kg
Clothing	40	kg
Spare Parts	95	kg
Total	550	kg

*3 Crew members, 4 Weeks (worst case)

**Assuming a buffer of 3 days

Table 29 Consumables mass budget

The atmosphere of the Free Flyer will be controlled in terms of air pressure, temperature, humidity, velocity, particulate and microbial concentrations. Intra-module air circulation is based on an air loop composed of a central fan, condensing heat exchanger, water separator, filters, ducts, diffusers and grids. Inter-module ventilation with attached elements is obtained through dedicated ducting, valves and fans. Fire detection is supported by cabin smoke sensors and monitoring of the electrical equipment. Fire suppression, within predefined internal enclosures, relies on the use of portable fire extinguisher. Summarizing, the Environmental Control & Life Support (ECLS) will be composed of four functions:

- Atmosphere Control and Supply
- Air Revitalization System (ARS)
- Oxygen Regeneration System (ORS)
- Fire Detection and Suppression (FDS)
- Temperature and Humidity Control (THC)
- Water Recovery System (WRS)

GNC

The major high level requirements for the Guidance Navigation and Control system (GNC) are:

- The Free Flyer shall provide self-attitude and orbit control
- The Free Flyer shall allow RvD and docking maneuvers with LEO orbital infrastructure
- The Free Flyer shall support to RvD and docking maneuvers of visiting vehicles
- The Free Flyer shall provide attitude control to docked visiting vehicles

The sensors for attitude, position, velocity acquisition and RvD with visiting vehicles and LEO orbital infrastructure:

- Star Tracker
- IMU
- GPS
- Sun Sensor Unit
- Telegoniometer
- LIDAR

OBDH

The On Board Data Handling Subsystem controls the operation of all other subsystems. The major high level requirements are:

- The OBDH shall provide on board storage resources for data to be later transmitted to the Ground
- The OBDH shall provide processing resources to support on-board software
- The OBDH shall provide automatic reconfiguration capabilities in case of detection of on board malfunctions
- The OBDH shall distributes commands generated on board (by software or hardware for reconfiguration purposes)
- The OBDH shall acquire data (housekeeping data from valves, sensors, relay status, attitude and position data, ECLSS data, etc.).
- The OBDH shall distribute commands (to attitude and orbit control actuators, to solar array drive mechanism, to the antenna steering mechanism, etc.)

The proposed equipment consists of:

- Master Control Computer (MCC)
- Mass Memory Module (MMM)
- Decentralized Command and Monitoring Units (CMU)
- HR Router
- Panels

Communication

The Free Flyer is a man-tended system that, for most part of its life, is uninhabited. It periodically hosts maximum 3 astronauts for up to 4 weeks (2 week are nominal). The major high level requirements are:

- The Free Flyer shall transmit telemetry to the Earth, during all its mission phases
- The Free Flyer shall receive commands from the Earth, during all its mission phases.
- The Free Flyer shall provide payload data collection, compression and storage
- The Free Flyer shall transmit payload data to the Earth when the experiments are on board
- The Free Flyer shall exchange audio data with the Earth during the crew missions
- The Free Flyer shall transmit video data to the Earth
- The Free Flyer shall support communications with visiting vehicles
- The Free Flyer shall interface with LEO infrastructure during proximity operations

Table 30 shows a preliminary estimation of the data rate budget for telemetry and commands, audio and video, based on the following assumptions:

- audio data shall be taken in consideration only when Man is on-board
- when crew is not on board, video data could be transmitted when required

The data rate required to be transmitted to Earth is ~8.9 Mbps during manned phases of the mission with payload data not included. The assumed payload total data rate is 50 Mbps.

Data	Upload (Kbit/s)	Download (Kbit/s)
Telemetry and Commands	120	10
Audio	64	64
Video	8700	8700
Payload Data	up to 50000	-

Table 30 Preliminary Estimation of Data Rate Budget

Figure 22 shows the hypothesized communication architecture. The Free-Flyer shall be able to communicate with the visiting vehicles, with crew during EVA and with the ground station. Direct link is possible with the crew during EVA, with the Earth surface and with the visiting vehicles when they are visible. A data relay system is necessary to allow communication with the ground station and with visiting vehicles when they are not visible from the Free-Flyer. The existing Tracking and Data Relay Satellite System (TDRSS) allows continuous communication link with the ground station. The S-band communication link is utilized to allow communication with visiting vehicle while Ka-band is utilized for the other links. Finally, VHF or UHF provide communication with EVA crewmembers.

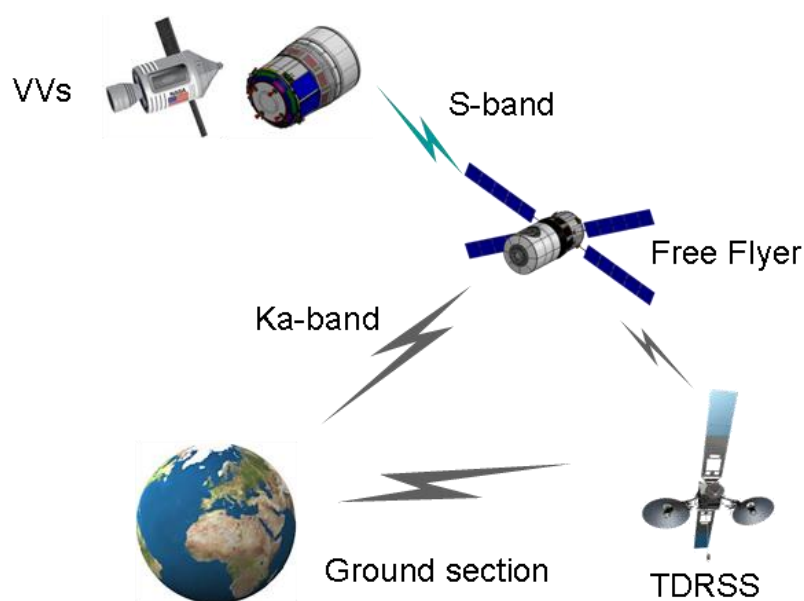


Figure 62 Communication architecture for Free Flyer

7.1.7 System budgets

7.1.7.1 Mass

The mass budget is done taking into account a subsystem margin variable from 5% to 20% (5% for fully developed systems, 10% for systems to be modified and 20% for system to be developed) on each single item and adding a System Margin of 20% on the sum of the designed parts. The mass budget has been performed implementing equation presented in section 4.

System	BEE Mass [kg]	Margin [%]	BEE Mass (w/ Margins)	
Structure	5037	10	5541	kg
TCS	844	10	929	kg
Mechanisms	900	20	1080	kg
Communications	102	10	112	kg
OBDH	91	10	100	kg
GNC	237	10	261	kg
Propulsion	638	10	702	kg
EPS	858	10	944	kg
ECLS	1376	20	1651	kg
Airlock	2500	20	3000	kg
Total Dry	10083		14319	kg
System margin (20%)		20	2864	kg
Experiments			0*	kg
Total Dry			17183	kg
Propellant			3000	kg
Total wet mass			20183**	kg

* Experiments and consumables provided by cargo mission to allow launch with A5ME

** Launcher adapter and separation mechanism not included in the mass budget

Table 31 Free Flyer mass budget

7.1.7.2 Power

Table 32 shows the power demand of the main subsystems for various mission phases, i.e. transfer phases in LEO environment, RvD, LEO with and without crew onboard and visiting vehicles attached. The power for battery recharging has been estimated considering an efficiency of the paths from the solar arrays through the batteries to the loads of 0.65 and an efficiency of the paths from the solar arrays directly to the loads of 0.9. The assumed duration of the daylight period is 55 minutes and of the eclipse period is 37 minutes.

The assumed power consumption for each subsystem derives from literature survey, ref. [2]. The power need for crew visiting vehicles has been assumed equal to 2 kW doing reference to NASA exploration crew vehicle. The crew vehicle average power need for the mission with crew on board is 4.5 kW. The assumed power need in attached configuration with solar array partially overshadowed and ECLS at reduced performances is equal to 2 kW. The power need for logistic visiting vehicles has been assumed equal to 0.9 kW doing reference to ATV heritage.

S/S	LEO- Transfer [W]	Rendezvous/ Docking [W]	LEO without crew [W]	LEO with crew [W]
Mechanisms	0	100	0	0
TCS	570	570	570	570
Communication	20	20	80	80
OBDH	590	590	590	590
GNC + Audio & Video	222	222	270	270
Propulsion	100	100	0	0
ECLS	0	0	500	2245
Sub Total	1502	1602	2010	3755
Payload:				
experiments	0	0	2500	1000
Payload: cVV	0	0	0	2000
Payload: LV	0	0	900	900
Harness Loss 5%	75	80	270	383
Battery recharging	1807	1927	6509	9211
Total	3384	3609	12189	17249

Table 32 Free Flyer power budget

7.1.7.3 Thermal

Total 5.7 kW (assuming self-thermal dissipation of visiting vehicles). Thermal budget is derived from power budget assuming that all the power to be produced shall be dissipated.

- Up to 5.2 kW for internal equipment
- Up to 0.5 kW for crew on board

7.1.7.4 Delta-velocity budget

The propulsion system of the Free Flyer shall be able to provide propulsion capability for RvD, orbit station keeping, attitude control and de-orbiting. The following table provides summary of ΔV .

ΔV budget				
System	FF + Airlock			
Maneuver	Altitude change (from 260 km to 400 km)	82	m/s	
Maneuver	ISS phasing	40	m/s	
Maneuver	ISS RvD maneuvers (+ backup attempt)	150	m/s	
System	FF + Airlock + Experiments			
Maneuver	ISS Departure	15	m/s	
Maneuver	Altitude change (from 400 km to 460 km)	35	m/s	
Maneuver	Station keeping LEO (10y at 460 km)	100	m/s	
Maneuver	Attitude Control (10y)	60	m/s	
Maneuver	De-orbiting	175	m/s	
Total		-	657	m/s

Table 33 Free Flyer ΔV budget

7.2 Cargo Logistic Vehicle

7.2.1 Mission objectives

The Cargo Logistic Vehicle (CLV) provides logistic support to orbital infrastructures in cis-lunar space.

The CLV provides re-supplying of:

- Pressurized payload
- Unpressurized payload

7.2.2 System requirements

Mission Requirements

- The mission design shall be compatible with an Ariane 5 ME launcher
- CLV shall deliver at least 2000 kg of pressurized payloads and at least 500 kg of unpressurized payloads to cis-lunar destinations (LLO, EML-1, EML-2)
- CLV mission shall be designed in order to permit ground supervision during all the critical phases of the mission

Interface Requirements

- CLV shall have a standard docking interface to the cis-lunar orbiting vehicles
- CLV shall be compatible with the Ariane 5 ME launcher interfaces requirements
- CLV shall be compatible with the cis-lunar station interfaces requirements
- CLV shall be designed to allow exchange of data (including status monitoring and relative navigation data) with the cis-lunar station interface during proximity operations

Functional Requirements

- CLV shall provide pressurized and unpressurized logistics to orbiting vehicles in cis-lunar space (LLO, EML-1, EML-2)
- CLV shall be able to perform autonomous RvD with a cooperating target in cis-lunar space
- CLV shall be able to provide power and thermal control to the payloads
- CLV shall be able to depart the cis-lunar station and be disposed in a way that poses no long term-threat to crew or other exploration systems.

Environmental Requirements

- CLV shall be designed to operate in a cis-lunar environment

Operational Requirements

- CLV shall have the capability to operate in an automated mode with ground supervision
- CLV shall be designed to permit the ground segment and the crew on board Cis-Lunar orbiting vehicles to trigger a collision avoidance maneuver

7.2.3 Mission Reference Scenario

CLV is launched in High elliptic orbit (HEO) by the Ariane 5ME. It performs autonomous maneuvers to reach and dock the cis-lunar space infrastructure. In case the crew is not present onboard the cis-lunar infrastructure, the Cargo transfer phase starts after cVV

arriving. The CLV remain docked to the infrastructure for all the time necessary to cargo unloading/loading. After, the CLV previously filled with waste undock and performs disposal maneuvers that put CLV in an orbit without long-term effects.

The CLV mission scenario, which is based on ATV mission profile, foresees five main phases, i.e. Launch Phase, Transfer Phase, Docking phase, Station Visit Phase, Departure. The detailed description of the operations performed in each phase follows here.

Launch Phase

- CLV is launched by Ariane 5 ME in HEO orbit (apogee 100000 km, perigee 300 km)
- After separation from the launcher, CLV performs on board systems initialization and the necessary orbit stabilization maneuvers
- The launch phase ends with the deploying of the CLV solar arrays

Transfer Phase

- CLV performs orbital maneuvers (Resonance Transfer) in accordance with proposed transfer strategies for each target

Proposed strategy to reach EML-1 [50 m/s; 3 months ÷ ~1 year]

- A5 launches CLV into HEO orbit
- CLV performs Resonance Transfer strategy to reach EML-1
- Required ΔV 50 m/s
- Transfer time: 3 months ÷ 1 year

Proposed strategy to reach EML-2 [190 m/s; 4 months ÷ ~1 year]

- A5 launches CLV into HEO orbit
- CLV performs Resonance Transfer strategy to reach EML-1
- Required ΔV 50 m/s
- Transfer time: 3 months ÷ 1 year
- Once in EML-1, CLV perform transfer maneuver to reach EML-2
- Required ΔV 140 m/s
- Transfer time: 1 month

Proposed strategy to reach LLO [690 m/s; 3 months ÷ ~1 year]

- A5 launches CLV into HEO orbit
- CLV performs Resonance Transfer strategy to reach EML-1
- Required ΔV 50 m/s
- Transfer time: 3 months ÷ 1 year
- Once in EML-1, CLV perform transfer maneuver to reach LLO
- Required ΔV 640 m/s
- Transfer time: >2 days (TBC)

Docking phase

- In proximity of the Cis-Lunar Space Station, CLV performs final approach and docking maneuvers automatically. During docking phase, CLV has the

automatic or manual (from ground) capability to trigger a collision avoidance maneuver should any problem occur at CLV or Station level

- After attachment accomplishment, CLV gets dormant operational mode if the docking phase is performed when Space Station uninhabited. CLV is supplied by space station with power

Station Visit Phase

- In case, before crew arriving, CLV performs systems initialization
- Cargo is manually unload by the visiting crew and possible consumables refurbishment (fuel, water, etc...) operations are powered and controlled by space station (up to 0,9 kW are available)
- Finally, CLV is loaded with waste (up to 2000 kg)

Departure

- The undocking phase starts after command by orbiting crew or ground station
- CLV performs automatically undocking and disposal maneuvers

The schematic of the mission scenario is provided in Figure 63.

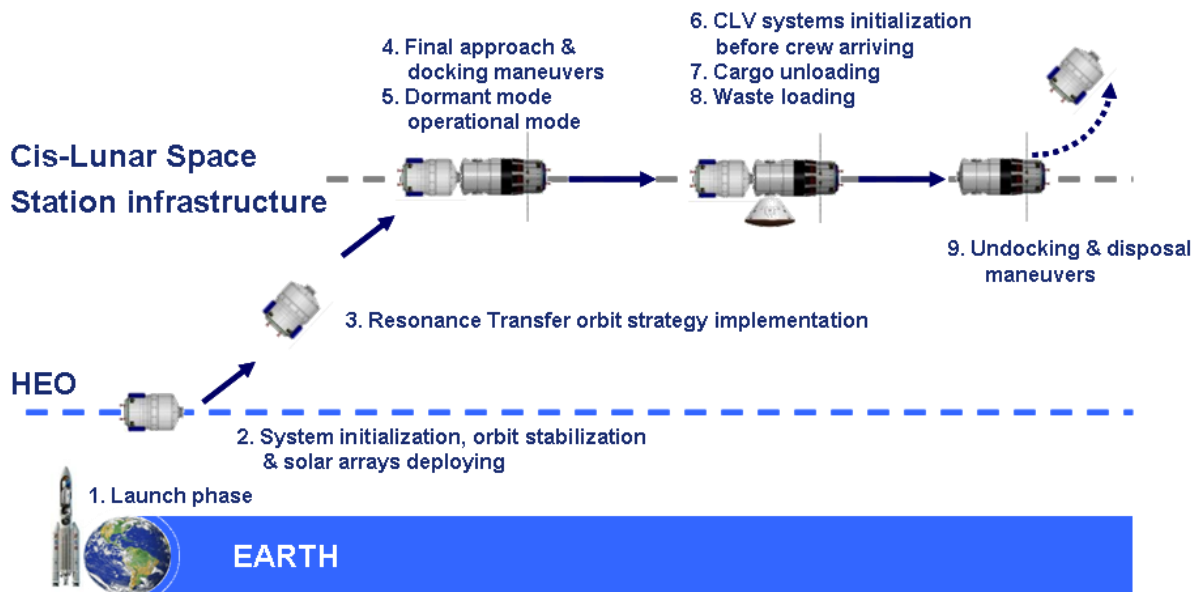


Figure 63 CLV mission scenario

7.2.4 System description

The design approach of the CLV is performed preserving (as much as possible) the ATV heritage. The chosen design approach allows:

- Possible re-use of existing technologies (after obsolescence analysis)
- Reduction of technological risks associated to new designs
- Reduction of development time
- Reduction of cost related to the system design complexity
- Potential subsystems design optimization

The system is composed of two main modules: a resource module (RM) and a pressurized module called Cargo Carrier (CC)

The resource module is composed of two main bays (propulsion bay and resource bay) and provides power capabilities (power generation and storage), Data Management, Thermal control, Communication, consumable storing, Orbit & attitude control capabilities

The pressurized module provides a pressurized compartment with ECLS basic and docking capabilities.

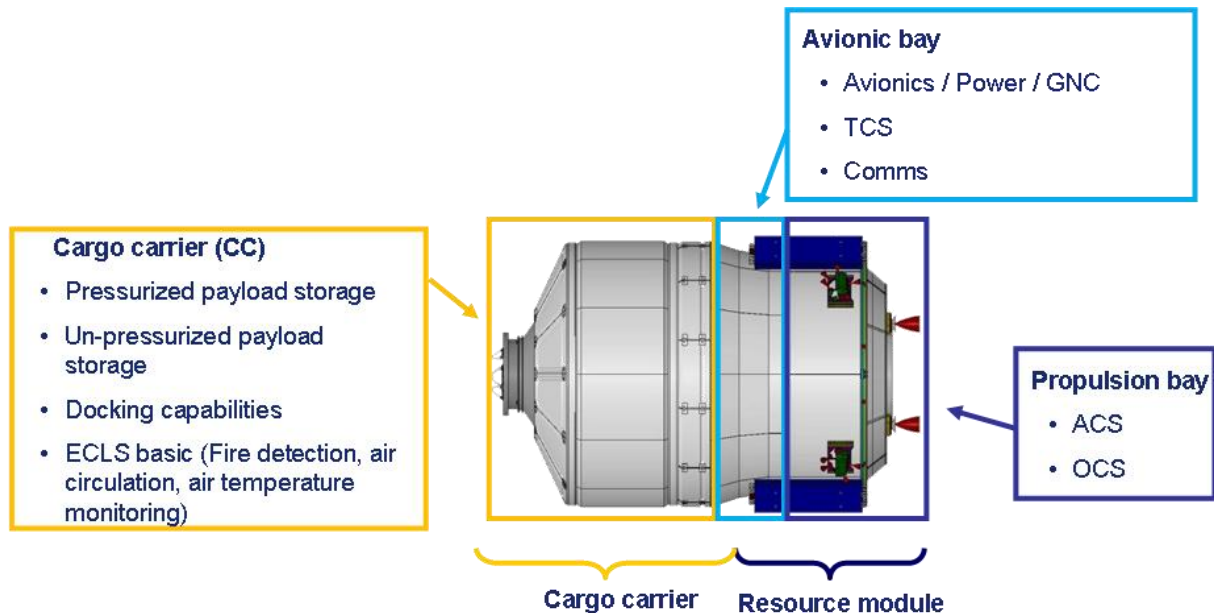


Figure 64 CLV functional configuration

7.2.4.1 Cargo Carrier design

The pressurized payload is disposed into payload bags (Cygnus like) which have been chosen instead of racks enhanced version because of higher storing efficiency in terms of mass and volume. Two kind of payload are possible:

- Passive payload
- Active payload (needs of dedicated power and thermal dissipation)

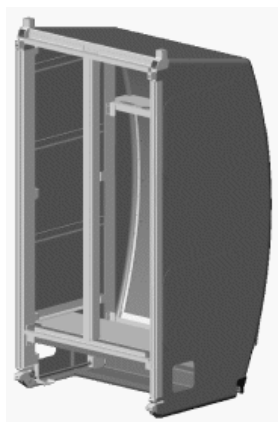


Figure 65 International standard rack enhanced version



Figure 66 Cargo bag

Payload configuration:

- Payload bags circumferentially disposed on 4 panels: payload bags have been chosen instead of racks enhanced version because of higher storing efficiency in terms of mass and volume
- The Active payload requires up to 850W for heater (ATV analogy, ref. [41])



Figure 67 CLV pressurized payload configuration, ref. [42]

Unpressurized payload (gas, liquids) is stored into external tanks (ATV analogy). The Payload tanks are located externally on the rear Cargo Carrier closure panel

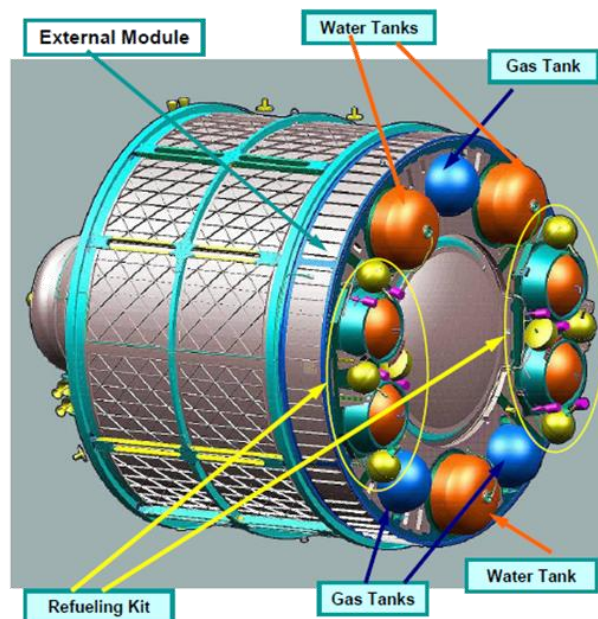


Figure 68 CLV unpressurized payload configuration, ref. [43]

The CLV shall be able to provide 2000 kg pressurized payload and 500 kg unpressurized payload. The assumed pressurized payload mean density is 245 kg/m³, thus 8 m³ of cargo volume must be provided. Doing reference to existing vehicles the necessary pressurized volume is 19.2 m³. The mass for secondary structure is assumed equal to 20% of payload 400 kg. Unpressurized payload (essentially fluids) is stored on external tanks (ATV analogy, ref. [41]).

The Cargo carrier diameter is 4.5 m and the length of the cylindrical section is 1.5 m which is compatible with the payload storage volume requirements with sufficient margin. The docking interface meets the International Docking System Standard (IDSS). The external diameter is equal to 1727 mm (ref. [44]) and the assumed mass is 300 Kg.

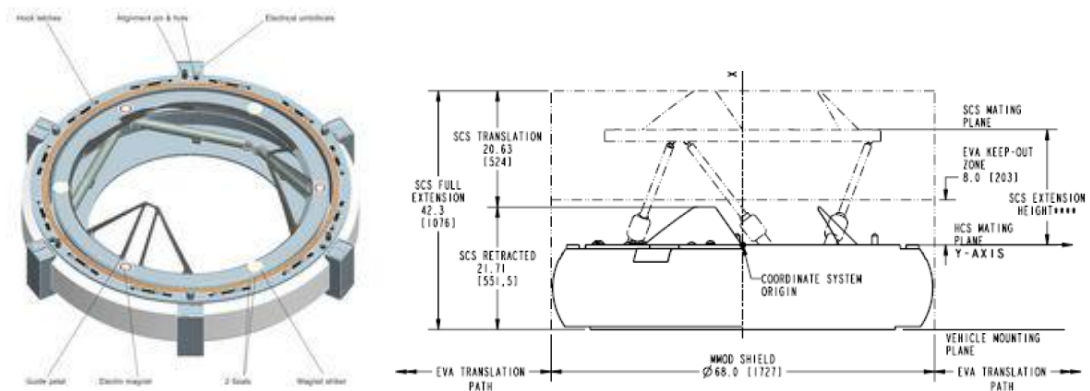


Figure 69 Docking interface, ref. [45]

Figure 70 shows Internal bags disposition, tanks of unpressurized payload disposition and envelopes of the cargo carrier section.

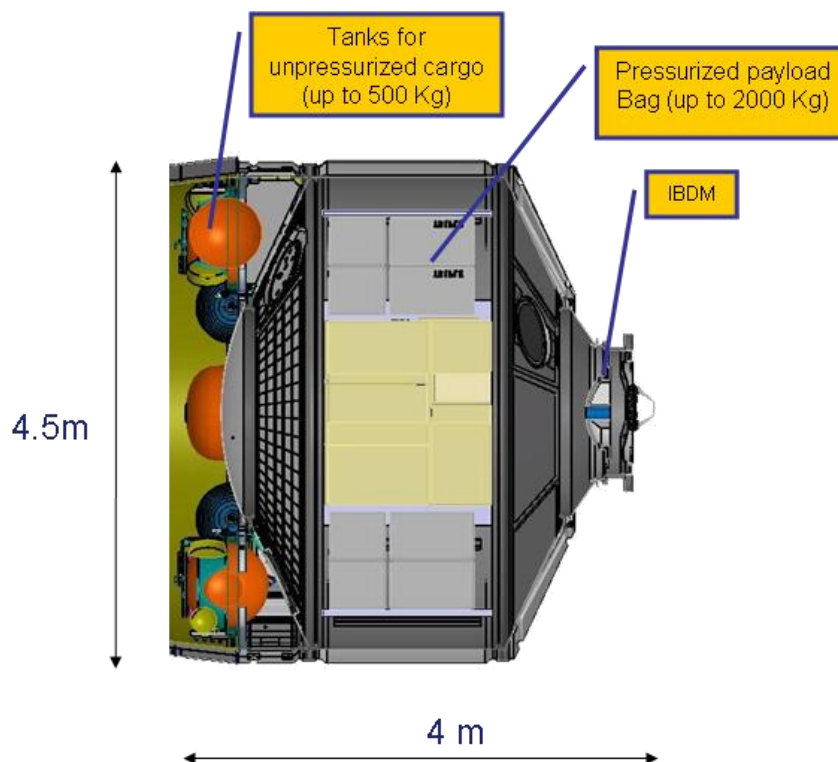


Figure 70 Internal bags, tanks of unpressurized payload and envelopes of the cargo carrier section

Other than baseline configuration (8 m^3 , 245 kg/m^3), a “Full volume” configuration has been studied: 11 m^3 (up to 2000 kg) of pressurized payload can be stored with mean density of 180 kg/m^3 . The last configuration provides:

- Up to 2000 kg of payload
- Up to 11 m^3 of payload ($\sim 180 \text{ kg/m}^3$ of payload density) with lower payload accessibility (see previously figure)

The full volume bags configuration assessment is provided in Table 34:

Bag Type	CTB eq.	#	TOT CTB eq	Volume
Single-size	0.5 CTB	10	50	2.6 m3
Double-size	1 CTB	4	4	0.2 m3
Triple-size	2 CTB	24	48	2.5 m3
M01	6 CTB	18	108	5.7 m3
TOTAL			210	11 m3

CTB: Cargo Transfer Bag

Table 34 Full volume bags configuration

Stand offs allow illumination and payload ventilation.

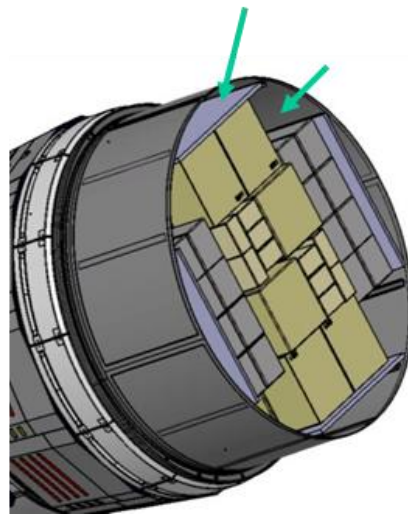


Figure 71 Stand-offs of the Cargo Carrier

7.2.4.2 External scientific platform assessment

Since the mission duration last up to 1 year, the option to perform scientific research during transfer shall be taken into account. The opportunity to perform scientific research increases the cost effectiveness of the CLV. The system exploits the high transfer time to perform experiments in different environmental condition from LEO.

The possible options for scientific payload accommodation are:

1. External payload platform: consists of platform(s) accommodating payload with power, thermal and control servicing. Since the fairing of A5ME does not allow lateral accommodation of the platform(s), these must be located on the frontal cone of the cargo carrier. To avoid mechanical interference during RvD, the payloads shall be located at safety distance from the docking plane. Two solutions have been investigated. The first one (Figure 72 left) foresees mechanisms which, once on orbit, move the platform away from critical zones. The second solutions (Figure 72 right) foresees bi-conical design of the frontal closure structure. Scientific payloads can be integrated at launch although experiments environmental compatibility in all the mission phases, from launch to orbit, shall be ensured.

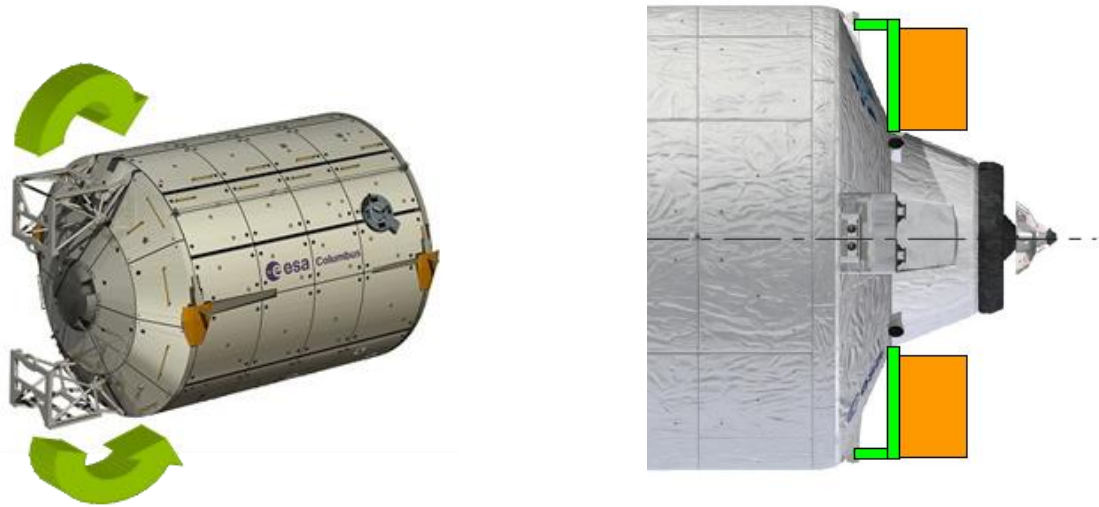


Figure 72 External payload platform

2. Unpressurized bay: a dedicated section for un-pressurized exposed experiments is located in the resource bay where unpressurized cargo is stored. Two different configurations are possible: totally exposed payload configuration (Figure 73 left) and partially exposed payload configuration (Figure 73 right). Both the solutions require complex experimental deployment mechanisms and structural configuration. Scientific payloads are integrated at launch and the environmental protection is provided by CLV during the critical mission phases.

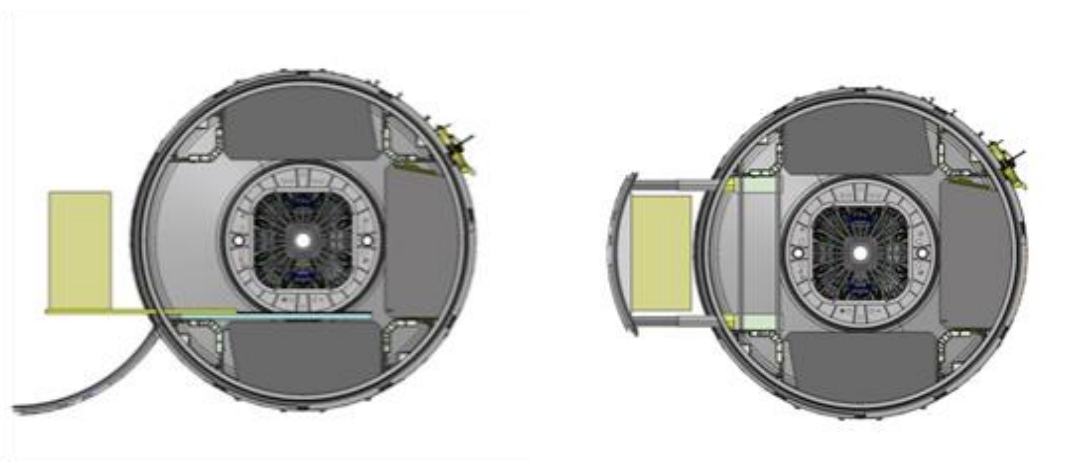


Figure 73 Unpressurized bay for experiments

Table 35 summarizes the main considerations about the possible solutions.

Options	Movable external platform	Fixed external platform	Unpressurized bay
Research capabilities Considered proportional to the available volume for scientific equipment	More external platforms could be accommodated	Limited number of platforms since RvD sensors interference	A limited volume can be devoted to payload accommodation
CLV impact	The platform shall be provided with mechanisms that, once on orbit, move the platform away from the frontal section. No particular impact on CLV	The bi-conic structure, necessary to shift the docking plane, implies mass penalties	Complex deployment mechanisms and structural configuration are necessary
Risk of primary mission failure	In case of deployment mechanism failure, the primary mission shall be aborted. The risk increases with the number of payload platforms	Parts of stay out volumes are occupied by payload envelopes. The risks in case of critical events during docking increases	No particular risks linked to mechanisms failure
Payload environmental compatibility	Payloads shall provide self-protection during launch	Payloads shall provide self-protection during launch	Experiments environmental protection during launch is provided by the CLV

Table 35 External scientific payload Trade off – rationale

	Research capabilities	CLV impact	Risk	Payload environmental compatibility	
Weighting factor	20	25	35	20	100
Movable external platform	1	1	-1	0	10
Fixed external platform	0	-1	0	0	-25
Unpressurized bay	0	-1	1	1	30

Table 36 External scientific payload Trade off – results

Risk have the higher weighting factor to heavily penalize the possibility that the CLV primary mission (i.e. provide logistic) fails due to a secondary mission (i.e. perform research). Then, the CLV impacts in term of complexity and mass penalty have been considered more important than the research issues because the potential negative effect on CLV logistic performance.

In conclusion, the best option is the unpressurized bay mainly because the lower risk of mission failure even though the mass and complexity of the CLV increase.

7.2.4.3 Resource module design

The resource module is composed of three main bays (propulsion bay, avionic bay and resource bay) and provides power capabilities (power generation and storage), Data Management, Thermal control, Communication, consumable storing, Orbit & attitude control capabilities.

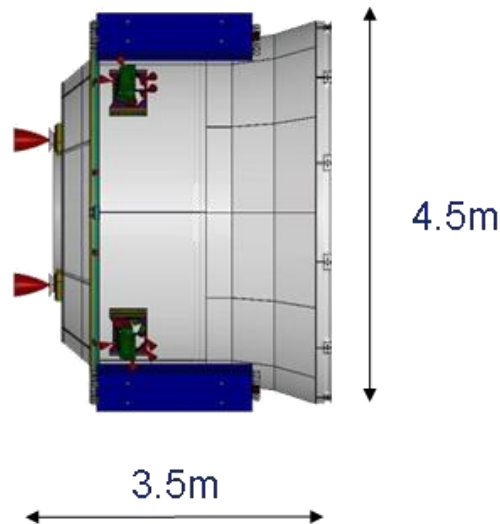


Figure 74 resource module envelope

Structure subsystem

The RM unpressurized structure provides support to the main RM subsystems: power, avionic, propulsion, thermal systems components. Mainly, it consists of a rigid cylindrical structure with external diameter equal to CC diameter (4.5 m). The external structure of the RM provides support to the solar arrays and to the body mounted radiator panels. Internally, the RM structure provides support, other than the avionics, also to the propulsion system tanks. The structure mass has been estimated equal to ~630 kg and it is compatible with up to 2100 kg of propellant.

The structure can be divided into three main sections. Starting from the bottom, the propulsion bay houses the propulsion equipment, supports the solar arrays and provides interface with the launcher. Above the propulsion bay, the avionic bay is located. It mainly houses the avionic equipment and support part of the radiators. Finally, the resource bay houses the unpressurized payload tanks and provide interface with the cargo carrier. In this section, unpressurized experiments can be located. The resource section provides support to the mechanisms necessary for exposition of the experiments.

The structural design of the Resource Module derives from ATV, reducing the number of propellant tanks and therefore the propulsion section length. The propellant tanks are equatorially disposed and are supported by a structural platform. Below the tanks, the separation plane with the launcher provides support to the thrusters. Above the propellant tanks, the external cylindrical structure supports the internal avionic equipment and the external radiators. The unpressurized payload is stored inside tanks that are located near the cargo carrier interface plane. These tanks are circumferentially disposed and equatorially supported by a further platform. Finally, internal shear panels collaborate to the sustaining of the mechanical loads. Figure 75 shows the Resource Module structural design.

Considering that the launcher puts the CLV directly in HEO, the Meteorite and Debris Protection System shall be conceived to provide protection of the CLV from Cis-lunar environment.

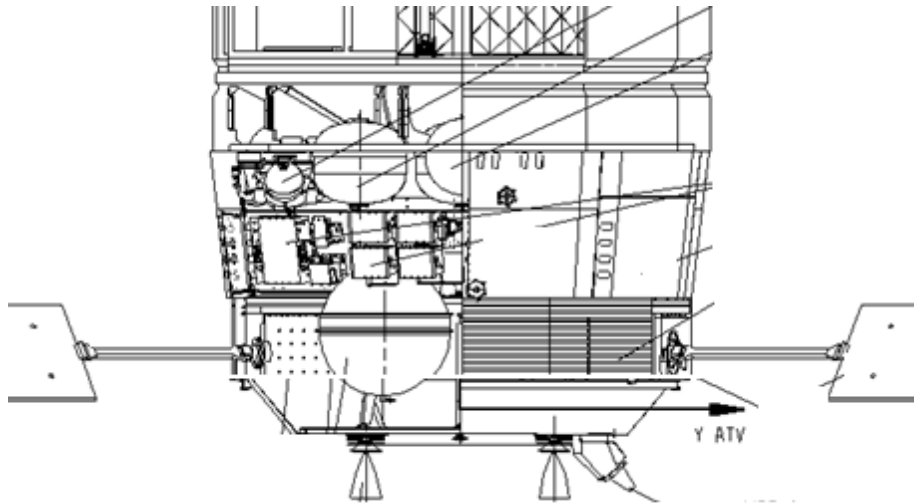


Figure 75 structural design

Power subsystem

The power system provides power generation, storage and distribution to the RM components and to the CC. The preliminary CLV power generation need is 5 kW (ATV, ref. [41]). Four GaAs solar wings, each consisting of 4 panels with rotating drive mechanism, provide the electrical power. The solar wing total area is 25 m². The solar wings are disposed at 22 deg from each other (X shape as ATV, ref. [41]).

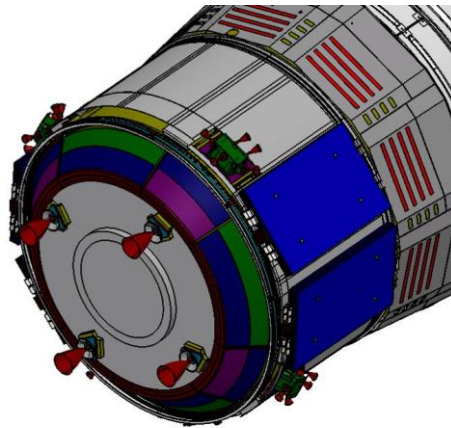


Figure 76 CLV power generation system

CLV maintain the ATV power system architecture, ref. [41]. Four PCDUs distribute power with a regulated voltage to the avionics units and with non-regulated voltage to the heaters. Each PCDU receives power from one panel of each solar wing so that, in case of wings shadow, the system provides balancing of power distribution. Figure 77 provides schematic of the power system configuration.

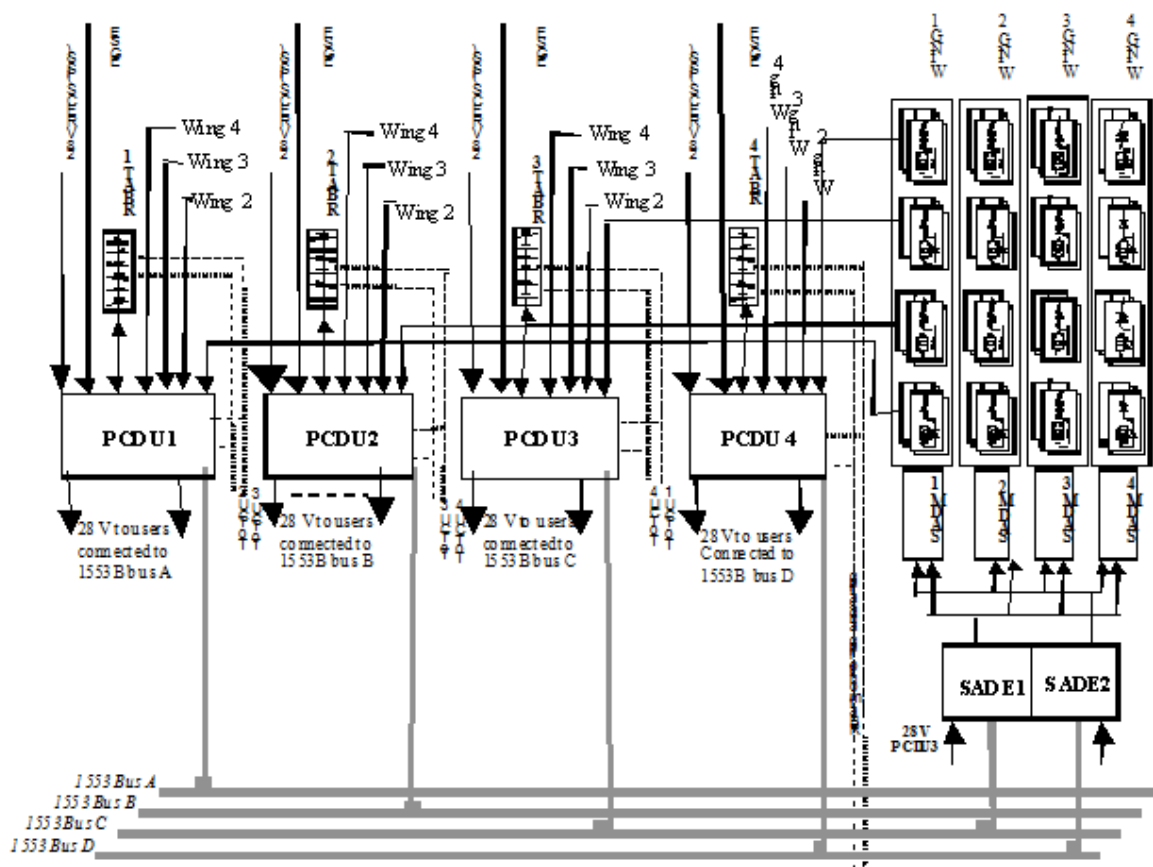


Figure 77 Power system configuration, ref. [46]

Rechargeable batteries have been chosen for power storage and power supplying during eclipse phases. Batteries have been chosen instead of fuel cells because their higher storage energy at low power level. Total mass estimated for power generation, storage and distribution is 775 kg. The technology considered for batteries is Li-Ion because although there are new technology with higher energy density, the Li-Ion are more suitable for long mission due to their lower memory effect.

Thermal subsystem

Multi-Layer Insulation material has been chosen to provide passive thermal control during all the mission phases. MLI provides protection of spacecraft surfaces directly exposed to space or covered by the radiator panels and MDPS protections.

Body mounted radiators (12 m^3) have been chosen to provide 1.5 kW of thermal dissipation. The architecture is based on a Single-phase Fluid Loop Architecture exploiting a HFE-7000 series as coolant to collect and transfer the heat load from both RM avionics (via cold-plates) and PM and reject it to dedicated body mounted radiators. The external radiator consists of an aluminum plate, fixed with insulating support brackets to the Avionics section structure to minimize heat leaks. The external radiator side is white painted to ensure the radiation of heat towards deep space with minimum solar flux perturbation. Finally, heaters are utilized to heat internal equipment. The estimate mass for thermal system components is 400 kg.

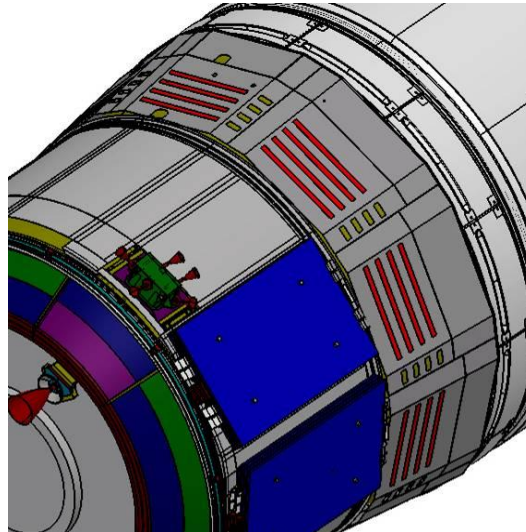


Figure 78 CLV radiators

Avionic

CLV avionic system performs the following functions: communication, data handling, GNC.

The On Board Data Handling Subsystem controls the operation of all other subsystems. It acquires data (from valves, sensors, relay status, attitude and position data, ECLSS data, etc.), provides data storage, provides processing of data to support on-board software, provides distribution of data and commands generated on board and finally provides automatic reconfiguration capabilities in case of detection of on board malfunctions.

CLV communication system shall be able to provide communication with the orbital facilities and with the ground. CLV exploits the same ATV short-range communication system architecture with new and more efficient components. Long-range communication system derives from ATV but it is modified to be compatible with Lunar Telecom Orbiter and higher distances.

The GNC system includes sensors for attitude, position and velocity acquisition and determination and for the rendezvous maneuvers. The sensors data are elaborated by the on board computers that calculate necessary correction maneuvers and send commands to the actuators of the propulsion system.

The sensors for attitude, position, velocity acquisition and RvD with orbital infrastructure are:

- Star Tracker
- IMU
- Sun Sensor Unit
- Tele-goniometer
- LIDAR

CLV antennas and non-optical sensors are located on the resource module. Optical sensors are on the cargo carrier to avoid deployable mechanisms.

Propulsion subsystem

The propulsion system allows the HEO-Cis-Lunar orbit transfer. The choice is to use ATV derived propulsion system. The main advantages are:

- CLV utilizes already space qualified components
- ATV flight heritage can be exploited
- Propellants can be stored for longer periods of time

- Hydrazine can be used also as monopropellant offering an increase in reliability although with decreased performances

The ATV propulsion system provides the spacecraft with the orbit transfer capability and the ISS re-boost support. ATV navigates using four main engines (490 N thrust from Aerojet) plus 28 smaller thrusters (220 N) for attitude control. Four control units connected to the main ATV computers control all valves and thrusters. There are eight titanium propellant tanks and two high-pressure helium tanks. The tanks hold up to seven tons of liquid propellants (MMH – Monomethylhydrazine, and N₂O₄ - nitrogen tetroxide). The propellant tanks are pressurized by helium stored in two high-pressure wound carbon fiber tanks.

ATV derived propulsion system (schematic in the Figure 79) has been considered compatible with the CLV. The estimated propulsion system mass is 830 kg, compatible with 2100 kg of propellant.

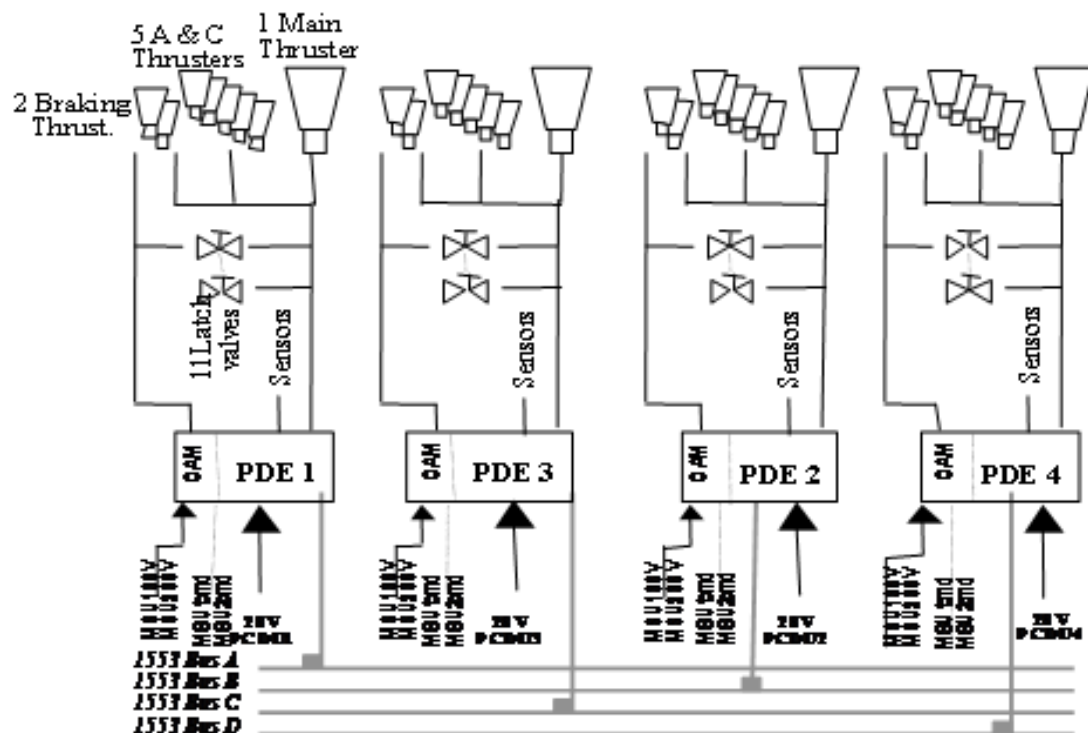


Figure 79 schematic of ATV derived propulsion system, ref. [46]

The thrust level is 1960 N and it is obtained through 4 engines of 490 N each. This gives a maximum vehicle acceleration of:

$$a = \frac{F}{m} = \frac{1960N}{10500kg} = 0.186 \frac{m}{s^2} \text{ or } 0.019g \quad [170]$$

Since we are using ATV propulsion system, we can consider an effective exhaust velocity of 3050 m/s (I_{sp} 311 s) feasible for an Oxidizer-to-Fuel Ratio of 1.65. The propellant mass can be estimated taking into account the exhaust velocity and the necessary ΔV (max 775 m/s for LLO). For the given total mass of 10500 kg, this leads to a propellant mass of 2100 kg. Using information on the Oxidizer-to-Fuel Ratio, propellant mass and propellant density we calculate for the propellant volume and mass of Oxidizer and fuel:

$$\text{Oxidizer: } \text{mass} = \frac{\text{Propellant mass}}{\left(1 + \frac{1}{1.65}\right)} = \frac{2100 \text{ kg}}{\left(1 + \frac{1}{1.65}\right)} = 1307 \text{ kg} \quad [171]$$

$$\text{volume} = \frac{\text{mass}}{\text{Oxidizer density}} = \frac{1307 \text{ kg}}{1450 \frac{\text{kg}}{\text{m}^3}} = 0.9 \text{ m}^3$$

$$\text{Fuel: } \text{mass} = \text{Propellant mass} - \text{Oxidizer mass} = 2100 - 1307 = 793 \text{ kg}$$

$$\text{volume} = \frac{\text{mass}}{\text{Oxidizer density}} = \frac{793 \text{ kg}}{866 \frac{\text{kg}}{\text{m}^3}} = 0.91 \text{ m}^3 \quad [172]$$

Since the propellant volumes are close, identical tanks for the two propellant constituents are selected. This significantly reduces tank development cost, since now only 1 tank needs to be developed (or acquired).

Selecting a regulated feed system and adding 10% ullage volume, we find a tank volume of $4 \times 0.5 \text{ m}^3$. Possible tank is showed in Figure 80. This is a 990 mm spherical pressure vessel able to store up to 503 liters of propellant. A PMD is provided to expel fuel under low or zero gravity conditions. Mounting is accomplished by a continuous flange parallel with and adjacent to the mid-plane.

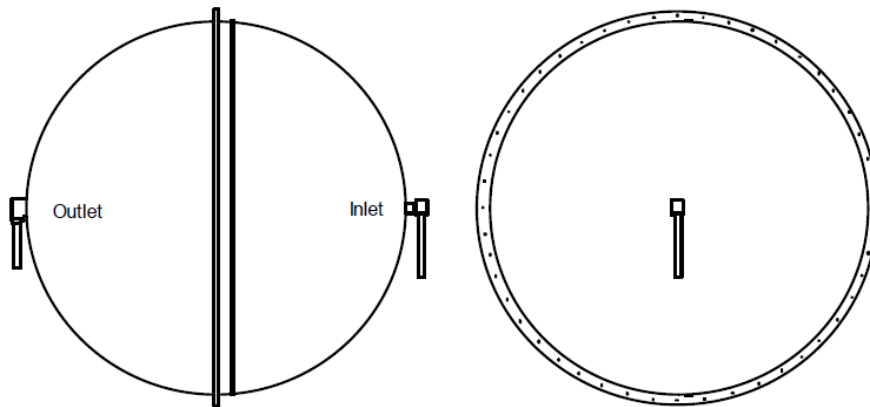


Figure 80 CLV propellant tank

In line with ATV an Helium pressurant system at 31 MPa has been selected. The necessary Helium is stored inside two pressurant tanks.

The design of the ACS is also based on ATV. The same set of thrusters are utilized for attitude control. The proposed equipment utilizes MON/NTO and consist of 28 secondary thrusters with thrust level equal 220N ($I_{sp} = 270 \text{ s}$).

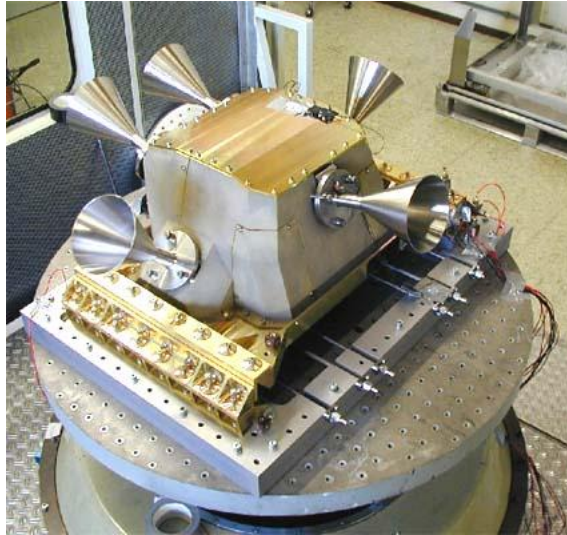


Figure 81 ACS thrusters

Communication subsystem

The CLV communication system shall provide communication with the orbital facility and with the ground. CLV exploits the same ATV short-range communication system architecture with new and more efficient components. Long-range communication system derives from ATV but it is modified to be compatible with Lunar Telecom Orbiter and higher distances.

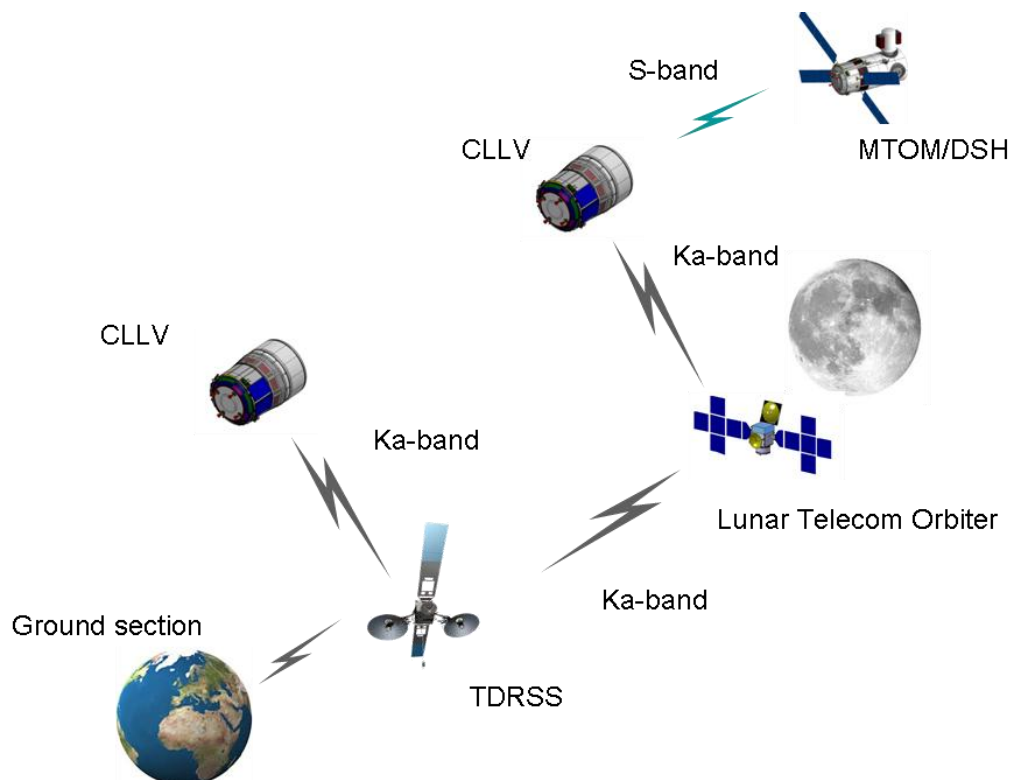


Figure 82 CLV communication links

As ATV communication system, two independent RF chains are foreseen to allow redundancy.

The long range communication system allows communication with the ground segment via TDRSS link when in proximity of the Earth and via Lunar Telecommunication

Orbiter when in the Cis-Lunar space. The assumed data rate is 1 kbps for tele-command and up to 64 kbps for telemetry (values derives from ATV, ref. [46]). The system transmits in Ka-band to be compatible with TDRS and Lunar Telecom Orbiter. To allow redundancy two transponders are foresees as for ATV. The two transponders receive in hot redundancy and transmit in cold redundancy. There are three antennas, two pointing (one for redundancy) towards nadir and one pointing toward the zenith.

The short range communication system allows proximity communication link with Moon outpost. The assumed data rate is 20 kbps for tele-command and for telemetry (also in this case values derives from ATV, ref. [46]). The system transmits in S-band as ATV so that heritage can be exploited. Also for the proximity link there are two transponders that receive in hot redundancy and transmit in cold redundancy. There are two antennas for proximity communication, one pointing towards nadir and one pointing toward the zenith.

Finally, the communication system foresees two CPF in hot redundancy for tele-command and telemetry.

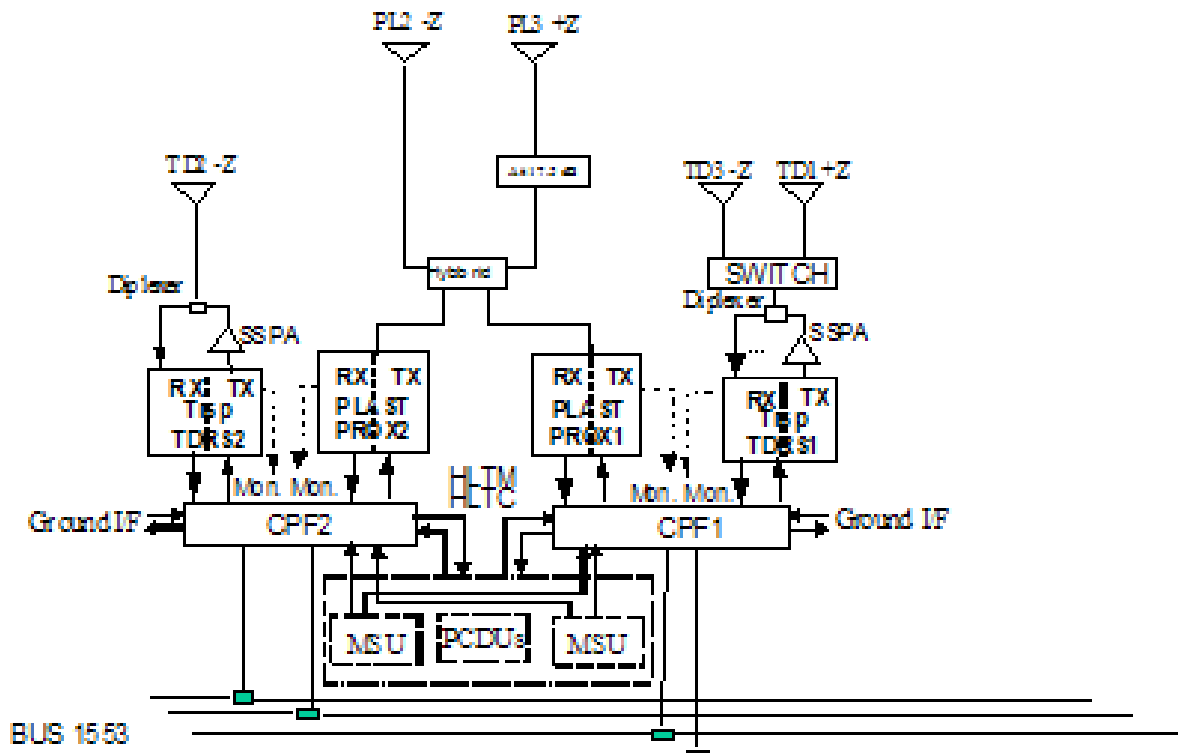


Figure 83 ATV communication system architecture, ref. [46]

7.2.4.4 Launch strategy T/O

In order to identify advantages and disadvantages of several launch strategies options with Ariane 5 ME including GTO, HEO and LTO, a trade-off has been performed considering:

- ΔV
- Time of Flight (TOF)
- Number of maneuvers

The results obtained are based on Literature analysis and Hohmann transfer analytical formulation. Considering that CLV is launched by Ariane 5ME, the following launcher performances have been considered:

Target orbit	Maximum payload mass
GTO	11.2 t
HEO	10.5 t*
LTO	9.7 t

Launch orbit characteristics

TLO 385600 km apogee; 300 km perigee
HEO 100 000 km apogee; 300 km perigee (assumption)
GTO 35786 km apogee; 300 km perigee

Target orbits assumptions

LLO 110km altitude
EML1 -57900 km from Moon
EML2 +64400 km from Moon

Table 37 Ariane 5ME performances, ref. [6]

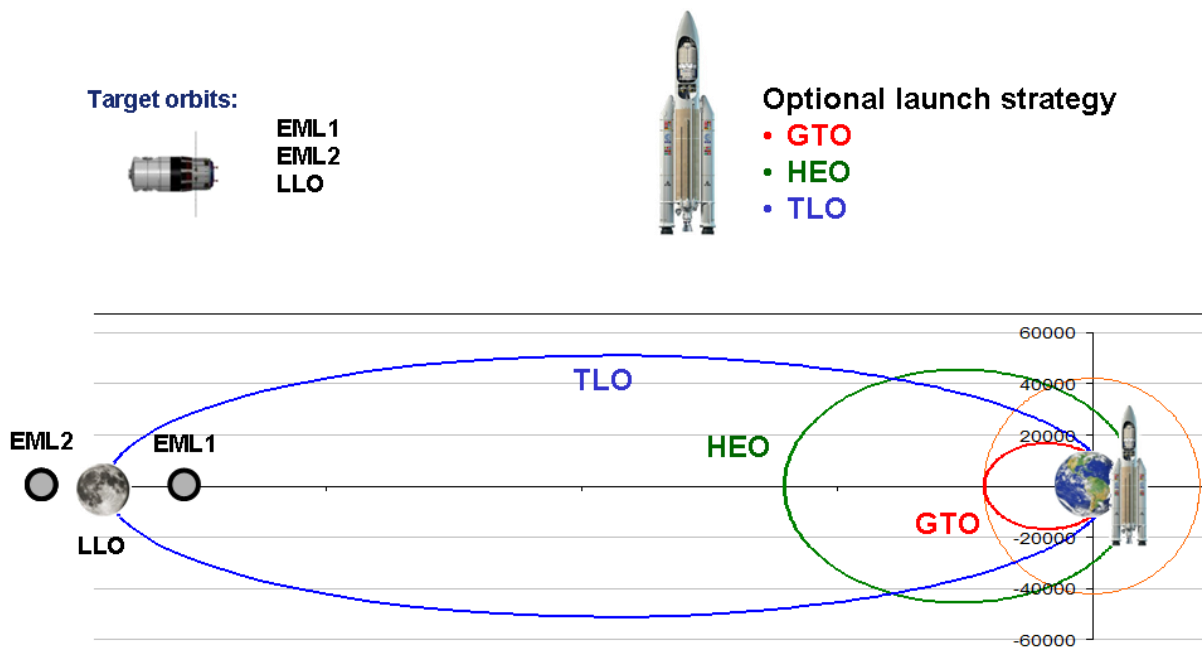


Figure 84 Launch strategies

The first analysis concerns the possibility to reach the target (Earth Moon Lagrangian points 1 or 2 (EML1, EML2), Low Lunar Orbit (LLO)) through classical Hohman transfer from Geo-stationary Transfer Orbit (GTO), High Elliptic Orbit (HEO) or Transfer Lunar Orbit. The analysis has been performed considering the ΔV in Table 38.

Hohmann transfer from GTO **ΔV (burn 1 + burn 2)**

to EML-1: 578 m/s + [600 ÷ 700] m/s (ref. [47])

- transfer time: 3,9 d
- ≥ 2 maneuvers necessary

to EML-2: 608 + [950 ÷ 1050] m/s (ref. [47])

- transfer time: 6,3 d ÷ 12 d (depending on thrust)
- ≥ 2 maneuvers necessary

to LLO: 594 + [820 ÷ 850] m/s (ref. [48])

- transfer time: 5 d ÷ 10 d (depending on thrust)
- ≥ 2 maneuvers necessary

Hohmann transfer from HEO **ΔV (burn 1 + burn 2)**

to EML-1: 218 + [600 ÷ 700] m/s (ref. [47])

- transfer time: high thrust 3,9 d (low thrust 7-10 d)
- low thrust: ≥ 2 maneuvers necessary (1 perigee burns)
- high thrust: 2 maneuvers necessary

to EML-2: 247 + [950 ÷ 1050] m/s (ref. [47])

- transfer time: 6,3 d
- ≥ 2 maneuvers necessary

to LLO: 234 + [820 ÷ 850] m/s (ref. [47])

- transfer time: 5 d
- 2 maneuvers – circularization

Hohmann transfer from TLO **ΔV (one burn necessary)**

to EML-1: 600 ÷ 700 m/s. (ref. [47])

- transfer time: high thrust > 5 d
- transfer time: low thrust: up to 10 d
- ≥ 2 maneuvers necessary

to EML-2: 950 ÷ 1050 m/s (ref. [47])

- low thrust: multiple long burns
- high thrust: 2 short burns
- transfer time: high thrust > 6 days (low thrust up to 12 d)

to LLO: 820 ÷ 850 m/s (circularization only) (ref. [47])

- low thrust: multiple apoapsis lowering maneuvers necessary
- high thrust: 1 maneuver for circularization
- transfer time: high thrust 5d (low thrust add approx. 2 d for circularization)

Table 38 ΔV , transfer time and numbers of maneuvers for Hohmann transfer

The analyses are performed considering Resource Module (RM) and Cargo Carrier (CC) module preliminary sizing:

- dry mass considered for RM is ~3400 kg
- dry mass for the CC is ~5600 kg

Table 39 shows that all the launch strategies exceed the A5 ME performances: the CLV mass exceed the maximum payload mass available on the launcher.

Alternative launcher systems (15 tons in GTO, 14 tons in HEO, 13 tons in TLO) have to be investigated if the Homan transfer strategy shall be utilized.

	ΔV	Fuel mass	Total mass	Diff (max A5ME 11200 kg)
From GTO to				
L1	1278	4650	13726	+2526
L2	1658	6450	15526	+4326
LLO	1444	5410	14486	+3286
From HEO to				
L1	918	3140	12216	+1716
L2	1297	4740	13816	+3316
LLO	1084	3820	12896	+2396
From TLO to				
L1	700	2310	11386	+1686
L2	1050	3680	12756	+3056
LLO	850	2880	11956	+2256

Table 39 CLV mass exceeding (Diff) w.r.t each launch strategy

Low energy transfer strategies have been investigated as alternative solution to Hohmann transfer. These strategies implies lower ΔV but higher transfer time (not problematic for un-manned missions) thus implying higher operational costs (mainly due to ground segment) and more stringent launch windows (few opportunities per years)

Possible low energy strategies are:

- Weak Stability Boundary (WSB) transfer (take advantage of Sun gravitational attraction perturbation) (ref. [49]), (ref. [50]), (ref. [51])
- Resonance Transfer (RT) (take advantage of Moon gravitational attraction perturbation) (ref. [48]), (ref. [51]), (ref. [52])

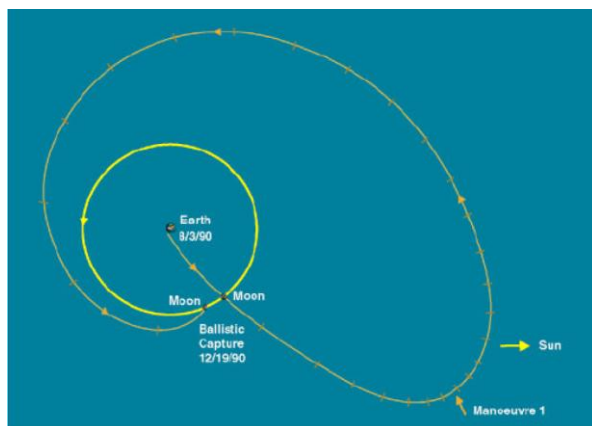


Figure 85 Weak Stability Boundary

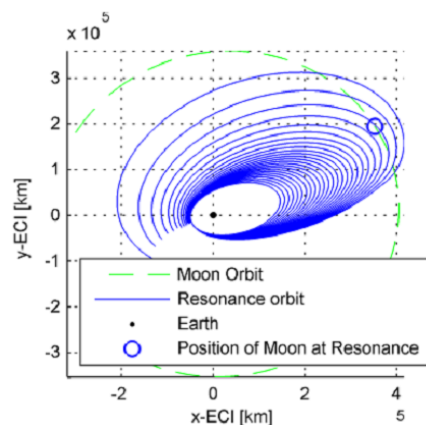


Figure 86 Resonance Transfer

When performing the resonance transfer strategy, the spacecraft takes advantage of Moon gravitational attraction perturbation. The transfer strategy starts from HEO where the Moon gravitational attraction is sufficient to implement the transfer strategy. There are two options to reach HEO: by the launcher or by itself. The hypothesized ΔV to reach HEO from LEO is less than 3000 m/s. Then, 50 m/s are necessary to reach the EML1 over a period ranging from 3 months to 1 year, (ref. [53]), (ref. [52]).

When performing the Weak Stability Boundary transfer strategy, the spacecraft takes advantage of Sun and Moon gravitational attraction perturbation. The spacecraft is injected in transfer lunar orbit and then performs correction maneuvers first to be automatically captured in an orbit around EML2. The necessary ΔV to be injected in the lunar transfer orbit is bigger than 3100 m/s and the ΔV necessary for correction maneuvers ranges from 1 to 10 m/s. The transfer time ranges from 1.5 to 3 months, (ref. [49]), (ref. [53]), (ref. [52]).

The following ΔV have been considered to move between EML1, EML2 and LLO using low energy strategies:

- To reach EML2 from EML1 or opposite, the necessary ΔV is 140 m/s and the transfer time reaches 1 month, (ref. [47]), (ref. [53])
- To reach LLO from EML1 or opposite, the necessary ΔV is 640 m/s and the transfer time exceed 2 days, (ref. [47])
- To reach LLO from EML2 or opposite, the necessary ΔV is 640 m/s and the transfer time exceed 2 days, (ref. [47])

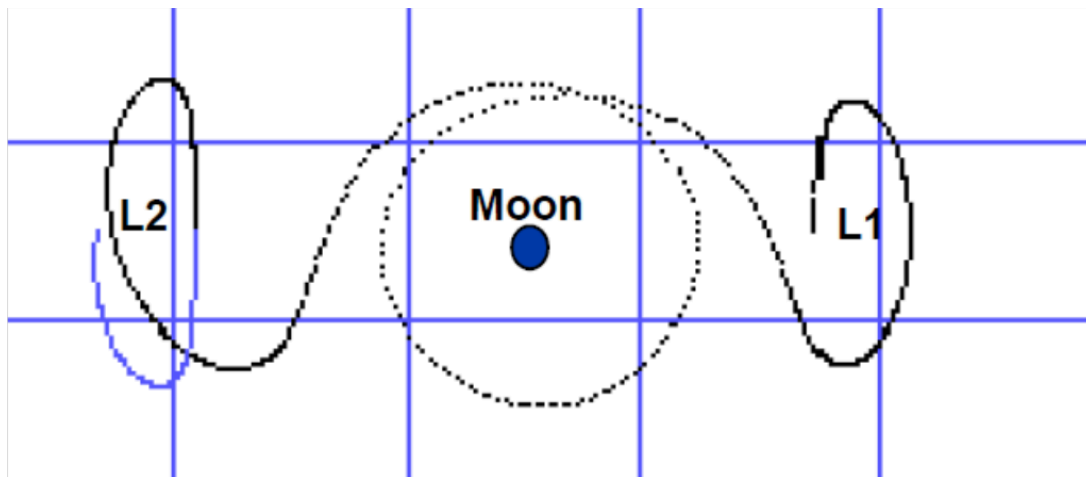


Figure 87 transfer from EML1 to EML2

In conclusion, WSB has been discarded:

- Launcher capabilities are not sufficient to inject CLV in the desired target orbit (assumed similar to a lunar transfer orbit). In fact, the launcher performances allow putting in LTO up to <9.7 tons that are not sufficient to deliver the CLV (LLO mission). Performing the injection maneuvers from LEO would be too much demanding for CLV propulsion system in terms of ΔV (>3 km/s).
- Low robustness: WSBs are highly influenced by gravitational perturbations. The risk of mission failure is high (w.r.t. RT) due to missing of the target orbit. Sensible additional ΔV to provide correction maneuvers must be taken into account (specific assessment requires specific optimization analyses)

At the end of the trade-off assessment the proposed transfer strategy foresees the implementation of Resonance Transfer:

- CLV is injected in HEO orbit by the launcher. Transfer from LEO to HEO is assumed to be done by A5 ME. Having not found the information about the performance of A5ME (HEO mission) in literature, 10,5 tons of payload in HEO have been assumed ($\Delta V \sim 3000$ m/s). Obviously the real payload performance depends by the HEO orbit chosen.
- CLV reaches EML1 by resonance transfer from HEO (with a ΔV of 50 m/s from HEO to EML1).
- In case low energy transfer is performed to reach EML2 or LLO

The detailed strategies to reach EML1, EML2 and LLO are here presented:

Proposed strategy to reach EML-1 [50 m/s; 3 months ÷ ~1 year]

- A5 launches CLV into HEO orbit: the transfer from LEO to HEO is assumed to be done by the launcher
- CLV performs Resonance Transfer strategy to reach EML-1
- Required ΔV 50 m/s
- Transfer time: 3 months ÷ 1 year

Proposed strategy to reach EML-2 [190 m/s; 4 months ÷ ~1 year]

- A5 launches CLV into HEO orbit: the transfer from LEO to HEO is assumed to be done by the launcher
- CLV performs Resonance Transfer strategy to reach EML-1
- Required ΔV 50 m/s
- Transfer time: 3 months ÷ 1 year
- Once in EML-1, CLV perform transfer maneuver to reach EML-2
- Required ΔV 140 m/s
- Transfer time: 1 month

Proposed strategy to reach LLO [690 m/s; 3 months ÷ ~1 year]

- A5 launches CLV into HEO orbit: the transfer from LEO to HEO is assumed to be done by the launcher
- CLV performs Resonance Transfer strategy to reach EML-1
- Required ΔV 50 m/s
- Transfer time: 3 months ÷ 1 year
- Once in EML-1, CLV perform transfer maneuver to reach LLO
- Required ΔV 640 m/s
- Transfer time: >2 days

7.2.5 System budgets

7.2.5.1 Mass Budget

The mass budget is done taking into account a subsystem margin variable from 5% to 20% (5% for fully developed systems, 10% for systems to be modified and 20% for system to be developed) on each single item and adding a System Margin of 20% on the sum of the

designed parts. The mass budget has been performed implementing equation presented in section 4.

CARGO CARRIER	
System	Mass Budget [kg]
Primary structure mass	1155
Secondary pressurized structure mass	388
Secondary unpressurized structure mass	315
IBDM	315
MDPS structure mass	63
MLI mass	105
ECLS (FDS, ventilation, sensors)	157
TCS (heaters, piping)	31
EPS (light, harness)	126
TOTAL MASS Cargo Carrier	2655
System margin (20%)	531
Payload*	2500 (1600)
TOTAL MASS Cargo Carrier + payload	5686 (4786)

* Low lunar target orbit reduces cargo capabilities to 1600 kg

Table 40 Cargo carrier mass budget

RESOURCE MODULE	
System	Mass Budget [kg]
Structure	633
Thermal Control	398
Communications	24
Data Handling	96
GNC	68
Propulsion	830
EPS	775
Total Dry	2825
System margin (20%)	565
Total Dry mass	3390

Table 41 Resource module mass budget

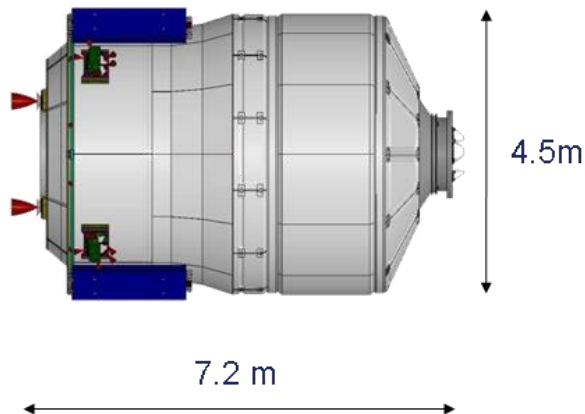


Figure 88 CLV envelope

CLV (CC+RM) Mass Budget			
	Mission to EML1	Mission to EML2	Mission to LLO
	[kg]	[kg]	[kg]
Vehicle dry mass	6576	6576	6576
Payload	2500	2500	1600
Total dry mass	9076	9076	8176
Propellant	410	850	2335
Mass at launch	9486	9926	10511

Table 42 CLV overall mass budget

7.2.5.2 Power Budget

The power estimate for the CLV derives from ATV design. ATV spacecraft generates up to 5 kW to supply subsystems of the resource module and cargo carrier during daylight and eclipse periods.

7.2.5.3 ΔV and Propellant Budget

Resonance Transfer strategy has been assessed the best option to reach the EML1, EML2 and LLO.

Proposed strategy to reach EML-1 [50 m/s; 3 months \div ~1 year]

- A5 launches CLV into HEO orbit
- CLV performs Resonance Transfer strategy to reach EML-1
- Required ΔV 50 m/s
- Transfer time: 3 months \div 1 year

Phase/Event	ΔV [m/s]	Propellant [kg]	Total Mass 9486 kg
HEO-EML1 transfer Resonance Transfer strategy: multiple burns (Cargo 2500 kg)	50	155	9331 kg
Docking	60	180	9151 kg
Disposal (waste: 2500 kg)	25	75	9076 kg
TOT	135	410	

Table 43 ΔV and propellant budget for EML-1

Proposed strategy to reach EML-2 [190 m/s; 4 months \div ~1 year]

- A5 launches CLV into HEO orbit
- CLV performs Resonance Transfer strategy to reach EML-1
- Required ΔV 50 m/s
- Transfer time: 3 months \div 1 year
- Once in EML-1, CLV perform transfer maneuver to reach EML-2
- Required ΔV 140 m/s
- Transfer time: 1 month

Phase/Event	ΔV [m/s]	Propellant [kg]	Total Mass 9926 kg
HEO-EML1 transfer Resonance Transfer strategy: multiple burns (Cargo 2500 kg)	50	160	9766 kg
EML1-EML2	140	435	9331 kg
Docking	60	180	9151 kg
Disposal (waste: 2500 kg)	25	75	9076 kg
TOT	275	850	

Table 44 ΔV and propellant budget for EML-2

Proposed strategy to reach LLO [690 m/s; 3 months \div ~1 year]

- A5 launches CLV into HEO orbit
- CLV performs Resonance Transfer strategy to reach EML-1
- Required ΔV 50 m/s
- Transfer time: 3 months \div 1 year
- Once in EML-1, CLV perform transfer maneuver to reach LLO
- Required ΔV 640 m/s
- Transfer time: >2 days

Phase/Event	ΔV [m/s]	Propellant [kg]	Total Mass 10511 kg
HEO-EML1 transfer Resonance Transfer strategy: multiple burns (Cargo 1600 kg)	50	169	10342 kg
EML1-LLO	640	1937	8405 kg
Docking	60	162	8243 kg
Disposal (waste: 1600 kg)	25	67	8176 kg
TOT	775	2335	

Table 45 ΔV and propellant budget for LLO

7.3 Rover Locomotion System

The section deals with the conceptual design, test and construction of the elastic wheel of a future large lunar rover. The accomplishment of the wheel design is part of a wider study in the framework of STEPS (Systems and Technologies for the ExPLoration of Space). STEPS is a research project, which has been co-financed by Piedmont Region (Italy), firms and universities of the Piedmont Aerospace District. The main purpose of STEPS has been the developing and testing new technologies for space exploration, including a demonstrator of a future large lunar rover.

The study of the wheel of the future large lunar rover has started from the conceptual design of the elastic wheel of the lunar rover (also called the “nominal” wheel). The activity has then proceeded with the design of the elastic wheel of a technological demonstrator of the lunar rover (the “resized” wheel). The manufacturing of a scaled model of the technological demonstrator wheel (the “scaled” wheel) has allowed the validation of the performance. Eventually, the resized wheels have been manufactured, tested and integrated.

The same design methodology, previously applied for the design of the Free Flyer and Cargo Logistic Vehicle, has been utilized. Thus, starting from the system requirements, performing the trade-offs necessary to assess the system design and sizing the system elements with utilization of analytical and numerical models, the definition of the wheel features was possible. Since the wheel should be built, the activity has continued with the construction of a prototype system on which tests were possible. The construction of the prototype was useful to assess the manufacturing process and to evaluate the real performance of the system. The tests highlighted that a second design loop was necessary since some parameters of the numerical model need to be rearranged. Eventually, the construction of the first resized wheel was useful to further assess the manufacturing process and to highlight criticalities to be definitively removed.

The detailed description of the tests performed on the wheel and of the design improvement process is beyond the scope of this document and information can be found in ref. [54]. The scope of this section is to demonstrate the effectiveness of the proposed design process since the manufacturing of a real product was possible. Considering that, the section provides detailed description of the wheel design methodology (mission objectives, requirements and wheel design). The wheel design has been accomplished through implementation of the analytical models described in section 4.11 and through definition of a numerical model (FEM model) that will be well described. These analytical and numerical models were useful to perform configuration trade-offs and detailed design assessment, thus definition of the system geometry and materials.

7.3.1 Applied design methodology

Figure 89 illustrates the applied methodology that has been considered for the design of the lunar rover elastic wheel. Once the mission statement has been established, the top level system requirements and constraints have been defined. Then a preliminary evaluation of the system performance has been accomplished on the basis of the Bekker theory. Taking into account the main system performance, different system architectures have been first considered and then evaluated through a qualitative trade-off analysis based on various parameters, like ride comfort, environment compatibility, stability, etc.. Two different concepts, i.e. the ellipse spring wheel and the spiral spring wheel (see next sections), of the lunar rover elastic wheel have been selected as the most promising result of this qualitative trade-off analysis. Both concepts have then been evaluated in terms of mass budget and internal stresses by carrying out their 3D CAD models and the first level FEM analyses. As a result of this trade-off analysis, the ellipse spring wheel concept has been chosen and then the low level system requirements and constraints have been defined. The system, i.e. the ellipse

spring wheel, has then been sized again by carrying out an improved (more detailed) 3D CAD model and the second level FEM analysis. Eventually the sized ellipse spring wheel has been evaluated, taking in particular into account whether the wheel concept is compliant or not with the system requirements. In case the system requirements are met, the applied methodology may either proceed with experimental tests to verify and validate the numerical models or end in case of confidence in the model. Otherwise the numerical results are not confirmed, the system numerical model must be corrected and the system sizing must be revised through an iterative process.

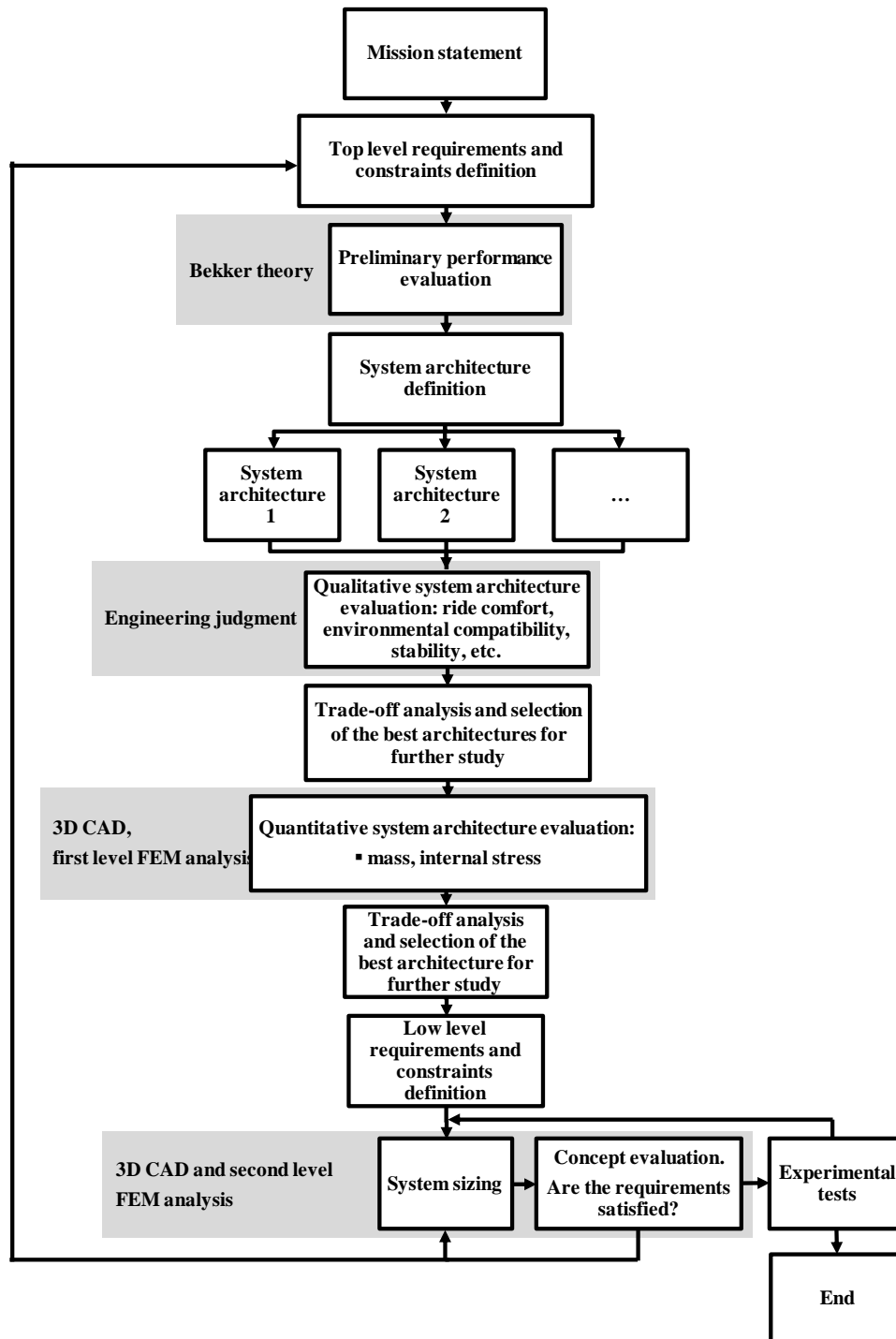


Figure 89 Flow-chart of the design methodology

7.3.2 Mission objective

The mission statement of the wheel system of the lunar rover is as follows: “to provide the ability to move objects supporting loads and ensuring adequate traction performances through rotating on an axle through its center”.

The wheel that will be developed shall therefore be able to move a large rover on a rugged terrain typical of the Moon surfaces. The vehicle specifications and performances come from preliminary studies conducted in the framework of the program STEPS and are shown in Table 46.

Operative scenario	Lunar surface exploration	[-]
Length	6000	[mm]
Width	4300	[mm]
High	3900	[mm]
Mass	7000	[kg]
Average speed (in plane)	10	[km/h]
Maximum speed (in plane)	15	[km/h]
Maximum terrain slope	30	[deg]
Number of wheel	6	[-]
Wheel diameter	~1	[m]
Wheel width	300	[mm]

Table 46 Vehicle specifications and performance

7.3.3 System requirements

From the wheel mission statement and the vehicle specifications and performances the top level requirements of the wheel system can be identified. The wheel top level requirements include functional, interfaces, environmental, physical, design, performance and operational issues. In Table 47 the top level requirements are summarized.

Requirements	Type
The wheel shall be able to rotate	Functional
The wheel shall ensure shock absorption capabilities	Functional
The wheel shall be able to transfer to the ground enough traction to have the motion	Functional
The motion resistances shall be as low as possible	Performance
The wheel shall be able to withstand the nominal continuous load (2000 N)	Performance
The wheel shall withstand a load factor of 2.5 without permanent strains.	Design
The maximum not continuous load is 5000 N	
The minimum contact surface between the wheel and the soil shall be 3 dm ² at nominal load	Performance
The wheel diameter shall be about 1 m	Physical
The wheel width shall be 300 mm	Physical
The wheel shall perform its mission in absence of atmosphere	Environmental
The wheel shall perform its mission in a temperature range between -180°C and +120 °C	Environmental
The wheel shall be able to interface with the electrical motor: the motor interface is on the circumferential surface of the motor's rotor (diameter initially equal to 426 mm and successively equal to 445.5 mm due to changes in the motor design)	Interface
The wheel shall transfer axial, radial and circumferential loads to the rotor of the motor	Interface

The wheel mass shall be as low as possible	Physical
The wheel tread shall be able to sustain stresses generated by the wheel-ground interaction	Functional
The wheel shall ensure an operative life of 5000 km.	Performance

Table 47 Wheel top level requirements

7.3.4 Preliminary performance

Taking into account the lunar soil parameters, listed in Table 48, and the rover features, described in section 7.3.3, as output of the mobility system requirements analysis, and on the basis of the Bekker semi-empirical theory presented in section 4.11, the wheel performance have been predicted, Table 49.

Symbol	Value	
g	1.635	$[m/s^2]$
ϕ	40	$[^\circ]$
c_c	170	$[N/m^2]$
γ	1680	$[kg/m^3]$
n	1	$[-]$
k_c	1400	$[N/m/n^1]$
k_ϕ	820000	$[N/m/n^2]$
θ	0	deg
f_r	0.025	-

Table 48 Lunar soil parameters. Ref. [22]

As previously said, the ability of the vehicle to move depends on the difference between H (or F , if the wheel motor is not enough powerful to generate the maximum traction H) and R (DP). From the data reported in Table 49, it is possible to observe that the motion of the vehicle is feasible, thanks to a certain amount of thrust left over (DP) to provide the vehicle with acceleration and to allow it to clear obstacles and to climb slopes. The total resistance is the sum of compaction, bulldozing and rolling resistance. The most important resistance component is due to compaction. As explained by Bekker in ref. [18], in order to reduce this component, the diameter of the wheel (or the length of the ground contact area) and/or the wheel width shall be increased. However, it is demonstrated that an increase of the wheel diameter reduces much faster the compaction resistance than a comparative increase of the wheel width [19]. Moreover, wide wheels increase the bulldozing effect, i.e. narrow wheels show less bulldozing resistance, as part of the soil is pushed towards the sides of the wheel itself. For these reasons the wheel width has not been modified. On the other hand, the wheel diameter cannot be significantly increased, in order to be compliant with the mobility system requirements. The wheel deflection is the unique variable useful to improve the wheel performances because it decreases the ground pressure: in fact, if the deflection grows, the contact area increases and the ground pressure (as well as the compaction resistance) decreases. Therefore one of the driving requirements of the wheel design is that the wheel shall be deformable and elastic, with adequate deflection, according to the strength of the material.

Symbol	Value
P_w	1070 [W]
T	193 [Nm]
DP (H-R)	1247 [N]
H	1686 [N]
R	439 [N]
R_c	291 [N]
R_b	98 [N]
R_r	50 [N]

Table 49 Performances of the mobility system in lunar environment – Flat surface

7.3.5 Wheel design assessment

A comparative evaluation of the most important architecture of lunar rover wheels, that have so far been studied, is shown in ref. [17]. The document does not recommend rigid or pneumatic wheels. Pneumatic wheels are not compatible with the lunar environment because of the rubber degradation due to the solar radiation. Rigid wheels, as the rigid rim wheel (ref. [17]), have not ride comfort. As far as the wire mesh wheels, ref. [17] (see the LRV's wheels of the Apollo missions, ref. [2]) are concerned, they cannot be scaled to heavier and longer range vehicles. The elliptical wheel (ref. [17]) and the hub-less system have reliability problems and high specific weight. Taking into account the above considerations, only two wheel configurations match the lunar rover requirements: the hoop spring wheel and the spiral spring wheel. Both these two wheel configurations ensure soft ground performance, i.e. low motion resistances, adequate thrust generation and good wear resistance. In particular, however, the hoop spring wheel seems to be lighter, more comfortable and more stable than the spiral spring wheel. In the following sections the ellipse spring wheel, which can be considered as a customized version of the hoop spring wheel, and the spiral spring wheel are described into the details.

7.3.5.1 Concept #1: the ellipse spring wheel

The ellipse spring wheel consists of several radial elements (or ellipse springs), a central hub and a tread. The wheel configuration concept is shown in Figure 90-a. The tread is the surface of the wheel that makes contact with the ground. The main function of the tread is to transmit the traction to the ground. The tread shall be deformable, in order to ensure the required ground contact area, and shall be able to sustain stresses generated by the wheel-ground interaction. The main function of the central hub is to transfer the axial, the radial and the circumferential loads, generated by wheel-ground interaction, to the wheel support. Eventually, the main function of the radial elements is to connect the hub and the tread. They act as elastic elements, in order to provide at the same time the wheel with load bearing and good shock absorption capabilities. Notwithstanding the similarity between the hoop spring wheel and the ellipse spring wheel, the ellipse spring wheel concept is substantially different from the hoop spring wheel one. In fact, while the hoop spring wheel consists of several independent hoop springs, the ellipse spring wheel consists of several springs that interact with one another to change the wheel stiffness. The wheel stiffness is the resistance of the wheel to the deformation, when a vertical load is applied to the wheel itself. The wheel configuration is characterized by a trend of stiffness, which increases when the deformation of the wheel causes the contact between the nearest displaced radial elements, as show qualitatively in Figure 90. The radial elements are deformable and close enough to be in contact when the loads exceeds a certain threshold. When two or three radial elements are in contact, the wheel becomes stiffer and the stresses are distributed over a larger number of radial elements. When the radial elements are not in contact, the FEM analyses show that one

or two radial elements withstand up to ninety percent of the total load. When the radial elements are in contact a larger number of them concur to withstand the vertical load acting on the wheel. Therefore this configuration should allow a more efficient use of the material of the wheel (and thus a lighter system) with respect to the hoop spring wheel concept, where there are no contacts amongst the radial elements.

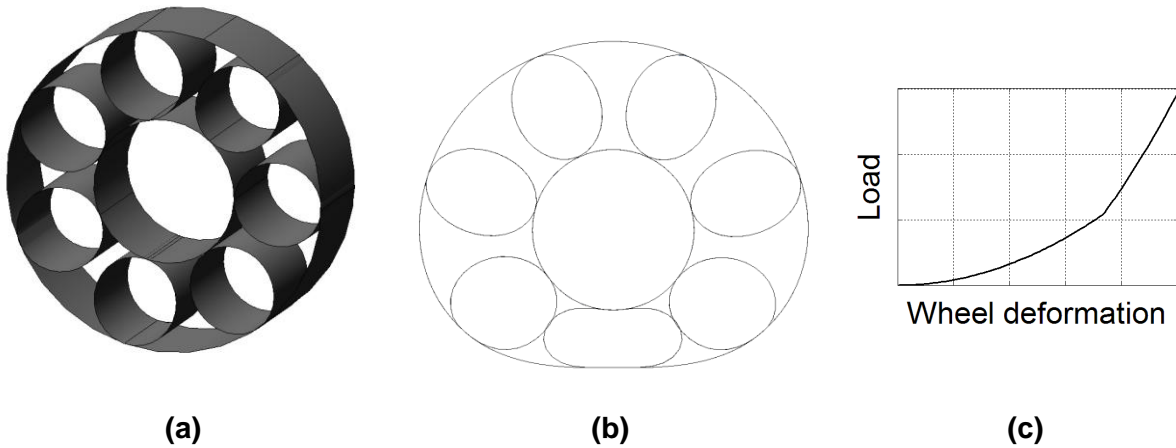


Figure 90 (a) ellipse spring wheel concept, (b) ellipse spring wheel displacement, (c) ellipse spring conceptual stiffness trend

7.3.5.2 Concept #2: the spiral spring wheel

The spiral spring wheel consists of a series of bi-tangent semicircles (or spiral springs), a central hub and a tread. The wheel configuration concept is shown in Figure 91-a. The tread, exactly as for the hoop spring wheel, is the surface that makes contact with the ground. Its main function is therefore to transmit the traction to the ground and to withstand the traction loads. Like for the first wheel concept, the tread shall be able to deform enough to ensure the required contact area. The spiral spring wheel central hub is very similar to the hoop spring wheel hub. It interfaces with the motor and transfers the wheel loads. Eventually the bi-tangent semicircles join the tread metal sheet and the central hub. As the ellipse springs, they act as elastic elements, in order to provide at the same time the wheel with load bearing and good shock absorption capabilities. This wheel configuration has a trend of stiffness which is constant when the load increases (Figure 91-c). The FEM analyses show that when the wheel is deformed, not significant interactions amongst radial elements occur.

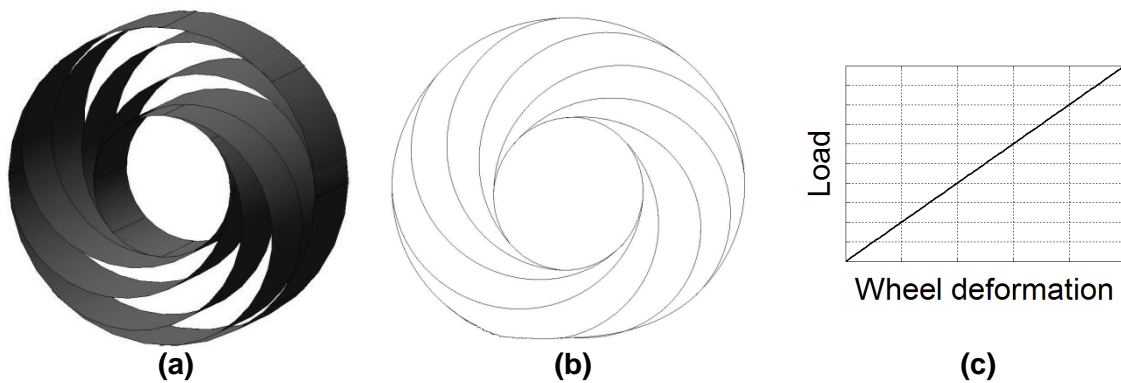


Figure 91 (a) spiral spring wheel concept, (b) spiral spring wheel displacement, (c) spiral spring conceptual stiffness trend

7.3.5.3 First level FEM analysis and selection of the best wheel architecture

A first level FEM analysis has been performed for the two wheel concepts. The main aim of the analysis is to choose the wheel architecture that meets the requirements with the minimum cost in terms of mass. The wheel configuration depends on a series of parameters. The values of some of them are dictated by the system requirements, like the wheel external diameter, the wheel width and the hub internal diameter, while the values of other parameters can be chosen and varied appropriately. These last parameters include the number of springs, their eccentricity and the plate wall thickness and material of the wheel components, i.e. the tread, the hub and the springs. For the first level FEM analysis different sets of values of these wheel parameters have been considered per each concept. The results of the activity have been the sizing of both wheel configurations compliant with the system requirements and the choice of the best one. For each wheel concept the aluminum has been considered (Young module equal to 72400 MPa, Poisson module equal to 0.3 and yield strength equal to 415 MPa) in the first level FEM analysis.

In order to simplify the analysis, some assumptions have been made to develop the 3D CAD and FEM models. The wheel structure has been modeled with 2-D surfaces. The mesh model has been carried out by means of parabolic triangular shell elements, as shown in Figure 92-a. The thickness of each metal sheet has been selected in the software properties module. Possible riveted joints between the metal sheets have been neglected and all the holes linked to rivets have been omitted, as they have very small dimensions. Contact elements have been utilized amongst surfaces that can be in contact. This allows to simulate the nonlinearities that characterize the ellipse spring wheel concept trend of stiffness. If two surfaces are in contact, no penetration occurs and the loads and the stresses are transmitted from the first surface to the second. The models for both wheel configurations have the same mesh global dimension (31 mm), in order to make the comparison between the results as more correct as possible. The total number of nodes and elements are respectively 15303 and 14118 for the ellipse spring wheel concept and 20423 and 9682 for the spiral spring wheel concept.

The FEM analysis has been performed for ultimate load only. The requirements impose a vertical load of 5000 N acting on the wheel. The vertical load is uniformly distributed on the wheel hub in order to simulate the wheel support loads transmission (Figure 92-a). No constraints have been directly applied onto the wheel. In the FEM model a plate has been introduced in order to simulate the ground. The wheel is free to move but the load pushes the wheel towards the plate that is fixed, as can be seen in Figure 92-a. Contact elements have been utilized between the wheel tread and the ground, thus no penetration occurs between the wheel and the ground. The evaluation of the contact area and the pressure distribution is a demanding activity in terms of computational effort. This model configuration allows to delegate the evaluation of the wheel-ground contact area to the FEM processor. Von Mises criteria have been assumed to evaluate stresses for all the materials. In Figure 92-b the stress map is showed.

As a result of this preliminary analysis, the ellipse wheel concept has shown a better behavior in terms of stiffness and mass. The analyses show that ellipse spring wheel withstands the loads with less mass than the spiral spring wheel, due to the fact that the stresses are more uniformly distributed over the wheel elements.

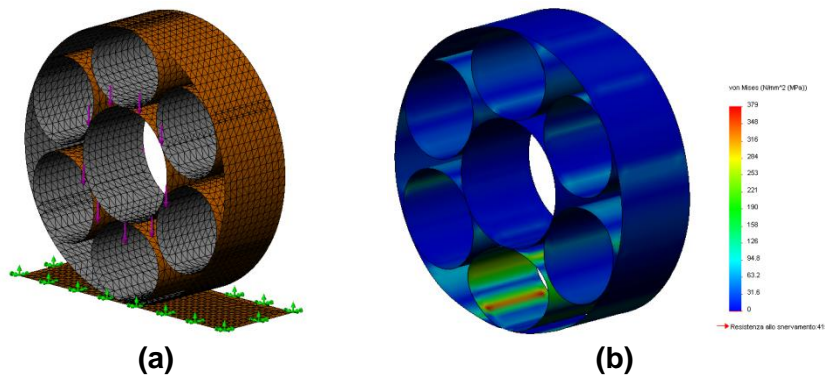


Figure 92 (a) FEM mesh model (b) Von Mises contour plot of the deformed wheels

Apart from the main aim of the analysis, other considerations can be drawn from the results of the FEM analysis. As far as the direction of motion is concerned, the ellipse spring wheel seems to have a symmetrical behavior for both the clockwise and counterclockwise rotations, while the spiral spring wheel has a preferred direction of rotation, as there is no symmetry on the wheel frontal view.

As far as the ride comfort and the stability are concerned, they are different for the two wheels. In Ref. [17] the authors give an engineering judgment of the wheel concepts. Ref. [17] shows that the spiral spring wheel has less ride comfort and stability than the ellipse spring wheel.

Taking all these considerations into account, the ellipse spring wheel concept has shown a better behavior in terms of stiffness, mass budget and dynamic performances.

7.3.6 Wheel sizing

7.3.6.1 Low level requirements and constraints

In the present section only the low level requirements, which greatly affect the whole wheel design, are considered and explained into the details. The top level requirements presented in section 7.3.3 are still applicable.

The first level FEM analyses have shown that, if the ellipse wheel has a particular geometrical configuration, the contact between the radial elements occurs. Otherwise the radial elements are too far and at maximum load there is no contact between them. As explained before, the contact between radial elements is important, in order to distribute high loads on more radial elements and allow less thick metal plates. Moreover, when there is contact between radial elements, the wheel becomes stiffer if compared to the case when there is no contact at all. Being the wheel stiffer, the deformation is much lower. On the basis of this consideration, the following low level requirement has been defined: the contact between radial elements shall occur at a load value higher than the nominal and lower than the ultimate value. This requirement is important to make it possible to understand that the ultimate load is forthcoming.

Being the number of radial elements not infinite, FEM analyses have shown that the wheel stiffness changes with the rotation of the wheel itself. This difference in stiffness generates vibrations that are then transmitted to the wheel suspensions. The intensity of the vibrations can be estimated as the root mean square value of the alternate quantity of the hub displacement. FEM analyses have demonstrated that, according to the value of the wheel geometrical characteristics, the intensity of the vibrations transmitted to the suspensions can be minimized under nominal load conditions. On the basis of these considerations, the following low level requirement has been defined: the intensity of the vibrations transmitted to the suspensions shall not exceed 1 m/s^2 , according to the standard regulations on acceptable

vibration values transmitted to the human body, considering that a large part of the vibrations are filtered by the soft ground and the wheel suspensions.

For every rotation of the wheel, each radial element is subjected to time-variant stresses, which induce fatigue phenomena. According to the top level requirements, the following low level requirement has been defined: the wheel shall ensure an operative life of $6.4 \cdot 10^6$ cycles, considering a safety factor equal to 4.

7.3.6.2 Second level FEM analysis

The first level FEM analyses have led to the selection of the wheel concept. The second level FEM analyses have been performed to optimize the wheel design, taking into account the low level wheel requirements. In particular the fatigue requirement has been very important for the wheel material selection and sizing (see section 7.3.6.2.1). The FEM model, that has been developed and implemented to complete this activity, is the same that has been described in section 7.3.5.3. The second level FEM analyses have been performed mainly to define the wheel components geometry and plate thickness, to evaluate the internal stresses, which depend on their turn on the radial elements geometry and on the plate thickness, to identify the wheel stiffness trend and the wheel behavior during rotation. In particular these activities include the identification of the wheel material, the number of radial elements, their eccentricity and plate thickness and eventually the identification of the tread plate thickness and diameter. Only standard values have been considered for the plate thickness, i.e. the thickness of the metal sheets changed discreetly upon the available industrial metal sheet thickness. The number of radial elements and their size have been dictated by geometrical considerations, in order to ensure their contact. Different configurations of the selected wheel concept have thus been defined, by changing the values of the input parameters (like for instance the geometrical features of radial elements and plate thickness), and then implemented and analyzed through the FEM models. The outputs of the study are the wheel deformation, the internal stress and the wheel mass. Therefore, starting from a first wheel configuration (characterized by certain values of the fundamental input parameters), the wheel configuration has been progressively modified, until the solution that better matches the requirements has been obtained. In order to perform this activity, the various influences of the design parameters on the wheel behaviors have been clearly identified. The wheel metal sheet thickness affects the maximum stress and the wheel stiffness: in fact, if the thickness increases, the maximum stress decreases and the wheel stiffness increases as well. The number of springs is very important in order to reduce the stresses and to obtain the desired stiffness trend. The spring eccentricity allows to match the requirement of the stiffening load, which is the load that causes the wheel stiffening.

7.3.6.2.1 *Choosing the wheel material: mass, fatigue and temperature phenomena*

At the end of the first level FEM analyses, the wheel concept has been chosen and a generic aluminum alloy has been considered as reference material, because of its lightness combined with good mechanical properties. However, at that stage no trade-off analysis has been performed, in order to select the best material for the wheel system. Thus at the beginning of the second level FEM analyses a trade-off analysis to choose the most appropriate material has been performed.

In order to meet the low level requirements, only the aluminum and the steel alloys have been considered to design the wheel. In particular the maraging steel ($\sigma_c = 1600$ MPa; $E = 186000$ N/mm²) and the aluminum 2024 ($\sigma_c = 415$ MPa; $E = 72400$ N/mm²) have been taken into account for their compatibility with the lunar environment, their density and mechanical features.

The main objective of the trade-off analysis amongst such materials has been to understand which alloy would allow to obtain the desired mechanical properties, in terms of wheel deformability and fatigue behavior, with the lowest achievable mass. In order to perform this trade-off analysis, a series of FEM simulations have been run. Considering both materials, the wheel concept has been re-elaborated mainly in terms of metal sheet thickness, in order to keep the internal stress within the mechanical limits at the ultimate load. The results of this activity showed that the employment of the aluminum allows a significant mass reduction. However, problems due to fatigue issues and temperature ranges, that are typical of the lunar environment, have to be taken into account.

As far as the fatigue is concerned, the fatigue analysis has been carried out considering a stress range, which has been evaluated by the Tresca's method. According to the requirements, the wheel shall accomplish its mission for $6.4 \cdot 10^6$ cycles. The wheel structure has been verified considering an applied load equal to the nominal one (2000 N). As far as the steel alloy wheel, the results of the FEM simulations show that at every rotation, the most stressed point on the wheel structure, is subjected to a complex time-variant stress with a maximum value of $\sigma_{\max} = 385 \text{ N/mm}^2$ and a minimum value of $\sigma_{\min} = 0 \text{ N/mm}^2$. As far as the aluminum alloy wheel, these stresses range between $\sigma_{\max} = 200 \text{ N/mm}^2$ and $\sigma_{\min} = 0 \text{ N/mm}^2$. In order to simplify the analysis, the complex sequence of loads has been reduced to a two stress level cycle. The results of the activity show that the steel wheel is verified, by the point of view of the fatigue, for infinite life, while the aluminum wheel can accomplish its mission for a number of cycles, which is just less than 10^5 .

As far as the temperature is concerned, it is well known that the temperature on the lunar surface ranges from $-180 \text{ }^\circ\text{C}$ to $120 \text{ }^\circ\text{C}$, with rapid temperature changes at sunset and sunrise, $5 \text{ }^\circ\text{C/hr}$, ref. [20]. The wheel material shall be able to withstand high internal stresses in a very wide range of temperature. From this point of view, all aluminum alloys show a more pronounced mechanical performance degradation than the maraging steel.

To conclude, the maraging steel has been chosen as the most appropriate material for the wheel. The mass penalty due to the highest specific density of the steel materials has been considered acceptable because of the necessity to withstand the fatigue and the temperature variations. Thus the maraging steel ellipse spring wheel has then been further optimized. The target of this optimization activity has been the achievement of a value of mass, which has to be as low as possible, according also to the stiffness trend and to the vibration requirements.

The result of the second level FEM analyses is presented in section 7.3.6.3.

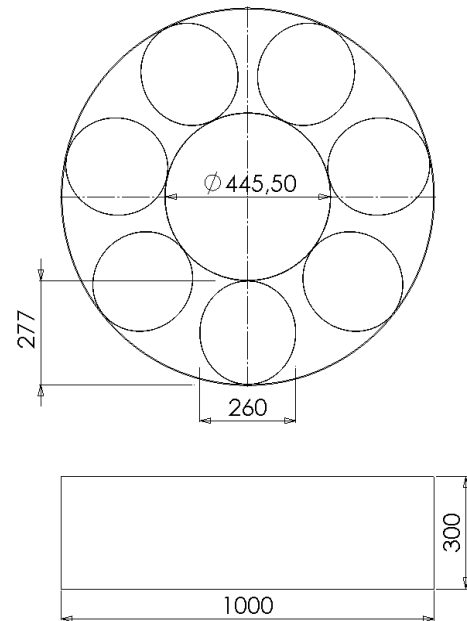
7.3.6.3 Results and discussion: lunar rover wheel synthesis

Taking into account the requirements defined in the previous sections, the final ellipse spring wheel design synthesis is shown in Table 50.

Wheel width	300	mm
Wheel diameter	1000	mm
Hub diameter	445.5	mm
Number of radial elements	7	-
Longer axis of radial elements	277	mm
Shorter axis of radial elements	260	mm
Total mass of wheel	36.5	kg
Maximum sustainable load	5000	N
Nominal load	2000	N
Stiffening load of the wheel	2500 ÷ 3000	N
Deflection at nominal load*	70	mm
Deflection at nominal load**	71	mm
Vibration intensity at nominal load due to rotation on a endlessy rigid and smooth surface	0.68	m/s ²

* wheel on a single radial element

**wheel on the gap between two radial elements



Material	Maraging Steel	-
Ultimate tensile strength	1800	N/mm ²
Yield strength	1600	N/mm ²
Fatigue limit	800	N/mm ²
Young's modulus	186000	N/mm ²
Density	8	kg/dm ³

Table 50 Wheel characteristics and FEM results

The wheel width is equal to 300 mm and the diameter is equal to 1000 mm according to the top level requirement. The hub diameter is imposed by the requirements and it cannot be changed. The wheel consists of 7 ellipse radial elements, whose longer axis is 277 mm and shorter axis is 260 mm. The ellipse longer axis is aligned with the wheel radial direction. The total wheel mass reaches the value of 38 kg. The nominal and maximum sustainable loads are respectively 2000 N and 5000 N, as stated by the requirements. In Figure 93 the trend of stiffness for different angles of rotation and load is shown. It has been observed that the wheel stiffness behavior changes, if the wheel stands on a single radial element (solid line) or on the gap between two radial elements (dashed line). In the first case, the wheel stiffness increases when the deformation leads to a contact between the nearest displaced radial elements. In the second case the wheel stiffness increases continuously with the applied load. The requirements impose that when the wheel stands on the gap between two radial elements, the contact between the two radial elements occurs for loads bigger than the nominal load. Figure 93 shows that the ellipse spring wheel meets this requirement. The change of stiffness during rotation causes vibrations transmission to the overall system. The amplitude of acceleration of the final wheel concept is 0.68 m/s². This value meets the requirement.

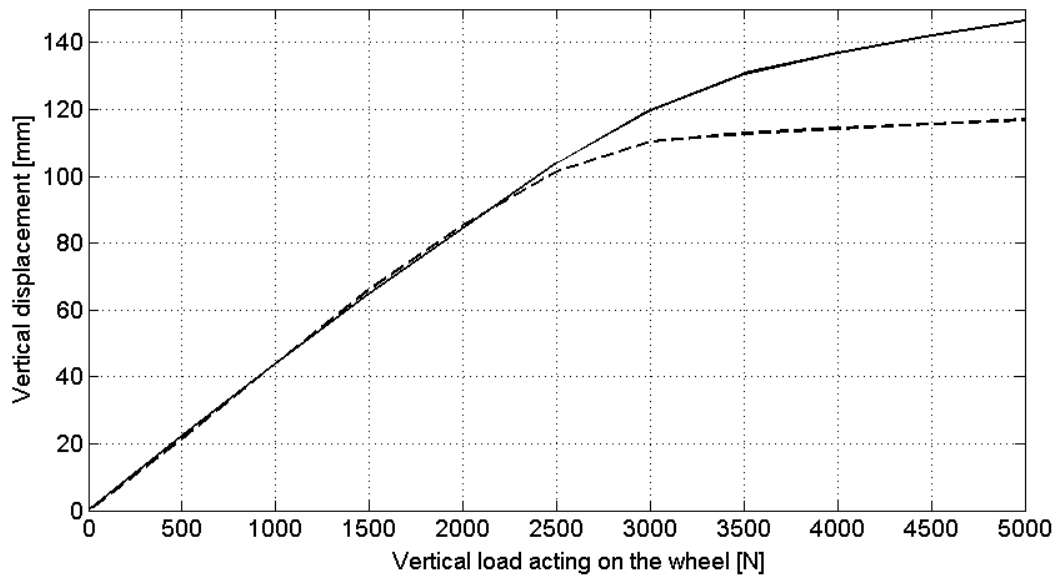
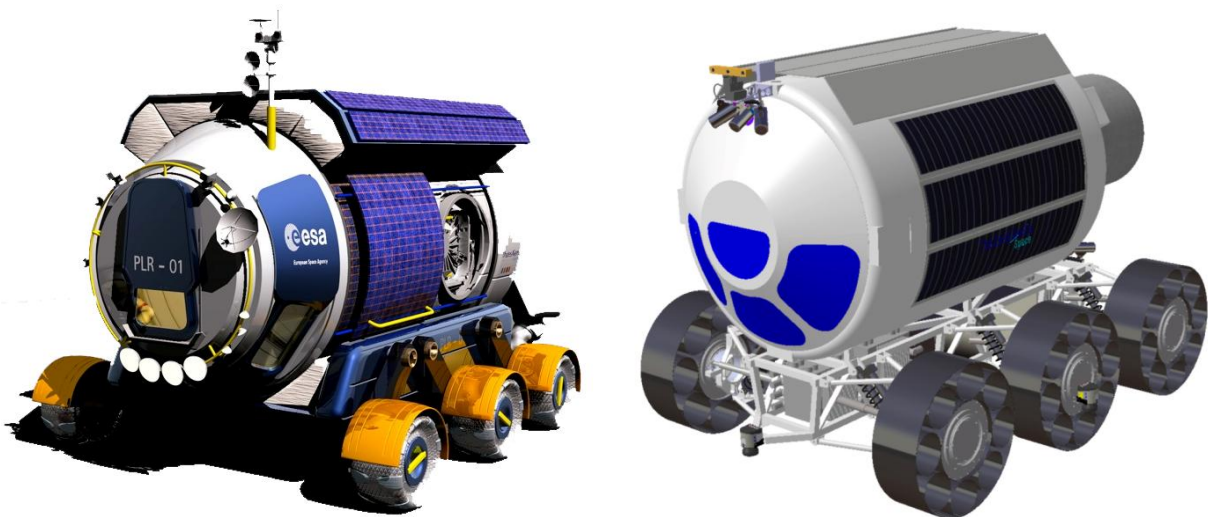


Figure 93 Wheel deformation trend when in rotation

7.3.7 Resized wheel

The rover demonstrator is a scaled version of a flight model that has been developed. It includes all the technological demonstrators' technologies coming from all the STEPS work packages. Mainly, the rover demonstrators' dimensions are 3.5 m length, 2.4 wide and 2.4 high. The rover total mass is 1500 kg and it is equipped with 6 motor-wheels with direct drive motors (one per each wheel), manufactured by Sicme Motori, see Figure 94.



Pressurized rover

- Lunar surface exploration (all regions)
- #4 to #8 crew members
- Mass: 7000 kg
- Life time 10 years - 5000 Km

Rover Demonstrator

- A test-bed for the technological results obtained in the STEPS research activities.
- Mass: 1500 Kg
- 5 Km/h to 20 Km/h speed

Figure 94 Pressurized rover and Rover Demonstrator (TAS courtesy)

The configuration of the demonstrator wheel comes from the design activities performed on the nominal wheel, even though the sizing is slightly different due to the fact that the wheel requirements have been partially rearranged, thus leading to a new design synthesis, which basically has the same architectural layout of the lunar rover elastic wheel, but slightly different values of the main geometrical characteristics and other materials. The wheel design is showed in Figure 95 and summarized in Table 51.

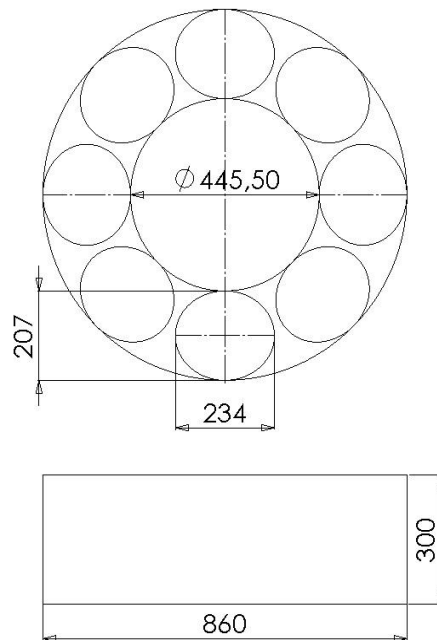


Figure 95 “Resized wheel” design

The resized wheel design activity started from the following requirements:

- The wheel shall be able to operate on a soil with physical characteristics similar to the Moon soil.
- The wheel diameter shall be 0,8 m.
- The wheel width shall be 0.3 m.
- The wheel shall be mounted on a motor. The motor diameter is 445.5 mm.
- The wheel shall be able to withstand a nominal vertical load of 2500 N.
- The wheel shall be able to withstand a contingency factor of 2 on the vertical load without permanent deformation. The ultimate load is 5000 N.
- The wheel shall transfer the axial, radial and circumferential loads from ground to the motor and vice versa.
- The wheel shall be able to provide the sufficient traction on the ground. At the nominal load, the minimum contact area shall be equal to 3 dm².
- The tread shall be resistant to the ground contact.
- The wheel shall be removable. When the motor-wheel system is still mounted on the suspension, the wheel shall be removable.

After the implementation of the design methodology that has been previously introduced and well described in section 7.3.1, the wheel design summarized in Table 51 has been obtained. Mainly, the wheel foresees eight radial elements located between the hub and tread. The radial elements are elliptical with longer axis equal to 234 mm and shorter axis equal to 206 mm. The hub diameter is 445.5 mm, the wheel diameter is 860 mm and the wheel width is 300 mm. The material selected is a harmonic steel (C72). The harmonic steel

C72 has been selected by analogy with the material considered for the “nominal wheel” and because allows lower production costs. The wheel total mass is 27.5 Kg. The wheel is characterized by a stiffness trend, which increases rapidly, when two adjacent radial elements are in contact as result of wheel deformation. When the radial elements are in contact, the wheel becomes stiffer and the stresses are distributed over a larger number of radial elements. This configuration allows a more efficient use of the wheel material and thus a lighter system with respect to a wheel design that does not allow radial element interaction. The proposed wheel configuration foresees the contact between the radial elements when the applied load reaches 2000 N. This stiffening load has been chosen in order to provide the “resized wheel” with the lower mass possible and in order to ensure the necessary wheel deformation capabilities.

Wheel width	300	mm
Wheel diameter	860	mm
Hub diameter	445.5	mm
Number of radial elements	8	-
Longer axis of radial elements	234	mm
Shorter axis of radial elements	207	mm
Total mass of wheel	27.5	kg
Maximum sustainable load	5000	N
Nominal load	2500	N
Stiffening load	2000	N
Material	C72	-

Table 51 “Resized wheel” design summary

7.3.8 Scaled wheel

In order to validate the numerical analyses, a study of a structural similitude model of the “resized wheel” and according to the structural models theory presented by Giuseppe Gabrielli (ref. [55]) has been performed. According to this theory, the ratio between the loads applied to the model and the loads applied to real wheel is equal to the square of the scale factor if the material is the same. In particular in the present case, being the “scaled wheel” a 1:3 scale model, the ratio of the applied loads is equal to 1/9.



Figure 96 A structural similitude model: the “scaled wheel”

The first tests on the “scaled model” have aimed to verifying the capability of bearing the maximum vertical axial and torque loads. The chosen wheel concept has successfully passed these tests, being always beneath the material yield limit, which is the same for the “scaled wheel” and the “resized wheel”. As far as the stiffness is concerned, the tests have shown that the “scaled model” stiffness is lower than that numerically estimated by means of the FEM models. The tests have therefore turned out to be quite useful to calibrate the FEM models themselves. The Figure 97 shows the trend of stiffness calculated by means of the numerical analysis, the trend of stiffness measured by test and the percentage difference amongst them. As can be observed in the Figure 97, it is evident that that the two stiffness curves have the same trend but also a significant deviation. The average percentage difference is equal to 18.5%. The differences amongst the analytical and test results can be attributed to FEM model simplifies assumptions, numerical approximations, test measurement errors, construction methodology of the “scaled model”, material proprieties of the “scaled model”, small geometrical differences between the “scaled model” and FEM models.

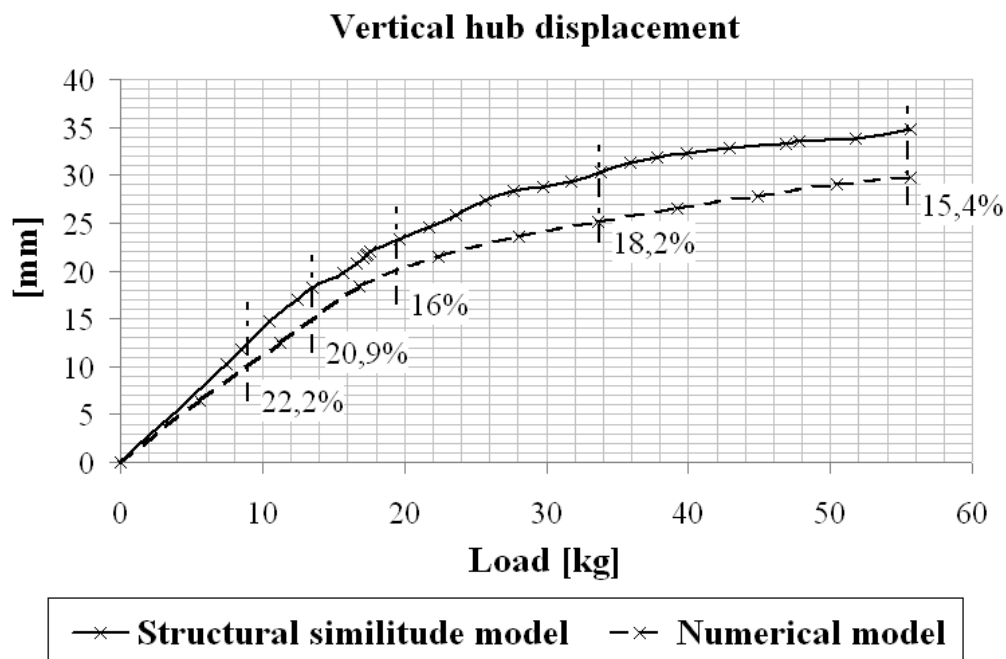


Figure 97 Vertical hub displacement: test and numerical results comparison

Figure 97 and Figure 98 show respectively the “scaled model” and an image of the tests performed on it. The wheel is mounted on a cylindrical element that reproduces the engine-wheel interface and houses a special beam able to support massive elements at the ends (wheel support). The wheel-wheel support assembly is placed inside a special structure that holds the wheel but allows wheel deflection (holding structure). Figure 98 shows the wheel under ultimate load conditions. The test procedure foresees to measure the initial weight of the wheel when it is mounted on the wheel support. Then, the wheel-wheel support assembly is put inside the holding structure so that eventual deflection resistances are annulled. Finally, with a surface gauge, incremental deflection of the wheel due to load increasing can be measured and annotated. The proposed test procedure has been performed several times and the results have been obtained after statistical elaboration.



Figure 98 Structural similitude model test activity

At the end of the test campaign the numerical model have been revised considering the average difference percentage to correct the results and to obtain as much as possible the matching of the numerical and test results.

7.3.9 Resized wheel design revision

The test results have shown that the developed and implemented analytical model overestimate the wheel stiffness. In particular an average difference percentage of 18.5% has been calculated. Thus considering the test results, a revision of the analytical model and of the wheel design has been considered necessary. In particular, a more stiff design than the previously proposed has been considered necessary.

The final “resized wheel” design is very similar to the first proposed sizing. The wheel design foresees the same geometry configuration of the first proposed solution but the thickness of the radial elements has been increased. As well explained in section 7.3.5.1, the main functions of the radial elements are to connect the hub and the tread, to provide load bearing and good shock absorption capabilities. The thickness and the eccentricity of these elements are the design parameters that allow the desired strength and load absorption features. If the thickness of the radial element increases the wheel become more stiff and the load of increasing stiffness (the wheel become more stiff when the radial elements are in contact due to wheel deformation) as the ultimate load increase. Considering the radial elements eccentricity, if this parameter increases, the radial elements are closer and the load of increasing stiffness decreases. For what concerns the “resized wheel”, the increasing of the radial elements metal sheet thickness has increased the wheel stiffness, the load of increasing stiffness and the ultimate load. This has been considered acceptable.

In conclusion the wheel foresees eight radial elements located between the hub and tread. The radial elements are elliptical with longer axis equal to 234 mm and shorter axis equal to 206 mm. The hub diameter is 445.5 mm while the wheel external diameter is 860 mm and the wheel width is 300 mm. The material selected is a harmonic steel (C72). The harmonic steel C72 has been selected by analogy with the material considered for the “nominal wheel” and because allow lower production costs. The wheel total mass is 27.5 Kg.

The following figures show the “resized wheel” vertical displacement for different angles of rotation and load. In particular Table 52 shows the applied vertical load and the calculated vertical displacement. In Table 52, it is also indicated the nominal load and the load of increasing stiffness when the wheel stands on a radial element (configuration 1).

Finally, Figure 99 graphically shows the information proposed in Table 52. It can be observed that wheel stiffness behavior changes, if the wheel stands on a single radial element (solid line) or on the gap between two radial elements (dashed line).

In the first case, the wheel stiffness increases when the deformation leads to a contact between the nearest displaced radial elements. In the second case the wheel stiffness increases continuously with the applied load.

Note	Load [N]	Configuration 1 [mm]	Configuration 2 [mm]
	0	0	0
	500	11	26
	1000	22	39
	1500	33	48
	2000	44	55
nominal load	2500	56	60
load of increasing stiffness	3000	66	61
	3500	75	63
	4000	80	64
	4500	85	65
	5000	88	66

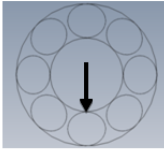
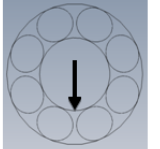



Table 52 Stiffness of the wheel when in rotation: vertical hub displacement

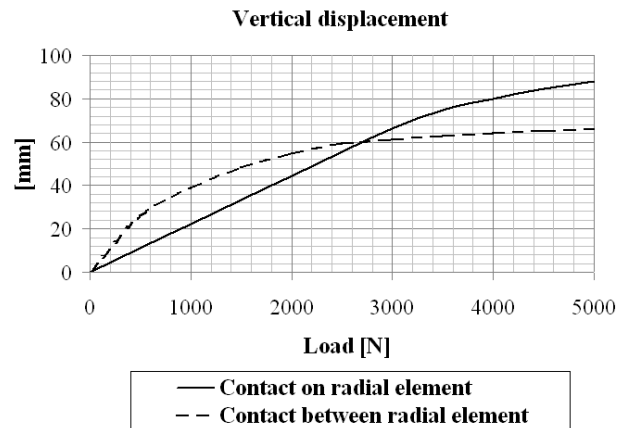


Figure 99 Stiffness of the wheel when in rotation: vertical hub displacement

At the end of the design process, six resized wheels have been produced to be eventually integrated on the rover demonstrator, see Figure 100.

The manufacturing process started with the production of the wheel components. The first wheel components was useful to perform further tests to evaluate eventual discrepancies amongst the real and expected performances, thus to identify possible criticalities induced by the manufacturing process. The activity highlighted the need to perform redesign of some particular of the wheel such as the interface components of the hub. After that the assembling of the first wheel has been completed, further tests have been performed on it. The test did not highlight any criticality and proved the matching of the resized wheel performances with the expected.

After the integration of the wheels with the rover demonstrator, the locomotion system completed the mission without any kind of failure. The locomotion performances allowed the system to move on a sandy soil, to cope with slopes and obstacles such as rocks.

The locomotion system of the rover demonstrator consists of six motor wheels. The mass of this subsystem is equal to 720 kg. Doing reference to equations [139] and [153], the estimation of the mass of the locomotion system a generic pressurized rover is possible. The rover demonstrator is the scaled model (scaling is performed on the mass since the different gravity of Earth and Moon) of the Moon pressurized rover, see Figure 94. The mass of the pressurized rover is 7000 kg. Doing reference to literature studies (ref. [4]), it can be assumed that the suspended mass is equal to the 86.5 % of the total mass. Thus, the assumed suspended mass of the pressurized rover is equal to 6055 kg. The drive power requirement can be assumed equal to 5 kW, since the similar performances of the pressurized rover and the design example in ref. [4]. Thus, the estimated mass of the locomotion system of the pressurized rover is 660 kg without the margin due to installation or estimation errors. If the mass of the rover demonstrator locomotion system is compared with the estimated mass, it is evident that the two values are closed proving the goodness of the analytical models.



Figure 100 Rover demonstrator

8 Mission design

8.1 Moon surface infrastructure support

The modeling framework, explained in the section 4, has been developed and used in three simple design sessions aimed to test and provide comparison of the results with similar studies that can be found in literature. The studies will be performed considering the reference mission architecture for Moon Exploration presented in the final report of the Exploration System Architecture Study (ESAS) by NASA, ref. [11]. This is a document aimed at defining the top-level requirements and the configurations of manned and cargo space elements to be developed to support a human and robotic lunar exploration mission.

The first study performed concerns the analysis of the effect of number of crew members and mission duration on Trans-Lunar Injected (TLI) mass for a crew mission. The second one is about an anytime-return scenario. In the last design session, the modeling framework has been utilized to design a support mission for a hypothetical human outpost on the Moon surface.

The reference mission architecture (ref. [11]) is studied to ensure global access to the Moon, i.e., the possibility of transportation of crew and cargo to and from anywhere on the lunar surface. The mission is very similar to the Apollo one for what concerns the surface activities but differs from the Apollo mission in the location of the “nodes”, i.e., the positions where a docking or a separation of modules occurs, ref. [56].

The most relevant space elements considered for this mission architecture are listed in Table 53.




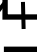

Description	Acronym	Symbol	ΔV [m/s]
Capsule	CAP		50
Service module	SM		1724
Lunar ascent module	LAM		1888
Lunar descent module	LDM		1900
Transfer stage	TS		3120

Table 53 Description of the main space elements with relative ΔV maneuvers of the space scenario, ref. [10]

The capsule is the vehicle capable of transporting and housing crew from Low Earth Orbit (LEO) to Low Lunar Orbit (LLO). The Service Module (SM) is an unpressurized system that provides propulsion, power and other supporting capabilities for the capsule. The Lunar Ascent Module (LAM) and the Lunar Descent Module (LDM) are docked together forming the so-called Lunar Surface Access Module (LSAM). The LAM is the module that supports the crew members from LLO to the lunar surface and back from the lunar surface to LLO. The LDM is an unpressurized module that performs the descent maneuvers from LLO. It provides life support for the crew members and power generation during the lunar activities. The Transfer Stage (TS) is a propulsion module that provides the necessary thrust to leave the LEO and inject the payload, formed by all the other modules docked together, into the Lunar Transfer Orbit (LTO).

In Figure 101 a schematic of the mission architecture is shown.

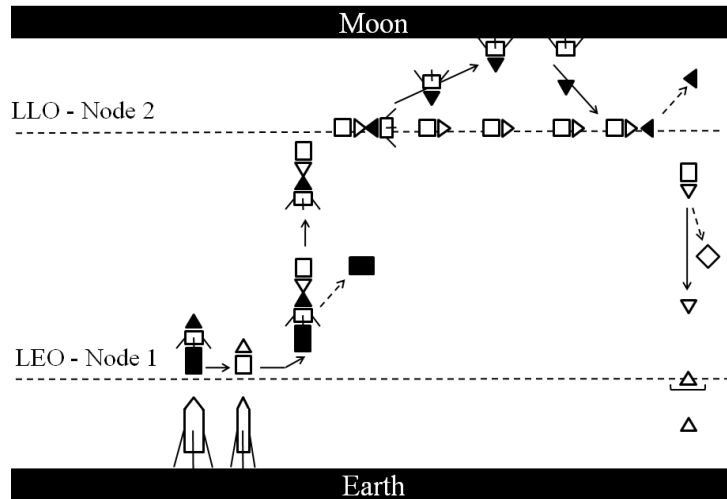


Figure 101 Schematic of the reference mission architecture

Two main mission nodes are considered. The first one is near the Earth, where the rendezvous and docking of the capsule and the service module with the transfer stage and the lunar access modules is performed. The second one is in the cis-lunar space. In particular, in the low lunar orbit the lunar surface access module undocks from the capsule and lands on the Moon.

Right after the docking of the capsule and the SM with the TS and the LSAM in low Earth orbit, the TS is injected. Once the trans-lunar injection maneuver is performed the TS is discarded. The Lunar Orbit Injection (LOI) maneuver is performed by the SM. Once in LLO all the crew members move from the capsule to the LAM. The LSAM then undocks from the capsule and lands on the Moon. Once the lunar activities have been completed, the return phase of the mission starts. The LDM is left on the Moon and LAM performs the maneuvers that put the crew members in LLO. Once in LLO, the LAM docks with the capsule and the crew moves back. The LAM is disposed while the SM performs an Earth transfer maneuver. In proximity of the Earth, the SM is disposed and the capsule performs a direct entry maneuver.

The capsule uses propellant to re-orient the vehicle to a proper attitude for the atmospheric re-entry. Additional propellant is used to correct the re-entry trajectory and to reduce eventual instabilities. The SM uses propellant to complete three main maneuvers. The first one is the rendezvous and docking with the LSAM and TS ($\Delta V = 119$ m/s), the second maneuver is a change of plane in LLO ($\Delta V = 156$ m/s), and the last one is the Trans-Earth Injection (TEI) from LLO ($\Delta V = 1449$ m/s). The LAM performs the ascent maneuvers from the Lunar surface. The main engine is sized to perform the ascent maneuver, with ΔV equal to 1866 m/s, while the secondary engines perform correction maneuvers only. The LDM performs two main maneuvers. The first one is the LLO insertion ($\Delta V = 1390$ m/s), the second one is the descent maneuver on the lunar surface ($\Delta V = 1900$ m/s). Finally, the TS provides a ΔV of 3120 m/s to put the other modules in LTO. The ΔV needed for all the maneuvers mentioned before are summarized in Table 53, retrieved from ref. [11].

For simplicity sake, we assumed that all the main and secondary maneuvers are performed with a single impulsive burn. Only for the LDM two different maneuvers are considered, one to brake from LTO to LLO and another one to descent on the moon.

Considering the mission architecture described in the previous section, with the analytical models of all the building blocks implemented with the equation described in section 4, a simulation was made to evaluate the masses of all the SoS elements. The mission requirements considered in the simulation are the following:

- Four crew members should be hosted in the capsule
- Capsule comfort level should be at least equal to performance limit, see Figure 12
- Capsule Mission duration should be at least 13.5 days
- All the crew members should land on the Moon
- The surface activities should last at least four days
- The LAM comfort level should be at least equal to performance limit, see Figure 12
- The required ΔV s are listed in Table 53 and the required Isp are listed in Table 54

System	I_{sp} [s]	Type of Propellant
Capsule	274	GOX-Ethanol
SM	363,6	LOX-LMET
LAM	363,6	LOX-LMET
LDM	435	LOX-LH2
TS	451,5	LOX-LH2

Table 54 Isp considered for each building block

The results of the simulations are listed in Table 55. The total mass of each building block of the SoS is reported together with a SoS mass break-down. The total mass placed on orbit is about 190 tons. It is evident that launchers that can transport such a large payload mass do not exist. Thus, the mission will have to be performed with two launches. The first launcher puts an unmanned payload in orbit, generally heavier than the manned one, composed of the departure stage docked with the LSAMs (165.5 t in total in this particular case). The second launch puts in orbit the manned payload, in this case composed of capsule and relative service module (25 t in total).

To verify the goodness of the SoS mathematical model, the results are compared with data available in the reference study, ref. [11]. The results of the comparison are shown in Table 56. As we can see, there are relatively small differences between the calculated masses and the reference data.

	Capsule [kg]	SM [kg]	LAM [kg]	LDM [kg]	TS [kg]
Structure	2000	829	887	1144	4648
Protection	840	168	86	93	476
Propulsion	632	1824	689	2444	12666
Power	850	419	587	459	820
Control	0	0	0	92	0
Avionics	435	117	385	69	195
Environment	1245	98	796	248	0
Other	1167	290	384	633	100
Growth	1434	749	763	1036	3781
Non-cargo	1008	569	1071	1114	1199
Cargo	100	0	100	0	0
Non-propellant	549	0	34	231	24
Propellant	182	9635	4010	27842	96355
Dry mass	8603	4494	4577	6219	22685
Inert mass	9711	5062	5747	7332	23884
Total Vehicle mass	10442	14698	9791	35406	120263

Table 55 Vehicle mass properties for all the building blocks of the reference mission scenario.

	Total System Mass		
	SoS model [Kg]	ESAS [Kg]	Δ
Capsule	10442	9506	9%
SM	14698	13647	7%
LAM	9791	10809	10%
LDM	35406	35055	1%
TS	120263	227250*	89%

Table 56: SoS model results v.s. ESAS data. *The TS mass evaluated in ref. [11] is retrieved from different design assumptions: the ESAS TS performs three maneuvers (LEO insertion, circularization and TLI burn); the TS modeled performs a single maneuver

8.1.1 Study 1: Number of crew members and mission duration

In Figure 102, the trend of the mass of the capsule as a function of the number of crew members and the duration of the mission is shown.

The mass of the capsule increases when the number of crew members increases and when the duration of the mission increases. The behavior is quite linear in both dimensions. It is also evident that the influence of the number of crew members is higher than the influence of the duration of the mission. This behavior is due to the fact that with the increasing number of crew members the increase in mass due to the presence of more astronauts, more provisions and supporting elements is higher than the increase in mass due to the increase in provisions and supporting elements with a constant number of astronauts.

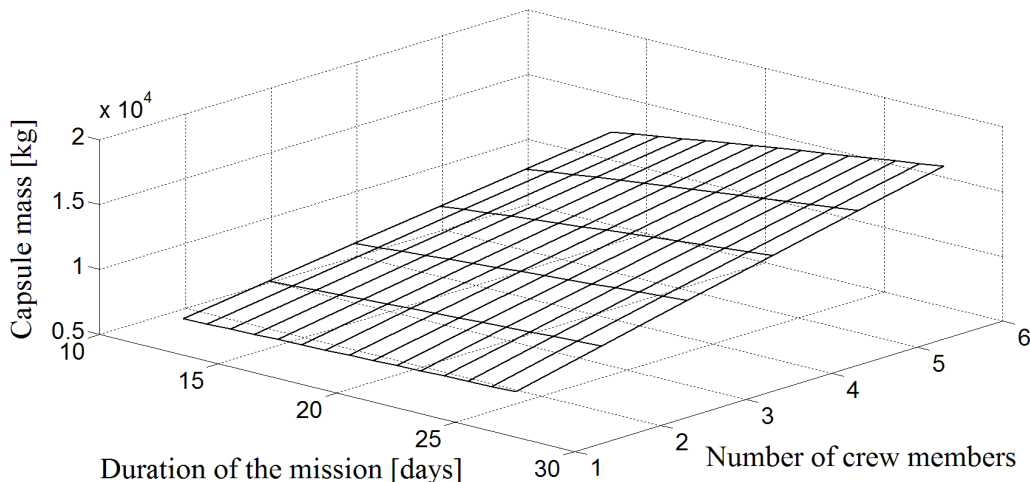


Figure 102 Mass of the capsule as a function of the number of crew members and the mission duration

At SoS level, the influence of design parameters on the TLI mass can be studied as well. The TLI mass is the sum of the masses of all the elements injected in lunar transfer orbit, i.e., the sum of the capsule, service module, lander and ascent module mass. In Figure 103, we can see that if the number of crew member increases, the TLI mass increases linearly. The number of crew members directly or indirectly influences the mass of all the other modules. We speak of direct influence when the module performances change due to the variation of a parameter of the module itself. For instance, the number of crew members affecting the capsule mass. We speak of parameter indirect influence when there is a variation of the performance of a module due to the variation of other modules characteristics. The amount of propellant on a spacecraft changes if the payload mass changes, e.g., the service-module propellant mass increases if the capsule mass increases, because the number of crew members increases. In this case the number of crew members has an indirect influence. In some other

cases the number of crew members directly affects the mass of unmanned modules. There are some systems that can be allocated to unmanned modules, but that are useful for manned modules. For example, the water system that is useful for the LAM and that has a mass that is directly proportional to the number of crew members, is allocated to the LDM in the SoS proposed.

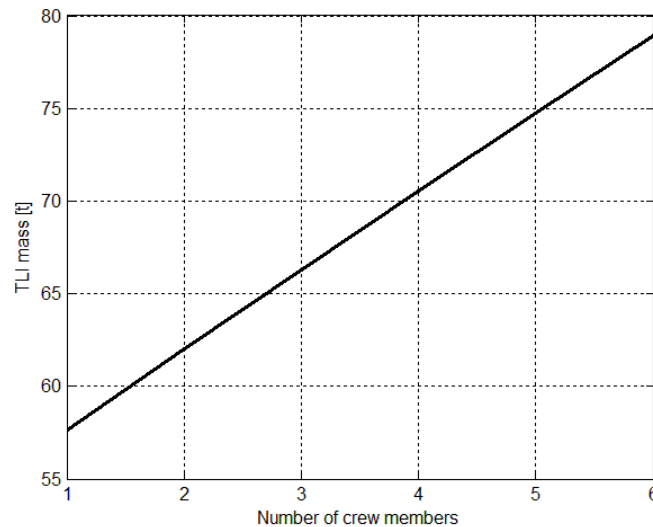


Figure 103 Influence of the number of crew members on the TLI mass

8.1.2 Study 2: Anytime return

For safety reasons, especially for a manned human mission to the Moon, abort strategies for each mission phase should be provided. In this section, the “*any-time return*” scenario will be studied as an abort strategy from the lunar vicinity.

Studying the anytime return conditions consists of determining the cost, in terms of mass, of the opportunity to allow the crew members to return from the lunar surface, independently from orbital plane alignment.

There are two main alternatives. The first one is to get back to the Earth by performing an orbital plane change around the Moon before entering in the transfer orbit. This is paid in terms of propellant mass. The second alternative is to wait in LLO until the orbits naturally aligns. This is paid in terms of crew provisions mass.

The results of this study are showed in Figure 104. The graph illustrates how the capsule and service module total mass, propellant mass, provisions mass and “*other*” mass vary as a function of loiter time in LLO and the required orbit plane change. The simulation starts when the orbital plane of the orbit around the Moon is perpendicular to the orbital plane of the Moon-Earth transfer orbit. In these conditions, if the loiter time is zero, a plane change of 90 deg is required for TEI (left side of the graph).

The trends show that when loitering is performed, the Service module mass and the capsule mass decrease. From the graph we can observe that for every day spent in LLO a reduction of about 120 kg of mass is obtained. This trend is due to the fact that the propellant mass decreases with loiter time more than crew provisions mass increases. The mass of the other elements remains approximately constant.

One of the reasons that can justify a modification of the schedule of the mission is an injury of a crew member. In this case loitering is allowed only if there are appropriate medical devices in the capsule.

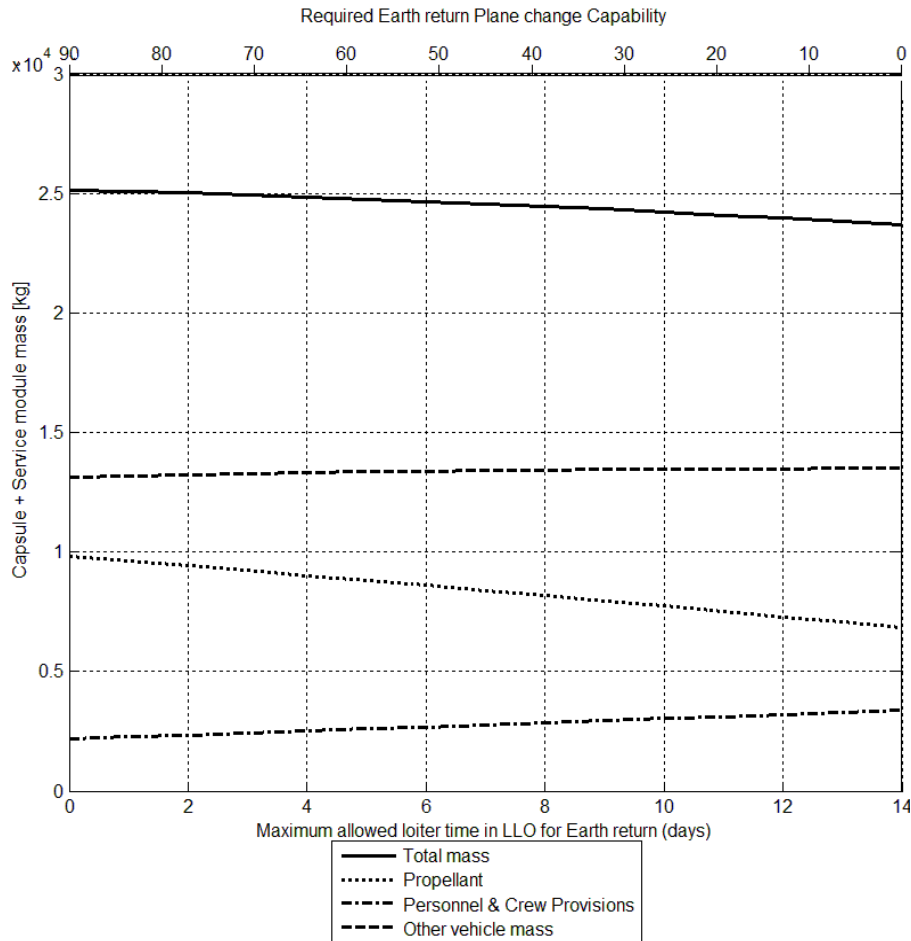


Figure 104 Study of anytime return

8.1.3 Study 3: Lunar Base

A final example of the utilization of the mathematical models and the modeling framework is provided in this subsection. The models are utilized to design a supporting mission for a hypothetical base on the lunar surface.

Suppose to have a human settlement on the Moon. Suppose that the construction phase of the Moon base is already completed. Further, suppose that there is a crew that conducts experiments in the lunar base. A certain number of astronautics must be transported from and to the Moon periodically, because they cannot stay on the Moon more than a certain period, defined by requirements. Let us consider the mission architecture described before as the baseline architecture designed to transport people to and from the Moon.

It would be interesting to understand what is the most advantageous strategy to efficiently put people on the Moon.

To conduct this investigation the following hypothesis will be considered:

- The operative life of the Moon base is equal to 15 years
- The crew members cannot stay on the Moon for more than 0.5 year (6 months)
- The number of crew members on the Moon is 8
- The number of astronauts that can be transported varies between 1 and 8

In Figure 105 we show, as a function of the number of crew members that are moved from Earth to Moon and return, two parameters defined to evaluate the mission efficiency, i.e., the total mass to put in orbit (with manned launches), and the total number of missions from the Earth to the Moon.

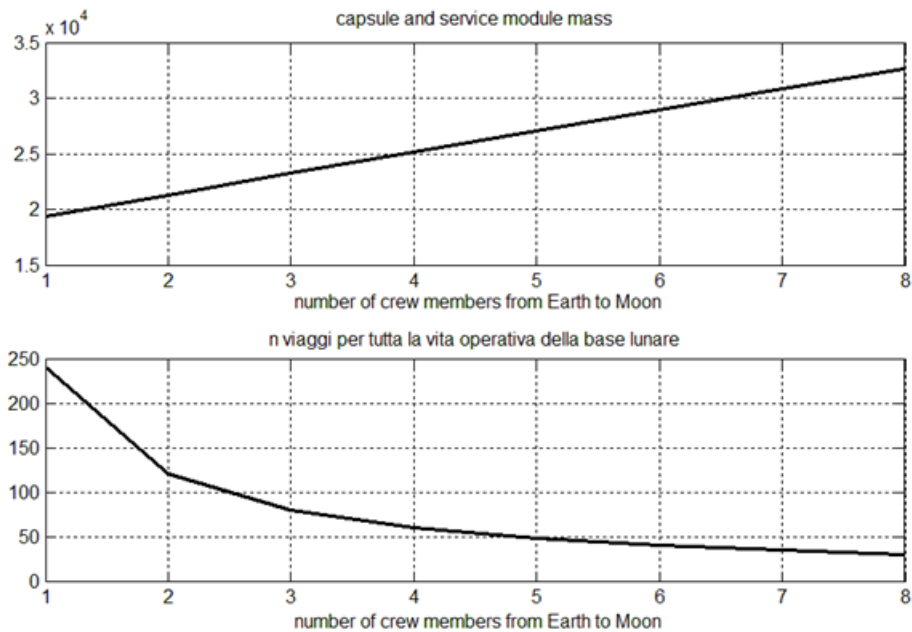


Figure 105 Moon base support System-of-Systems

As already said, if the number of crew members on the capsule increases the mass of the capsule and the relative service module increases as a consequence. However, at SoS level it is important to notice that the total number of travels from Earth to Moon, in the timeframe of the operative life of the Moon base, decreases. So multiplying the total mass of capsule and SM by the total number of missions, we obtain the total capsule and SM mass injected in orbit by the crewed launcher in the operative life of the Moon base, as shown in Figure 106.

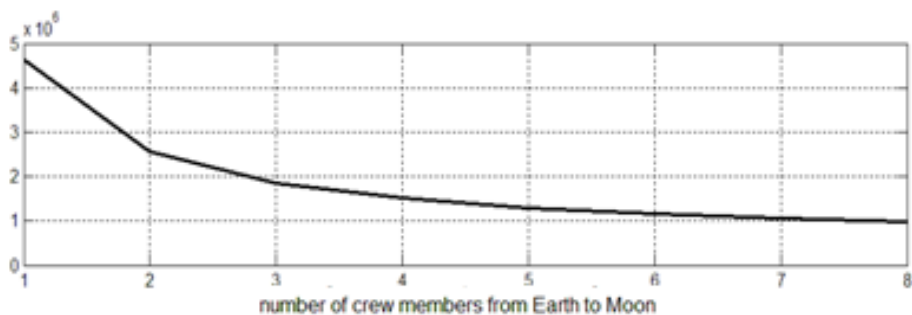


Figure 106 Moon base support System of Systems, total mass injected in orbit by the manned launchers, during the whole operational life of the base

The unfeasible solutions, i.e., those solutions for which the capsule mass plus the service module mass exceeds the launcher available mass are not shown in the graph of Figure 106.

The more astronauts in the capsule, the more efficient is the SoS, since the total injected mass decreases. This is true if the launcher can accommodate a payload as large as a capsule that can host eight astronauts plus the relative service module.

For a more realistic analysis, we set the constraint on the launcher capability, i.e., the launcher cannot accommodate a payload that is larger than a certain threshold, specific for each launcher.

In Figure 107, we can observe that if we want to have 4 astronauts from Earth to Moon, a single manned launch is sufficient, with the requirements settings as described before. With more than 4 astronauts, we observe that more than one launch is required, i.e., more launches

of smaller capsules, because the mass of the capsule plus the service module exceeds the launcher mass availability on orbit. For instance, if we want to send six astronauts to the Moon, we must launch two smaller capsules (two capsules sized for three people, for instance). As a consequence, we observe that it is not convenient to increase the number of astronauts that travel for each mission, because, even if the total number of launches decreases, the total injected mass, during the timeframe of the operative life of the base, increases as well, see Figure 108.

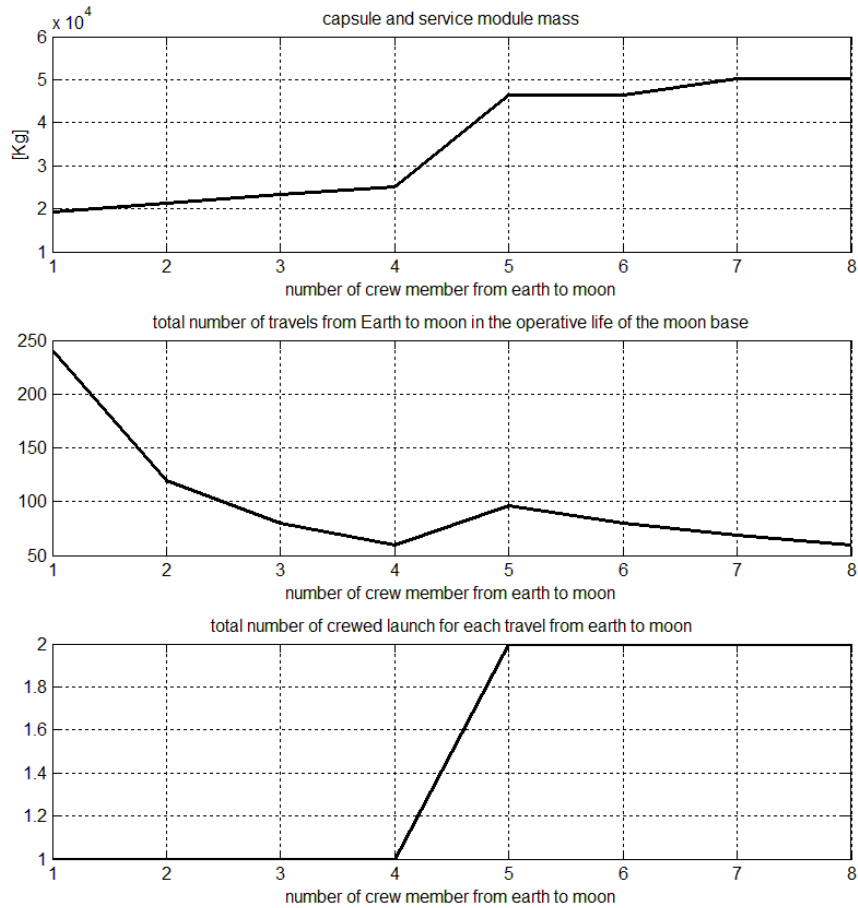


Figure 107 Moon base support System of Systems, with constraint on the launcher available mass on orbit

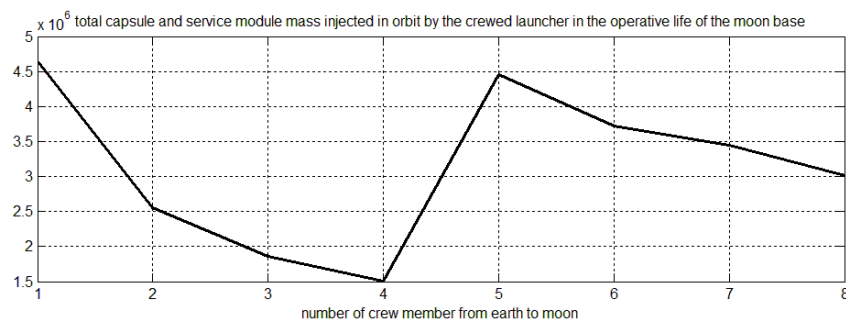


Figure 108 Moon base support System of Systems, total mass injected in orbit by the manned launchers, during the whole operative life of the base, with constraint on the launcher available mass on orbit

Already with this simple example, using only one variable and two objectives, with one constraint, it is clear that there is not a unique solution, as it usually happens in engineering problems. Only varying the number of crew members, we obtained opposite trends for the two selected objectives. When more variables are considered at the same time, the task of selecting the best combination of their levels becomes particularly hard.

8.2 Cis-Lunar infrastructure delivering

The space-exploration scenario envisages the insertion of a manned space station in a low orbit around the Moon. Two main system-architectures are considered. The first one consists of a multi-element space station composed of two modules, i.e., a service module (SSSM, Space Station Service Module) and a node module (SSN, Space Station Node). The second one is a single-element space station, Skylab like.

The SSSM provides electrical power, propulsion, guidance and control, communications capabilities, thermal control, and life support during all the mission phases of the space station. The SSN provides docking, berthing, and research (pressurized or not) capabilities. The SSSM is a rigid, cylindrical, element consisting of a pressurized and an unpressurized section. The pressurized section houses the pressurized avionic, the crew accommodation equipment, and part of the research equipment. These systems are located into racks and into the standoff volumes. The propulsion bay mainly accommodates the propulsion subsystem, i.e., the propellant tanks, the main engines and the sub-system control equipment. Other avionic equipment as the batteries, the communication equipment, and part of the power and GNC systems are located inside the non-pressurized avionic bay. The deployable solar arrays and radiators are externally mounted. The SSN is a rigid, cylindrical, pressurized element closed at the extremes by two conical segments. The SSN can accommodate up to six docking ports which are mounted at the edges of the cylindrical body of the SSN and on the lateral surface. The SSN accommodates eight racks that house the research equipment and the necessary avionic systems needed by the internal equipment and to support eventual additional systems attached to it. In Figure 109 the on-orbit configuration of the multi element space station is represented.

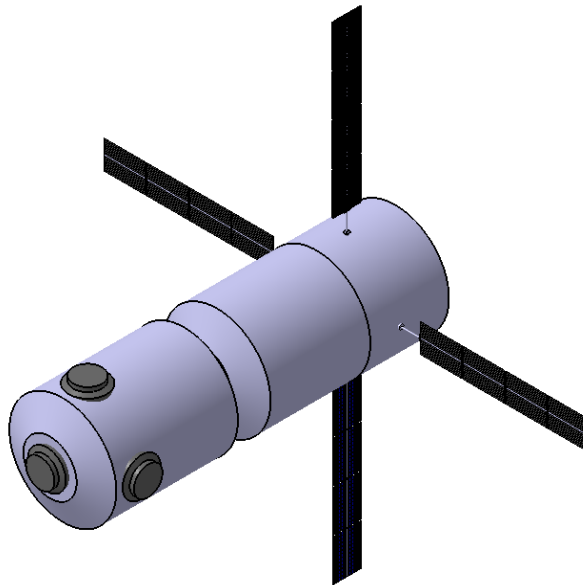


Figure 109 On-orbit configuration of the SSSM+SSN

The Skylab-like space station consists of a single integrated module only (SSIM, Space Station Integrated Module). It provides electrical power, propulsion, guidance and control, communications capabilities, thermal control, and life support during all the mission phases, as well as docking, berthing, and research (pressurized or not also in this case) capabilities. The SSIM is very similar to the SSSM of the multi-element space station but it is longer to ensure the total required habitable volume. It also houses the docking ports. As the SSSM module, it has a cylindrical shape and it is divided into a pressurized and a non-pressurized section. The pressurized section houses the pressurized avionic systems, the crew

accommodations, and the research equipment. All these elements are arranged into racks and *standoff* volumes. The SSIM can accommodate up to five docking ports which are mounted at the extremes of the cylindrical body and on the lateral surface, as shown in Figure 110. Thus, both the multi-element space station and the Skylab-like space station can ensure docking capabilities up to five visiting vehicles or generic support systems. The unpressurized section on the SSIM is located in the aft part of the module. The service compartment houses the non-pressurized avionic systems and the propulsion bays. The propulsion bays accommodate the propulsion sub-system, i.e., the propellant tanks, the main engines and the relative control equipment. The non-pressurized avionic bay accommodates avionic equipment, the batteries, the communication equipment and part of the power and GNC systems. The deployable solar arrays and radiators are mounted externally in correspondence of the non-pressurized avionic bay. In Figure 110 the on orbit configuration of the Skylab-like space station is represented.

Both the system architectures are designed to perform every-day station-keeping and on-orbit maneuvers using the propulsion system.

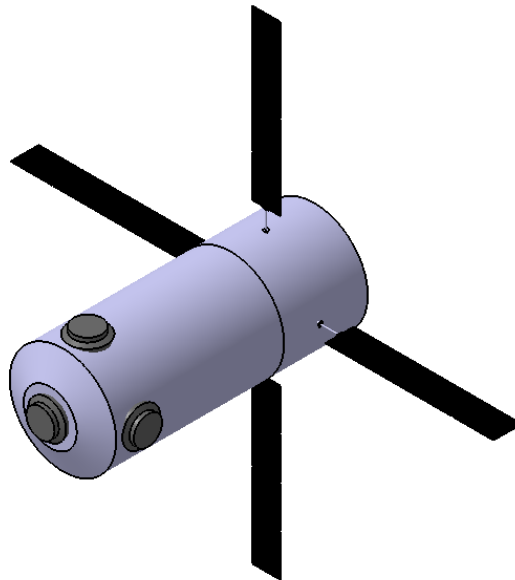


Figure 110 On-orbit configuration of the SSIM

A single-element or multi-element space station can be deployed in a low lunar-orbit according to a large variety of mission architectures. In fact, considering all the possible combinations of number and type of building blocks, one can think of many different solutions to the problem. Some of the proposed mission scenarios foresee that the orbit maneuvers are performed by the space station modules themselves, while some of them foresee that the orbit maneuvers are performed by a transfer stage (TS).

The TS is a propulsion module that provides the necessary thrust to leave the initial orbit and inject the payload into the target orbit. The external shape of the transfer stage is cylindrical. The length of the TS module is proportional to the propellant tank length. The propellant tank dimensions are computed as a function of the propellant mass which is proportional to the required ΔV and to the total mass that the propulsion system must accelerate. The structure of the TS consists of an unpressurized structure with dedicated tank supports. The unpressurized structure provides structural support to the other subsystem components as secondary propulsion devices, power and avionic equipment and ensures the proper interface with the launcher and the payload. In Figure 111 the configuration of the transfer stage is represented.

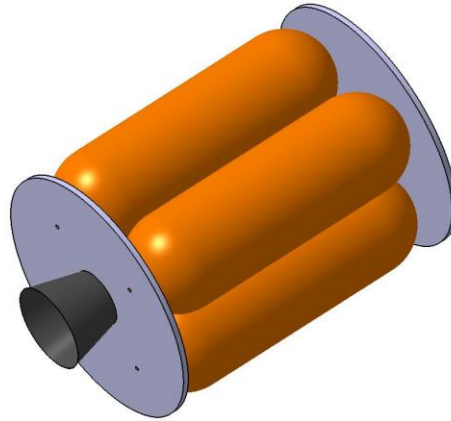


Figure 111 Configuration of the TS

The type of mission architectures considered is neither exhaustive nor complete. They are examples used to demonstrate how a combined sensitivity analysis and optimization method could help the engineering team in reducing the number of feasible solutions to analyze, even for a complex system as a lunar-orbiting space station.

Three mission architectures have been considered for the deployment of the Skylab-like space station and seven mission architectures have been considered for the deployment of the multi-element space station. The building blocks considered for all the mission architectures are listed in Table 57.

Description	Acronym	Symbol
Space station integrated module	SSIM	
Space station service module	SSSM	
Space station node	SSN	
Transfer stage	TS	

Table 57 Description of the main building blocks

The mission architectures considered for this study foresee two main mission-nodes. The first node is near the Earth, in Low Earth Orbit (LEO), while the second one is in the cis-lunar space. This node is called Low Lunar Orbit and it represents the orbit where we want the space station to be in its final configuration. All the mission architectures begin by launching the building blocks in LEO.

The first mission architecture is presented in Figure 112. This is the simplest one proposed. It is only made of a single building block, i.e., the SSIM. Once the SSIM is inserted in LEO, it performs the Trans-Lunar Injection (TLI) and Lunar Orbit Injection (LOI) maneuvers. The mission scenario does not foresee any staging or Rendezvous and Docking.

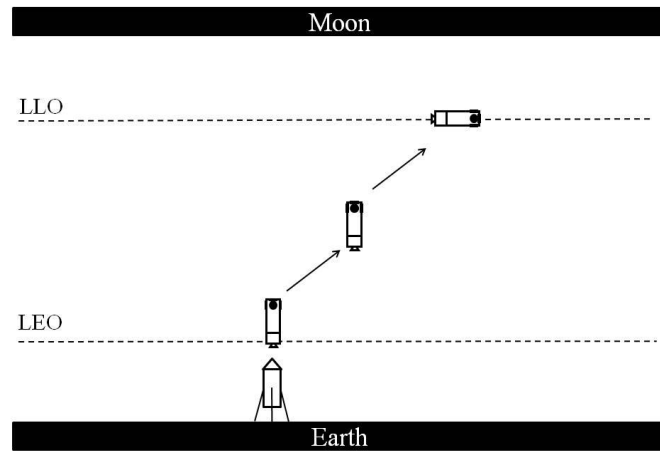


Figure 112 Space station deployment mission architecture#1

The second mission architecture (see Figure 113) foresees two building blocks. The SSIM and the TS are inserted on orbit by one or two launches. Once in orbit, the systems perform the TLI and LOI maneuvers, in a docked configuration. Unlike the first mission architecture, the maneuvers are not performed by the SSIM. Indeed, they are performed by the TS. Once the TLI maneuver is completed the TS is discarded.

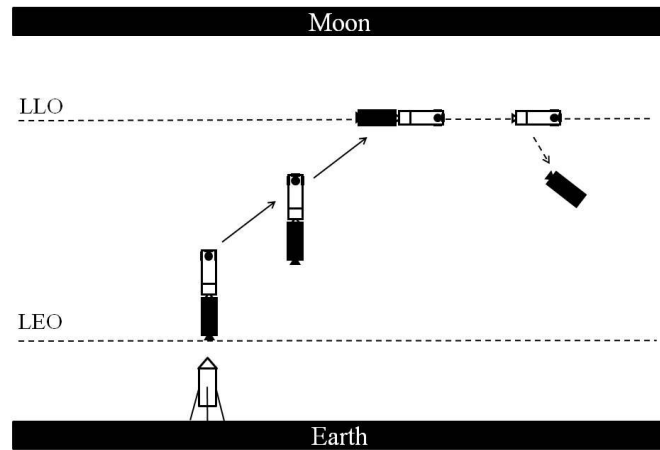


Figure 113 Space station deployment mission architecture#2 Fig. 5

The building blocks considered for the third mission architecture are the SSIM and the TS, as in the previous one. In this case the TS module performs the TLI maneuver only. Once the TLI is completed, the TS is discarded and the SSIM performs the LOI maneuvers using its own propulsion system. This mission architecture is presented in Figure 114.

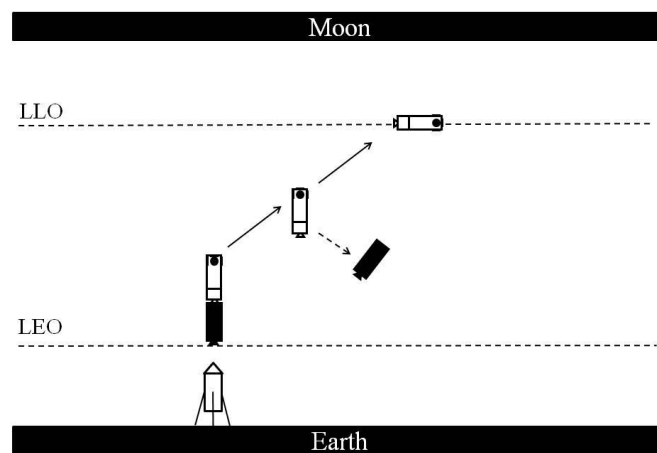


Figure 114 Space station deployment mission architecture#3 Fig. 6

Mission architecture #4 (see Figure 115) is very similar to mission architecture #1. The SSSM and the SSN are inserted on orbit by one or two launches. In case of the two-launches mission, the RvD of the two modules is completed in LEO. Once the systems are in LEO, the SSSM performs the TLI and LOI maneuvers. As for the first mission architecture, this mission does not foresee staging and the RvD (if needed) is completed in LEO.

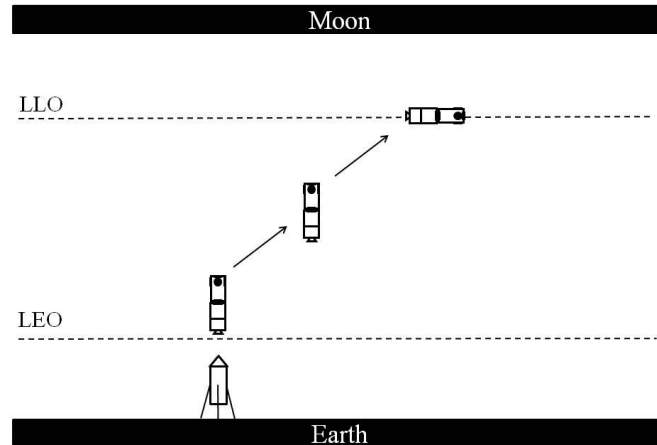


Figure 115 Space station deployment mission architecture#4 Fig. 7

The number of building blocks increases to three considering mission architecture #5 (see Figure 116). The mission begins when the SSSM, the SSN, and the TS are docked together in LEO. If a one-launch solution is considered, the building blocks are launched in the docked configuration. If the two-launch solution is considered, instead, the first launcher inserts the SSSM on orbit while the second launcher inserts the TS and the SSN modules docked together on orbit. This one-launch or two-launches configurations will be considered for all the remaining mission architectures. The two-launch solution foresees RvD in LEO. Once all the systems are docked in LEO, the mission architecture #2 foresees that the TS performs the TLI and LLO insertion maneuvers, and it is discarded at the end.

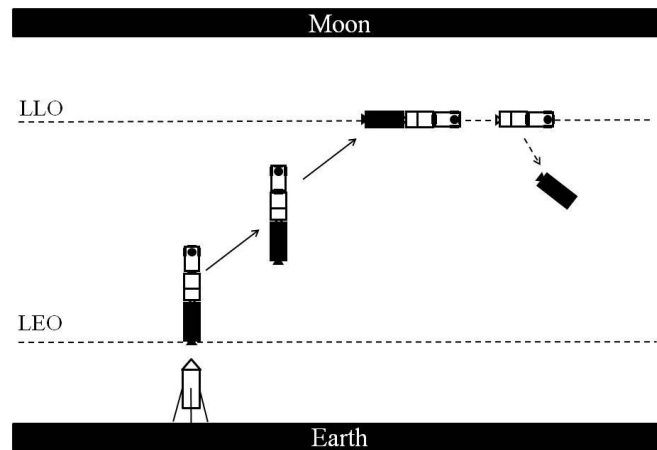


Figure 116 Space station deployment mission architecture#5 Fig. 8

In the architecture #6 (see Figure 117), the one-launch or two-launches solutions are possible. Once on orbit, the SSSM performs the TLI and LOI maneuvers. When the SSSM is in LLO, the mission of the SSN and TS begins. The TS performs the TLI and LLO injection maneuvers and at the end of these, it is discarded. Once the SSSM and SSN are in LLO a RvD maneuver is performed to finally assemble the space station.

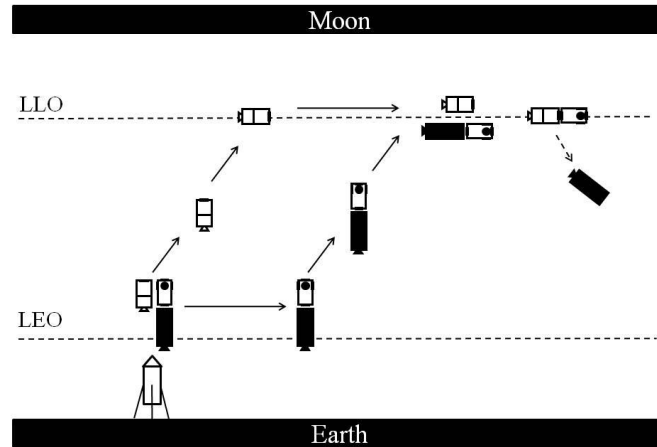


Figure 117 Space station deployment mission architecture#6 Fig. 9

According to the mission architecture #7, the mission begins with the TS module providing the necessary acceleration to reach the TLO to the SSSM and the SSN. Once the systems are accelerated, the undocking of the SSSM occurs. The SSSM and the SSN-TS assembly reaches LLO separately. The TS is discarded when the necessary SSSM-SSN docking maneuvers are completed.

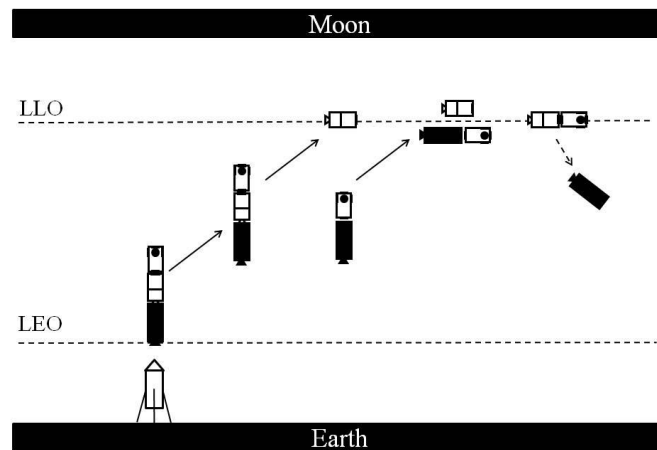


Figure 118 Space station deployment mission architecture#7 Fig. 10

The mission architecture #8, foresees that once the TS, the SSSM, and the SSN perform the TLI maneuver docked together, the TS module is discarded and the SSSM provides the ΔV needed to reach the LLO.

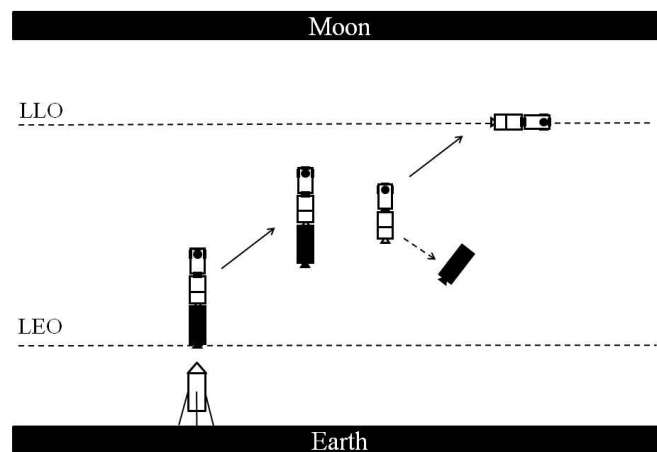


Figure 119 Space station deployment mission architecture#8 Fig. 11

The last two architectures foresee the utilization of two TSs. The first TS is docked to the SSSM and the second one is docked to the SSN. The mission starts when TS puts the SSSM in TLO and then in LLO. When the SSSM reaches LLO the first TS module is discarded and the mission of the SSN begins. The second TS performs the TLO and LLO injection maneuvers and then it is discarded. Once the SSSM and the SSN are in LLO, they perform a docking maneuver.

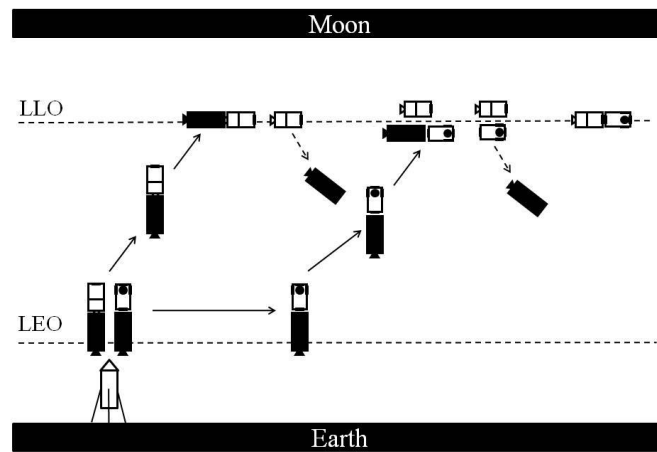


Figure 120 Space station deployment mission architecture#9 Fig. 12

In the last mission architecture the first TS, which is attached to the SSSM, is discarded at the end of the TLO injection maneuver and the SSSM performs the LLO injection maneuver. Once the SSSM reaches the LLO, the mission continues as described already for the mission architecture #9. The second TS inserts the SSN in TLO and then in LLO. It is discarded at the end. Finally, the SSSM and the SSN perform a docking maneuver.

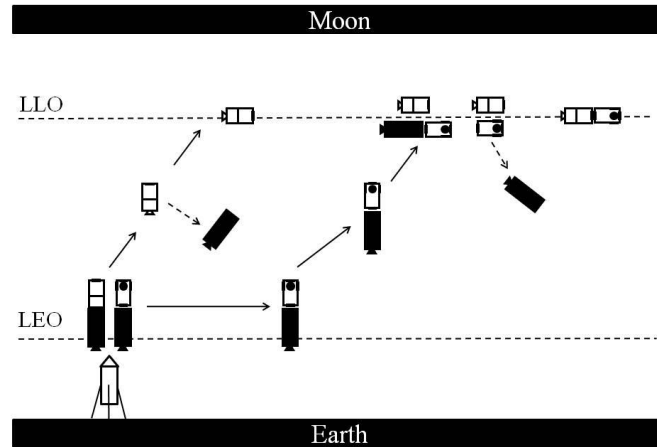


Figure 121 Space station deployment mission architecture#10 Fig. 13

The ΔV for the maneuvers considered for the mission architectures described before are presented in Table 58.

Maneuver	Value	Unit
LEO - TLO	3120	m/s
TLO - LLO	1390	m/s

Table 58 ΔV manoeuvres of the space scenarios, ref. [11]

The design variables taken into account for the analysis presented are described in Table 59.

Design Variable	Code	Type	Intervals		
			Min	Max	Levels
Type of Mission	A	Disc.	1	10	10
# of Launches	B	Disc.	1	2	2
# of Crew members	C	Disc.	3	6	4
Volume distribution Node/SM	D	Cont.	40%	60%	-
# of Hatches SM	E	Disc.	1	5	5
# of Hatches Node	F	Disc.	1	5	5
# of Hatches IM	G	Disc.	1	5	5
SM Diameter [m]	H	Cont.	3.5	5.5	-
Node Diameter [m]	I	Cont.	3.5	5.5	-
IM Diameter [m]	J	Cont.	3.5	5.5	-
# of Racks SM	K	Disc.	4	10	7
# of Racks Node	L	Disc.	4	10	7
# of Racks IM	M	Disc.	6	18	13
Moon Orbit Altitude [Km]	N	Cont.	80	150	-
Mission Duration [days]	O	Cont.	25	35	-
I_{sp} SM [s]	P	Cont.	250	350	-
I_{sp} IM [s]	Q	Cont.	250	350	-
Min. Habitable Volume [m ³]	R	Cont.	35	45	-
Racks SM mass [Kg]	S	Cont.	160	200	-
Racks Node mass [Kg]	T	Cont.	160	200	-
Racks IM mass [Kg]	U	Cont.	160	200	-
Max. Power Required SM [KW]	V	Cont.	8.5	11.5	-
Max. Power Required IM [KW]	Z	Cont.	8.5	11.5	-
I_{sp} TS [s]	X	Cont	350	450	-

Table 59 Design factors used in the simulation and relative design intervals

The “*type of mission*” design variable allows choosing amongst one of the ten mission architectures described in the previous section. Each mission architecture foresees a specific number and type of modules, a combination of orbit maneuvers and staging phases. All these mission features characterize the mission architecture with pros and cons. If the number of docking and undocking maneuvers increases, for instance, the mission-success ratio decreases. In this case, however, the entire mission results more *flexible*. As said already, each mission architecture can be deployed using one or two launches. The variable “*# of Launches*” allows choosing between the one-launch solution and the two-launch solution. If the one-launch solution is selected, all the building blocks are launched in the docked configuration. As a consequence, on-orbit docking maneuvers are avoided but the launcher payload mass increases. If the two-launch solution is chosen, instead, the launcher payload mass and the launcher cost decrease. In this case the launch reliability increases but on-orbit docking maneuvers became necessary, with the consequence that the mission-success ratio decreases.

The “# of Crew members” represents the number of astronauts that the space station can support. The number of crew members ranges between a minimum of 3 astronauts to a maximum of 6 astronauts. If the number of crew members increases the habitable volume that must be guaranteed on the space station increases. A larger space station becomes also heavier and more expensive. The variable “*Volume distribution Node/SM*” is related to the multi-element space station architecture. This variable defines how much habitable volume is allocated to the SSSM and how much on the SSN. The allocation of more or less habitable volume to one module influences the module characteristics as the external layout and the mass proprieties. The variables “# of Hatches SM”, “# of Hatches Node” and “# of Hatches IM” are the number of hatches on the SSSM, on the SSN and on the SSIM. The number of hatches influences the mass proprieties of the systems and it is representative of the capability of the space station to support more or less visiting/additional vehicles. It is also an indicator of the scalability of the space station itself. The variables “*SM Diameter*”, “*Node Diameter*” and “*IM Diameter*” are the external diameter of the SSSM, of the SSN and of the SSIM, respectively. If the modules of the multi-element space station have different external diameters, the space station cost increases because the production cost increases. The model considers the additional cost as exponentially-increasing with the modules diameter difference. The variables “# of Racks SM”, “# of Racks Node” and “# of Racks IM” are the number of racks that can be stored on the SSSM, the SSN and the SSIM, respectively. The racks provide accommodation to part of the space station subsystems (i.e. life support systems and crew accommodation) and to experimental equipment. If the number of racks is at the minimum value, this implies that volume dedicated to experimental equipment is also reduced. The “*Moon Orbit Altitude*” is the altitude of the space station orbit around the Moon. The orbit altitude influences the power subsystem, amongst the others. The “*Mission Duration*” is related to the crew mission-duration inside the space station. A large mission duration implies a large habitable volume that must be guaranteed on the station to comply with the necessary comfort levels. Moreover, the mission duration influences the amount of consumables that must be stored on board of the space station. The “*I_{sp} SM*”, “*I_{sp} IM*” and “*I_{sp} TS*” are the specific impulses of the SSSM, SSIM and TS propulsion-system propellants, respectively. The value of these design variables is related to the propulsion technology adopted by each specific building block. If the specific impulse increases, the amount of necessary propellant mass decreases. Further, the mathematical model takes into account also the fact that if the modules have different propellants, the total production costs increase. This is due to the consideration that different infrastructures for propellant managing are necessary. The “*Min. Habitable Volume*” variable is representative of the minimum habitable volume that the space station must guarantee. The “*Racks SM mass*”, “*Racks Node mass*” and “*Racks IM mass*” are the mass of the rack of the SSSM, the SSN and the SSIM, respectively. The “*Max. Power Required SM*” and the “*Max. Power Required IM*” are the maximum power required by the power system of the SSSM and by the SSIM, respectively.

To implement the value analysis (see equation [162]) to the previously described mission scenario, the following space mission functionalities have been identified as the most important and representative of the system:

- The pressurized volume of the space station (V_p) is representative of the capabilities of the system to accommodate a crew. If the pressurized volume increases the space station offers a higher level of comfort, or it is able to accommodate a larger number of astronauts, or it is able to support astronauts for a longer period of time. The pressurized volume of the space station is also indicative of the *research potentialities* of the system. The research potentialities of the space station can be considered proportional to the pressurized volume that can be allocated to the experimental equipment.

- The number of crew members (n_{crew}) that the space station can support and their maximum allowed on-board permanence time, t_{mission} , are representative, amongst other factors, of the research capabilities on board of the station. Further, a larger number of crew members and a larger permanence time could allow for more maintenance and operations (in general) capabilities of the space station.
- The space station number of hatches (n_{hatches}) is representative of the capability of the space station to support more or less visiting vehicles and to be expandable.
- The racks provide research equipment accommodation. Therefore, with an increasing number of racks (n_{rack}) and their total mass (m_{rack}), the potentialities for research increase as well.

The indicator representative of the system global functionality (f , see eq. [173]) can be obtained by the sum of each system function multiplied by a proportionality factor. The proportionality factors ($\alpha_1, \alpha_2, \dots, \alpha_n$) indicates the relative importance of the system functions.

$$f = \alpha_1 V_p + \alpha_2 n_c + \alpha_3 t_m + \alpha_4 n_h + \alpha_5 n_r + \alpha_6 m_r \quad [173]$$

The method implemented and adopted to estimate the building-blocks cost is based on the advanced missions cost model (AMCM) proposed by NASA. The mathematical model for costs has been described in section 4.13.

The mission success ratio (p) is the indicator that is proportional to the probability of mission success. The mission success ratio is proportional to the launches and docking/undocking success probability. The launcher model has been described in section 4.12. It estimates the launch probability of success (as well as the launch cost) on the basis of the launcher payload mass. The statistical survey shows that the higher is the launcher payload mass, the higher is the launch costs and the lower is the probability of mission success. The probabilities of docking/undocking success as well as the reliability of the space building blocks have been assumed constant. The mission success-ratio model takes into account the number of launches and the number of RvD (n_{RvD}). It evaluates the mission success-ratio (p) by multiplying the launch probability-of-success (p_l) by the RvD probability of success (p_{RvD}). The equation used is the following:

$$p = p_l (p_{\text{R\&D}} n_{\text{R\&D}}) \quad [174]$$

To efficiently use the mathematical model of the cis-lunar space station mission and system, the analysis is divided into two subsequent activities. At first, the screening analysis is carried out to have a first impression on the relative importance of the design factors in Table 59 on the performances. Then, the multi-objective optimization process is executed considering the most relevant factors only, fixing the others. This allows reducing the design space dimensionality to facilitate and speed up the optimization process.

In Figure 122 (a), it can be observed that concerning the Cost of the mission, the type of mission architecture (A), the I_{sp} of the service module and the integrated module (P and Q, respectively), the node diameter (I), and the integrated module diameter (J) are the most relevant design variables. The screening analysis also tells us that the specific impulse of the propellant of the integrated module is involved in some (not better specified since it is a qualitative method) interactions with other factors. A zoom in the region of the origin of the

axes is presented in Figure 122 (b). Besides the relative importance of all the other design variables on the determination of the mission Cost (that can be read from the figure), the analysis shows limited sensitivity of the mission Cost to the number of launches (B), the Volume distribution Node/SM (D), the lunar-orbit altitude (N), and the maximum power required by the service module and the integrated module (V and W, respectively).

The cost of a space system is estimated on the basis of the system complexity and the mass, mainly. The total cost of the mission architecture is obtained, instead, by adding all the building-blocks cost. The type, number, and mass of the building blocks are strongly related to the “*type of mission*”. In fact, this design variable is responsible of how the mission will work in practice, i.e., it defines for each building block its type, the quantity, the payload and the maneuvers to perform. Therefore, costs are strongly influenced by the “*type of mission*” design variable. Costs are also influenced by the service module and integrated module I_{sp} . It must be considered that the cost model assumes that highly complex systems (e.g. the SSIM and the SSSM) are more expensive than less complex systems (i.e., the TS) and that the higher the system mass is, the higher is its cost. Therefore, if in the mission architecture it is determined that the SSSM and the SSIM shall perform maneuvers, their mass is influenced by their I_{sp} , and on turn the cost is influenced. The analysis shows that the mass of the propulsive bay is affected by the amount of propellant, which in turn is determined as a function of the I_{sp} and the mission architecture, and the module diameter. Sub-optimal values of the diameter generate solutions with heavier systems (thus more expensive) because they are not optimized with respect to the tanks.

The other variables have a limited influence on the cost since they have also a limited influence on the mass of the systems. The fact that the design characteristics of the TS scarcely influence the mission cost is not surprising. Indeed, this is considered a not-so-complex system, with a significantly lower cost if compared to the other more-complex systems. The number of launches (B) does not affect the cost variation much. This is due to the fact that the overall cost of two smaller launches is almost equal (slightly higher) to the cost of a larger launcher, according to the model developed.

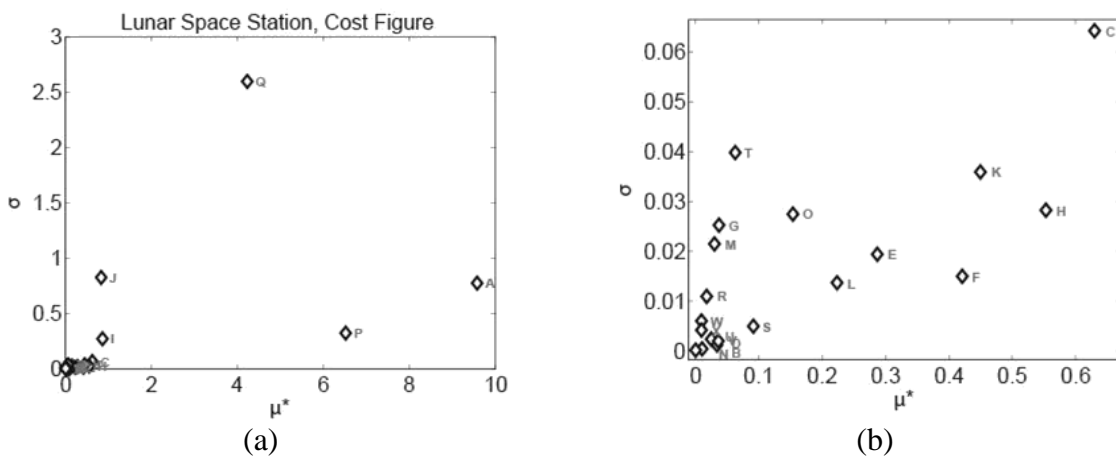


Figure 122 Lunar-Orbiting Space Station Cost Figure. Screening analysis results using the method of Morris. (b) Zoom of figure (a)

In Figure 123 (a) the method of Morris identified the factors, Q, J, A, and P, as quite relevant also in the determination of the mission-functionality, i.e., the probability of completing functions. It is calculated as the product of the global system functionality and the mission success ratio, $F_m = f \times p$.

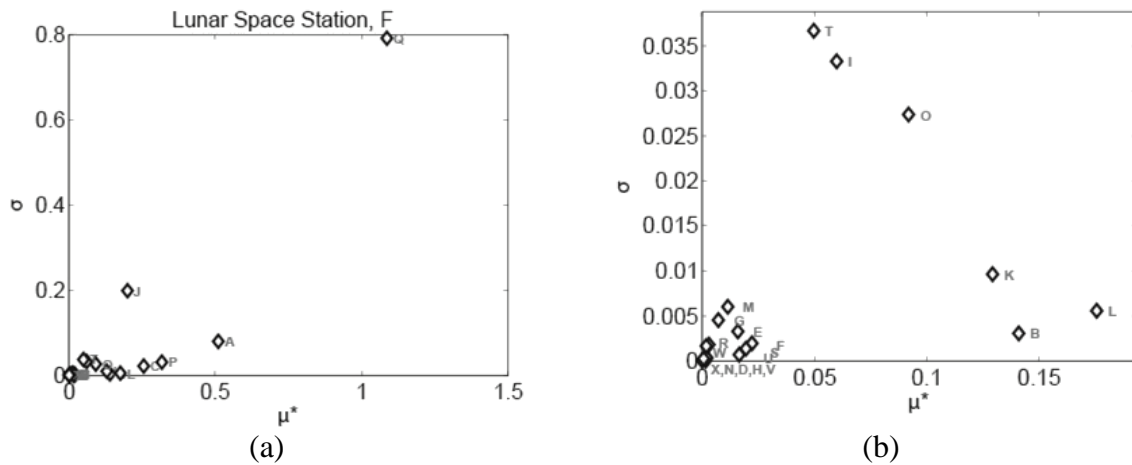


Figure 123 Lunar-Orbiting Space Station Value Figure. Screening analysis results using the method of Morris. (b) Zoom of figure (a). Fig. 15

As previously discussed, the system global functionality, f , indicates the potentiality of the space station to deploy scientific experiments, to provide functionalities as a node, and to connect other space systems. It also represents the space station scalability. These characteristics have been hypothesized as proportional to the pressurized volume, to the number of crew members, to the duration of the mission on board, to the number of hatches, and to the number and the mass of the racks. A sensitivity analysis on f , would identify the already known behavior of f , see equation [173]. The analysis is therefore performed on the mission-functionality. In Figure 123 (b), instead, it can be observed that the Volume distribution Node/SM (D), the diameter of the service module (H), the lunar-orbit altitude (N), the maximum power required by the service module and the integrated module (V and W, respectively), and the specific impulse of the departure stage have a limited effect on the mission functionality figure-of-merit. The design variables Q, J, and P have a relevant effect on F. This is due to the fact that they have an influence on the mass of the modules. Indeed, the launch probability of success is proportional to the mass of the payload. The mission architecture (A) is relevant because it determines the number of maneuvers and docking/undocking (every maneuver has a certain success probability, thus with an increasing number of maneuvers the overall probability decreases). The effect of the number of launches (B) on the mission success ratio is more relevant than its influence on the mission cost. This effect is due to the fact that a small launcher has a higher success ratio than a larger one. However, the overall success ratio, in the case of two launches, is computed as the product of the success ratios of the two launchers. This could lead to a reduced overall mission success ratio in case of two launches

The optimization of the Cis-lunar space station problem is executed using only the most relevant design variables detected with the screening analysis presented before. In particular the factors A, B, C, E, F, G, H, I, J, K, L, M, O, P, and Q (see Table 59) are considered for the analysis while the other design variables are fixed to a level that is intermediate compared to the ranges presented in Table 59.

In Figure 124, the Pareto front obtained using the MOEA/D is presented. All the solutions tend towards the upper-left corner of the graph, i.e., the point with minimum cost and maximum mission-functionality index. As expected, for all the solutions on the Pareto front it is not possible to improve one objective without worsening the other. Therefore, all the solutions in Figure 124 are optimal solutions. It is up to the engineering team, at this point of the analysis, selecting the most suitable design.

The Pareto front is discontinuous in the Cost objective. This means that starting from *Solution3* (see Figure 124) an improvement in the mission-functionality index can only be obtained at a much higher cost. Indeed, the optimal solutions are obtained from two mission architectures, namely the architecture #2 and #5, with the architecture 5 being in general more expensive but more *functional* than architecture 2.

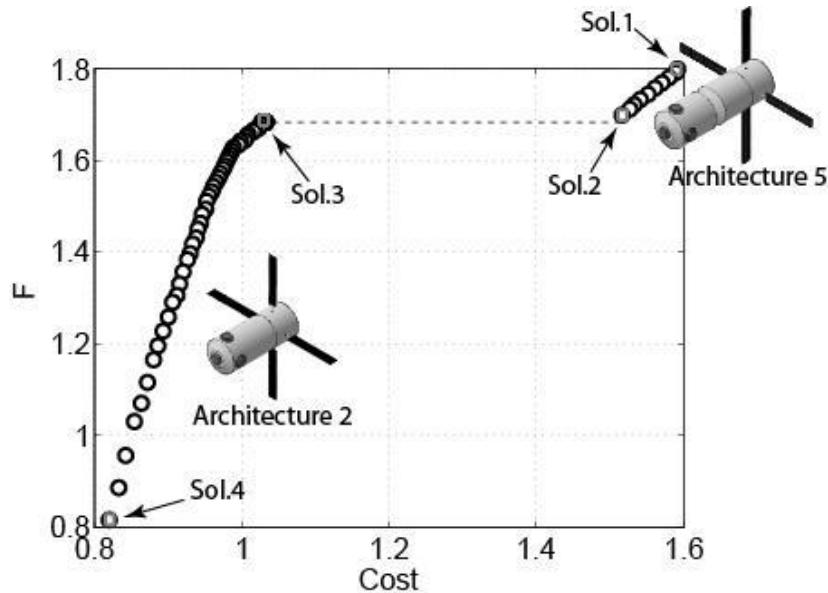


Figure 124 Numerical Pareto-front of the Cis-lunar space station problem

In the discussion of the results we will refer to the 1st leg of the Pareto front indicating those solutions obtained with the architecture #5, and to the 2nd leg of the Pareto front for those obtained with the second architecture. In the first leg of the Pareto front, the solutions go from a high-cost and high-mission-functionality index (Solution 1) to a lower cost and lower mission-functionality index (Solution 2) with the variable trends described in Table 60.

Design Variable	Code	<u>Sol.1</u>	<u>Sol.2</u>	<u>Sol.3</u>	<u>Sol.4</u>
<u>Type of Mission</u>	A	5	5	2	2
<u># of Launches</u>	B	1	1	1	1
<u># of Crew members</u>	C	6	6	6	3
<u>Volume distribution Node/SM</u>	D	0.5	0.5	0.5	0.5
<u># of Hatches SM</u>	E	5	2	-	-
<u># of Hatches Node</u>	F	6	1	-	-
<u># of Hatches IM</u>	G	-	-	5	1
<u>SM Diameter [m]</u>	H	5	5	-	-
<u>Node Diameter [m]</u>	I	5	5	-	-
<u>IM Diameter [m]</u>	J	-	-	5.5	5.2
<u># of Racks SM</u>	K	10	10	-	-
<u># of Racks Node</u>	L	10	10	-	-
<u># of Racks IM</u>	M	-	-	18	6
<u>Moon Orbit Altitude [Km]</u>	N	100	100	100	100
<u>Mission Duration [days]</u>	O	35	34	35	25

<u>I_{sp} SM</u> [s]	P	250	250	-	-
<u>I_{sp} IM</u> [s]	Q	-	-	270	250
Min. Habitable Volume [m ³]	R	40	40	40	40
Racks SM mass [Kg]	S	187.5	187.5	-	-
Racks Node mass [Kg]	T	187.5	187.5	-	-
Racks IM mass [Kg]	U	-	-	187.5	187.5
Max. Power Required SM [KW]	V	10	10	-	-
Max. Power Required IM [KW]	W	-	-	10	10
<u>I_{sp} TS</u> [s]	X	450	450	450	450

Table 60 Design-variable settings for 4 optimal solutions of the Cis-lunar space station problem. The design variables considered in the optimization process are underlined, the other factors are fixed

The number of hatches is the parameter that influences the solutions in that region of the design space the most. Many hatches make sure that the space station is more flexible, allowing for increased capabilities in supporting docking and un-docking of more space elements, e.g., crew vehicle, space haven and supporting vehicle all at the same time. On the other hand, the mass-on-orbit increases with the number of hatches and so does the overall design complexity, leading to an increased cost figure-of-merit.

The second leg of the Pareto front, instead, present solutions with a decreasing cost and mission-functionality index going from Solution 3 to Solution 4 with the trends shown in Table 60.

The number of crew-members, the duration of their mission on-board of the space station and the number of racks for scientific experiments affects the objectives the most, in this region of the design space. The mission-functionality and the cost decrease for a decreasing trend of all these three variables. The diameter of the integrated module is responsible for the volume available on board. The mission-functionality and the cost decrease also because of this design variable that decreases.

Figure 125 is aimed to demonstrate that indeed the other mission architectures and space-station configurations previously discussed present worse performances if compared to those found by the optimization algorithm. The results have been obtained using the design-variable settings presented in Table 61.

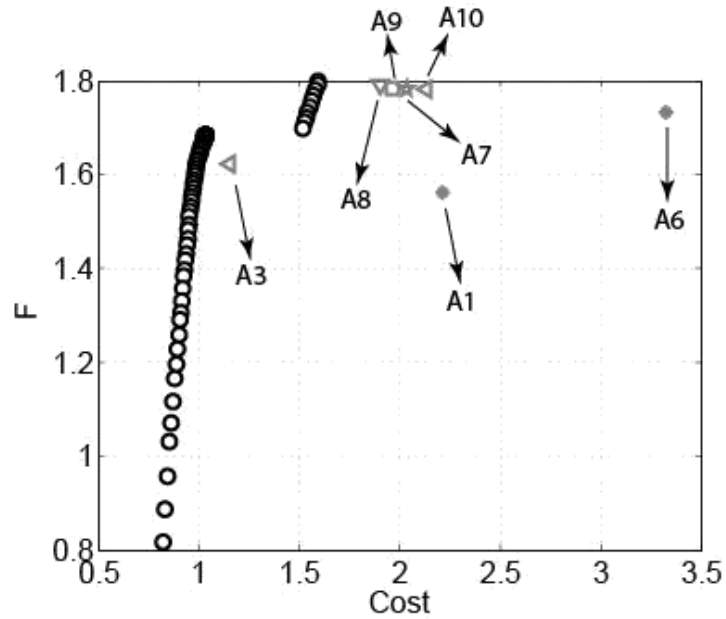


Figure 125 Comparison of all the architectures on the objective space

Design Variable	Code	A1-A10
<u>Type of Mission</u>	A	1-10
<u># of Launches</u>	B	1
<u># of Crew members</u>	C	6
Volume distribution Node/SM	D	0.5
<u># of Hatches SM</u>	E	5
<u># of Hatches Node</u>	F	6
<u># of Hatches IM</u>	G	3
<u>SM Diameter [m]</u>	H	5
<u>Node Diameter [m]</u>	I	5
<u>IM Diameter [m]</u>	J	5.5
<u># of Racks SM</u>	K	10
<u># of Racks Node</u>	L	10
<u># of Racks IM</u>	M	17
Moon Orbit Altitude [Km]	N	100
<u>Mission Duration [days]</u>	O	35
<u>I_{sp} SM [s]</u>	P	350
<u>I_{sp} IM [s]</u>	Q	350
Min. Habitable Volume [m ³]	R	40
Racks SM mass [Kg]	S	187.5
Racks Node mass [Kg]	T	187.5
Racks IM mass [Kg]	U	187.5
Max. Power Required SM [KW]	V	10
Max. Power Required IM [KW]	W	10
<u>I_{sp} TS [s]</u>	X	450

Table 61 Design-variable settings for the comparison of the architectures on the objective space, see Figure 125

8.3 Cis-Lunar infrastructure Logistic

The exploration scenario envisages the deployment of an outpost in Low Lunar Orbit and its logistic support with crew and cargo. The outpost consists of a free flyer which is periodically visited by the crew and logistic vehicles. The design of the outpost is derived from that of section 7.1 with the addition of a further inflatable module to provide extension of the free flyer performance capabilities in terms of human support.

The simulation software tool, presented in section 6, will be utilized to assess the mission concepts for the outpost deployment, the crew outpost access, the cargo delivering mission and the inflatable module delivering. The tool will be useful to estimate mass budget of each building block and overall costs. The estimation will concern the cost of each building block and cost spreading throughout the entire outpost lifetime.

To perform the study, some assumptions have been performed. Thus, the time between 2 crew visits is six month, while the logistic mission is performed one time per year. The lifetime of the outpost is 10 years. At midlife (5 years), the extension of the outpost capabilities is foreseen. A further inflatable module is attached to the outpost and provides it with the capabilities to support a permanent crew up to 1 year. Periodic logistic missions are foreseen to support the outpost every 6 months.

Considering the hypothesized exploration scenario, the building blocks identified necessary are listed in Table 62.



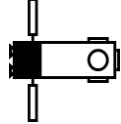




Description	Acronym	Symbol
Capsule	CAP	
Service Module	SM	
Outpost	OP	
Inflatable module	IM	
Logistic Vehicle	LV	
Transfer Stage	TS	
Launch System	LS	

Table 62 Description of the main building blocks

The capsule (CAP) is the vehicle capable of transporting and housing crew from Low Earth Orbit (LEO) to Low Lunar Orbit (LLO). The Service Module (SM) is an unpressurized system that provides the capsule with propulsion, power and other supporting capabilities. The outpost (OP) is the orbital infrastructure that allows extended autonomous free-flying and supports a crew of 4 people up to 4 weeks in the Cis-lunar environment. At midlife (5 years) the outpost is extended by a inflatable module (IM) that increases the habitable volume and provides the outpost with the capabilities to support a permanent crew of 4 people up to 1 year. The logistic vehicle (LV) provides the orbital infrastructure with logistic support. It provides the outpost with pressurized and unpressurized cargo every 12 months. The transfer stage (TS) is a propulsion module that gives the necessary thrust to leave Low Earth Orbit

(LEO) and inject the payload into the LLO. Finally the launch system (LS) allows the launch of the systems in orbit.

The analytical models of the capsule, service module and transfer stage have been developed through utilization of the mathematical models presented in section 4 and design methodology described and applied in section 7. The detailed concept of the logistic vehicle is described in section 7.2. Finally, the design of the inflatable module has been derived from literature. The inflatable module allows extension of the outpost performances, in terms of crew permanence time, providing additional habitable volume and higher closure Environmental Control and Life Support functionalities. Since inflatable systems have a higher Volume/Mass ratio than conventional space structures, the additional module consists of a primary internal rigid structure that supports the external flexible structure. The primary structure is cylindrical with two docking ports at the extremities. The first one allows the docking of the inflatable module with the outpost. The second one allows the docking of visiting vehicles or accommodation of the airlock. The flexible structure consists of a multilayer skin that maintains the internal pressure and provides the system with thermal and micrometeoroid penetration protection. The internal configuration of the module envisages two floors where astronauts find crew quarters and can perform experimental and/or research activities. The thermal control system collects heat from internal equipment and atmosphere and through a heat exchanger transfers it to the outpost. Passive thermal control is provided by MLI integrated in the flexible skin. The electrical power system essentially allows power distribution and illumination. The life support system consists of an oxygen recovery system, a fire detection system, an air circulating system and crew accommodation. The crew accommodation includes a galley system, a personal hygiene system, recreational equipment, sleep accommodation and crew health care equipment. In order to meet the requirement of protection from GCR (Galactic Cosmic Rays), equipment and consumables are located on the outer diameter of the shell. To protect from SPE (Solar Particle Events), a crew quarter area is envisaged inside the rigid structure where the shelter protection provided by structures and equipment have been considered sufficient. The external envelop of the inflatable module consists of a cylinder with a diameter Φ equal 7 m and a length l equal to 7 m. The estimated mass is 20 tons.

The mission exploration scenario foresees three mission nodes: Low Earth Orbit (LEO), High Elliptical Orbit (HEO) and Low Lunar Orbit (LLO).

In Figure 126 a schematic of the Outpost deployment mission architecture is shown. As yet demonstrated in section 8.2 the best mission architecture to deploy an outpost with design and performances similar to that assumed for the study in LLO foresees the utilization of a transfer stage that performs the TLI and LOI maneuvers prior to be discarded. Thus, we refer to the same mission architecture: the OP and the TS are inserted into orbit by the launcher. Once in orbit, the systems perform the TLI and LLO orbit insertion maneuvers, in a docked configuration. The maneuvers are performed by the TS. Once the LLO orbit insertion maneuver is completed the TS is discarded.

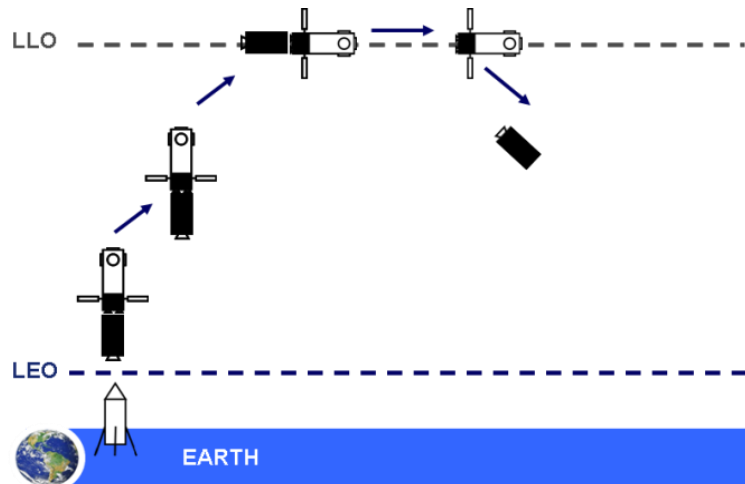


Figure 126 Outpost deployment mission

Once the outpost has been deployed in LLO, the crew and logistic missions start. Figure 129 shows the mission architecture considered for the crew visit mission. The described mission architecture has been obtained, after an activity of sensitivity analysis and multi-objective optimization. Three mission architectures have been considered. The first one (mission architecture “A”) envisages that the TS performs the TLO injection and LLO insertion maneuvers prior to be discarded. The SM will provide direct return on Earth. The second one (mission architecture “B”) envisages that the TS performs only the TLO injection prior to be discarded. The SM will provide LLO insertion and direct return to Earth. The third architecture (mission architecture “C”) envisages that all necessary maneuvers to reach LLO and return to Earth are performed by the SM.

The sensitivity analysis has been performed with the intention of identifying the design variables that mostly affect the mission total cost. The design variables that have been considered are the crew size, the comfort level, the specific impulse of the SM, the specific impulse of the TS and the mission architecture. The results show that the service module specific impulse, the capsule comfort level, the mission architecture and finally the capsule crew size are the design variables with the greatest influence.

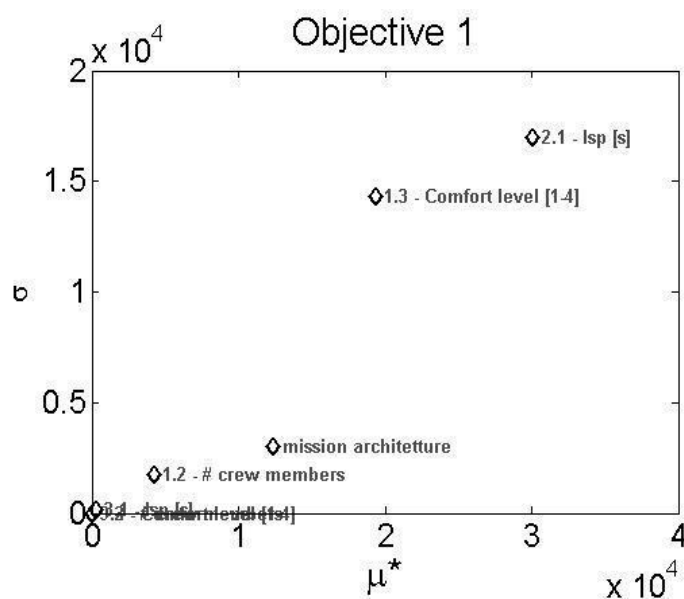


Figure 127 Sensitivity analysis result

On the basis of the sensitivity analysis results, a multi-objective optimization analysis has been performed, considering only the most affecting design variables, i.e. service module specific impulse, the capsule comfort level, the mission architecture and finally the number of crew members. The objectives of the optimization are the reduction of costs and the increase of human transportability, i.e. the ability to transport as many astronauts as possible with the maximum comfort. Figure 128 shows that an optimal single solution that maximizes transportability and minimizes the cost does not exist. On the contrary, there are many system configurations that are characterized by different values of cost and transportability but for which the global system value is the same. It is worth remembering that the choice of the system configuration cannot be performed only on the basis of technical issues but it must take into consideration also programmatic, technological and political issues. Within the considered design variables, only the mission architecture can be chosen on the basis of technical issues. In fact, all solutions on the Pareto front are obtained for the design variable at level 1, i.e. the mission architecture A (Figure 129). The other design variables are chosen considering technology already developed in Europe. For example the specific impulse of the service module has been chosen equal to 315 s as that of ATV. The same specific impulse has been chosen for the LV so that commonalities and synergies can derive from the development of the two building blocks.

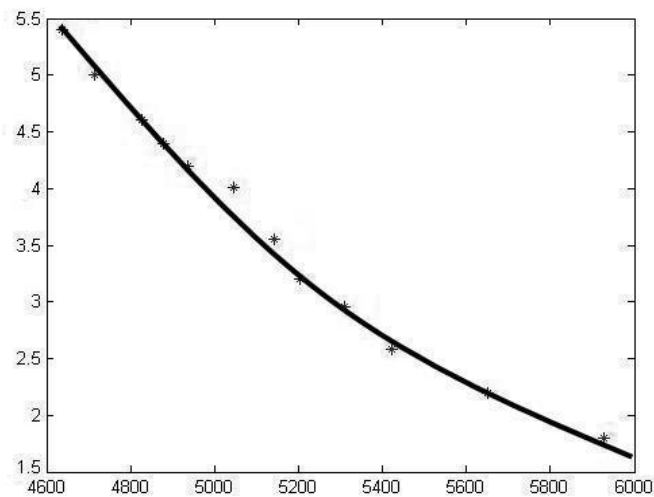


Figure 128 Multi-objective analysis result

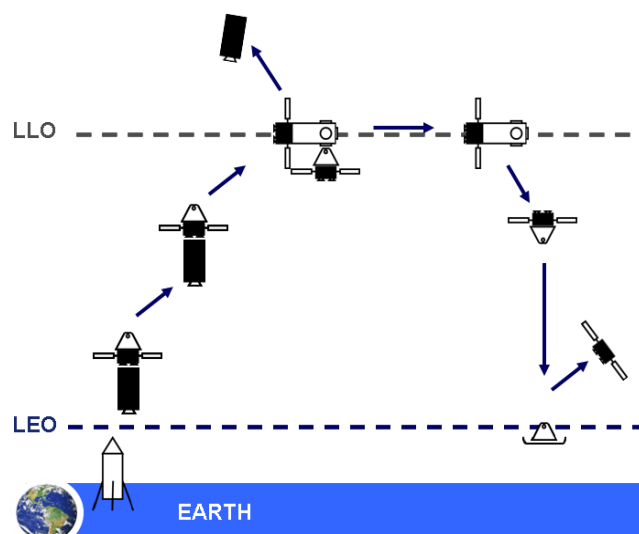


Figure 129 Crew mission

Figure 130 shows the mission architecture for the logistic mission. The LV is launched in HEO orbit by the launcher. It performs autonomous resonance transfer strategy to reach and dock to the outpost in LLO. In case the LV docks to the outpost before crew arrival, it remains docked in dormant mode. After crew arrival, it remains docked to the outpost for all the time necessary to cargo unloading/loading. Then the LV, previously filled with waste, undocks and performs disposal maneuvers that put LV in an orbit without long-term effects. The crew mission lasts until the scheduled conclusion.

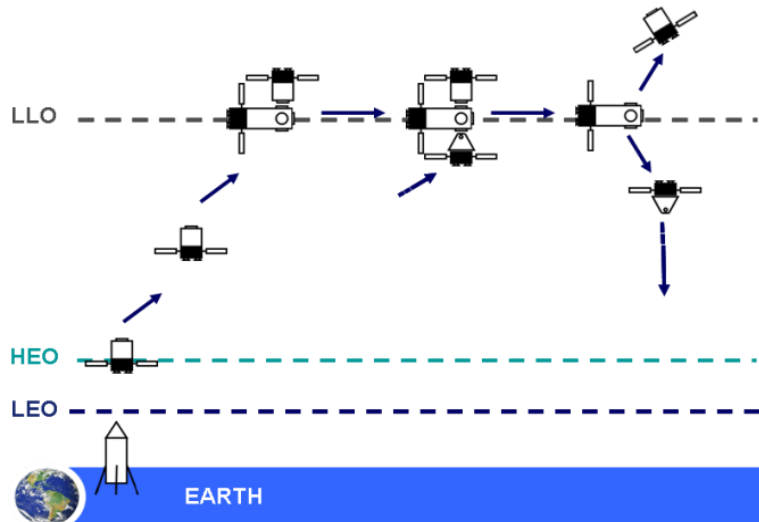


Figure 130 Logistic mission

Figure 131 shows the hypothesized mission architecture for the delivering of the inflatable module. The inflatable module, docked to TS, is injected in LEO orbit by the launcher. The TS performs the transfer orbit injection and arrival maneuvers. Once in proximity of the outpost, the TS performs the RvD maneuvers prior to be discarded.

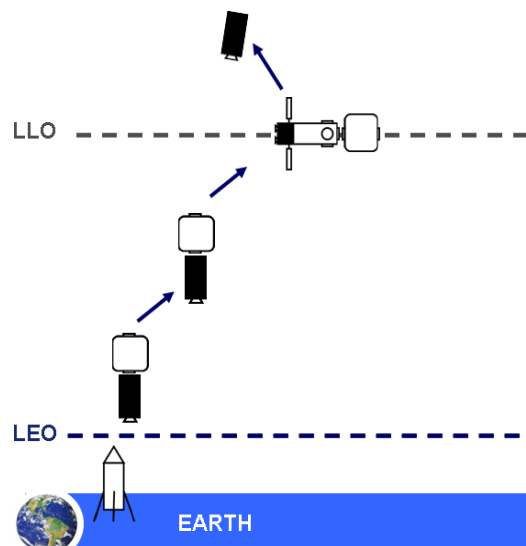


Figure 131 Inflation module delivering

The described architectures have been implemented within SET tool. Through SET interface, each architecture has been implemented in the scenario tab and saved, the design parameters of each building block have been set to the chosen value in the building block tabs. Table 63 shows for each building block the main performance parameters and the total mass

that has been calculated thanks to SET. Since the model of the launcher does not allow estimating the total mass of such system, the launcher total mass has been omitted.

Building block	Performances	Mass [t]
Capsule	Crew members: 4	10.4
Service Module	Crew permanence: 15d I _{sp} : 315 s; ΔV: 1300 m/s	10.8
Outpost	Crew members: 4 Crew permanence: 28 days Comfort level: average	19.4
Inflatable module	High closure ECLS Cargo: 2000 kg	20
Logistic Vehicle	I _{sp} : 315 s ΔV: 690 m/s Resonance transfer strategy Transfer time: 3m÷~1y	12.1
Transfer Stage (Outpost deployment mission)	I _{sp} : 451,5 s ΔV: 4500 m/s	82.2
Transfer Stage (Crew mission)	I _{sp} : 451,5 s ΔV: 4500 m/s	91.5
Transfer Stage (Inflatable module delivering)	I _{sp} : 451,5 s ΔV: 4500 m/s	83.7
Launch System (Outpost deployment mission)	Class: 100 tons	-
Launch System (Crew mission)	Class: 110 tons	-
Launch System (Logistic mission)	Class: 12 tons	-
Launch System (Inflatable module delivering)	Class: 100 tons	-

Table 63 Building blocks performance and mass

Table 64 shows the estimates of the development and production costs of each spacecraft obtained through the cost model previously presented and integrated within SET. Costs are expressed in millions of dollars (2004\$). Other than the cost of a single unit Table 64 shows the total cost to produce all units necessary to ensure the outpost support for its entire lifetime. Obviously, the bigger is the number to be produced (#), the lower is the production cost of each single unit because development costs are distributed on the entire fleet. Thus development and production costs of the capsule and service module are spread on 15 units, development and production costs of the logistic vehicle are spread on 10 units, and finally development and production costs of the transfer stage are spread on 17 units. In the latter case, the assumption is that TS is sized to support the crew mission, which envisages the maximum amount of fuel, whereas in the other missions it is filled with a lower quantity of fuel.

As an assumption, 2025 has been assumed as the date in which the spacecraft (outpost, capsule, service module, logistic vehicle and transfer stage) are first launched. The inflatable module will be launched in the 2030. The difficulty factor represents the level of programmatic and technical difficulty anticipated for the new system. The considered value is an average value for all systems, except the inflatable module. The inflatable module is the

most costly building block, as technical difficulties have been assumed high because of the low TRL of inflatable systems.

The logistic vehicle is the least costly system because of the assumption that it is an ATV design evolution: the level of design inheritance has therefore been considered high with respect to the other systems.

Building block	Cost [M\$]	#	Total cost
Capsule	1253	15	18801
Service Module	537	15	8055
Outpost	2394	1	2394
Inflatable module	5040	1	5040
Logistic Vehicle	532	10	5323
Transfer Stage (Outpost deployment mission)	1588	1	1588
Transfer Stage (Crew mission)	1588	15	23820
Transfer Stage (Inflatable module delivering)	1588	1	1588
Launch System (Outpost deployment mission)	478	1	478
Launch System (Crew mission)	521	15	7815
Launch System (Logistic mission)	103	10	1030
Launch System (Inflatable module delivering)	485	1	485
Total scenario cost [M\$]			76417

Table 64 Development and production cost of the building blocks

Figure 132 shows graphically the spreading of the costs on annual basis for the entire Cis-lunar outpost lifetime. The first year is the most expensive because the outpost shall be deployed and supported. Then the annual cost decreases because only crew and logistic mission are foreseen. The annual cost increases again when the inflatable module shall be deployed. Nevertheless, since the outpost is then able to support a crew up to 1 year, crew rotating missions are reduced, thus allowing a general decreasing of the annual cost.

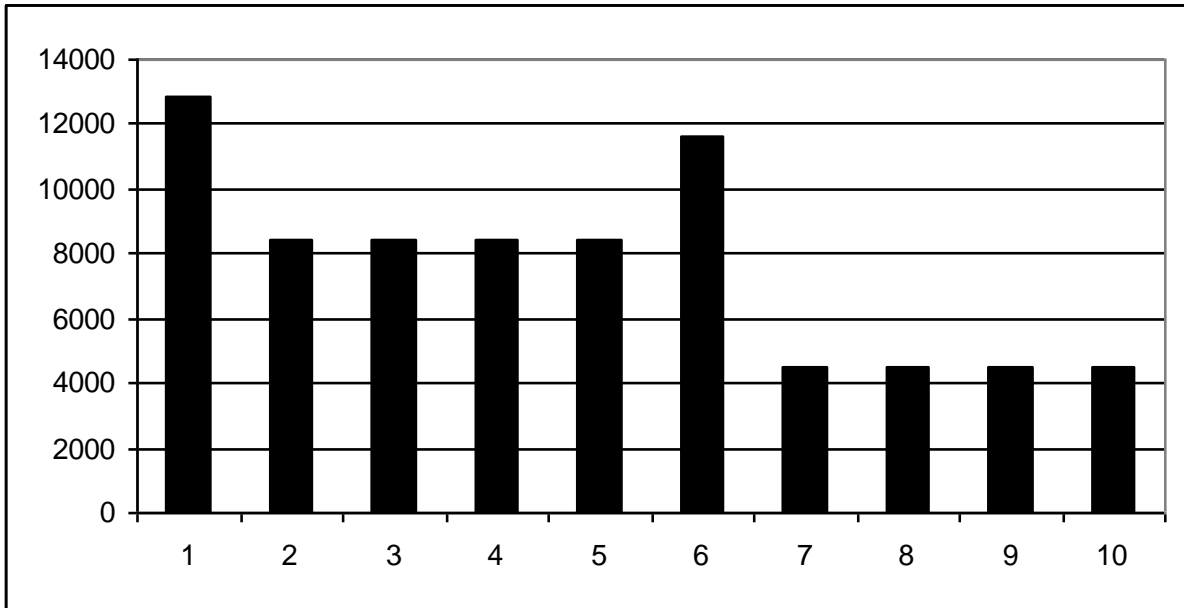


Figure 132 Cost spreading above the entire Cis-lunar outpost lifetime

The results have been obtained implementing the exploration scenario within SET. The post processing of the results has allowed to show graphically the cost spreading on annual base for the entire Cis-lunar outpost lifetime. The results show that although the cost of development, production and delivering associated to a permanent crewed space station are higher than a man-tended facility, the cost of logistic support decreases. A final consideration shall be performed on the obtained cost values. These shall be considered as indicative values that are more suitable for trade off analyses amongst similar system configuration or to understand a general trend. In fact the costs of space system are very difficult to be predicted mostly because of the limited number of space vehicle developed and the limited information available in literature.

9 Conclusions

The exploration of the space foresees the closed observation of the objects in the space with the objective to discover resources and/or information that otherwise are not available. Space exploration is very costly because of the need to travel up to the site of interest. Nevertheless, the economical, technical and social benefits deriving from space activities that affect everyday life shall be considered in the balance of advantages and disadvantages of space exploration. Space exploration stimulates industries and investors to create new employments thus contributing to the redistribution of money. New technologies, which are available today, have been developed to compete with the technical difficulties linked to space exploration. Eventually space exploration represents an opportunity of collaboration between nations that stimulates people to share knowledge and resources.

Nevertheless, today, the new ambitious space programs and the reduced resources push the industries to develop new and more efficient systems because of the need to save money. To reach this objective, it is necessary to learn how to manage the increased complexity of the space exploration systems. Thus, the traditional design approach is no longer adequate to compete with the challenge deriving from space system design because there are significant uncertainties in environmental and system parameters.

The traditional systems design approach creates artificial communication boundaries amongst people, which evolve to inefficient design solutions. For this reason, the traditional design approach results to be inflexible and instable and makes the costs of the final product increase. For these reasons, today, an alternative design approach has been developed. The concurrent engineering is a systematic approach structured so that co-operation and sharing are pursued. The resulting design activity is iterative and more efficient also because all the issues concerning the lifecycle of a system are taken into account since the first development phases. The basic idea is that since every system component affects the others, if any design change is propagated through the system, the resulting design solution reaches the optimal configuration. In concurrent engineering, the design process results to be more challenging than the traditional approach. Nevertheless, if tools are utilized to assist the design activity, the development time, costs and inefficiencies can be reduced. The main scope of the tools is to support communication, to allow integration of the design process, to evaluate and in case relax dependencies, to optimize the design reducing the time and calculation effort.

The scope of the research is to identify and develop a methodology, based on models, methods and tools, to support the decision makers during the space exploration scenarios design and evaluation activity in line with the concurrent design philosophy. To reach this scope, the following objectives have been identified:

- to develop a methodology and identify the tools to support the decision makers during the space exploration scenarios design and evaluation activity;
- to develop a modeling framework and the mathematical models for mission architecture, system engineering and assessment;
- to develop a software tool to support the space mission design process (mission architect and space elements engineering) to reduce time and computational effort.

The identification and development of a methodology for the mission and spacecraft conceptual design have allowed the fulfilment of the first objective. The developed methodology is suitable for the initial phases of the design process (phases 0 and A) so that the output becomes input for the more detailed design phases (B, C). The methodology can be

divided into two parts. The first one allows the definition of the mission concept baseline including the identification of the spacecraft and the mission operation concepts. The second one allows the preliminary definition of each spacecraft which is part of the mission scenario. Thus, starting from the needs, which are assumed as inputs, the mission objectives, the mission requirements set and the mission functional architecture are obtained. This information is then useful to generate the set of possible mission concepts to be evaluated. Once the baseline mission concept is chosen, the design of each spacecraft is performed. The spacecraft definition includes the requirements set, the functional architecture and the spacecraft baseline design, which includes information about the technologies to be considered, the operations concept, the mass budget and the cost of the spacecraft.

The several mission concept options are evaluated on the basis of performance parameters such as launched mass, cost of the space elements and cost-effectiveness (or value), which is a ratio between the benefits and the cost of a system. To assess the optimal mission and/or spacecraft design configuration, sensitivity and optimization analyses have been developed and implemented. The sensitivity analysis allows assessing the relative importance of the design parameters on the performances. This means to understand how a subset of input factors affects the model outputs. The optimization analysis allows identifying the sets of system configurations that optimize the considered performances.

To implement the design methodology, a modelling framework together with the mathematical models of the spacecraft and the analysis tools has been developed. The modelling framework has been developed pursuing a SoS approach. A SoS is formed of several interacting elements and sub-elements, whose overall behavior is usually different than the sum of the effects of the single elements. The modeling framework allows implementing the mathematical model of the mission scenario, including the model of the several space elements, coupling together elementary models able to of the exchange information at any SoS level. The structure of the modeling framework pursues modularity as basic requirement that allows for a certain degree of flexibility and expandability of the modeling framework itself. The elementary models initially provided can be easily substituted and/or reassembled, thus allowing the design team to adapt the models to the actual necessities. For example the design team can introduce new technologies to be considered or change the model accuracy.

The mathematical models of the spacecraft are obtained by coupling together the elementary models of the main subsystems components. Thus, the models of the main components of the structure, TCS, EPS, Propulsion system, ECLS system, communication system, locomotion system and mechanisms have been developed and implemented. Obviously, the list of components models presented in the document is not exhaustive but it allows the accomplishment of the design of the most common technologies considered for space exploration. The chosen level of modeling detail is sufficient for a phase A because more advanced design phases require more detailed models such as numerical models that were out of the scope of this research.

The mission concept defines how people and systems will work to meet the mission objectives and to satisfy the needs. The model of the mission concept organize the interactions amongst the several space elements allowing interactions and synergies that otherwise would not be observable.

Finally, the cost and value model allows completing the set of information concerning the space elements.

The implemented cost model (AMCM by NASA) allows the estimation of the cost of a spacecraft considering mainly information about mass, spacecraft mission, system complexity, maturity level of the considered technologies, heritage of the industry, technological risks. Although, the implemented cost model takes into account several design factors, it is not accurate and the mission cost has been considered as an index useful to

perform trade off analysis of different solutions. More accurate cost models could be developed but they require design information and access to industries cost database that are not available.

The value analysis allows defining the cost-effectiveness of a mission considering the related benefits, costs and probability of mission success. Although, this is a qualitative method, it allows performing the trade-off between similar options. The method allows reduction of the design team subjectivity but this is still important in the choice of parameters to be considered for the determination of the mission benefits and for their weighting factors.

In conclusion, a software tool useful to support the space mission design process and the space elements engineering has been created and has been named Scenario Evaluator Tool (SET). SET derives from putting together the developed modeling strategies and design methodologies with a functional graphical user interface. The tool is conceived so that it allows defining the mission architecture and the spacecraft design to characterize, compare and optimize exploration scenarios and space elements. The main information provided includes mass budget of the space elements, cost indexes and exploration capabilities.

SET has been inspired by the ESA - Concurrent Design Facility (CDF) and by the SpaceNet software tool developed by MIT for NASA.

The CDF is a infrastructure that support the work of the design team during space mission studies. It is structured to allow as much as possible communication amongst the several specialists who are involved in the activity. Basically, it consists of an integrated design model shared by a multidisciplinary team through a dedicated facility. The ESA – CDF is mainly aimed to the concurrent design of spacecraft. Unlike ESA - CDF, SET is conceived for the analysis of mission scenarios. For this reason, ESA – CDF implements more detailed spacecraft models than SET, to perform more accurate analysis at system and subsystem level. In SET the spacecraft models are utilized for the analysis of the mission scenario thus less accurate models are sufficient.

In ESA – CDF, the models of the spacecraft are implemented into an Excel file so that every specialist has a dedicated sheet on which the subsystem model can be implemented providing the necessary interfaces with the other subsystem models.

The modeling infrastructure of SET has been developed with the same modeling philosophy of ESA - CDF. Thus, the model of the space elements are obtained merging opportunely the models of several spacecraft components. Nevertheless, these models are implemented on files and not on Excel sheets. This choice has been performed because, in case of necessity, changing of a model results to be more easily. The files are provided with a suitable interface that allows exchanging inputs and outputs. The model of a system component can be changed by simply changing its file. This features of the modeling environment provides the tool with higher flexibility. For example, the detail level of the model can be easily changed or the model of a new spacecraft can be easily obtained by merging in a different way the models already developed or by introducing new models.

SpaceNet is a NASA-funded and integrated modelling and simulation software environment for analysis of space exploration missions and campaigns mainly from a logistics point of view. It assists the work of the decision makers to assess what is needed to support (manned) space exploration missions in the Earth, Moon and Mars system. The software does not allow the design of space elements but, considering their features, assesses a particular mission architecture and supply chain strategy. This is also the main limitation of the tool which is provided with a database of spacecraft models that cannot be changed or expanded. Although the tool allows customization of the mission scenario, the analyses are limited to the utilization of the predefined spacecraft. SET allows the user to customize the design of the spacecraft, which will then be utilized in the implemented mission concept. This is possible

because the user can set the spacecraft design parameters or, in case, can change the model of a spacecraft.

SpaceNet is provided with the possibility to optimize a mission scenario. In the same way, SET has been provided with the possibility to optimize a mission scenario providing information about the set of equivalent system configurations once the target performances are chosen.

In the second part of the document, the developed design methodology and software tool have been utilized to support the design of space elements and mission scenarios.

The studies concerning the space elements were about two spacecraft, a Free Flyer and a Cargo Logistic Vehicle, and a rover locomotion system. The studies concerning the two spacecraft have been performed in the framework of the ESA scenarios studies for Human Space-Flight and Exploration. These studies are aimed to define an integrated architecture for exploration of Moon, Libration Points, Near-Earth Objects (NEO) and Mars responding to the objectives and requirements of European stakeholders and to integrate this architecture within the international context in order to identify European priorities and roadmaps for space exploration. The study concerning the rover locomotion system has been performed in the framework of the STEPS research project. STEPS is a research project, which has been co-financed by Piedmont Region (Italy), firms and universities of the Piedmont Aerospace District. The main purpose of STEPS has been the developing and testing new technologies for space exploration, including a demonstrator of a future large lunar rover.

The studies about the mission scenarios concern the analysis of a Moon surface infrastructure support, a Cis-lunar orbiting infrastructure delivering and finally its support.

The document shows the main results deriving from the analysis of mission objectives, high level requirements and trade-offs performed. The results concerning the Free Flyer and the Cargo Logistic Vehicle have been discussed and accepted by ESA providing the achieved results with good feedback from the scientific community. The presented studies have been performed with a level of detail sufficient for a phase A. More advanced design phases would require utilization of more detailed analysis such as numerical analysis for the design of the subsystems (e.g. structure and TPS). This has been performed for the design of the rover locomotion system. The design methodology has been applied allowing the design of the wheel of the rover locomotion system. Then, the information has been utilized for the detailed design of the wheel to be constructed. The effectiveness of the design methodology has been demonstrated by the fact that the wheel, after to be constructed, completed successfully its mission.

The studies about the design of the mission scenarios, where possible, have been compared with analogue studies found in literature thus providing an opportunity to test and validate the results provided by the simulation environment and discussed with the scientific community.

Future additional research activities will be about the further development of the Scenario Evaluator Tool – SET. In particular, the future activities will be performed with the objective to reduce the analysis time and to increase the software potentialities and flexibility. In this prospective, the tool will be integrated with an instrument for assembling new spacecraft models, for the further development of new components models and for the link with external models to be considered as black box.

Other future developments will concern the possibility to perform dynamical simulation of the mission concept to provide the design team with visual information of how the mission concept effectively works.

Finally, it shall be considered that for a particular mission statement there are a lot of possible mission concept options that shall be assessed. There could be some cases for which

the number of possible mission options is very high and the assessment of each of them is not possible. In these cases, today, the number of possible options is reduced by the experiences and engineering judgment with the possibility that a good solution is discharged. For this reason, SET will be integrated with a tool able to generate all possible mission concepts compatible with a set of requirements and constraints and to assess each of them. This will be a very powerful instrument that will expand the potentialities of the software.

The future research development will be performed with the objective to reduce the time and computational effort performed for the studies of Gap-analysis. Gap-analysis is an assessment of gaps between the current state and the future state of a system or process and it is the beginning point for the implementation of a system improvement process. In particular, the Gap-analysis is a structured process that, considering space missions, allows identification of the gaps between existing technologies and technologies needed to complete a space exploration mission. In this framework, the Gap-analyses are aimed to answer to questions such as: What is necessary to complete a mission? Where is it necessary? When is it necessary? This is the idea that is behind the Figure 133. Nowadays, the main exploration mission targets considered by agencies are exploration of Moon, Mars or NEO objects. Nevertheless, is not well clear how the targets can be reached and when and what kinds of space elements are really essential. Moreover, it must be considered that budgets are reduced every day and the costs of space programs and project have become more important. For these reasons, the main space agencies have proposed and continue to propose studies concerning new exploration scenarios and enabling technologies to investigate on more efficient solutions. Thus, it is necessary to investigate on new system design that accounts for cost, particularly for large-scale effort. SET has been conceived to help the decision makers to perform this investigation reducing the time of preliminary assessment and trade off of new system configurations.

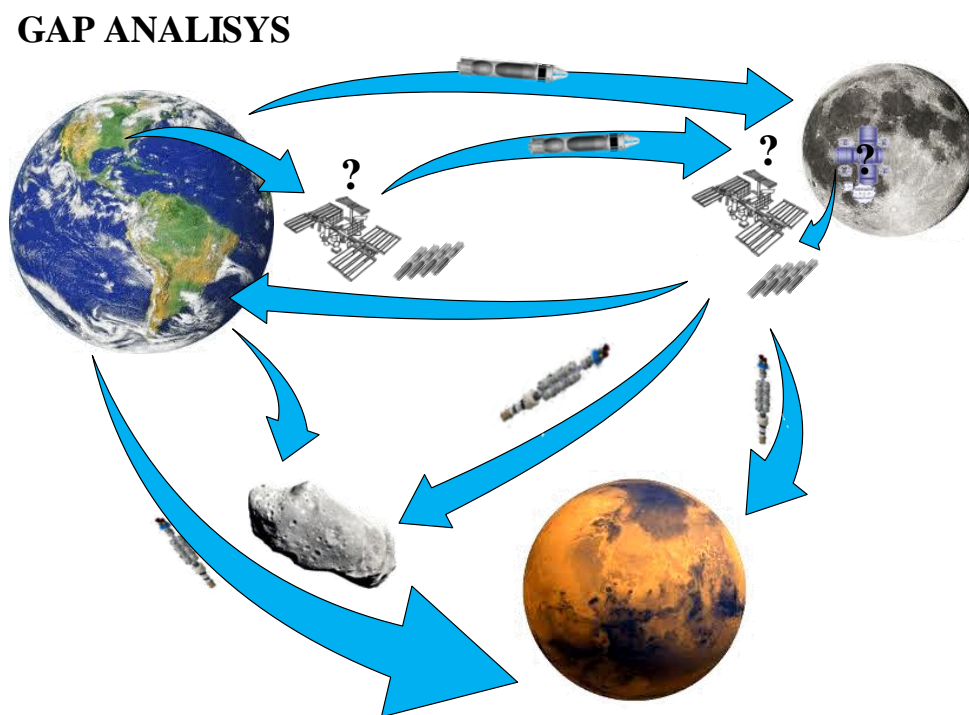


Figure 133 Space GAP analysis

Bibliography

- [1] Oxforddictionaries.com, Oxford: Oxford University Press, 2012, retrieved in January 2013, available at <http://oxforddictionaries.com>
- [2] NASA.gov, Washington: NASA Public Communications Office, 2013, retrieved in January 2013, available at www.nasa.gov
- [3] B. Schwerin, L. Rademakers, D. Coleman, J. Jones, "*Spinoff - NASA Technologies Benefit Society*", NASA, Washington, 2011, DC 20402-0001, ISBN 978-0-16-089850-1
- [4] W. J. Larson, L. K. Prake, "*Human spaceflight: mission analysis and design*", The McGraw-Hill Companies Inc., New York, USA, 2007, 0-07-236811-X
- [5] NASA Langley Research Center, Washington: NASA Public Communications Office, 2013, retrieved in January 2013, available at www.larc.nasa.gov
- [6] Frascati: ESA Communication Department, retrieved in January 2013, available at www.esa.it
- [7] O. L. De Weck, D. Simchi-Levi, R. Shishko, J. Ahn, E. L. Gralla, D. Klabjan, J. Mellein, S. A. Shull, A. Siddiqi, B. K. Bairstow, G. Y. Lee, "*SpaceNet - User's Guide*", NASA Center for AeroSpace Information, Hanover, USA, 2007, NASA/TP—2007–214725
- [8] European Space Agency for the members of ECSS, "*Space project management - Project planning and implementation*", Rev. 1, ESA-ESTEC, Noordwijk, The Nederland, 2009, ECSS-M-ST-10C
- [9] NASA, "*Man-System Integration Standards*", Vol. II, rev. B, NASA, Washington, USSA, 1995, NASA-STD- 3000
- [10] EEA Erasmus Experiment Archive, ESA, "*ESA, Automated Transfer Vehicle-3*", rev. 2.0, ESA-HSO-COU-023
- [11] D. Stanley, S. Cook., J. Connolly, "*NASA's Exploration Systems Architecture Study*", NASA, Washington, USA, 2005, TM 214062, 2005
- [12] "*Columbus, Europe's laboratory for the ISS*", Astrium, 2007
- [13] W. J. Larson, J. R. Wertz, "*Space Mission Analysis and Design*", 3th Edition, United States Air Force Academy, Microcosm Press, El Segundo, California, 1999, ISBN 1881883108
- [14] Thrusters database, Bremen: Astrium GmbH, Ground System Engineering Department, 2013, retrieved in January 2013, available at <http://cs.astrium.eads.net/>
- [15] NSTS 1988 News reference manual, Florida: NASA/KSC Information Technology Directorate/Telescience, 2010, retrieved January 2013, available at <http://science.ksc.nasa.gov>
- [16] ESA, "*Exploration Architecture Trade Report*", Issue 1, strategy and architecture office, ESA-ESTEC, Noordwijk, The Nederland, 2008, HME-HS/STU/TN/JS/2008-XXX
- [17] V. Asnani, D. Delap, C. Creager, "*The Development of Wheels for the Lunar Roving Vehicle*", Glenn Research Center, Cleveland, USA, 2009, NASA/TM-2009-215798
- [18] M. G. Bekker, "*Theory of land locomotion: the mechanics of vehicle mobility*", University of Michigan press, Ann Arbor, 1956, ASIN B0007EAPN6
- [19] M. G. Bekker, "*Off-the-road locomotion: research and development in terramechanics*", University of Michigan press, Ann Arbor, 1960, ISBN 978-0472041428
- [20] G. H. Heiken, D. T. Vaniman, B. M. French, J. Schmitt, "*Lunar Sourcebook: A User's Guide to the Moon*", Cambridge university press, Cambridge, 1991, ISBN 978-0521334440

- [21] D. S. Apostolopoulos, “*Analytical Configuration of wheeled robotic locomotion*”, Carnegie Mellon University, Pittsburgh, Pennsylvania, 2001, CMU-RI-TR-01-08
- [22] P. Nildeep, G. P. Scott, A. Ellery, “*Application of Bekker Theory for Planetary Exploration through Wheeled, Tracked and Legged Vehicle Locomotion*”, Space 2004 conference and exhibit, San Diego, California, 2004, AIAA 2004-6091
- [23] M. Faragalli, D. Pasini, P. Radziszewski, “Performance evaluation of compliant lunar wheels in lunar soil”, IAC 2011, Prague, Czech Republic, 2011
- [24] K. Terzaghi, “*Theoretical soil mechanics*”, John Wiley & Sons, New York, 1944, ISBN 978-0471853053
- [25] Current launchers vehicle data, retrieved January 2013, 2011, available at <http://www.faqs.org/faqs/space/launchers/>
- [26] Advanced missions cost model (AMCM), Washington: NASA, retrieved 08, 2011, available at <http://cost.jsc.nasa.gov/AMCM.html>
- [27] B. S. Blanchard, “*Logistics engineering and management*”, Prentice-Hall, Prentice-Hall international series in industrial and systems engineering, 1974, ISBN 978-0135400470
- [28] G. Ridolfi, “Space Systems Conceptual Design. Analysis methods for engineering-team support”, Politecnico di Torino, Torino, Italy, 2013
- [29] M. D. Morris, “*Factorial sampling plans for preliminary computational experiments*”, Technometrics, Vol. 33, No. 2, pp. 161-174, 1991
- [30] A. Saltelli, S. Tarantola, F. Campolongo, M. Ratto, “*Sensitivity Analysis in Practice: A Guide to Assessing Scientific Models*”, John Wiley & Sons Ltd, Chichester, West Sussex, England, 2004, ISBN 978-0470870938
- [31] F. Campolongo, , J. Cariboni, A. Saltelli, “*An effective screening design for sensitivity analysis of large models,*” Environmental Modelling & Software, Vol. 22, No. 10, pp. 1509-1518, 2007
- [32] K. C. Tan, E. F., Khor, T. H. Lee, Y. J. Yang, “*A Tabu-Based Exploratory Evolutionary Algorithm for Multiobjective Optimization*”, Artificial Intelligence Review, Vol. 19, pp. 231-260, 2003
- [33] N. Srinivas, K. Deb, “*Multiobjective Optimization Using Nondominated Sorting in Genetic Algorithms*”, Journal of Evolutionary Computation, Vol. 2, No. 3, pp. 221-248, 1994
- [34] K. Deb, A. Pratap, S. Agarwal, T. Meyarivan, “*A Fast and Elitist Multiobjective Genetic Algorithm: NSGA-II*”, IEEE Transactions on evolutionary computation, Vol. 6, No. 2, 2002
- [35] C. A. Coello, G. T. Pulido, M. S. Lechuga, “*Handling Multiple Objectives With Particle Swarm Optimization*”, Ieee transactions on Evolutionary Computation, Vol. 8, No. 3, 2004
- [36] J. Kennedy, R. C. Eberhart, Y. Shi, “*Swarm Intelligence*”, The Morgan Kaufmann Publishers, 2001, ISBN 978-1558605954
- [37] Q. Zhang, H. Li, “*MOEA/D: A Multiobjective Evolutionary Algorithm Based on Decomposition*”, IEEE Transactions on Evolutionary Computation. Vol. 11, No 6, pp. 712-731, 2007
- [38] E. Zitzler, K. Deb, L. Thiele, “*Comparison of Multiobjective Evolutionary Algorithms: Empirical Results*”, Evolutionary Computation, Vol. 8, No. 2, pp. 173-195, 2000
- [39] K. Deb, L. Thiele, M. Laumanns, E. Zitzler, “*Scalable test problems for evolutionary multiobjective optimization*” in A. Abraham, L.C. Jain, and R. Goldberg (eds.), “*Evolutionary Multiobjective Optimization: Theoretical Advances and Applications*”, pp. 105-145, Springer, Berlin, 2005

- [40] K., Deb, *“Multi-Objective Optimization using Evolutionary Algorithms”*, Wiley Interscience Series in Systems and Optimization, Vol. 16, Wiley, 2001, ISBN 978-0470743614
- [41] K. Capelle, *“ATV-2 Operations “Up to the ISS and Back””*, ESA - Toulouse control center, 2011
- [42] Cygnus racks configuration, Thales’ Multimedia department, retrieved in January 2013, available at <http://www.thalesgroup.com/Space/>
- [43] ATV Jules Verne - Launch Kit, EADS Astrium, Kourou, 2008
- [44] W. Gerstenmaier, A. Krasnov, T. Reiter, G. Leclerc, Y. Kato, *“International Docking System Standard (IDSS)”*, NASA, Roscosmos, ESA, CSA, MEXT, 2011, IDSS IDD
- [45] International Berthing Docking Mechanism (IBDM), ERASMUS Centre - Directorate of Human Spaceflight, ESA, ESA-HSF-COU-027
- [46] H.P. Leiseifer , *“The ATV2 Flight Segment”*, ESA, 2011
- [47] Mars/Moon/Earth Delta-Vs, Stack exchange Inc., retrieved in January 2013, available at <http://physics.stackexchange.com/questions/31948/is-there-a-map-of-the-interplanetary-transport-network>
- [48] J. Spurmann, *“Lunar Transfer Trajectories”*, DLR, 2010, TN 10-02
- [49] E. A. Belbruno, J. P. Carrico, *“Calculation of Weak Stability Boundary Ballistic Lunar Transfer Trajectories”*, AIAA, 2000, AIAA2000-4142
- [50] V. Krish, E. A. Belbruno, *“An Investigation Into Critical Aspects of a New Form of Low Energy Lunar Transfer, the Belbruno-Miller Trajectories”*, AIAA, 1992, AIAA-92-4581-CP
- [51] A. Ohndorf, B. Dachwald, E. Gill, *“Optimization of Low-Thrust Earth-Moon Transfers Using Evolutionary Neurocontrol”*, IEEE, Computing & Processing (Hardware/Software), Trondheim, 2009, ISBN 978-1-4244-2958-5
- [52] F. Topputo, *“Low-Thrust Non-Keplerian Orbits: Analysis, Design, and Control”*, Politecnico di Milano, March, 2007
- [53] M. T. Ozime, K. C. Howell, *“Low-Thrust Transfers in the Earth–Moon System, Including Applications to Libration Point Orbits”*, Journal of guidance, control, and dynamics, Vol. 33, No. 2, March–April, 2010
- [54] D. Cardile, N. Viola, S. Chiesa, V. Bruno, L. Pegolo, *“Motor-wheel (STEPS annex 2011)”*, Torino, 2011
- [55] G. Gabrielli, *“Lezioni sulla scienza del progetto degli aeromobili”*, Vol. I e Vol. II, Levrotto e Bella, Torino, 1974
- [56] B. Lyndon, *“Apollo program summary report”*, NASA - Johnson Space Center, Houston, Texas, 1975, TM X 68725

